Université de Montréal

Synthetic Approach to Room Temperature Luminescent Ruthenium(II) Complexes With Tridentate Ligands

presented by

Jianhua Wang

Département de chimie

Faculté des arts et des sciences

A thesis presented to Faculté des études supérieures

for the degree of Master of Science in Chemistry

Montréal, Quebéc, Canada

April, 2005

Université de Montréal

Faculté des arts et des sciences

Thesis titled:

Synthetic Approach to Room Temperature Luminescent Ruthenium(II) Complexes With Tridentate Ligands

presented by

Jianhua Wang

was evaluated by the committee composed of the following persons:

1. Prof. Christian Reber, committee president

.....

2. Prof. Garry S. Hanan, research supervisor

.....

3. Prof. Frank Schaper, committee member

.....

Thesis accepted on 13/06/05.

Master's thesis

Title: *Synthetic approach to room temperature luminescent ruthenium(II) complexes with tridentate ligands*

Author: Jianhua Wang

Corrections:

1st corrections:

General corrections:

1. Removal of the blanks in the lifetime data.
2. Addition of the relative percentage of ESI-MS as well as the common solvents for MS samples.
3. Addition of elemental analysis of compound in Chapter 3 and Chapter 5 with comments for unsatisfactory results.
4. Addition of standard counteranion exchange procedure in Chapter 1, General experimental section.
5. Addition of residue solvent peaks in ^{13}C NMR general experimental.
6. Addition of R1 and wR2 factors in all XRD data, separation of target molecules with solvents in the molecular formula for XRD data.
7. Correction of names in the acknowledgements.
8. Addition of comments on the agreement of the isotope patterns in HRMS.
9. Correction of NMR discussion in Chapter 2, Chapter 3 and Chapter 5 and ^{1}H NMR of ligand Cl-pm-tpy in CD_3CN was added in Chapter 2 and 3 for reference.

Other specific corrections:

1. Cover: addition of committee members'name.
2. Page numbers of Table of contents and all the lists for tables, figures, schemes, charts.
3. p3: Addition of more details about the thermal-deactivation hypothesis. Revised discussion about the ligand field strength and the activation energy for crossing from the $^{3}MLCT$ to the ^{3}MC state.

4. p9-11: Experimental section: (i) solvent peaks in ^{13}C NMR; (ii) standard counteranion exchange procedure; (iii) isotope agreement comments for HRMS; (iv) radiation sources for XRD.

5. p26: Figure 2.1 assignments of the proton NMR.

6. p29: 2-D COSY NMR.

7. p35 and 36: round the distances.

8. p56: Explanation of the luminescence quenching mechanism of complex $Ru(tpy\text{-}An)_2^{2+}$ in ref 20 in Chapter 2.

9. p68: discussion of unsatisfactory refinement of complex **3b**.

10. p83-89: elemental analysis results.

11. p108: revised structure discussion.

12. p110: more data for Table 4.4 and revised discussion for complex **2d**.

13. p138: Ligand **1a-c** ^1H NMR in CD_3CN and revised discusson.

14. p139: discussion of the symmetry of ligand **1a**.

15. p142: discussion of unusual *Z* number of complex **3b**.

16: p150: last sentence, revised discussion.

17: p192: change "could also give rise to" to "has opened the gate to".

18: A1: *Synlett.* **2005**, *8*, 1251 and the annexed real paper.

19. A2-8: Addition of supplementary data for complex **2b** in Chapter 5.

Explanations for unchanged suggestions:

1. The styles of reporting values of LRMS and *J* values of ^1H NMR. The reporting styles follow the conventional reporting styles for publication in our journals of choice.

2nd corrections:

General corrections:

1. Change of the numbering schemes of single crystal structures to match the numbers in the supplementary data.

2. Addition of all the fractional atomic coordinates and equivalent isotropic displacement parameters for XRD supplementary data.

3. Correction of the discussion of solid structure symmetry of ligand **1a** in Chapter 5.

Summary

Abstract

In my research thesis, the different synthetic approaches to prolong the excited state lifetime of Ru(II) complexes with deliberately designed tridentate ligands are presented. Initially, the "chemistry-on-the-complex" method was used to build up dimetallic Ru(II) species with multi-chromophoric approach (**Chapter 2**). The bimetallic Ru(II) complexes were efficiently synthesized through palladium(0)-catalyzed homocoupling reactions. These newly synthesized Ru(II) species had intriguing photophysical properties.

Even though the approach used in **Chapter 2** has been proven to be an efficient strategy to optimize the photophysical properties of Ru(II) terpyridine complexes, their syntheses also depend on sequential reactions in order to incorporate two chromophores into the same ligand. The optimized multi-chromophoric approach is then presented in **Chapter 3**. In this new approach, the 9-anthryl chromophore (the energy reservoir) is grafted onto the tpy moiety not involved in the ^{3}MLCT emitting state level, while the 2-pyrimidyl-tpy subunit is involved in extended electron delocalization.

The introduction of electron-donating or -accepting 4'-substituents onto $Ru(tpy)_2^{2+}$ has several advantages over multi-chromophoric species due to their easier syntheses and simpler monoexponential decay. In this approach, Ru(II) complexes of 4'-

cyano-tpy, which were not accessible from a classical approach, were first synthesized through palladium(0)-catalyzed cyanation reactions(**Chapter 4**). The introduction of the strongly electron-withdrawing cyano group has yielded exceptional photophysical properties in Ru(II) complexes, with prolonged rt luminescence lifetimes as well as relatively high quantum yields as compared to $Ru(tpy)_2^{2+}$.

Due to the importance of ligand design in coordination chemistry, the exploration of new ligands as well as the new methodology to synthesize known ligands is a major concern in inorganic chemistry. In **Chapter 5**, a new family of tridentate ligands, 2,6-*bis*(pyrimid-2'-yl)pyridines, were convergently synthesized with high yields. The application of this new family of ligands to Ru(II) coordination chemistry has proven the strongly π-electron accepting nature of these ligands.

Since 4'-aryl-tpy ligands have been used as ubiquitous ligands in coordination chemistry, new synthetic method to obtain these ligands is in great need. The new synthetic methodology to sterically hindered and non-hindered 4'-aryl-tpy ligands is shown in **Chapter 6**. This one-pot method has several advantages over previous reported methods: (i) milder reaction conditions; (ii) higher yields and (iii) easier purification. In this method, even the sterically hindered 9-anthryl group can be incorporated into the tpy moiety in one step.

Keywords

excited state lifetime, ligand design, ^{3}MLCT, ruthenium, terpyridine

Sommaire

Résumé

Dans mon mémoire de maîtrise sont présentés des différentes approches de prolonger la durée de vie de l'état excité des complexes de ruthénium(II) avec des ligands tridentates. Dans une première étape, la méthode « chimie-sur-complexe » a été utilisée pour construire des espèces multi-chromophoriques dimétalliques de Ru(II) (**Chapitre 2**). Les complexes bimétalliques de Ru(II) ont été efficacement synthétisés par une réaction de homocouplage, en utilisant palladium(0) comme catalyseur. Ces nouvelles espèces de ruthénium ont démontré des propriétés photophysiques très intéressantes.

Bien que l'approche utilisée dans le **Chapitre 2** soit révélé utile pour optimiser les propriétés photophysiques des complexes de Ru(II) avec des ligands terpyridines, leur synthèse dépendent aussi sur des réactions consécutives, pour que deux chromophores soient incorporés dans le même ligand. L'approche multi-chromophore optimisée est ensuite présentée dans le **Chapitre 3**. Dans cette nouvelle approche, le chromophore 9-anthryle (le réservoir d'énergie) est greffé sur la partie tpy qui n'est pas impliquée dans l'état émetteur ^{3}MLCT, tandis que la sous-unité 2-pyrimidyle-tpy est entraînée dans la délocalisation électronique.

L'introduction de substituents accepteurs ou donneurs d'électrons dans la position 4' du ligand dans les complexes $Ru(tpy)_2^{2+}$ présente des avantages par comparaison aux espèces multi-chromophoriques, grâce à leur synthèse facile et le déclin monoexponentielle simple. Par cette approche, des complexes de Ru(II) avec des ligands de type 4'-cyano-tpy ont été synthétisés pour la première fois par l'intermède d'une

réaction de cyanuration catalysée par Pd(0) (**Chapitre 4**). La présence du groupement cyano, très fort accepteur d'électron, a amené des propriétés photophysiques exceptionnelles aux complexes de Ru(II), avec des longues durées de vie, aussi que des grands rendements quantiques comparés aux $Ru(tpy)_2^{2+}$.

L'importance de la nature du ligand dans la chimie de coordination mène vers l'exploration des nouveaux ligands, aussi que vers des nouvelles méthodes de synthèse des ligands déjà connus. Dans le **Chapitre 5**, une nouvelle famille des ligands tridentates, 2,6-*bis*(pyrimid-2'-yl)pyridines, a été synthétisée avec des bons rendements. L'application de cette nouvelle famille sur la chimie de coordination du Ru(II) a démontré la capacité forte accepteuse de ces ligands.

Les résultats exceptionnels obtenus par l'utilisation des ligands de type 4'-aryle-tpy dans la chimie de coordination ont démontré la nécessité de trouver des nouvelles méthodes de synthétiser ces ligands. Ainsi, une nouvelle méthodologie de synthèse des ligands de type 4'-aryle-tpy encombrant et non-encombrant stérique est présentée dans le **Chapitre 6**. La méthode présente quelques avantages par rapport à celles présentées jusqu'à maintenant : (i) des conditions de réactions pas trop drastiques; (ii) grands rendements; (iii) très facile purification. Par cette méthode, même le groupement encombrant 9-anthryle peut être incorporé dans le ligand tpy dans une seule étape.

Mots clé

durée de vie de l'état excité, design de ligand, ^{3}MLCT, ruthénium, terpyridine

Table of Contents

Summary i

Sommaire iii

Table of Contents v

List of Tables xiii

List of Figures xv

List of Schemes xvii

List of Charts xix

Abbreviations xx

Acknowledgements xxiii

Chapter 1

Introduction 1

1.1 Ruthenium polypyridyl complexes 1

1.2 Ligand design in coordination chemistry 6

1.3 General experimental 9

1.4 References 12

Chapter 2

The Multi-chromophore Approach to Prolonged Room Temperature Luminescence Lifetimes in Ru(II) Complexes Based on Tridentate Polypyridine Ligands 16

Abstract 16

2.1 Introduction 17

2.2 Results and discussion 20

2.2.1 Synthesis 20

2.2.2 ^{1}H NMR spectroscopy 26

2.2.3 Crystallography 30

2.2.4 Electrochemistry 36

2.2.5 Spectroscopic properties 38

2.2.6 Photophysical properties[gsh1] 40

2.3 Conclusion 42

2.4 Experimental 43

2.4.1 General methods 43

2.4.2 X-Ray crystallography 43

2.4.3 Synthesis 45

(AnPmtpy)Ru(tpy) $(PF_6)_2$ **(3a)** 45

(AnPmtpy)Ru(tpyPmAn) $(PF_6)_2$ **(3b)** 46

(AnPmtpy)Ru(tpyPmCl) $(PF_6)_2$ **(3c)** 47

[(tpy)Ru(tpyPmPmtpy)Ru(tpy)]$(PF_6)_4$ **(4a)** 49

[(AnPmtpy)Ru(tpyPmPmtpy)Ru(tpyPmAn)]$(PF_6)_4$ **(4b)** 50

2.5 References 52

Chapter 3

Luminescent Ruthenium(II) Complexes of 4'-(9-Anthryl)-2,2':6',2"-Terpyridine: Equilibrating Organic Chromophore and ^{3}MLCT Over Large Distance 57

Abstract 57

3.1 Introduction 58

3.2 Results and discussion 61

3.2.1 Synthesis 61

3.2.2 NMR spectroscopy 63

3.2.3 Crystal structure determination 67

3.2.4 Electrochemistry 71

3.2.5 Spectroscopic properties 72

3.2.6 Photoluminescence measurements 74

3.3 Conclusion 77

3.4 Experimental 78

3.4.1 General methods 78

3.4.2 X-Ray crystallography 79

3.4.3 Ligands synthesis 80

4'-(Pyrimid-2-yl)-2,2':6',2"-terpyridine (**2a**) 80

4'-(5-Chloro-pyrimid-2-yl)-2,2':6',2"-terpyridine (**2b**) 81

4'-(5-Phenyl-pyrimid-2-yl)-2,2':6',2"-terpyridine (**2c**) 81

4'-(5-*p*-Bromo-phenyl-pyrimid-2-yl)-2,2':6',2"-terpyridine (**2d**) 82

3.4.4 Metal complexes preparation 83

(An-tpy)$RuCl_3$ (**4**) 83

[(An-tpy)Ru(**2a**)]$(PF_6)_2$ (**3a**) 83

[(An-tpy)Ru(**2b**)]$(PF_6)_2$ (**3b**) 85

[(An-tpy)Ru(**2c**)]$(PF_6)_2$ (**3c**) 86

[(An-tpy)Ru(**2d**)]$(PF_6)_2$ (**3d**) 87

[(An-tpy)Ru(tpy)]$(PF_6)_2$ (**3e**) 88

3.5 References 90

Chapter 4

Synthesis and Properties of the Elusive Cyano-complexes: Facile Palladium-Catalyzed Cyanation on the Ru(II) Terpyridine Complexes 94

4.1 Introduction 94

4.2 Result and discussion 100

4.2.1 Synthesis 100

4.2.2 NMR spectroscopy 105

4.2.3 Crystal structure determination 106

4.2.4 Electrochemistry 109

4.2.5 Absorption and emission measurements 110

4.3 Conclusion 115

4.4 Experimental 116

4.4.1 General methods 116

4.4.2 Materials 116

4.4.3 Syntheses 117

Synthesis of 1,5-di-2-pyridylpentane-1,3,5-trione (**6**) 117

Synthesis of 2,6-*bis*(2'-pyridyl)-4-pyridone (**7**) 118

Synthesis of 4'-chloro-2,2':6',2''-terpyridine (**4**, Cl-tpy) 118

Synthesis of 4'-cyano-2,2':6',2''-terpyridine (**5**, NC-tpy) 118

[(NC-tpy)Ru(tpy)]$(PF_6)_2$ (**2a**) 119

[(NC-pm-tpy)Ru(tpy)]$(PF_6)_2$ (**2c**) 120

[(NC-ph-pm-tpy)Ru(tpy)]$(PF_6)_2$ (**2d**) 121

[$(NC\text{-}tpy)_2$Ru]$(PF_6)_2$ (**2b**) 122

4.5 References 124

Chapter 5

Synthesis of 2,6-*bis*(5'-Substituted-pyrimid-2'-yl)pyridine Ligands and Their Ruthenium(II) Complexes 129

Abstract 129

5.1 Introduction 130

5.2 Results and discussion 134

5.2.1 Syntheses 134

5.2.2 NMR spectroscopy 137

5.2.3 Solid state structure 139

5.2.4 Electrochemistry 146

5.2.5 UV-vis spectroscopy 148

5.3 Conclusion 154

5.4 Experimental 155

5.4.1 General methods 155

5.4.2 X-Ray crystallography 156

5.4.3 Syntheses of Ligands **1a-c** 157

2,6- pyridine-bisamidine · 2HCl (**6**) 157

2,6-*bis*(pyrimyd-2'-yl)pyridine (**1a**) 157

2,6-*bis*(5'-chloro-pyrimyd-2'-yl)pyridine (**1b**) 158

2,6-*bis*(5'-phenyl-pyrimyd-2'-yl)pyridine (**1c**) 158

5.4.3 Syntheses of complexes **2a-c** and **3a-c** 159

$Ru(\mathbf{1a})_2(PF_6)_2$ (**2a**) 159

$Ru(\mathbf{1b})_2(PF_6)_2$ (**2b**) 160

$Ru(\mathbf{1b})(\mathbf{1b})Cl(PF_6)_2$ (**2b'**) 160

$Ru(\mathbf{1c})_2(PF_6)_2$ (**2c**) 161

$Ru(\mathbf{1a})(tpy)(PF_6)_2$ (**3a**) 162

$Ru(\mathbf{1b})(tpy)(PF_6)_2$ (**3b**) 163

$Ru(\mathbf{1c})(tpy)(PF_6)_2$ (**3c**) 163

5.5 References 165

Chapter 6

A Facile Route to the Sterically Hindered and Non-hindered 4'-Aryl-2,2':6',2"-Terpyridines 170

Abstract 171

6.1 Introduction 172

6.2 Results and discussion 174

6.3 Conclusion 178

6.4 Experimental 170

6.4.1General methods 179

6.4.2 Materials 179

4'-phenyl-2,2':6',2"-terpyridine (**1**) 179

4'-*p*-Tolyl-2,2':6',2"-terpyridine (**2**) 180

p-Cyanophenyl-2,2':6',2"-terpyridine (**3**) 181

p-Hydroxyphenyl-2,2':6',2"-terpyridine (**4**) 181

p-bromophenyl-2,2':6',2"-terpyridine (**5**) 182

p-(*N,N*-dimethylaminophenyl) -2,2':6',2"-terpyridine (**6**) 182

p-nitrophenyl-2,2':6',2"-terpyridine (**7**) 183

p-methoxyphenyl-2,2':6',2"-terpyridine (**8**) 183

4'-(2,3-dimethoxyphenyl)-2,2':6',2"-terpyridine (**9**) 184

4'-(4-diphenyl)-2,2':6',2"-terpyridine (**10**) 184

4'-(1-naphthyl)-2,2':6',2"-terpyridine (**11**) 185

4'-(9-anthryl)-2,2':6',2"-terpyridine (**12**) 185

4'-(2-furyl)-2,2':6',2"-terpyridine (**13**) 186

4'-(4-pyridyl)-2,2':6',2"-terpyridine (**14**) 187

6.5 References 188

Chapter 7

Conclusions and Future Proposals 191

7.1 Conclusions 191

7.2 Future proposals 193

7.2.1 Tridentate ligands 193

7.2.2 Complexes 194

7.2.3 Synthetic methodology 195

7.3 References and notes 198

Appendix A1

A-1 Papers published A1

A-2 Supplementary data of single crystal structures A2

List of Tables

Table 1.1 Major approaches to prolong the room temperature excited state lifetimes of ruthenium(II) polypyridyl complexes based on tridentate ligands. 5

Table 2.1 Effect of catalyst and temperature variation on the mono-coupling reaction. 24

Table 2.2 ^{1}H NMR chemical shifts for Ru(II) complexes **3a-c**, **4a-b**, **2a-b** and ligand **1**.. 30

Table 2.3 Selected bond lengths and bond angles for complexes **3a** and **3b**. 34

Table 2.4 π-Stacking distances in the two stacked motifs. 36

Table 2.5 Electrochemical redox potentials for complexes **3a-c**, **4a-b** and **5**. 37

Table 2.6 Electronic spectra data of complexes **3a-c**, **4a-b** and **5**. 40

Table 2.7 Luminescence data of complexes **3a-c** and **4a-b**. 41

Table 2.8 Crystallography data for complexes **3a** and **3b**..... 44

Table 3.1 Chemical shifts of ^{1}H NMR signals of complexes **3a-e**. 65

Table 3.2 Selected bond lengths and angles for complexes **3b** and **3d**..... 68

Table 3.3 Cyclic voltammetric potentials of complexes **3a-e**. 72

Table 3.4 Electronic absorption spectra for complexes **3a-e**. 73

Table 3.5 Luminescence data of complex **3a-e**. 76

Table 3.6 Crystallography data for complexes **3b** and **3d**. 79

Table 4.1 ^{1}H NMR data of complex **1a-e** and complexes **2a-e**..... 105

Table 4.2 Crystallography data for complex **2c**. 108

Table 4.3 Selected bond lengths and angles in complex **2c**. 109

Table 4.4 Electrochemical data of complexes **2a-e**..... 110

Table 4.5 Absorption spectra data of complexes **2a-d**..... 113

Table 4.6 Luminescence data of complexes **2a-e**. 114

Table 5.1 ^{1}H NMR resonances for ligands **1a-c**..... 138

Table 5.2 ^{1}H NMR resonances for complexes **2a-c** and **3a-c**. 139

Table. 5.3 Selected bond lengths and bond angles for complexes **2a-b** and **3b**.. 146

Table 5.4 Half-wave potentials for complexes **2a-c** and **3a-c**..... 148

Table 5.5 Absorption spectra data of ligands **1a-c**..... 150

Table 5.6 Absorption spectra data of complexes **2a-c**, **3a-c**. 153

Table 5.7 Crystallography data for complexes **2a-b** and **3b**. 156

Table 6.1 Reaction conditions and yields of 4'-aryl-2,2':6',2"-terpyridines compared with the methods previously reported. 176

List of Figures

Figure 1.1 Octahedral structures of $Ru(bpy)_3^{2+}$ and $Ru(tpy)_2^{2+}$ complexes with their energy diagrams of photo-excited states. 2

Figure 1.2 Schematic representations of $M(bpy)_3^{n+}$ and $M(tpy)_2^{n+}$ complexes and of their disubstituted derivatives 3

Figure 1.3 Schematic representations of two approaches to synthesize metal complexes with newly designed ligands: **(A)** ligand approach; **(B)** "chemistry-on-the-complex" approach. 8

Figure 2.1 ^1H NMR spectrum of complex **4b** with proton labelling. 26

Figure 2.2 2-D COSY spectrum of complex 3b with labelling and schematic representation of the deshielding effect of 9-anthryl group to the chemical shifts of $T_{3',5'}$ and $Pm_{4,6}$ protons. 29

Figure 2.3 Two ORTEP plots of the X-ray crystal structure of complex **3a**. 32

Figure 2.4 Two ORTEP plots of the X-ray crystal structure of complex **3b**. 33

Figure 2.5 Two intramolecular π-stacking motifs observed in complex **3b.** 35

Figure 2.6 Electronic absorption spectra for **3a-c** and **4b**. 39

Figure 2.7 Schematic representation of the luminescence quenching mechanism of homoleptic $Ru(tpy\text{-}An)_2^{2+}$ complex. 56

Figure 3.1 ^1H NMR spectra of complexes **3a-e**. 67

Figure 3.2 ORTEP plots of the X-ray crystal structure of complex **3b**. 70

Figure 3.3 ORTEP plots of the X-ray crystal structure of complex **3d**. 71

Figure 3.4 Electronic absorption spectra for **3a-e**. 74

Figure 4.1 Energy diagram of the frontier orbitals of $Ru(tpy)_2^{2+}$ complexes. 96

Figure 4.2 A recent example of di-ruthenium system. 98

Figure 4.3 ORTEP plots of the X-ray crystal structure of complex **2c**. 107

Figure 4.4 Absorption and emission spectra of **2b**. 111

Figure 4.5 UV-vis spectra of complexes **2a** (solid line), **2c** (dashed line) and **2d** (dotted line) in acetonitrile solution. 112

Figure 5.1 Dynamic Behavior of [bppy]PdR complexes. 131

Figure 5.2 Proposed structure of complex **2b'**. 136

Figure 5.3 ORTEP plot of the X-ray crystal structure of **1a**·$2H_2O$. 140

Figure 5.4 ORTEP plots of the three-dimensional structure of **1a**·$2H_2O$ viewed from Z-axis (top) and viewed along Z-axis (bottom). 141

Figure 5.5 ORTEP plots of the X-ray crystal structure of complex **2a**. 143

Figure 5.6 ORTEP plot of the X-ray crystal structure of complex **2b**. 144

Figure 5.7 ORTEP plots of the X-ray crystal structure of complex **3b**. 145

Figure 5.8 Absorption spectra of ligands **1a-c**. 149

Figure 5.9 Absorption spectra of complexes **2a-c**. 151

Figure 5.10 Absorption spectra of complexes **3a-c**. 152

List of Schemes

Scheme 2.1 Synthesis of complexes **3a-b**. 21

Scheme 2.2 Palladium-catalyzed mono-coupling reaction on the $Ru(tpy\text{-}pm\text{-}Cl)_2^{2+}$ complex **2b**..... 23

Scheme 2.3 Palladium-catalyzed homo-coupling reaction on complexes **2a** and **3c**..... 25

Scheme 3.1 Synthesis of 5-R-pyrimid-2-yl-2,2':6',2"-terpyridine ligands **2a-d**. 61

Scheme 3.2 Synthesis of the ruthenium complexes **3a-d**..... 63

Scheme 4.1 Possible intramolecular electron-transfer processes taking place after light excitation of the mixed-valent Ru(II)-Ru(III) dimer. 98

Scheme 4.2 Original synthesis of 4'-cyano-2,2':6',2"-terpyridine ligand. 100

Scheme 4.3 Synthesis of 4'-cyano-2,2':6',2"-terpyridine through palladium(0)-catalyzed cyanation of 4'-chloro-2,2':6',2"-terpyridine. 101

Scheme 4.4 Classical approach to the Ru(II) 4-cyano-2,2':6',2"-terpyridine complex..... 102

Scheme 4.5 Palladium-catalyzed cyanation of Ru(II) complexes of 4'-chloro-2,2':6',2"-terpyridine..... 103

Scheme 4.6 Palladium catalyzed cyanation on Ru(II) complexes **1c-d**. 104

Scheme 5.1 Reported synthesis of bppy ligand..... 133

Scheme 5.2 Synthesis of 2,6-*bis*(5'-R-pyrimid-2'-yl)pyridine ligands (Rbppy) **1a-c**. 134

Scheme 5.3 Synthesis of $[(Rbppy)_2Ru](PF_6)_2$ complexes **2a-c**. 135

Scheme 5.4 Synthesis of heteroleptic $[(Rbbpy)Ru(tpy)](PF_6)_2$ complexes **3a-c**. 136

Scheme 6.1 Facile one-pot synthesis of 4'-aryl-2,2':6',2"-terpyridine. 174

Scheme 7.1 Target ligand, 4'-(oligo-2,5-pyrimidine)-tpy ligand with unsuccessful attempts to synthesize oligo-2,5-pyrimidine. 196

List of Charts

Chart 3.1 Numbering scheme for complex [(an-tpy)Ru(tpy-pm-R)]$(PF_6)_2$ **3a-d**..... 66

Chart 5.1 Tridentate ligands: 2,2':6':2"-terpyridine (tpy) and tpy analogues **A-F**. 131

Chart 7.1 Proposed target ligands for ligand approach in coordination chemistry. 194

Abbreviations

2-D	two-dimensional
abs	absolute
Ac	acetyl
An	9-anthryl
Ar	aryl
bppy	2,6-*bis*(pyrimid-2'-yl)pyridine
bpy	2,2'-bipyridine
Calcd	calculated
COSY	correlated spectroscopy
CV	cyclic voltammetry
d	doublet (NMR)
dba	dibenzylideneacetone
dd	doublet of doublets (NMR)
ddd	doublet of doublet of doublet
DMA	*N,N*-dimethylacetamide
DMF	*N,N*-dimethylformamide
DMSO	dimethyl sulfoxide
dppf	1,1'-*bis*(diphenylphosphino)ferocence
e	electron
equiv.	equivalent
ESI-MS	electro-spray ionization mass spectrometry

Et	ethyl
FAB-MS	fast atom bombardment mass spectrometry
GS	ground state
h	hour
HOMO	highest occupied molecular orbital
Hz	hertz
J	spin coupling constant
L	ligand
LC	ligand centered
LC-MS	liquid chromatography mass spectrometry
LUMO	lowest unoccupied molecular orbital
m	multiplet (NMR)
M	metal
MC	metal-centered (transition)
Me	methyl
mL	milliliter
MLCT	metal-to-ligand charge transfer (transition)
mmol	millimole
mol	mole
mp	melting point
MS	mass spectrometry
m/z	mass to charge
^{n}Bu	*n*-butyl

NMR	nuclear magnetic resonance
nm	nanometer
ns	nanosecond
$Pd_2(dba)_3$	*tris*(dibenzylideneacetone)dipalladium chloroform complex
$Pd(PPh_3)_4$	*tetrakis*(triphenylphosphine)palladium
Ph	phenyl
pm	pyrimidine
ppm	parts per million
Py	pyridine
RC	reaction center
Rf	retention factor
rt	room temperature
s	singlet (NMR)
SCE	siliver chloride electrode
SHE	standard hydrogen electrode
t	triplet (NMR)
^{t}Bu	*tert*-butyl
td	triplet of doublets (NMR)
Tf	triflate
THF	tetrahydrofuran
TLC	thin-layer chromatography
tpy	2,2':6',2''-terpyridine
UV-vis	ultraviolet and visage spectrascopy

To my mother, Suzhen Li

To my wife, Yuan Zhang

Acknowledgements

First of all, I'd like to thank my supervisor, Prof. Dr. Garry S. Hanan, for his endless support on my research projects. It's he who helped me to restore the interests on the chemistry when I felt depressed on the scientific research. His enthusiasm, encouragement, diligence and guidance have taught me a lot and made my research have more pleasure as it should have. I should also thank Garry for the generous financial aid as well as his help on the application for the waiver of international student fees.

I would like to thank the Hanan team: Michael W. Cooke, Elaine A. Medlycott, Elena Ioachim and all the undergraduates. All of them made my life wonderful in Canada. And also I thank the former Hanan team members, especially Yuan-Qing Fang for his research advices. Helps and joys from other groups such as André Beauchamp's, Christian Reber's, Davit Zargarian's, André Charette's and Hélène Lebel's are also highly appreciated. The combined helps from these groups gave me a lot of convenience in my research. The financial aid of a TA scholarship from Département de chimie, Université de Montréal is also greatly acknowledged.

Prof. Dr. S. Campagna's group at Università di Messina is also acknowledged for the photophysical measurements. I would also like to thank Elaine and Francine Bélanger-Gariépy in Université de Montréal, Dr. Constandin A. Udachin in NRC (Ottawa, Canada) for their great work on the crystal structures. Dr. Alexandre Furtos and Dr.

Dalbir Singh Sekhon are thanked for their excellent work on the high resolution mass spectra and ESI-MS, respectively.

I'd like to send my acknowledgements to Dr. Claudio F. Sturino and Dr. Zhaoyin Wang in Merck Frosst, Canada for their constant helps on my road to be a synthetic chemist.

I would like to express my gratefulness to my wife, Yuan Sabrina Zhang, who has shared all the happiness and depression with me. I am indebted to my families (my sister, my father and my family-in-law) for their constant support.

Finally I want to dedicate this thesis to my mother, Suzhen Li, who passed away during my master's studies. It is my mother who made me fearless on the future.

Chapter 1

Introduction

1.1 Ruthenium polypyridyl complexes

One of the main topics in coordination chemistry is the study of luminescence and redox properties of ruthenium(II) complexes due to their rich photophysical properties, which can be used as potential photosensitisers in artificial light-harvesting devices.[1]

Among these complexes, the prototype, $Ru(bpy)_3^{2+}$ (bpy = 2,2'-bipyridine), is one of the most simple, yet interesting, systems due to its potential application in light-harvesting devices (**Figure 1.1**).[2] Due to the strong ligand field strength of bpy (activation energy, $\Delta E = 4000\ cm^{-1}$), the metal-centered triplet state of the $Ru(bpy)_3^{2+}$ is not easily accessible from the ^{3}MLCT emitting state[2] and complexes based on $Ru(bpy)_3^{2+}$ have relatively longer lifetimes than their $Ru(tpy)_2^{2+}$ analogues, which give rise to their wide applications.

However, $[Ru(bpy)_3]^{2+}$ complexes suffer from a stereochemical disadvantage when used to build up multimetallic supramolecular arrays due to the presence of Δ and Λ enantiomers that exist in D_3-symmetrical $Ru(L_2)_3$ complexes (L_2: bpy-type bidentate ligand) (**Figure 1.2**).[1a] Moreover, asymmetric substituents on the bpy ligands can give rise to *fac*- and *mer*- geometrical isomers for $Ru(LL')_3$ complexes (LL' = unsymmetrical bidentate ligand, **Figure 1.2**).

In recent years, research work concerning Ru(II) polypyridyl complexes has focused on $Ru(tpy)_2^{2+}$-type complexes (tpy = 2,2':6',2"-terpyridine) since complexes based on the tridentate tpy ligand offered several structural and synthetic advantages as compared to those based on the bidentate bpy ligand.[1a,1f] The substituents on the 4'-position of the $Ru(tpy)_2^{2+}$ complexes maintain a *C2*-axial symmetry and, thus, make the purification and characterization of these *C2*-symmetric molecules easier than those of $Ru(bpy)_3^{2+}$ complexes. Subsequently, it's much easier to use the functionalities on the 4'-position of tpy ligands to build up linear polymetallic arrays or dendrimers for their application in artificial light-harvesting devices.

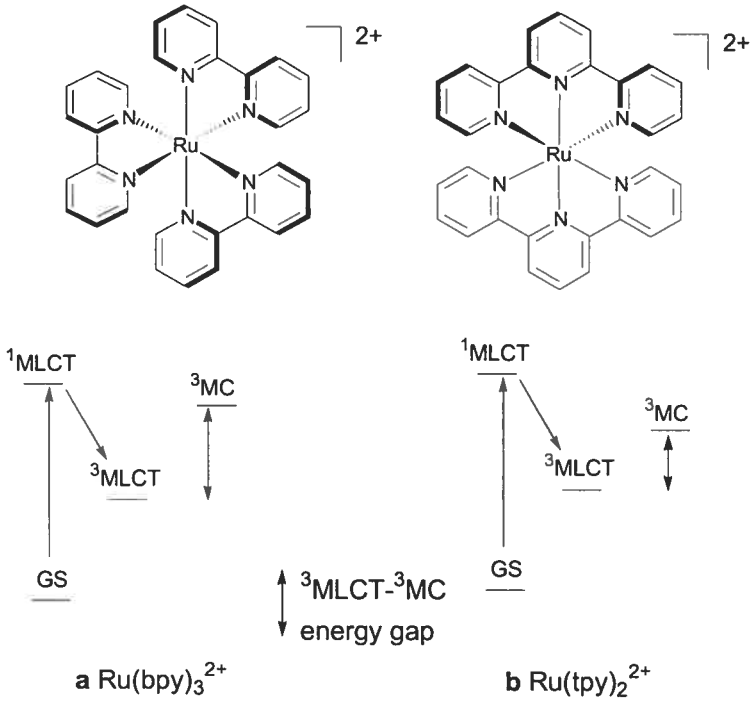

Figure 1.1 Octahedral structures of $Ru(bpy)_3^{2+}$ and $Ru(tpy)_2^{2+}$ complexes with their energy diagrams of photo-excited states.[1a,1f]

In rigid matrix at 77 K $Ru(tpy)_2^{2+}$ has a strong, long-lived luminescence characteristic of a ^{3}MLCT emitter. However, on increased temperature, the $Ru(tpy)_2^{2+}$ luminescence intensity and lifetime decreased, attributed to the equilibration of ^{3}MLCT state with high-spin metal-based dd state.[3] $Ru(tpy)_2^{2+}$-type complexes (**Figure 1.1**) exhibit *pseudo*-octahedral coordination, which is extremely distorted from idealized octahedral configuration.[4] The ligand field strength of tpy with this geometry is much smaller than that of bpy and subsequently has a lower ^{3}MC excited state energy and a smaller separation between the ^{3}MLCT and ^{3}MC states, as estimated from the smaller activation energy (ΔE = 1500 cm^{-1}) for crossing between the two states in $Ru(tpy)_2^{2+}$.[5] Therefore, the ^{3}MLCT state of $Ru(tpy)_2^{2+}$ can access the ^{3}MC state at rt through a Boltzmann distribution. Subsequently, $Ru(tpy)_2^{2+}$ complexes have an extremely short excited state lifetime (< 0.25 ns), which is far from useful for practical applications at rt.[6]

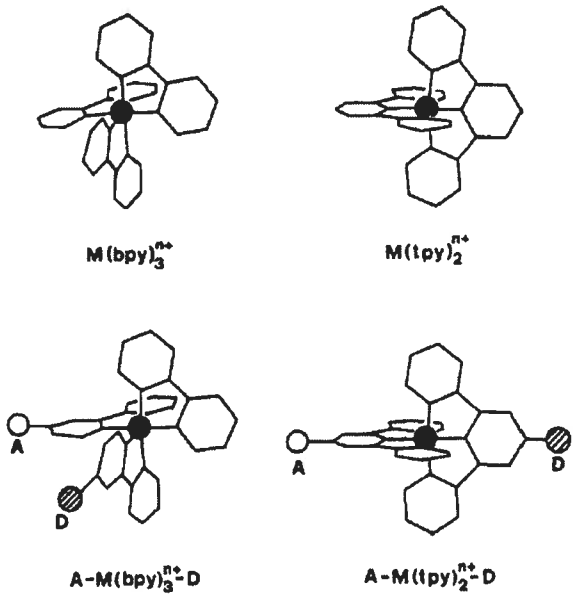

Figure 1.2 Schematic representations of $M(bpy)_3^{n+}$ and $M(tpy)_2^{n+}$ complexes and of their disubstituted derivatives.[1a]

To be applied in a practical device, it would be convenient if Ru(II) tpy complexes had relatively long-lived excited states at rt. A variety of strategies have been employed to prolong the rt excited state lifetimes of Ru(II) complexes based on tridentate ligands.[1f] Several major approaches to improve the luminescence lifetime of ruthenium *bis*-tridentate complexes have been summarized in **Table 1.1**. The first two approaches are based on fine-tuning the separation in the excited energy levels of the complexes in order to minimize the population of the ^{3}MC state from the ^{3}MLCT state, which is the main deactivation process in $Ru(tpy)_2^{2+}$ complexes.[7] A great number of tpy derivatives have been incorporated into the Ru(II) coordination sphere in order to tune the relative energy of the excited states in an aim to prolong the rt lifetimes of their complexes. Through the introduction of electron-rich tridentate ligands, the longest lifetime, 3100 ns, was acquired in the Ru(II) *bis*-carbene complex in water with bromides as counteranions.[8]

Recently, a third approach, namely a multi-chromophoric approach, has appeared as a successful strategy to prolong the rt excited state lifetime of Ru(II) polypyridine chromophores through the introduction of an energy storage element into the system to delay the non-radiative decay by excited state energy equilibration.[10] The efficient energy equilibration between the ^{3}MLCT of Ru(II) polypyridyl chromophore and an isoenergetic triplet state of the organic chromophore (^{3}OC) delayed the luminescent ^{3}MLCT radiative decay to the GS and resulted in biexponential decay in bichromophoric species, which have two lifetimes attributed to ^{3}MLCT radiative decay and the ^{3}MLCT equilibrated with ^{3}OC state, respectively.[10f] Previous research in our lab has showed that the homoleptic $[Ru(tpy\text{-}pm\text{-}an)_2](PF_6)_2$ complex has a rt excited state lifetime as long as 1.8 μs.[10f]

Table 1.1 Major approaches to prolong the room temperature excited state lifetimes of ruthenium(II) polypyridyl complexes based on tridentate ligands.

mechanisms	approaches	representative complex, λ_{max}, r.t. lifetime[a][b]
lowering the energy of the ^{3}MLCT state	electron withdrawing group approach	$[(4'\text{-}MeSO_2\text{-}tpy)Ru(tpy)]^{2+}$,679 nm, 75 ns[1b]
	π-accepting group approach	$[(R\text{-}pm\text{-}tpy)Ru(tpy)]^{2+}$, 669-713 nm, 8-200 ns[9a]; $[(6'\text{-}ph\text{-}trz)Ru(tpy)]^{2+}$, 740 nm, 9 ns[9b];
increasing the energy of the ^{3}MC state	cyclometallation approach	$[(bpb)Ru(tpy)]^{+}$, 784 nm, 4.5 ns[9c];
	σ-donor heterocycles	$[(ttz)Ru(tpy)]^{2+}$, 680-702 nm, 24-77 ns[9d]
	carbene approach	$[(NHC)_2Ru]Br_2$, 532 nm, 3100 ns[8[c]]
energy equilibration	bichromophoric approach	$[(pyrene\text{-}CH{\equiv}CH\text{-}tpy)Ru(tpy)]^{2+}$, 698 nm, 580 ns[9e]; $[(an\text{-}pm\text{-}tpy)_2Ru]^{2+}$, 675 nm, 1806 ns[10f].

[a] Unless stated otherwise, λ_{max} and lifetime were measured at rt in acetonitrile. [b] trz = 2,4-bis(pyrid-2-yl)-1,3,5-triazine, bpb = 1,3-bi(pyrid-4-yl)benzene, ttz = 2,6-bis(1,2,3,4-tetrazol-5-yl)pyridine, NHC = 2,6-bis(1-methylimidazolium-3-yl)pyridine. [c] Measured at rt in H_2O as bromide salt.

However, the chemistry of Ru(II) tridentate complexes is a developing area, in which some of the main challenges still remain. The optimization of the photophysical properties of Ru(II) complexes based on tridentate ligands is still a promising research area. The possible improvements are: (1) to simplify the syntheses of the tridentate

ligands as well as the complexes; (2) to increase the quantum yields of the luminescent Ru(II) species; (3) to prolong the rt excited state lifetimes to an extent at which practical applications become feasible. The synthetic approach to optimize the photophysical properties of Ru(II) species with tridentate ligands is the main aim of this research thesis.

1.2 Ligand design in coordination chemistry

The nature of coordination chemistry is to explore the interactions between metals and ligands, as well as the aftermaths from the interactions. Two distinctive approaches to novel complexes prevail in the literature. The first approach, namely a ligand approach, is the application of a variety of ligands to a specific metal cation, whose complexes have the novel properties derived from the interaction with the ligands. Application of a specific family of ligands to a variety of metals can be named as a metal approach, which focuses on the deliberate selection of metal cations.[11] Nonetheless, in the two different approaches, ligands play crucial roles. The elegant design of ligands is one of the main topics in coordination chemistry nowadays.[12] Ligand design has been widely used: in bioinorganic chemistry to mimic the enzymes, such as zinc based *carbonic anhydrase* and *liver dehydrogenase*;[13] in material science for the invention of new materials and devices;[11] in environmental chemistry for the recovery of heavy metals;[14] as well as in organic chemistry in the pursuit of novel catalysts.[15]

In the sub-area of ruthenium chemistry, the ligand can still contribute significantly to the pursuit of novel complexes with novel properties.[1] The desired optical properties of Ru(II) complexes can be afforded through the fine-tuning of the energy of the ^{3}MLCT state. One successful ligand design in Ru(II) polypyridyl chemistry is the synthetic

approach to black MLCT chromophores which exhibit significant absorption throughout the visible region.[16] The systematic application of the rigidity and delocalization was deliberately directed by theoretical calculation of the acceptor ligand on MLCT excited state decay.[17]

Considering the importance of ligand design in coordination chemistry, the exploration of new family of ligands for Ru(II) coordination chemistry is one of the concerns in this thesis. The approaches to deliberately designed tridentate ligands were mainly accomplished either through the syntheses of new families of ligands (**A** in **Figure 1.3**) or through the "chemistry-on-the-complex" approach (**B** in **Figure 1.3**).[18] The "chemistry-on-the-complex" approach has been used to: (1) activate function group for chemical modification;[4a] (2) selectively create new binding site for the syntheses of mixed-polymetallic complexes[19] and (3) introduce sensitive functionalities onto metal complexes.[20] In some case, the functionality introduced "on-the-complex" may only be possible through a "chemistry-on-the-complex" approach.

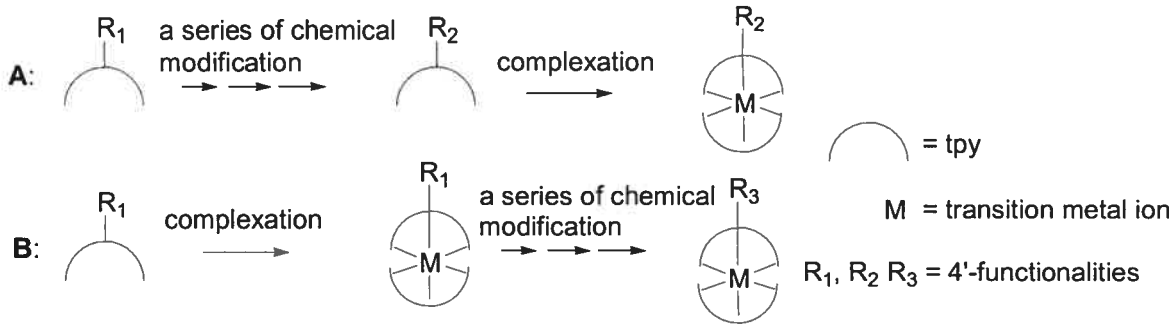

Figure 1.3 Schematic representations of two approaches to synthesize metal complexes with newly designed ligands: (A) ligand approach; (B) "chemistry-on-the-complex" approach.

1.3 General experimental

All the synthetic procedures were carried out at Département de chimie, Université de Montréal.

All the dry solvents for the reactions were pre-purified and dried by the Pure-Solv Solvents Purification System (Innovative Technology Inc.) in Organic Lab, Université de Montréal.

Nuclear magnetic resonance (NMR) spectra were recorded at room temperature on a Bruker AV 400 spectrometer at 400 MHz or AV 300 spectrometer at 300 MHz for ^{1}H NMR and at 100 MHz or 75 MHz for ^{13}C NMR, respectively. Chemical shifts are reported in part per million (ppm) relative to residual protonated solvents () and the carbon resonance of the solvents (40.3 ppm for DMSO-d_6, 77.5 ppm for chloroform-d and 118.3 ppm for acetonitrile-d_3).

Analytical thin layer chromatography (TLC) was performed on Kieselgel 60 F_{254} plastic plate precoated with a 0.20 mm thickness of silica gel and aluminium oxide 60 F_{254} plastic plate precoated with a 0.25 mm thickness of neutral aluninium oxide gel. The TLC plates were visualized with UV light and/or by staining with ferrous ammonium sulfate in MeOH/H_2O (1:1) (for tpy ligands). Column chromatography was performed using Kieselgel 60 (230-400 mesh) silica gel or neutral aluninium oxide gel (5-8% H_2O deactivated) with the eluents indicated.

Counteranion exchanges for Ru(II) complexes from their chloride salts or nitrate salts to the corresponding hexafluorophosphate salts were achieved through the general procedure: Aqueous NH_4PF_6 solution (~0.01g/mL, 30 mL) was added to metal complex chloride salt or nitrate salt in acetonitrile (~50 mL) and the resultant solution was

equilibrated for 5 min followed by the addition of CH_2Cl_2 (~5 mL). The acetonitrile phase was separated and washed two times with aqueous NH_4PF_6 solution (~0.01g/mL, 30 mL), followed by washing with H_2O (~50 mL). Removal of the solvent, acetonitrile, yielded metal complex hexafluorophosphate salt.

Melting points were measured on an Electrothermal Mel-Temp 1101D without correction.

Fast-atom bombardment (FAB, positive mode) spectra were recorded on a ZAB-HF-VB-analytical apparatus in an *m*-nitrobenzylalcohol (*m*-NBA) matrix and Ar atoms were used for the bombardment (8 KeV). ESI-MS were measured in the Quebec Combinatorial Chemistry Consortium in Chemistry Department, Université de Montréal. ESI-MS samples of ligands and complexes were prepared as ~1 mg/mL solution in $CHCl_3$ and CH_3CN, respectively. MALDI-TOF spectra were measured in the Mass Spectroscopy Facilities in Département de chimie, Université de Montréal. All the observed isotope patterns of the reported MALDI-TOF results in this thesis agreed the calculated isotope patterns.

Electrochemistry data was collected in Ar-purged acetonitrile with 1.0 M $^nBu_4NPF_6$ on a BAS CV-50W Voltammetric Analyzer. Redox potentials were corrected by the internal reference to ferrocence (395 mV).

Single crystal X-ray diffraction structure determination was carried out by Francine Bélanger-Gariépy and Elaine A. Medlycott in Université de Montréal or by Dr. Constandin A. Udachin in NRC, Ottawa. Unless stated otherwise, the radiation sources for the single crystal structure determination were Cu $K\alpha$ radiation.

Elemental analyses were done in the Elemental Analyses Lab in Département de chimie, Université de Montréal.

Routine absorption spectra and emission spectra were measured in spectroscopic quality acetonitrile at rt on a Cary 500i UV-vis-NIR Spectrophotometer and a Cary Eclipse Fluorescence Spectrophotometer, respectively.

Lifetime measurements were accomplished by the collaborators in Prof. Dr. Sebastiano Campagna's group in Dipartimento di Chimica Inorganica, Chimica Analitica e Chimica Fisica, Università di Messina, Italy.

1.4 References

1 (a) Sauvage, J. P.; Collin, J. P.; Chambron, J. C.; Guillerez, S.; Coudret, C.; Balzani, V.; Barigelletti, F.; De Cola, L.; Flamigni, L. *Chem. Rev.* **1994**, *94*, 993. (b) Maestri, M.; Armaroli, N.; Balzani, V.; Constable, E. C.; Thompson, A. M. W. C. *Inorg. Chem.* **1995**, *34*, 2759. (c) El-Ghayoury, A.; Harriman, A.; Khatyr, A.; Ziessel, R. *Angew. Chem. Int. Ed.* **2000**, *39*, 185. (d) Barigelletti, F.; Flamigni, L. *Chem. Soc. Rev.* **2000**, *29*, 1. (e) Encinas, S.; Flamigni, L.; Barigelletti, F.; Constable, E. C.; Housecroft, C. E.; Schofield, E. R.; Figgemeier, E.; Fenske, D.; Neuburger, M.; Vos, J. G.; Zehnder, M. *Chem. Eur. J.* **2002**, *8*, 137. (f) Medlycott, E. A.; Hanan, G. S. *Chem. Soc. Rev.* **2005**, *34*, 133.

2 Juris A.; Balzani, V.; Barigelletti, F.; Campagna, S.; Besler, P.; Von Zelewsky, A. *Coord. Chem. Rev.* **1988**, *84*, 85.

3 Fink, D. W.; Ohnesorge, W. E. *J. Am. Chem. Soc.* **1969**, *91*, 4995.

4 (a) Constable, E. C.; Cargill Thompson, A. M. W.; Tocher, D. A.; Daniels, M. A. M. *New J. Chem.* **1992**, *16*, 855. (b) Pyo, S.; Perez-Cordero, E.; Bott, S. G.; Echegoyen, L. *Inorg. Chem.* **1999**, *38*, 3337.

5 Hacker, C. R.; Gushurst, A. K. I.; McMillin, D. R. *Inorg. Chem.* **1991**, *30*, 538.

6 Winkler, J. R.; Netzel, T. L.; Creutz, C.; Sutin, N. *J. Am. Chem. Soc.* **1987**, *109*, 2381.

7 Calvert, J. M.; Caspar, J. V.; Binstead, R. A.; Westmoreland, T. D.; Meyer, T. J. *J. Am. Chem. Soc.* **1982**, *104*, 6620.

8 Son, S. U.; Park, K. H.; Lee, Y.-S.; Kim, B. Y.; Choi, C. H.; Lah, M. S.; Jang, Y. H.; Jang, D.-J.; Chung, Y. K. *Inorg. Chem.* **2004**, *43*, 6896.

9 (a) Fang Y.-Q.; Taylor, A. J.; Hanan, G. S.; Loiseau, F.; Passalacqua, R.; Campagna, S.; Nierengarten, H.; Van Dorsselaer, A. *J. Am. Chem. Soc.* **2002**, *124*, 7912. (b) Polson, M. I. J.; Medlycott, E. A.; Hanan, G. S.; Mikelsons, L.; Taylor, N. J., Watanabe, M.; Tanaka, Y.; Loiseau, F.; Passalacqua, R.; Campagna, S. *Chem. Eur. J.* **2004**, *10*, 3640. (c) Beley, M.; Chodorowski, S.; Collin, J.-P.; Sauvage, J.-P.; Flammigni, L.; Barigelletti, F. *Inorg. Chem.* **1994**, *33*, 2543. (d) Duati, M.; Tasca, S.; Lynch, F. C.; Bohlen, H.; Vos, J. G.; Stagni, S.; Ward, M. D. *Inorg. Chem.* **2003**, *42*, 8377. (e) Harriman, A.; Mayeux, A.; De Nicola, A.; Ziessel, R. *Phys. Chem. Chem. Phys.* **2002**, *4*, 2229.

10 (a) Ford, W. E.; Rodgers, M. A. J. *J. Phys. Chem.* **1992**, *96*, 2917. (b) Wilson, G. J.; Launikonis, A.; Sasse, W. H. F.; Mau, A. W.-H. *J. Phys. Chem. A* **1997**, *101*, 4860. (c) Simon, J. A.; Curry, S. L.; Shemehl, R. H.; Schatz, T. R.; Piotrowiak, P.; Jin, X.; Thummel, R. P. *J. Am. Chem. Soc.* **1997**, *119*, 11012. (d) Tyson, D. S.; Luman, C. R.; Zhou, X.; Castellano, F. N. *Inorg. Chem.* **2001**, *40*, 4063. (e) Maubert, B.; McClenaghan, N. D.; Indelli, M. T.; Campagna, S. *J. Phys. Chem. A* **2003**, *107*, 447. (f) Passalacqua, R.; Loiseau, F.; Campagna, S.; Fang, Y.-Q.; Hanan, G. S. *Angew. Chem. Int. Ed.* **2003**, *42*, 1608. (g) McClenaghan, N. D.; Leydet, Y.; Maubert, B.; Indelli, M. T.; Campagna, S. *Coord. Chem. Rev.* **2005**, in press.

11 Ioachim, E. *Master's Thesis* **2005**, Département de Chimie, Université de Montréal, Montréal, Canada.

12 Elsevier, C. J.; Reedijk, J.; Walton, P. H.; Ward, M. D. *J. Chem. Soc., Dalton Trans.* **2003**, 1869. and reference therein.

13 (a) Trosch, A.; Vahrenkamp, H. *Inorg. Chem.* **2001**, *40*, 2305. (b) Seebacher, J.; Shu, M. H.; Vahrenkamp, H. *Chem. Commun.* **2001**, 1026. (c) Walz, R.; Vahrenkamp, H. *Inorg. Chim. Acta* **2001**, *314*, 58. (d) Kimblin, C.; Bridgewater, B. M.; Churchill, D. G.; Parkin, G. *Chem. Commun.* **1999**, 2301.

14 Smith, A. G.; Tasker, P. A.; White, P. J. *Coord. Chem. Rev.* **2003**, *241*, 61.

15 See examples of ligand design in organic synthesis: (a) Dai, L.-X.; Tu, T.; You, S.-L.; Deng, W.-P.; Hou, X.-L. *Acc. Chem. Res.* **2003**, *36*, 659. (b) Desimoni, G.; Faita, G.; Quadrelli, P. *Chem. Rev.* **2003**, *103*, 3119. (c) McManus, H. A.; Guiry, P. J. *Chem. Rev.* **2004**, *104*, 4151.

16 Anderson, P. A.; Strouse, G. F.; Treadway, J. A.; Keene, F. R.; Meyer, T. J. *Inorg. Chem.* **1994**, *33*, 3863.

17 Treadway, J. A.; Loeb, B.; Lopez, R.; Anderson, P. A.; Keene, F. R.; Meyer, T. J. *Inorg. Chem.* **1996**, *35*, 2242.

18 (a) Chodorowski, S.; Beley, M.; Collin, J.-P.; Sauvage, J.-P. *Tetrahedron Lett.* **1996**, *37*, 2963. (b) Tzalis, D.; Tor, Y. *Chem. Commun.* **1996**, 1043. (c) Hissler, M.; Ziessel, R. *New J. Chem.* **1997**, *21*, 843. (d) Coudret, C.; Fraysse, S.; Launay, J.-P. *Chem. Commun.* **1998**, 663. (e) Osawa, M.; Hoshino, M.; Horiuchi, S.; Wakatsuki, Y. *Organometallics* **1999**, *18*, 112. (f) Kelch, S.; Rehahn, M. *Macromolecules* **1999**, *32*, 5818. (g) Storrier, G. D.; Colbran, S. B. *Inorg. Chim. Acta* **1999**, *284*, 76. (h) Aspley, C. J.; Gareth Williams, J. A. *New J. Chem.* **2001**, *25*, 1136. (i) Harriman, A.; Hissler, M.; Khatyr, A.; Ziessel, R. *Eur. J. Inorg. Chem.* **2003**, 955.

19 (a) Johansson, K. O.; Lotoski, J. A.; Tong, C. C.; Hanan, G. S. *Chem. Commun.* **2000**, 819. (b) Fang, Y.-Q.; Polson, M. I. J.; Hanan, G. S. *Inorg. Chem.* **2003**, *42*, 5.

20 For example as the introduction of the cyano group into $Ru(tpy)_2^{2+}$ complexes: Wang, J.; Fang, Y.-Q.; Hanan, G. S.; Loiseau, F.; Campagna, S. *Inorg. Chem.* **2005**, *44*, 5.

Chapter 2

The Multi-chromophoric Approach to Prolonged Room Temperature Luminescence Lifetimes in Ru(II) Complexes Based on Tridentate Polypyridine Ligands

---

Abstract

Synthetic approaches to a new series of ruthenium(II) complexes with multi-chromophoric behaviours are presented based on a "chemistry-on-the-complex" approach. Complexes **3a** and **3b** were synthesized through the Pd-catalyzed Suzuki coupling reaction between 9-anthrylboronic acid and the chloro-ligands on **2a** and **2b**, respectively. The mono-coupling product **3c** was also synthesized as the starting complex for a dimetallic complex under optimized Suzuki coupling conditions. The palladium(0)-catalyzed homocoupling reaction on complexes **2a** and **3c** led to dimetallic Ru(II) species **4b** and **4a**, respectively. The newly synthesized complexes were extensively studied with a variety of physical measurements. The solid structures of complexes **3a-b** were characterized by single crystal X-ray diffraction. The lifetime measurements of complexes **3a-c** and **4b** showed that multi-chromophoric behaviours exist in these species, which have 9-anthryl groups as energy storage elements for the repopulation of the ^{3}MLCT state. The rt lifetimes of the monometallic complexes **3a-b** have been significantly prolonged to 402 ns and 1806 ns, respectively, with the introduction of the secondary chromophore(s), anthracene, as an energy storage element.

2.1 Introduction

Luminescent multicomponent systems (LMS) are important targets in supramolecular chemistry as they play important roles in fields connected to solar energy conversion and storage of light and/or electronic information at the molecular level.[1] Although their synthesis normally requires elaborate procedures, recent advances in the 'chemistry-on-the-complex' methodology has facilitated the development of an important class of LMS based on ruthenium(II) polypyridine complexes.[1i] For example, multinuclear complexes with up to 22 Ru(II) centres were prepared by a series of protection/deprotection sequences.[2] These light-harvesting complexes were shown to channel excited energy based on the substitution pattern of the dendrimers.[3] More recently, new binding sites were created in metal complexes by organometallic coupling reactions catalyzed by nickel (0)[4] and palladium(0).[5] These new building blocks could be exploited for further metal ion coordination or as ion sensors.[6]

$Ru(bpy)_3^{2+}$ (bpy = 2,2'-bipyridine) complexes have been widely used for building up polymetallic complexes because they show a much sought after combination of chemical stability, and suitable redox and photophysical properties.[7] However, $[Ru(tpy)_2]^{2+}$ (tpy = 2,2':6',2"-terpyridine) complexes have stereochemical advantages when incorporated in multinuclear supramolecular arrays due to the absence of Δ and Λ enantiomers that exist in D_3-symmetrical $Ru(bpy)_3^{2+}$ complexes.[8] Unfortunately, $Ru(tpy)_2^{2+}$ complexes are practically non-luminescent at room temperature (rt) and have a short rt excited state lifetime (< 0.25 ns).[8o] With such a short excited-state lifetime, energy transfer from the triplet metal-to-ligand charge transfer (^{3}MLCT) state of the

ruthenium complexes to other suitable acceptor molecules is difficult to study and to apply.

Prolonging the rt excited state lifetimes of $Ru(tpy)_2^{2+}$ complexes is still a major challenge, and as a result the chemistry of $Ru(tpy)_2^{2+}$ complexes is far less developed than that of $Ru(bpy)_3^{2+}$. Several strategies have recently been employed to prolong the room temperature excited-state lifetime of ruthenium complexes with tridentate polypyridyl ligands,[6q] including the use of (i) electron deficient ligands,[9] (ii) strongly electron-donating ligands,[8m-n] (iii) electron withdrawing and/or donor substituents on terpyridine,[8o-p] and (iv) ligands with extended acceptor orbitals.[10] The first three strategies increase the energy gap between the ^{3}MLCT and ^{3}MC excited states, thereby minimizing the thermally-activated surface crossing which in turn lowers the extent of MLCT deactivation processes. The last strategy is based on modification of the Frank-Condon factors for non-radiative decay. Quite recently, an approach to increase the luminescence lifetime of metal polypyridine complexes has emerged: the combination of metal complexes and organic chromophores which have triplet excited states at similar energies.[11] The prolonged excited state lifetimes were attributed to the energy equilibrium between ^{3}MLCT and triplet states of the secondary chromophores, which served as energy storage elements in the LMS.

An alternative approach to prolonged rt excited state lifetime of $Ru(tpy)_2^{2+}$ was based on complexes by introducing a coplanar pyrimidyl (pm) substituent on the tpy ligands to increase electron delocalization and enlarge the ^{3}MLCT-^{3}MC energy gap.[10e] Through this approach the rt excited state lifetime of $Ru(tpy\text{-}pm\text{-}R)_2^{2+}$ (tpy-pm-R = 4'-(5-substituted-2-pyrimidyl)-2,2':6',2"-terpyridine) complexes can be prolonged up to 200 ns.

Following these encouraging results, $Ru(tpy\text{-}pm\text{-}R)_2^{2+}$ complexes based on the fusion of two approaches were prepared, that is, the coupling of ligands with extended π^* orbitals and an organic chromophore with a triplet state energy level similar to the ^{3}MLCT state of the metal complex. The energy level of the ^{3}MLCT emitting state of $Ru(tpy\text{-}pm\text{-}R)_2^{2+}$ complexes (between 1.83 eV and 1.87 eV with various 5-substituents on pm) can be tuned to the energy level of the non-emissive triplet state of an anthracene subunit (^{3}An, E^{00} = 1.85 eV),[12] which acts as the storage element in the bichromophoric approach.

Herein we present our synthetic approach to incorporate anthracene subunits into $Ru(tpy\text{-}pm\text{-}R)_2^{2+}$-based complexes and the extraordinary results of these newly synthesized Ru(II) multichromophoric species.

2.2 Results and Discussion

2.2.1 Synthesis

Complexes **3a** and **3b** were synthesized using the "chemistry-on-the-complex" methodology, in which the 4'-(5-(9-anthryl)pyrimid-2-yl))-2,2':6',2"-terpyridine (an-pm-tpy) ligands were synthesized while directly attached to the metal ion. This approach is particularly powerful when used in conjugation with organometallic catalysts to form carbon-carbon bonds. Previous work has shown that the chloro substituent in the 5-position of a pyrimidine group is relatively inert to Stille coupling reactions since it is *meta* to both nitrogen atoms.[13] However, the ruthenium cations in **2a** and **2b** effectively activates the 5-chloro group on the conjugated pyrimidine ring by an inductive effect.[14] Thus, ruthenium complexes **2a** and **2b** were allowed to react with 9-anthryl boronic acid[18] under Suzuki coupling conditions at elevated temperatures to afford complexes **3a** and **3b**, respectively (**Scheme 2.1**).[15]

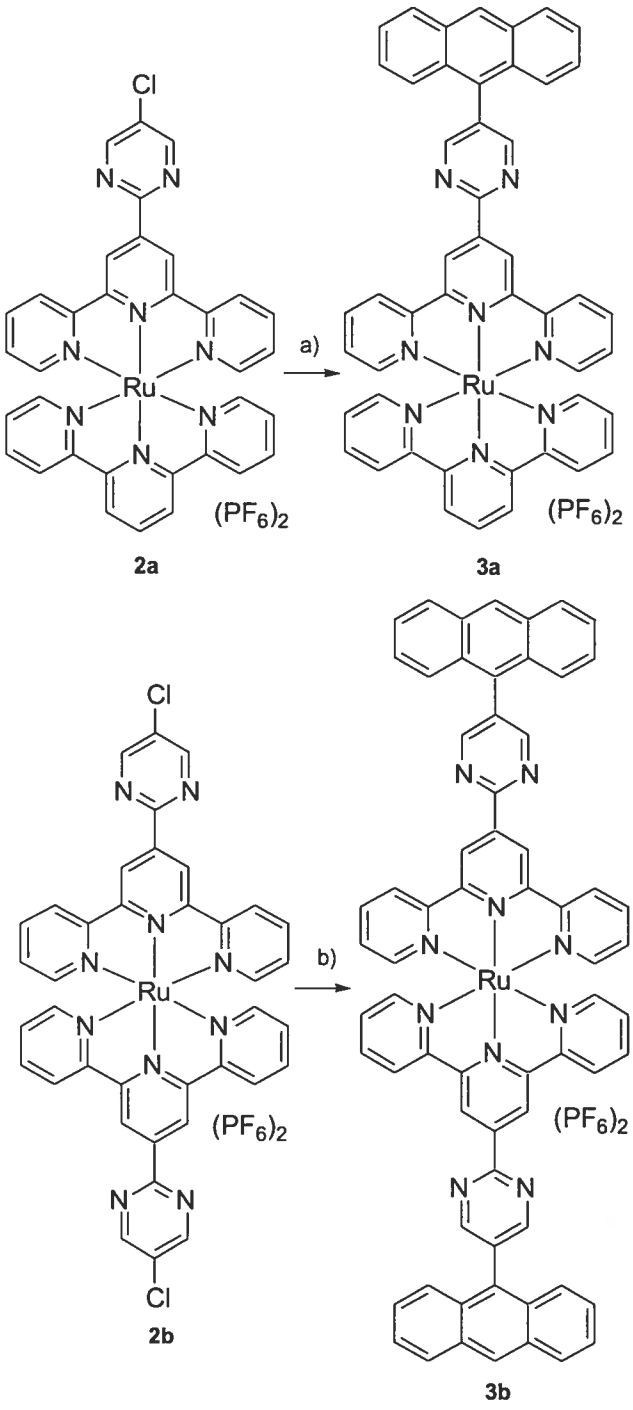

Scheme 2.1 Synthesis of complexes **3a-b** through palladium-catalyzed cross-coupling reaction. Reagents and conditions: a) excess 9-anthryl boronic acid, $(PPh_3)_2PdCl_2$, K_2CO_3, DMF, 110 °C, 12 h. b) excess 9-anthryl boronic acid, $(PPh_3)_2PdCl_2$, K_2CO_3, DMF, 140 °C, 12 h.

The synthesis of the heteroleptic complex, [(Cl-pm-tpy)Ru(tpy-pm-an)]$(PF_6)_2$ (**3c**), was initially attempted using the standard approach used to construct 5-substituted pyrimidyl groups in the R-pm-tpy ligands. We envisioned the formation of the an-pm-tpy ligand through a pyrimidine ring forming condensation reaction between 2-(9-anthryl)-1,3-*bis*(dimethylamino)trimethinium hexaflurophosphate and 2,2':6',2"-terpyrid-4'-ylamidine hydrochloride. However, conversion of 9-anthraceneactic acid[16] to the vinamidine hexaflurophosphate salt under various reaction conditions failed,[17] presumably due to the sterically hindered 9-anthryl group.

Then a "chemistry-on-the-complex" approach, in which a palladium-catalyzed cross-coupling was adopted to incorporate the bulky anthryl group into the $Ru(tpy)^{2+}$ moiety was attempted.[15] Treatment of complex **2b** with 9-anthryl boronic acid[18] under optimized Suzuki coupling reaction (**Table 2.1**) conditions afforded mono-coupling product, complex **3c**, which was purified by silica chromatography (**Scheme 2.2**). In surveying suitable catalysts and reaction conditions, reactions catalyzed by $Pd(PPh_3)_4$ at 90°C were found to show the best activity and selectivity for the mono-coupling reaction with 83% yield after recovering starting complex **2b** (**Table 2.1**, Entry 5). A slightly lower temperature and an optimized reaction time were preferred for control of the mono-coupling reaction. Pre-reduced palladium catalyst, $Pd(PPh_3)_4$, afforded a better yield than $Pd(PPh_3)_2Cl_2$, due to the inefficient transmetallation of the latter with bulky 9-anthrylboronic acid.

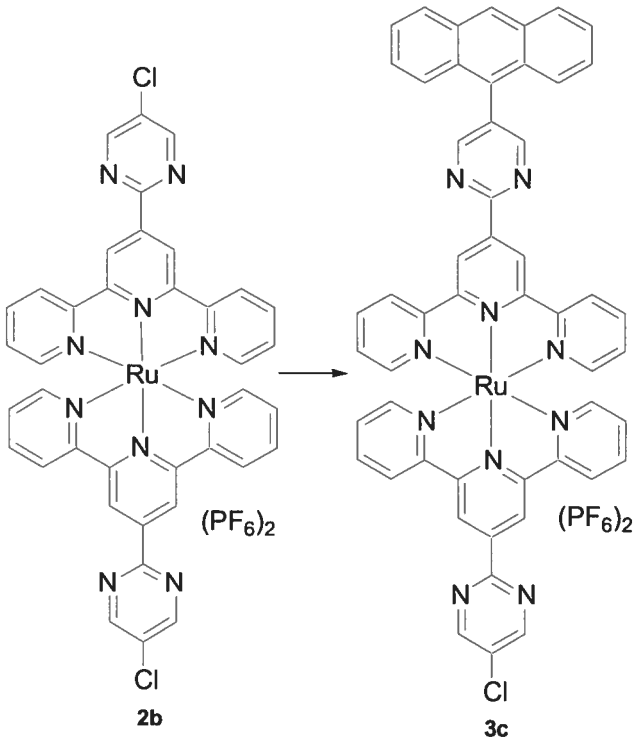

Scheme 2.2 Palladium-catalyzed mono-coupling reaction on the $Ru(tpy\text{-}pm\text{-}Cl)_2^{2+}$ complex **2b**. Reagents and conditions: 9-anthrylboronic acid, $Pd(PPh_3)_4$, K_2CO_3, DMF, 110 °C, 16 h.

The syntheses of bimetallic Ru(II) species were achieved through palladium-catalyzed homocoupling reactions on the appropriate chlorides in the monometallic complexes, **3c** and **2a**, respectively. Treatment of complex **3c** with the Pd(0) catalyst, generated *in situ* by the combination of $Pd(OAc)_2$ with 2-(di-*t*-butylphosphino)biphenyl, led to the homo-coupled bimetallic complex **4b (Scheme 2.3)**. Treatment of complex **2a** under the same homo-coupling conditions yielded bimetallic complex **4a**. It is interesting to note that the standard Ni-catalyzed reaction normally used to homocouple two fragments failed to generate **4a-b** under a variety of conditions.[4]

Table 2.1 Effect of catalysts and temperature variation on the mono-coupling reaction.[a]

Entry	Catalyst (10 mol% Pd)	T [°C]	T [h]	Yield [%][b]
1	$Pd(PPh_3)_2Cl_2$	140	24	12
2	$Pd(PPh_3)_2Cl_2$	110	48	33
3	$Pd(PPh_3)_4$	140	24	16
4	$Pd(PPh_3)_4$	110	4	20[c]
5	$Pd(PPh_3)_4$	110	16	49[d]
6	$Pd(PPh_3)_4$	110	48	36[c]

[a] Reaction with 1.0 equiv. **2b**, 1.2 equiv. 9-anthryl boronic acid, 2.0 equiv. K_2CO_3, DMF. [b] Isolated yield for mono-coupling complex **3c** without recovering starting complex **2b**. [c] HPLC yield for mono-coupling complex **3c** without recovering starting complex **2b**. [d] 83% yield based on recovering starting material **2b**.

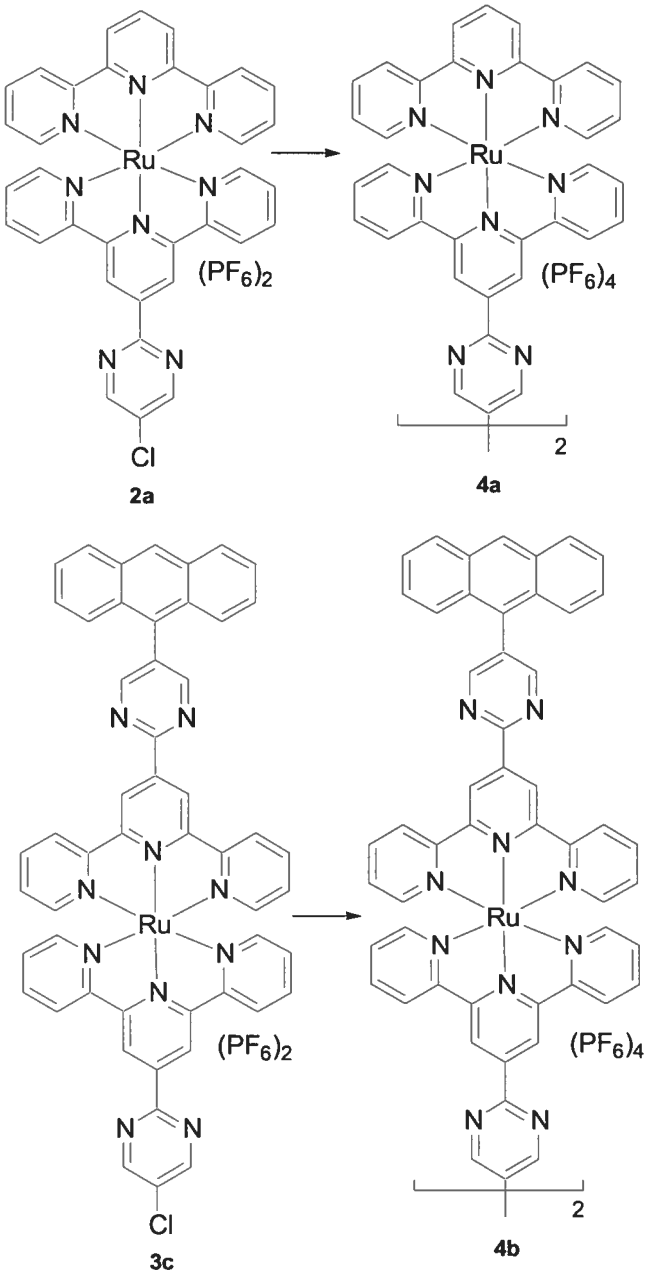

Scheme 2.3 Palladium-catalyzed homo-coupling reaction on the Ru(II) tpy complexes **2a** and **3c**. Reagents and conditions: 1.0 equiv. **2a** or **3c**, 15 mol% $Pd(OAc)_2$, 30 mol% tBu$_2$P(biph), 2.0 equiv. K_2CO_3, DMF, 110°C, 24 h .

2.2.2 ^{1}H NMR spectroscopy

All of the newly synthesized complexes **3a-c** and **4a-b** were characterized by ^{1}H NMR spectroscopy. The ^{1}H NMR chemical shift data for complexes **3a-c** and **4a-b** and reference complexes **2a-b** are compiled in **Table 2.2**. In the ^{1}H NMR spectra of the complexes, although there are more than 20 protons at the chemical shift range of 7-10 ppm, all of the signals are well separated and assignable with the assistance of two-dimensional experiments, such as COSY experiments (for example **Figure 2.1** for complex **4b**)

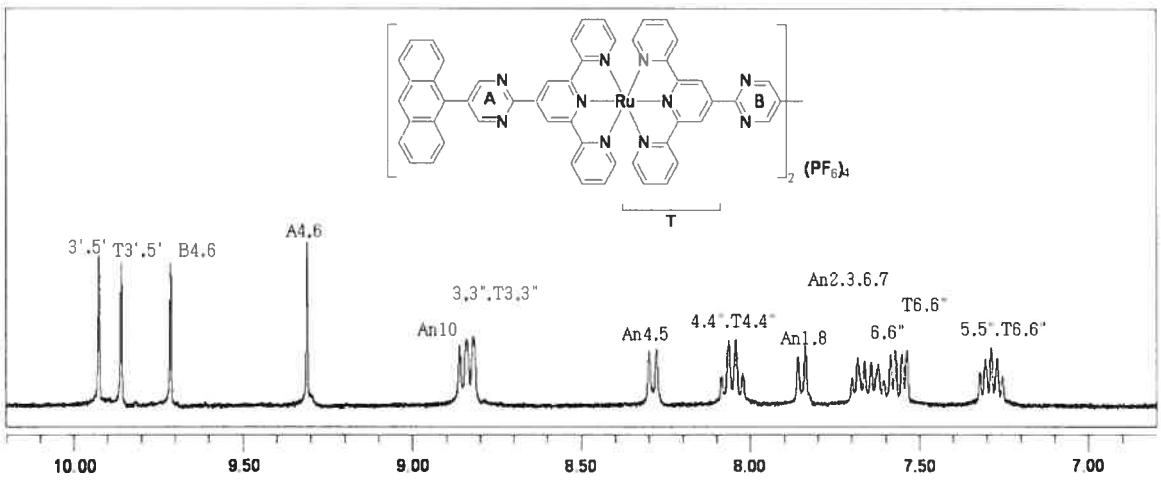

Figure 2.1 ^{1}H NMR spectrum of complex **4b** with proton labelling (See experimental for labelling scheme). Spectrum was recorded at rt in CD_3CN at 400 MHz.

Comparison between the chemical shift of the free ligand **1** and the complexes gives some interesting information. Upon coordination of the ligand with the ruthenium metal cation, the changes of the chemical shift on the ligand are quite significant, showing the electronic and conformational changes induced by metal ion coordination.

The $H_{Pm\,4,6}$ and $H_{3',5'}$ signals shift 0.14 ppm and 0.25 ppm downfield, respectively, which can be justified as coordination delocalizes the charge of Ru(II) to the whole complex.

All the $H_{3',5'}$ in the complexes with pyrimidine substituents shifted around 0.6 - 0.9 ppm downfield compared with reference complex **6**, $Ru(tpy\text{-}Ph)_2^{2+}$, due to the deshielding effects of the hydrogen boding between N lone pair in pyrimidine ring and $H_{3',5'}$ protons.

Upon coupling with an anthryl group, the proton signals from the $Ru(tpy)_2^{2+}$ moieties of complexes **3** and **4** are slightly shifted to lower field by about 0.1 ppm, indicating slightly deshielding of $Ru(tpy)_2^{2+}$ when coupling with non-conjugated chromophore(s).

Interestingly, complex **3c**, which has electron withdrawing ligand Cl-pm-tpy instead of the tpy ligand of complex **3a**, displayed significant downfield shifts in the $T_{3',5'}$ and $T_{3,3''}$ resonances due to the deshielding from the pyrimidine lone pairs with $T_{3',5'}$ shifting downfield by 0.88 ppm. A slight deshielding effect was also observed for $T_{3',5'}$ and $Pm_{4,6}$ protons in complex **3b** with the an-pm-tpy ligand. The orthogonal 9-anthryl group in **3b** creates a deshielding shielding plane to the neighbouring $Pm_{4,6}$ and $H_{3',5'}$.[19] A roughly quantified effect of anthracene subunit to $Pm_{4,6}$ and $H_{3',5'}$ was obtained as 0.11 ppm and 0.17 ppm downfield, respectively, from the comparison of complex **3a** with complex **7a**, $(tpy)Ru(tpy\text{-}pm)_2^{2+}$, which has a proton at the 5-position of the pyrimidine ring.

Dramatic chemical shifts were found in complexes **4a-b**, which have the back-to-back tpy-pm-pm-tpy ligand bridging the two Ru(II) centers. Complex **4b** has two sets of

$Ru(tpy\text{-}pm)_2^{2+}$ moieties along with two anthracene chromophores. The H signals from the back-to-back pyrimidyl group ($H_{B\,4,6}$) are shifted to lower field by 0.53 ppm from the starting complex **3c** (*cf.* **Table 2.2**), in accord with the strong electron-withdrawing effect of two Ru(II) cations in complex **4b**. Other signals from the $Ru(tpy\text{-}pm)_2^{2+}$ moieties are all shifted to lower field by 0.4-0.8 ppm, due to the deshielding effect of the dimetallic Ru(II) centers. The proton signals from complex **4a** follow the same trend as those in complex **4b**, only there is more electron density on the tpy-pm-pm-tpy ligand due to the absence of electron-withdrawing pm group on the back of tpy ancillary ligands.

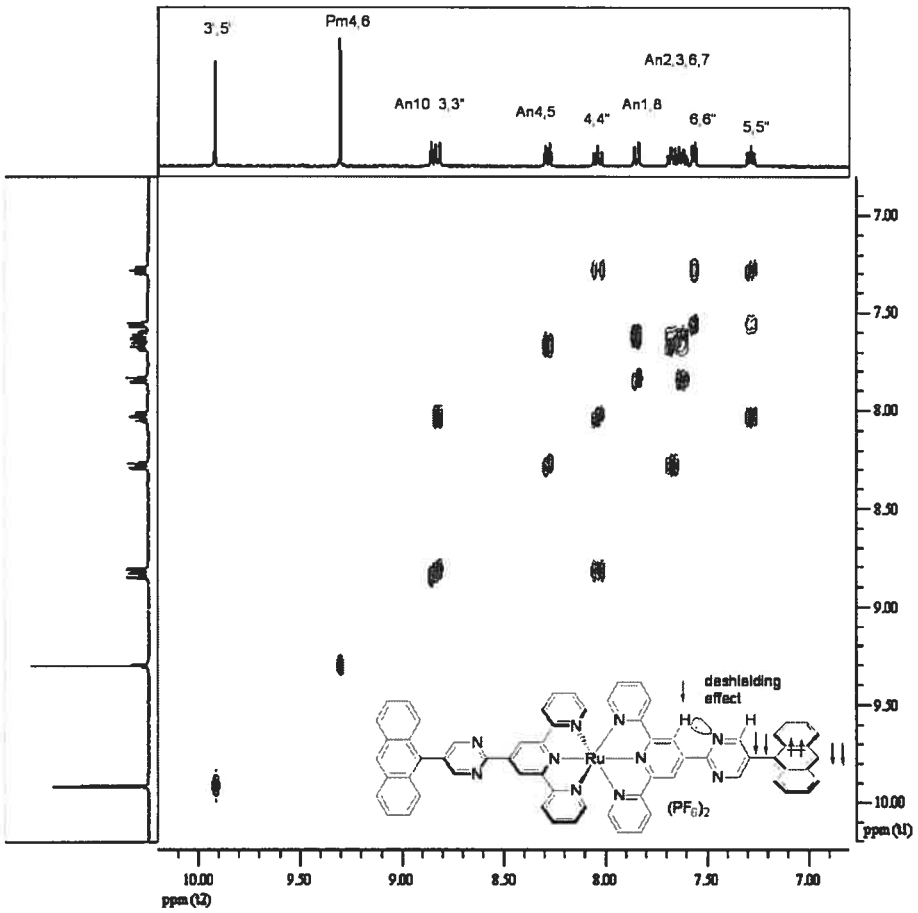

Figure 2.2 2-D COSY spectrum of complex **3b** with labelling and schematic representation of the deshielding effect of 9-anthryl group to the chemical shifts of $T_{3',5'}$ and $Pm_{4,6}$ protons.

It should be noted that the H signals from anthracene chromophores in complex **3a-c** and **4b** were nearly unchanged upon coupling with the $Ru(tpy\text{-}pm)_2^{2+}$ moieties, indicating that the chromophores are not conjugated in these complexes. Combined with the solid state structure data (*cf.* X-ray single crystal structures), the more favourable perpendicular configuration of the anthracene chromophores minimizes the electronic interaction with $Ru(tpy\text{-}pm)_2^{2+}$ moieties.

Table 2.2 ^{1}H NMR chemical shifts for Ru(II) complexes **3** and **4**, **2a-b** and ligand **1** (Cl-pm-tpy).[a]

Cpd	3,3"	4,4"	5,5"	6,6"	3',5'	T 3,3"	T 4,4"	T 5,5"	T 6,6"	T 3',5'	T 4'	A4, 6[b]	B 4,6	An 10	An 1,8	An 3,6	An 4,5	An 2,7
3a	8.76	7.98	7.23	7.47	9.86	8.54	7.96	7.20	7.42	8.80	8.47	9.26	---	8.82	7.82	7.65	8.25	7.59
3b	8.83	8.04	7.29	7.57	9.92							9.31	---	8.86	7.85	7.68	8.29	7.62
7a[h]	8.69	7.96	7.21	7.41	9.69	8.51	7.92	7.15	7.39	8.78	8.45	9.15						
3c	8.79	8.00	7.25	7.52	9.89	8.75	8.00	7.21	7.48	9.68		9.27	9.18	8.83	7.82	7.62	8.26	7.62
4a	8.53	7.95	7.15	7.44	8.80	8.76	8.00	7.24	7.41	9.79	8.47[e]		9.66					
4b	8.83	8.05	7.29	7.58	9.93	8.83	8.05	7.29	7.54	9.86		9.31	9.71	8.86	7.85	7.65	8.29	7.65
5[c]	8.50	7.42	7.17	7.34	8.76	8.50	7.42	7.17	7.34	8.76								
2a[d]	8.69	7.93	7.21	7.40	9.63	8.51	7.69	7.15	7.39	8.78	8.45	9.15						
2b[d]	8.71	7.97	7.19	7.44	9.66							9.16						
6[f]	8.64	7.95	7.18	7.43	9.01							8.21[f]						
1[d]	8.65	7.86	7.34	8.75	9.40							8.84						
1[g]	8.74	8.01	7.50	8.79	9.41							9.02						

[a] In acetonitrile-d_3, 400 MHz. Assignments of the signals were assisted by two-dimensional experiments, NOESY or COSY. See the experimental section for proton labeling scheme. [b] H $_{Pm\,4,6}$ for complex **3a-d**. [c] From reference 8o, **5** = $Ru(tpy)_2^{2+}$. [d] In $CDCl_3$, from reference 10e. [e] 4'-proton in tpy moiety. [f] From reference 8o, **6** = $Ru(tpy\text{-}Ph)_2^{2+}$, A 4,6 = Ph 4, 6.[g] In CD_3CN. [h] From reference 10e, **7a** = $(tpy)Ru(tpy\text{-}pm)^{2+}$.

2.2.3 Crystallography

The solid-state structures of the complexes **3a** and **3b** were determined by single crystal X-ray crystallography. The ORTEP diagrams of the cations of complexes **3a** and **3b** are shown in **Figure 2.3** and **Figure 2.4**, respectively, while selected bond parameters are listed in **Table 2.3**.

The bond lengths and bond angles are typical $Ru(tpy)_2^{2+}$ moieties, which adopt a *pseudo*-octahedral coordination sphere. The pm rings in the two complexes are nearly coplanar (dihedral angles of 7.8° in **3a**, 4.0° and 12.4° in **3b**, respectively) to the tpy moieties. The coplanar pyrimidyl rings serve to extend the electron delocalization, which is crucial to develop the bichromophoric behaviour. The secondary chromophores, anthracenes, have large dihedral angles to the pm-tpy moieties (dihedral angles of 75° in **3a**, 55° and 64° in **3b**, respectively), which diminishes conjugation, thus allowing the subunits to maintain their independent properties in the complexes. The combination of the coplanar pyrimidyl ring and perpendicular anthracene chromophore is crucial to the enhancement of the rt luminescence lifetimes (*c.f.* photophysical properties).

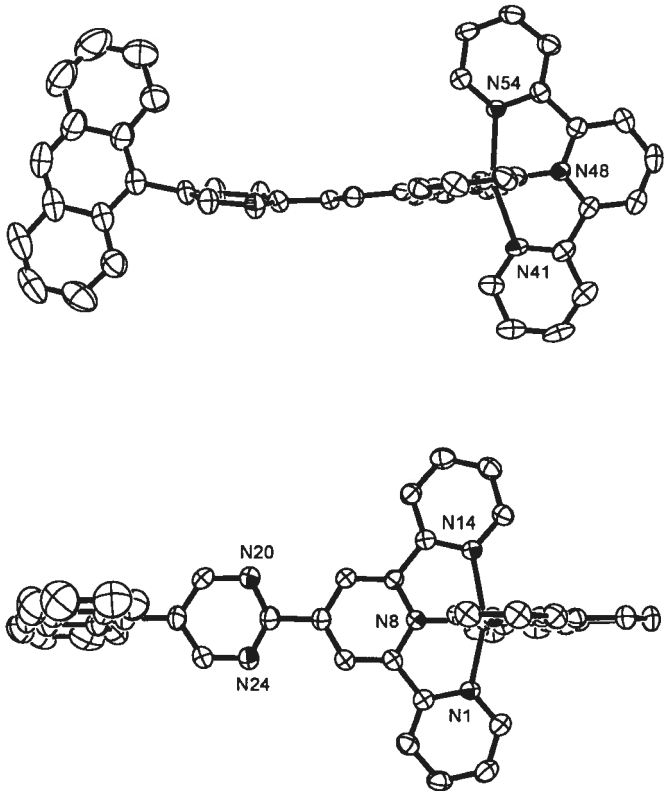

Figure 2.3 Two ORTEP plots of the X-ray crystal structure of complex **3a** exposing the tpy ligand (top) and, after a 90° rotation, the 4'-(5-(9-anthryl)-pyrimid-2-yl)-tpy ligand (bottom). Thermal ellipsoids are set at 50% probability with the counteranions, solvent and hydrogen atoms omitted for clarity.

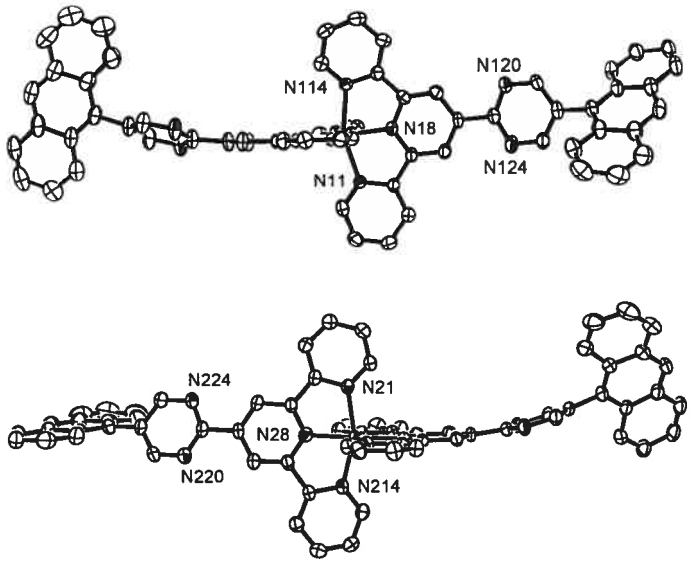

Figure 2.4 Two ORTEP plots of the X-ray crystal structure of complex **3b** exposing the 4'-(5-(9-anthryl)pyrimid-2-yl)-tpy ligand (top) and, after a 90° rotation, the other 4'-(5-(9-anthryl)pyrimid-2-yl)-tpy ligand (bottom). Thermal ellipsoids are set at 50% probability with the counteranions, solvent and hydrogen atoms omitted for clarity.

Table 2.3 Selected bond lengths (Å) and bond angles (°) for complexes **3a** and **3b**.

Bond distances (Å) for **3a**		Bond distances (Å) for **3b**	
Ru	N54 2.093(3)	Ru	N114 2.064(4)
Ru	N48 1.983(3)	Ru	N18 1.993(4)
Ru	N41 2.068(3)	Ru	N11 2.070(3)
Ru	N14 2.081(3)	Ru	N21 2.087(4)
Ru	N8 1.978(3)	Ru	N28 1.981(5)
Ru	N1 2.084(3)	Ru	N214 2.086(4)
Bond angles (°) for **3a**		Bond angles (°) for **3b**	
N54 Ru N2	78.78(13)	N114 Ru N18	79.05(15)
N54 Ru N41	157.59(13)	N114 Ru N11	157.88(14)
N48 Ru N41	78.84(14)	N18 Ru N11	78.86(16)
N48 Ru N8	178.9(2)	N18 Ru N28	178.2(2)
N14 Ru N8	78.90(18)	N21 Ru N28	79.13(17)
N14 Ru N6	157.89(12)	N21 Ru N214	157.96(14)
N8 Ru N1	79.05(17)	N28 Ru N214	78.86(16)

In both complexes, the molecules are distorted to a bow-shaped form by more favorable intermolecular forces in the solid states. This is exemplified in **Figure 2.5** where the two molecules of **3b** are stacked one beside the other with two different stacking forces: (1) intramolecular tpy-tpy stacking and (2) intramolecular anthracene-anthracene stacking. The atom distances in the two stacking motifs are compiled in **Table 2.4**.

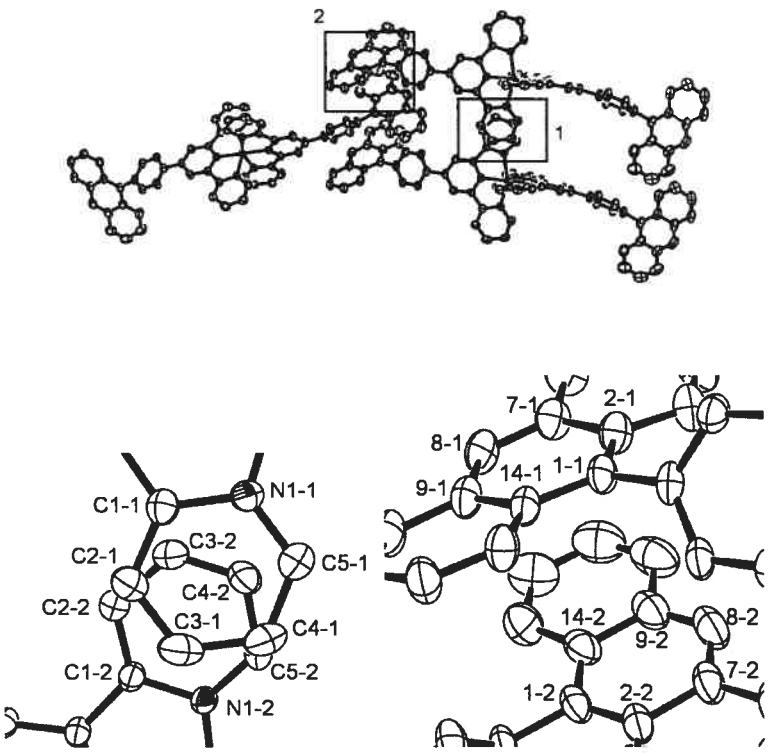

1 **2**

Figure 2.5 Two intramolecular π-stacking motifs observed in complex **3b**: (1) tpy-tpy (motif **1**, left, centroid-to-centroid distance: 4.02 Å); (2) anthryl-anthryl (motif **2**, right, centroid-to-centroid distance: 4.07 Å).

Table 2.4 π-Stacking distances in the two stacked motifs in complex **3b**.

motif **1**		motif **2**	
A B	distances (Å)	A B	distances (Å)
N1-1 C3-2	4.41	1-1 7-2	4.16
C1-1 C2-2	4.25	2-1 8-2	3.90
C2-1 C1-2	4.17	7-1 9-2	3.90
C3-1 N1-2	3.90	8-1 14-2	3.97
C4-1 C5-2	3.65	9-1 1-2	4.16
C5-1 C4-2	3.71	14-1 2-2	4.32

2.2.4 Electrochemistry

The electrochemical data for complexes **3** and **4** are listed in **Table 2.5**. In all of the complexes with anthracene substituents, only *quasi*-reversible oxidation of Ru(II) to Ru(III) were found. In all cases, the 4'-pyrimidine substituents on the tpy have very little effect on $Ru(tpy)^{2+}$ moiety, showing that the pyrimidines have negligible effect on the metal-centered d_π orbitals, and only lower the ligand-based π^* orbitals without disturbing the metal-based d_π orbitals to a great extent. The oxidation potentials have shifted to slightly more positive potentials by 25-50 mV as compared with reference complex **5**, $Ru(tpy)_2^{2+}$, (+1.30 V vs SCE), due to a slight stablization of the metal-based orbitals by the electron accepting pyrimidine substituents on the tpy ligands.

Table 2.5 Electrochemical redox potentials for complexes **3a-c, 4a-b** and reference complex **5** in argon-purged acetonitrile solutions.[a]

Compd	Potential/V			
	$E_{1/2ox}$ (V) (ΔE_p (mV))	$E_{1/2red}$ (V) (ΔE_p (mV))		
3a	1.32	-1.10 (65)	-	-
3b	1.36	-1.06 (70)	-	-
3c	1.35 (65)	-1.11 (84)	-1.32 (ir)	-1.68 (ir)
4a	1.31 (70)	-1.06 (70)	-1.25 (ir)	
4b	1.34 (80)	-1.05 (70)	-.125 (ir)	
5[b]	1.30	-1.24	-1.49	

[a] Scan rate 100 mV s^{-1}. $E_{1/2}$ = ½ (E_{pa} + E_{pc}), where E_{pa} and E_{pc} are the anodic and cathodic peak potential respectively. $\Delta E_p = E_{pa} - E_{pc}$. ir = irreversible. Potentials are corrected by internal reference to ferrocene (395 mV); [b] **5** = $Ru(tpy)_2^{2+}$, from ref 6n.

Heteroleptic complex **3a** is slightly easier to oxidize than homoleptic complex **3b**, which has two pyrimidine rings on each sides, as it has more electron density donated from the $Ru(tpy)^{2+}$ moiety. Complex **3c** has an oxidation potential between that of **2b** and **3b**, in accordance with the presence of an electron-withdrawing Cl group.

Upon homo-coupling, the dimetallic complex **4b** becomes easier to oxidize than its starting complex **3c**, due to the substitution of the electron withdrawing chloride atom with a non-conjugated back-to-back pyrimidine. The two metal centers in complex **4b** are homogeneous without any pronounced interaction since the oxidation potential is nearly the same as that of complex **3b**. In the reference bimetallic complex **4a**, which has nearly

the same oxidation potential as that in complex **3a**, the oxidation potential is less positive than that in complex **4b**, due to the electron-donating tpy ligands. The anthryl groups on the pyrimidines have no effect on the metal-based d_π orbitals due to their nonconjugated perpendicular configuration to the $Ru(tpy)_2^{2+}$ centers.

The reduction processes of the newly synthesized complexes have dramatically changed to more positive potentials as compared with $Ru(tpy)_2^{2+}$. In the reduction processes, usually more than one reversible reduction process can be observed with only the first process being reversible. The reduction patterns are different for the homoleptic and heteroleptic complexes. For the heteroleptic complexes, the first single-electron reduction is assigned to the pyrimidyl-substituted ligand and the second is on the non-substituted tpy moiety. Compared to the heteroleptic complexes, the first single-electron reduction of the homoleptic complexes occurs at almost the same potential (slightly higher by 40-50 mV) than that of their heteroleptic analogue. The second reduction processes are less negative than that in heteroleptic counterparts.

2.2.5 Spectroscopic properties

The UV-vis spectra of the newly synthesized complexes **3** and **4** are dominated by spin-allowed MLCT bands in the visible and by spin-allowed polypyridine ligand centered (LC) bands in the UV region (**Figure 2.6**, **Table 2.6**).

Complexes **3a-c** and **4b** all have anthracene signatures due to the population of the ^1L_a state in 350-400 nm region and the population of the ^1B_a state around 254 nm. As expected the molar absorptivities of the anthracene based absorption bands in **3b** and **4b** are larger than those in **3a** and **3c**, respectively. It can be noted that the ^{1}MLCT bands of

complexes **3a-c** and **4b** are red-shifted to lower energy (498~505 nm) as compared with the prototypical $Ru(tpy)_2^{2+}$ (474 nm) complex (**Table 2.6**). The lowering in energy of the absorption band can be attributed to the extended acceptor orbital since the 9-anthryl group has little electronic interaction with tpy-pm moieties due to its orthogonal arrangement. This delocalization is crucial to the prolonged lifetime as compared to $Ru(tpy\text{-}an)_2^{2+}$ (tpy-an = 4'-(9-anthryl)-2,2':6',2"-terpyridine), in which the excited state is totally quenched by the non-emissive ^{3}An state.[20]

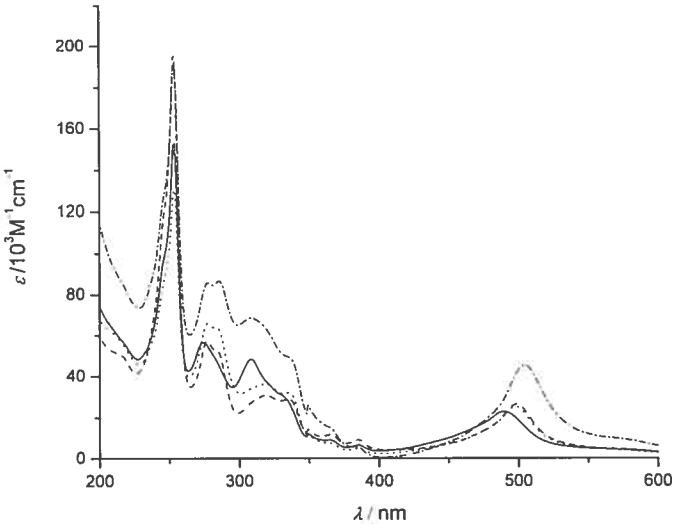

Figure 2.6 Electronic absorption spectra for **3a** (solid line), **3b** (dashed line), **3c** (dotted line), **4b** (intermittent line). The spectra were recorded at rt in acetonitrile.

Table 2.6 Electronic spectra data of complexes **3a-d**, **4b** and $Ru(tpy)_2^{2+}$ (**5**).[a]

Compd	λ_{max} (nm) (ε (10^3 M^{-1} cm^{-1})
3a	489 (22.9); 308 (48.3); 274 (56.5); 254 (152.8)
3b	499 (39.6); 319 (46.3); 277 (85.8); 254 (292.6)
3c	498 (38.1); 319 (54.4); 278 (98.6); 254 (195.7)
4b	505 (65.7); 308 (99.2); 286 (125.7); 254 (278.5)
5[b]	476 (10.4), 309 (46.2), 270 (28.1)

[a] Data was collected in spectroscopic quality acetonitrile at rt. [b] **5** = $Ru(tpy)_2^{2+}$, from reference 6o.

2.2.6 Photophysical properties[gsh1]

The luminescence data are compiled in **Table 2.7**. The rt emission spectra of **3a-b** are typical of MLCT emitters with prolonged rt luminescence lifetimes. The enhancement in the luminescence lifetimes of **3a-b** is attributed to the presence of ^{3}An state in addition to the effect of the extended π^* orbitals. Due to the lowered energy state of the ^{3}MLCT resulting from the conjugated pyrimidine ring, the bichromophoric behaviour became possible in the newly synthesized species. The equilibration between the ^{3}MLCT and the triplet anthracene states (by Boltzmann distribution) results in the significant increase of the rt ^{3}MLCT luminescence lifetime.

Table 2.7 Luminescence data

Compd	298 K[a]			77K[b]	
	λ_{max} (nm)	τ (ns)	Φ	λ_{max} (nm)	τ (ms)
3a	680	5.5; 402	1.3×10^{-4}	692	3.5
3b	675	5.8; 1806	1.8×10^{-4}	694	3.5

[a] In deaerated acetonitrile; [b] In butyronitrile.

2.3 Conclusion

The secondary chromophores, anthracene subunits, were successfully incorporated into the $Ru(tpy)_2^{2+}$ framework with a delocalizating pyrimidyl group through palladium-catalyzed Suzuki cross-coupling reactions. The palladium(0)-catalyzed homocoupling reaction on complexes **2a** and **3c** led to dimetallic Ru(II) species **4a** and **4b**, respectively. The fusion of two design strategies, extending the acceptor orbital and a bichromophoric approach, afforded long-lived luminescence in Ru(II) complexes at rt In particular, the multichromophoric approach proved to be very efficient and allowed novel species **3a-c** to be obtained, which displayed impressive long-lived MLCT luminescence lifetimes at room temperature.

2.4 Experimental Section

2.4.1 General

All reactions were performed under a dry argon atmosphere using standard Schlenk or glove box techniques. All the reactions with anthryl were protected from full lab light. Solvents for the reaction were pre-dried using Pure-Solv Solvent Purification System (Innovative Technology Inc.). Catalytic palladium catalysts and ligands were purchased from STREM. All other chemicals, except where stated otherwise, were purchased from Sigma-Aldrich and used as received.

Nuclear magnetic resonance (NMR) spectra were recorded in $CDCl_3$ or CD_3CN at room temperature (rt) on a Bruker AV400 spectrometer at 400 MHz for ^1H NMR and at 100 MHz for ^{13}C NMR. Chemical shifts are reported in part per million (ppm) relative to residual solvents proton and the carbon resonance of the solvents. ESI-MS was done by the Service de spectrométrie de masse at the Université de Montréal. Routine absorption spectra and emission spectra were measured in deaerated acetonitrile at rt on a Cary 500i UV-Vis-NIR Spectrophotometer and a Cary Eclipse Fluorescence Spectrophotometer, respectively. Electrochemistry data were collected in deaerated acetonitrile with 0.1 M $^nBu_4NPF_6$ on a BAS CV-50W Voltammetric Analyzer. Redox potentials were corrected by the internal reference ferrocence (395 mV vs SCE).

2.4.2 X-Ray crystallography

Recrystallization of **3a** and **3b** from acetonitrile solution by slow diffusion of diethyl ether vapour provided red single crystal suitable for X-ray crystallography.

Crystal parameters and details of the data collection and refinement for **3a** and **3b** are given in **Table 2.8**.

Table 2.8 Crystallography data for complexes **3a, 3b**.

Compd	**3a**	**3b**
Molecular formula	$C_{48}H_{32}N_8Ru(PF_6)_2$ ·CH_3CN	$C_{66}H_{42}N_{10}Ru(PF_6)_2$ ·$2CH_3CN$
M	1152.88	1448.21
Crystal system	monoclinic	monoclinic
a/Å	8.9632 (1)	13.1378 (2)
b/Å	8.7648 (1)	12.1410 (2)
c/Å	30.6115 (4)	39.3588 (6)
α/°	90	90
β/°	92.1247 (8)	92.449 (1)
γ/°	90	90
U/Å^3	2403.21 (5)	6272.23 (17)
Space group	P21	Cc
Z	2	4
Dc/Mg m^{-3}	1.593	1.534
Temperature/K	220 (2)	220 (2)
R1	0.0401	0.0493
wR2	0.0973	0.1224

2.4.3 Synthesis

Pyrimidyl-tpy ligands were synthesized from terpyridylamidine hydrochloride and vinamidium hexaflurophosphate salt.[17] Complexes **2a-b** were synthesized as we previously reported.[10e] 9-Anthrylboronic acid[18] was prepared following the literature methods.

Complex **3a**: (an-pm-tpy)Ru(tpy)$(PF_6)_2$

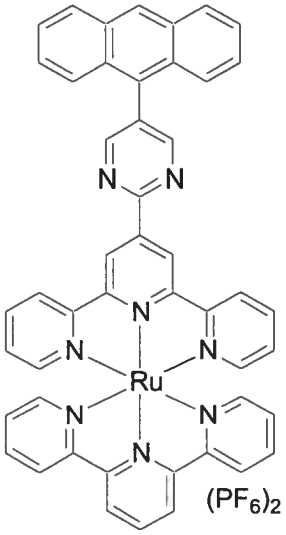

Complex [(Cl-pm-tpy)Ru(tpy)]$(PF_6)_2$ (**2a**, 0.100 g, 0.10 mmol), 9-anthryl boronic acid (0.100 g, 0.46 mmol), $(PPh_3)_2PdCl_2$ (8.0 mg, 10 mol%) and K_2CO_3 (0.140 g, 1.0 mmol) were added into anhydrous DMF (10 mL). The reaction mixture was heated to 110 °C for 12 hours under argon. The mixture was then poured into deaerated aqueous NH_4PF_6 and filtered through celite. The residue was chromatographed on silica gel with 7:1 acetonitrile and aqueous saturated KNO_3 solution as eluent. After anion exchange to hexafluorophosphate with NH_4PF_6, pure red product **3a** (0.095 g, 85%) was isolated. ^{1}H NMR (500 MHz, CD_3CN): δ 9.86 (s, 2H, $H_{3',5'}$), 9.26 (s, 2H, $H_{P\,3',5'}$), 8.82 (s, 1H, H_{An}

$_{10}$), 8.80 (d, J = 8.2 Hz, 2H, H $_{T\,3',5'}$), 8.76 (d, J = 8.1 Hz, 2H, H $_{3,3''}$), 8.54 (d, J = 8.0 Hz, 2H, H $_{T\,3,3''}$), 8.47 (t, J = 8.2 Hz, 1H, H $_{T\,4'}$), 8.25 (d, J = 8.5 Hz, 2H, H $_{An\,4,5}$), 7.98 (td, J^t = 8.2 Hz, J^d = 1.2 Hz, 2H, H $_{4,4''}$), 7.96 (td, J^t = 7.8 Hz, J^d = 1.3 Hz, 2H, H $_{T\,4,4''}$), 7.82 (d, J = 8.8 Hz, 2H, H $_{An\,1,8}$), 7.65 (m, 2H, H $_{An\,3,6}$), 7.59 (m, 2H, H $_{An\,2,7}$), 7.47 (d, J = 5.6 Hz, 2H, H $_{6,6''}$), 7.42 (d, J = 4.9 Hz, 2H, H $_{T\,6,6''}$), 7.23 (ddd, J = 7.4, 5.7, 1.1 Hz, 2H, H $_{5,5''}$), 7.20 (ddd, J = 7.5, 5.7, 1.1 Hz, 2H, H $_{T\,5,5''}$). ^{13}C NMR (75 MHz, CD_3CN): δ 160.5, 159.9, 158.0, 158.0, 156.2, 155.2, 152.7, 152.6, 144.6, 138.3, 138.2, 136.3, 132.9, 131.4, 130.7, 128.9, 128.9, 128.3, 127.7, 127.6, 127.0, 125.9, 125.5, 124.9, 124.6, 123.9, 121.7 (br). Anal. Calcd for $C_{48}H_{32}F_{12}N_8P_2Ru\cdot1.5H_2O$: C, 50.62; H, 3.10; N, 9.84. Found: C, 50.78; H, 2.73; N, 9.56. ESI-MS: 411.2 ([M-2PF_6]$^{2+}$, 100%).

Complex **3b**:(an-pm-tpy)$_2$Ru(PF_6)$_2$

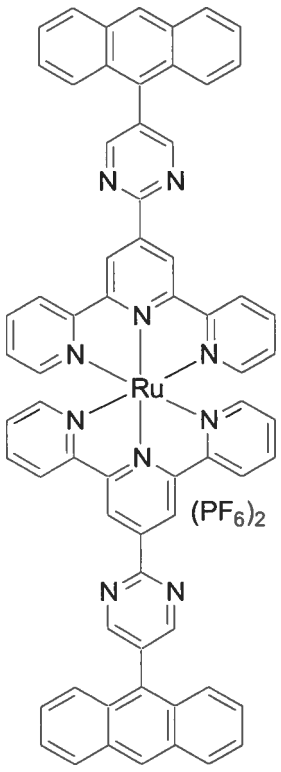

Complex (Cl-pm-tpy)$_2$Ru(PF_6)$_2$ (**2b**, 0.080 g, 0.074 mmol), 9-anthryl boronic acid (0.090 g, 0.41 mmol), (PPh_3)$_2$$PdCl_2$ (11.0 mg, 20 mol%) and K_2CO_3 (0.065g, 0.47 mmol) were added into dry anhydrous DMF (10 mL). The mixture was heated at 140 °C for 12 h under argon and poured into deaerated aqueous NH_4PF_6 and filtered through celite. The residue was chromatographed on silica gel with 10:1 acetonitrile and aqueous saturated KNO_3 solution as eluent. After anion exchange to hexafluorophosphate with NH_4PF_6, pure red product **3b** (0.061 g, 60%) was isolated. ^{1}H NMR (500 MHz, CD_3CN): δ 9.92 (s, 4H, H $_{3', 5'}$), 9.31 (s, 4H, H $_{P\ 4, 6}$), 8.86 (s, 2H, H $_{An\ 10}$), 8.83 (d, J = 8.0 Hz, 4H, H $_{3, 3''}$), 8.29 (d, J = 8.4 Hz, 4H, H $_{An\ 4, 5}$), 8.04 (td, J^t = 7.9 Hz, J^d = 1.3 Hz, 4H, H $_{4, 4''}$), 7.85 (d, J = 8.8 Hz, 4H, H $_{An\ 1, 8}$), 7.68 (m, 4H, 2H, H $_{An\ 3, 6}$), 7.62 (m, 4H, H $_{An\ 2, 7}$), 7.57 (dd, J = 5.6, 0.6 Hz, 4H, H $_{6, 6''}$), 7.29 (ddd, J = 7.5, 5.7, 1.2Hz, 4H, H $_{5, 5''}$). ^{13} C NMR (75 MHz, CD_3CN): δ 160.5, 160.0, 158.0, 156.0, 152.8, 145.0, 138.4, 133.0, 131.4, 130.7, 128.9, 128.3, 127.8, 127.4, 127.0, 125.9, 125.5, 125.1, 121.8. Anal. Calcd for $C_{66}H_{42}F_{12}N_{10}P_2Ru\cdot 2H_2O$: C, 56.54; H, 3.31; N, 9.99. Found: C, 56.66; H, 3.15; N, 10.17. ESI/LR-MS: 1221.1 ([M-PF_6]$^+$, 64%); 538.5 ([M-2PF_6]$^{2+}$, 100%).

Complex **3c**: (an-pm-tpy)Ru(tpy-pm-Cl)(PF_6)$_2$

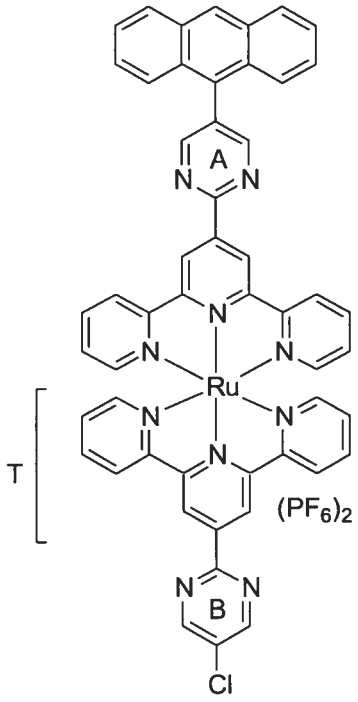

Complex (Cl-pm-tpy)$_2$Ru(PF$_6$)$_2$ (**2b**, 0.087 g, 0.080 mmol), 9-anthryl boronic acid (0.022 g, 0.099 mmol), (PPh$_3$)$_4$Pd (9.0 mg, 0.008 mmol, 10 mol%) and K_2CO_3 (0.027 g, 0.20 mmol) were added into anhydrous DMF (10 mL). The mixture was heated at 90 °C for 24 h under argon and poured into deaerated aqueous NH_4PF_6 and filtered through celite. The residue was chromatographed on silica gel with 15:1 acetonitrile and aqueous saturated KNO_3 solution as eluent. After anion exchange to hexafluorophosphate with NH_4PF_6, pure red product **3c** (0.039 g, 49%, 83% after recovery of starting material **2b**) was isolated. ^{1}H NMR (400 MHz, CD_3CN): δ 9.89 (s, 2H, H $_{3',5'}$), 9.68 (s, 2H, H $_{T\,3',5'}$), 9.27 (s, 2H, H $_{A\,4,6}$), 9.18 (s, 2H, H $_{B\,4,6}$), 8.83 (s, 1H, H $_{An\,10}$), 8.79 (d, J = 8.0 Hz, 2H, H $_{3,3''}$), 8.75 (d, J = 8.1 Hz, 2H, H $_{T\,3,3''}$), 8.26 (d, J = 8.4 Hz, 2H, H $_{An\,4,5}$), 8.00 (t, J = 7.9 Hz, 4H, H $_{4,4'',T\,4,4''}$), 7.82 (d, J = 8.4 Hz, 2H, H $_{An\,1,8}$), 7.62 (m, 4H, H $_{An\,2,3,6,7}$), 7.52 (d, J = 5.7 Hz, 2H, H $_{6,6''}$), 7.48 (d, J = 5.6 Hz, 2H, H $_{T\,6,6''}$), 7.25 (t, J = 7.6 Hz, 2H, H $_{5,5''}$), 7.21(t, J = 7.5 Hz, 2H, H $_{T\,5,5''}$). ESI-MS: 467.0 ([M-2PF$_6$]$^{2+}$, 100%).

Complex **4a**: $[(tpy)Ru(tpy\text{-}pm\text{-}pm\text{-}tpy)Ru(tpy)](PF_6)_4$

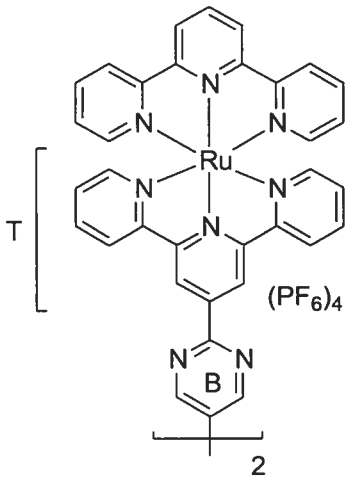

Complex $[(tpy)Ru(tpy\text{-}pm\text{-}Cl)](PF_6)_2$ (**2a**) (31.1 mg, 0.032 mmol), $Pd(OAc)_2$ (1.1 mg, 0.005 mmol, 15 mol%), $tBu_2P(biph)$ (2.9 mg, 0.010 mmol, 30 mol%) and K_2CO_3 (11.0 mg, 0.80 mmol) were added into anhydrous DMF (5 mL). The mixture was heated at 110 °C for 24 h under argon and poured into deaerated aqueous NH_4PF_6 and filtered through celite. The residue was chromatographed on silica gel with 7:1 CH_3CN and aqueous saturated KNO_3 solution as eluent. After anion exchange to hexafluorophosphate with NH_4PF_6, pure red product **4a** (22.5 mg, 0.012 mmol, 75%) was isolated. ^1H NMR (500 MHz; CD_3CN) δ 9.79 (s, 4H, $H_{T\,3',5'}$), 9.66 (s, 4H, $H_{Pm\,4,6}$), 8.80 (d, J = 8.2 Hz, 4H, $H_{3',5'}$), 8.76 (d, J = 8.0 Hz, 4H, $H_{T\,3,3''}$), 8.53 (d, J = 8.2 Hz, 4H, $H_{3,3''}$), 8.47 (t, J = 8.2 Hz, 2H, $H_{4'}$), 8.00 (td, J^t = 7.8 Hz, J^d = 1.4 Hz, 4H, $H_{T\,4,4''}$), 7.95 (td, J^t = 7.8 Hz, J^d = 1.3 Hz, 2H, $H_{4,4''}$), 7.44 (d, J = 5.5 Hz, 4H, $H_{6,6''}$), 7.41 (d, J = 5.7 Hz, 4H, $H_{T\,6,6''}$), 7.24 (ddd, J = 7.5, 5.5, 1.1 Hz, 4H, $H_{T\,5,5''}$), 7.15 (ddd, J = 7.5, 5.7, 1.1 Hz, 4H, $H_{5,5''}$). ^{13}C NMR can not be obtained due to the small molar concentration in CD_3CN. ESI-MS: 322.0, $[M\text{-}4PF_6]^{4+}$; 478.4, $[M\text{-}3PF_6]^{3+}$; 789.6, $[M\text{-}2PF_6]^{2+}$.

Complex **4b**: [(an-pm-tpy)Ru(tpy-pm-pm-tpy)Ru(tpy-pm-an)]$(PF_6)_4$

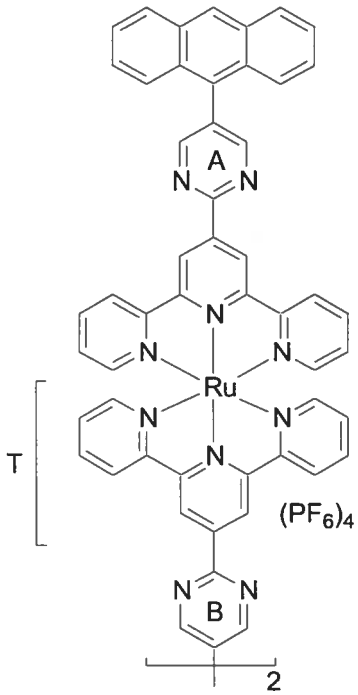

Complex (an-pm-tpy)Ru(tpy-pm-Cl)$(PF_6)_2$ (**3c**) (42.4 mg, 0.031 mmol), $Pd(OAc)_2$ (1.1 mg, 0.005 mmol, 15 mol%), *t*Bu_2P(biph) (2.9 mg, 0.010 mmol, 30 mol%) and K_2CO_3 (18.5 mg, 0.13 mmol) were added into anhydrous DMF (10 mL). The mixture was heated at 110 °C for 24 h under argon and poured into deaerated aqueous NH_4PF_6 and filtered through celite. The residue was chromatographed on silica gel with 7:1 ACN and aqueous saturated KNO_3 solution as eluent. After anion exchange to hexafluorophosphate with NH_4PF_6, pure red product **4b** (12.5 mg, 49%, 62% after recovery of starting material **3c**) was isolated. ^{1}H NMR (400 MHz, CD_3CN): δ 9.93 (s, 4H, $H_{3',5'}$), 9.86 (s, 4H, $H_{T3',5'}$), 9.71 (s, 4H, $H_{B4,6}$), 9.31 (s, 4H, $H_{A4,6}$), 8.86 (s, 2H, H_{An10}), 8.83 (dd, J = 8.2 Hz, 8H, $H_{3,3'',T3,3''}$), 8.29 (d, J = 8.8 Hz, 4H, $H_{An4,5}$), 8.05 (dt, J = 8.5 Hz, 8H, $H_{4,4'',T4,4''}$), 7.85 (d, J = 8.4 Hz, 4H, $H_{An1,8}$), 7.65 (m, 8H, $H_{An2,3,6,7}$), 7.58 (d, J = 5.6 Hz, 4H, $H_{6,6''}$), 7.54 (d, J = 5.7 Hz, 4H, $H_{T6,6''}$), 7.29 (dt, J = 6.7 Hz, 8H, $H_{5,5'',T5,5''}$). ^{13}C NMR can

not be obtained due to the small molar concentration in CD_3CN. ESI-MS: 450.2 ($[M-4PF_6]^{4+}$, 86%); 648.2 ($[M-3PF_6]^{3+}$, 87%); 1045.0 ($[M-2PF_6]^{2+}$, 100%).

2.5 References

1 (a) V. Balzani, F. Scandola, *Supramolecular Photochemistry*, Horwood,, Chichester, **1991**; (b) G. L. Closs, J. R. Miller, *Science* **1988**, *240*, 440. (c) M. R. Wasielewski, *Chem. Rev.* **1992**, *92*, 435; (d) K.D. Jordan, M. N. Paddon-Row, *Chem. Rev.* **1992**, *92*, 395; (e) V. Balzani, L. De Cola, *Supramolecular Chemistry,* Vol. *371*, Kluwer, Dordrecht **1992**; (f) D. Gust, T.A. Moore, A.L. Moore, *Acc. Chem. Res.* **1993**, *26*, 198; (g) K.P. Ghiggino, T.A. Smith, *Prog. React. Kinetics* **1993**, *18*, 375; (h) R. A. Bissel, A. P. de Silva, H. Q. N. Gunaratne, P. L. M. Lynch, G. E. M. Maguire, C. P. McCoy, K. R. A. S. Sandanayake, *Topics Curr. Chem.* **1993**, *168*, 223; (i) V. Balzani, A. Juris, M. Venturi, S. Campagna, S. Serroni, *Chem. Rev.* **1996**, *96*, 759; (j) V. Balzani, F. Scandola, In: D.N. Reinhoudt, Editor, *Comprehensive Supramolecular Chemistry,* Vol. *10*, Pergamon,, Oxford (**1996**), 1.

2 (a) S. Serroni, G. Denti, S. Campagna, A. Juris, M. Ciano, V. Balzani, *Angew. Chem. Int. Ed. Engl.* **1992**, *31*, 1493. (b) S. Campagna, G. Denti, S. Serroni, A. Juris, M. Venturi, M. Ricevuto, V. *Chem. Eur. J.* **1995**, *1*, 211.

3 V. Balzani, S. Campagna, G. Denti, A. Juris, S. Serroni, M. Venturi, *Acc. Chem. Res.* **1998**, *31*, 26.

4 K. O. Johansson, J. A. Lotoski, C. C. Tong, G. S. Hanan, *Chem. Commun.* **2000**, 819.

5 Y.-Q. Fang, M. I. J. Polson, Garry S. Hanan, *Inorg. Chem.* **2003**, *42*, 5.

6 F. Loiseau, R. Passalacqua, S. Campagna, M. I. J. Polson, Y.-Q. Fang, G. S. Hanan, *Photochem. Photobiol. Sci.* **2002**, *1*, 982.

7 (a) T. J. Meyer, *Pure Appl. Chem.* **1986**, *58*, 1193; (b) A. Juris, V. Balzani, F. Barigelletti, S. Campagna, P. Belser, A. von Zelewsky, *Coord. Chem. Rev.* **1988**, *84*, 85; (c) K. Kalyanasundaram, *Photochemistry of Polypyridine and Porphyrin Complexes*, Academic Press, London, **1991**; (d) V. Balzani, F. Barigelletti, L. De Cola, *Topics Curr. Chem.* **1990**, *158*, 31; (e) G. J. Karvanos, *Photoinduced Electron Transfer*, VCH, New York, **1993**.

8 (a) E.C. Constable, *Prog. Inorg. Chem.* Vol. *42*, Wiley, New York, **1994,** 67; (b) E. M. Kober, J. L. Marshall, W. J. Dressick, B. P. Sullivan, J. V. Caspar, T. J. Meyer, *Inorg. Chem.* **1985**, *24*, 2755; (c) C. R. Hecker, A. K. I. Gushurst, D. R. McMillin, *Inorg. Chem.* **1991**, *30*, 538; (d) E. Amouyal, M. Mouallem-Bahout, G. Calzaferri, *J. Phys. Chem.* **1991**, *95*, 7641; (d) C. R. Arana, H. D. Abruña, *Inorg. Chem.* **1993**, *32*, 194; (e) J.-P. Collin, S. Guillerez, J.-P. Sauvage, F. Barigelletti, L. De Cola, L. Flamigni, V. Balzani, *Inorg. Chem.* **1991**, *30*, 4230; (f) J.-P. Collin, S. Guillerez, J.-P. Sauvage, F. Barigelletti, L. De Cola, L. Flamigni, V. Balzani, *Inorg. Chem.* **1992**, *31*, 4112; (g) V. Grosshenny, R. Ziessel, *J. Chem. Soc., Dalton Trans.* **1993**, 817; (h) V. Grosshenny, R. Ziessel, *J. Organomet. Chem.* **1993**, *453*, C19; (i) A. Harriman, R. Ziessel, *Chem. Commun.* **1996**, 1707; (j) F. Barigelletti, L. Flamigni, V. Balzani, J.-P. Collin, J.-P. Sauvage, A. Sour, E. C. Constable, A. M. W. Cargill Thompson, *J. Chem. Soc., Chem. Commun.* **1993**, 942; (k) F. Barigelletti, L. Flamigni, V. Balzani, J.-P. Collin, J.-P. Sauvage, A. Sour, E. C. Constable, A. M. W. Cargill Thompson, *J. Am. Chem. Soc.* **1994**, *116*, 7692; (l) F. Barigelletti, L. Flamigni, V. Balzani, J.-P. Collin, J.-P. Sauvage, A. Sour, *New J. Chem.* **1995**, *19*, 793; (m) J.-P. Sauvage, J.-P. Collin, J.-C.

Chambron, S. Guillerez, C. Coudret, V. Balzani, F. Barigelletti, L. De Cola, L. Flamigni, *Chem. Rev.* **1994**, *94*, 993. (n) S. U. Son, K. H. Park, Y.-S. Lee, B. Y. Kim, C. H. Choi, M. S. Lah, Y. H. Jang, D.-J. Jang, Y. K. Chung, *Inorg. Chem.* **2004**, *43*, 6896. (o) M. Maestri, N. Armaroli, V. Balzani, E. C. Constable, A. M. W. Cargill Thompson, *Inorg. Chem.* **1995**, *34*, 2759; (p) J. Wang, Y.-Q. Fang, G. S. Hanan, F. Loiseau, S. Campagna, *Inorg. Chem.* **2005**, *44*, 5-7; (q) E. A. Medlycott, G. S. Hanan, *Chem. Soc. Rev.* **2005**, *34*, 133.

9 M. I. J. Polson, E. A. Medlycott, G. S. Hanan, L. Mikelsons, N. J. Taylor, M. Watanabe, Y. Tanaka, F. Loiseau, R Passalacqua, S. Campagna, *Chem. Eur. J.* **2004**, *10*, 3640.

10 (a) A. El-ghayoury, A. Harriman, A. Khatyr, R. Ziessel, *Angew. Chem.* **2000**, *112*, 191; (b) A. Harriman, R. Ziessel, *Chem. Comm.* **1996**, 1707; (c) A. C. Benniston, A. Harriman, V. Grosshenny, R. Ziessel, *New. J. Chem.* **1997**, *21*, 405; (d) A. El-ghayoury, A. Harriman, A. Khatyr, R. Ziessel, *J. Phys. Chem. A* **2000**, *104*,1512; (e) Y.-Q. Fang, N. J. Taylor, G. S. Hanan, F. Loiseau, R. Passalacqua, S. Campagna, H. Nierengarten, A. Van Dorsselaer, *J. Am. Chem. Soc.* **2002**, *124*, 7912.

11 (a) W. E. Ford, M. A. J. Rodgers, *J. Phys. Chem.* **1992**, *96*, 2917; b) G. J. Wilson, A. Launikonis, W. H. F. Sasse, A. W.-H. Mau, *J. Phys. Chem. A* **1997**, *101*, 4860; c) J. A. Simon, S. L. Curry, R. H. Schmehl, T. R. Schatz, P. Piotrowiak, X. Jin, R. P. Thummel, *J. Am. Chem. Soc.* **1997**, *119,* 11012; d) D. S. Tyson, C. R. Luman, X. Zhou, F. N. Castellano, *Inorg. Chem.* **2001**, *40*, 4063; e) B. Maubert, N. D.

McClenaghan, M. T. Indelli, S. Campagna, *J. Phys. Chem. A*, **2003**, *107*, 447; e) J. Wang, G. S. Hanan, F. Loiseau, S. Campagna, *Chem Comm.* **2004**, 2068.

12 S. L. Murov, I. Carmichael, G. L. Hug, In: *Handbook of Photochemistry*, Marcel Dekker, New York, **1993**.

13 V. Farina, V. Krishnamurthy, W. J. Scott, *The Stille Reaction*, Wiley, New York, **1998**.

14 Same inductive effect has been observed in the 4'-position of tpy ligands in Ru(II) complex: E. C. Constable, A. M. W. C. Thompson, D. A. Tocher, M. A. M. Daniels, *New J. Chem.* **1992**, *16*, 855.

15 (a) N. Miyaura, T. Yanagi, A. Suzuki, *Synth. Commun.* **1981**, *11*, 513; (b) A. Suzuki, *Pure Appl. Chem.* **1985**, *57*, 1749; (c) A. Suzuki, *Pure Appl. Chem.* **1991**, *63*, 419; (d) A. R. Martin, Y. Yang, *Acta Chem. Scand.* **1993**, *47*, 221; (e) A. Suzuki, *Pure Appl. Chem.* **1994**, *66*, 213; (f) N. Miyaura, A. Suzuki, *Chem. Rev.* **1995**, *95*, 2457; (g) S. P. Stanforth, *Tetrahedron* **1998**, *54*, 263; (h) N. Miyaura, *Advances in Metal-organic Chemistry* Libeskind, L. S., Ed.; Jai: London, **1998**, *6*, 187–243; (i) A. J. Suzuki, *Organomet. Chem.* **1999**, *576*, 147; (j) A. Suzuki, In *Organoboranes for Syntheses.* ACS Symposium Series 783; P. V. Ramachandran, H. C. Brown, Eds.; American Chemical Society: Washington, DC, **2001**; pp 80–93.

16 (a) E. *J.* Ciganek, *Org. Chem.* **1980**, *45*, 1497. (b) R. A. Gardner, J.-G. Delcros, F. Konate, F. Breitbeil III, B. Martin, M. Sigman, M. Huang, O. Phanstiel IV, *J. Med. Chem.* **2004**, *47*, 6055.

17 I. W. Davies, J.-F. Marcoux, J. Wu, M. Palucki, E. G. Corley, M. A. Robbins, N. Tsou, R. G. Ball, P. Dormer, R. D. Larsen, P. J. Reider, *J. Org. Chem.* **2000**, *65*, 4571.

18 Z. H. Li, M. S. Wong, Y. Tao, M. D'Iorio, *J. Org. Chem.* **2004**, *69*, 921.

19 A similar effect was reported previously: R. P. Thummel, Y. Jahng, *Inorg. Chem.* **1986**, *25*, 2527.

20 G. Albano, V. Balzani, E. C. Constable, M. Maestri, D. R. Smith, *Inorg. Chim. Acta* **1998**, *277*, 225. See schematic representation below for the quenching mechanism:

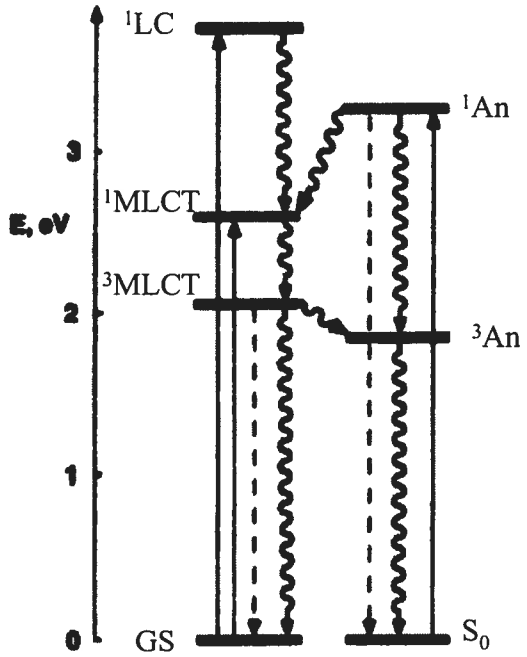

$Ru(tpy)_2^{2+}$ An

Figure 2.7 Schematic representation of the luminescence quenching mechanism of homoleptic $Ru(tpy\text{-}An)_2^{2+}$ complex. MLCT = metal-to-ligand charge transfer, ^{1}LC = ligand-centered singlet state, GS = ground state, S0 = ground state of An, ^{3}An = non-emissive triplet state of An, 1An = singlet excited state of An.

Chapter 3

Luminescent Ruthenium(II) Complexes of 4'-(9-Anthryl)-2,2':6',2"-Terpyridine: Equilibrating Organic Chromophore and ^{3}MLCT Over Large Distance*

Abstract

A new series of ruthenium(II) complexes, based on 4'-(9-anthryl)-2,2':6',2"-terpyridine (an-tpy), has been synthesized from the Ru(III) precursor (an-tpy)$RuCl_3$ (**4**). These new Ru(II) complexes, [(an-tpy)Ru(tpy-pm-R)] (R= H, **3a**; Cl, **3b**; phenyl, **3c**; *p*-bromophenyl, **3d**), with extended π-conjugation through the 4'-substituted pyrimidyl group, have been characterized by analytical and spectroscopic methods, and X-ray single crystal structure determination for **3b** and **3d**. Lifetime measurements have shown that the anthryl chromophore has greatly increased the room temperature (r.t.) excited-state lifetimes of the complexes, even though it is not directly connected to the ligand involved in the metal-to-ligand charge transfer (^{3}MLCT) emitting state. An equilibrium exists between the anthryl triplet state and the ^{3}MLCT state even though the two are physically separated by more than one nanometer.

3.1 Introduction

Ruthenium complexes based on polypyridines are one of the main topics of research in the field of coordination chemistry due to their potential application in light-harvesting devices and molecular electronics.[1] The prototype, $Ru(bpy)_3^{2+}$ (bpy = 2,2'-bipyridine), has been well-studied and used in several photosensitizers because of its relative long room temperature (r.t.) excited-state lifetime (up to 1 μs).[2a,3] However, the application of this type of complex in polynuclear light-active arrays is compromised by their structural disadvantages: (i) $[Ru(bpy)_3]^{2+}$ is a mixture of *Δ* and *Λ* enantiomers; (ii) mono-substitution of bpy ligands introduces *fac* and *mer* isomerism; (iii) a linear arrangement of such chromophores, useful for the design of molecular wires and, consequently, vectorial energy and electron migration, is difficult to obtain.

In order to overcome the structural disadvantages and subsequent problems in the synthesis and characterization of $Ru(bpy)_3^{2+}$ based complexes, more focus has been applied to the inherently *achiral* $Ru(tpy)_2^{2+}$ motif (tpy = 2,2':6',2"-terpyridine) in the last decade. However, $Ru(tpy)_2^{2+}$ has a very short r.t. excited-state lifetime, less than 250 ps, which is not useful for practical applications since the non-radiative decay from the triplet metal-to-ligand charge transfer state (^{3}MLCT) to the triplet metal-centered state (^{3}MC) quenches the r.t. luminescence before energy or electron transfer can take place. To be applied in a practical device, it would be convenient if these complexes had relatively long-lived room temperature (r.t.) excited states.[1f] Approaches based on the chemical modification on the 4'-position of tpy in $Ru(tpy)_2^{2+}$ have been widely adopted to prolong its r.t. lifetime as well as to retain its structural advantages. A linear arrangement could be easily obtained by adding substituents on the 4'-position of the tpy

ligands in the $Ru(tpy)_2^{2+}$ motif. The approaches include the incorporation of various structural modifications to tpy: cyclometallating groups[4], electron-donating and/or -accepting substituents[5] and delocalization of π-system[6]. All of these modifications work by increasing the energy gap between the ^{3}MLCT and ^{3}MC excited states, thereby minimizing the thermally-activated surface crossing which dominates the MLCT deactivation processes.

Recently, the multi-chromophore approach has emerged as a very efficient tool to increase the excited-state lifetime of metal polypyridine complexes: the combination of metal complexes and organic chromophores, which have long-lived triplet excited states due to their strongly forbidden deactivation processes, at energies close to that of the ^{3}MLCT state of the metal chromophore.[7] This requires the synthesis of multichromophoric species, in which the various metal- and organic-based chromophores are only weakly interacting, so that their individual properties are essentially maintained in the multichromophoric complex. We have previously reported that Ru(II) complexes of a tpy with a coplanar pyrimidine and a 9-anthryl chromophore have greatly increased luminescence lifetimes due to bichromophoric effect, in which the ^{3}MLCT is in equilibrium with the anthracene triplet state (^{3}An), which acts as an excited-state energy storage element.[7f] In all the case in which bichromophoric states are known for Ru(II) polypyridine complexes, the organic chromophore used as the energy storage element is incorporated into the polypyridine ligand which is directly involved in the ^{3}MLCT emitting state. These complexes display exceptional properties; however, their syntheses also depend on several sequential reactions in order to incorporate the two chromophores into the same ligand. Herein we report on a new series of Ru(tpy)-type complexes in

which the excited-state storage element (an anthracene subunit) is linked to a ligand which is not involved in the ^{3}MLCT emitting level, and demonstrate that the multichromophoric approach is still effective in spite of the large (nanometric) spatial separation between the subunits.

3.2 Results and Discussion

3.2.1 Synthesis

The substituent pyrimidyl tpy ligands **2a-d** were synthesized through base-catalyzed ring-forming reaction between (2,2':6',2"-terpyrid-4-yl)amidium hydrochloride and vinamidine hexafluorophosphate salt **1a-d** (**Scheme 3.1**). These ligands were isolated as off-white to yellow solid in moderate to high yields and fully characterized by NMR spectroscopy as well as satisfactory microanalysis results.

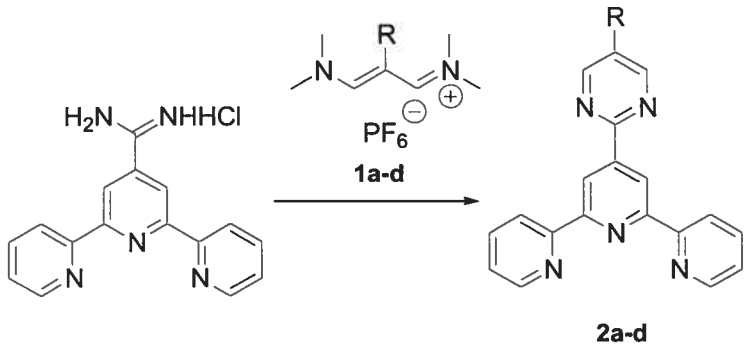

Scheme 3.1 Synthesis of 5-R-pyrimid-2-yl-2,2':6',2"-terpyridine ligands **2a-d** from terpyridyl amidium chloride and vinamidine hexaflurophosphate salt **1a-d** (R = H, **1a**; Cl, **1b**; Ph, **1c**; *p*-bromo-Ph, **1d**). Reagents and conditions: MeONa, MeOH, reflux, 12 h.

For the sake of convergence, we chose to introduce the an-tpy ligand into Ru(II) coordination sphere to obtain the Ru(III) precursor **4**, (an-tpy)$RuCl_3$, for the synthesis of heteroleptic complexes **3a-d** (**Scheme 3.2**). Thus, treatment of an-tpy ligand and $RuCl_3 \cdot 3H_2O$ with excess lithium chloride in anhydrous DMF at reflux afforded (an-

tpy)$RuCl_3$ (**4**) with 84% yield without the formation of the byproduct, homoleptic complex, $[(an\text{-}tpy)_2Ru]_2^{2+}$. The formula of complex **4** was confirmed by the satisfactory results from positive FAB-MS and microanalysis.

The reaction of each of ligands **2a-d** with one equivalent of **4**, in the presence of three equivalent of dechlorinating reagent, in anhydrous DMF at reflux readily afforded heteroleptic complexes **3a-d** in good yields (**Scheme 3.2**). Reference heteroleptic complex **3e**, $[(an\text{-}tpy)Ru(tpy)]^{2+}$, was also synthesized from **4** and tpy ligand with similar procedure. The pure complexes **3a-e** were afforded through silica chromatography and counteranion exchange with ammonium hexafluorophosphate. The formulae of the complexes were confirmed by NMR spectroscopy, ESI-MS, MALDI-TOF MS and elemental analysis. However, satisfied elemental analysis results for complexes **3a**, **3d-e** can not be obtained, presumably due to the incomplete counteranion exchange.

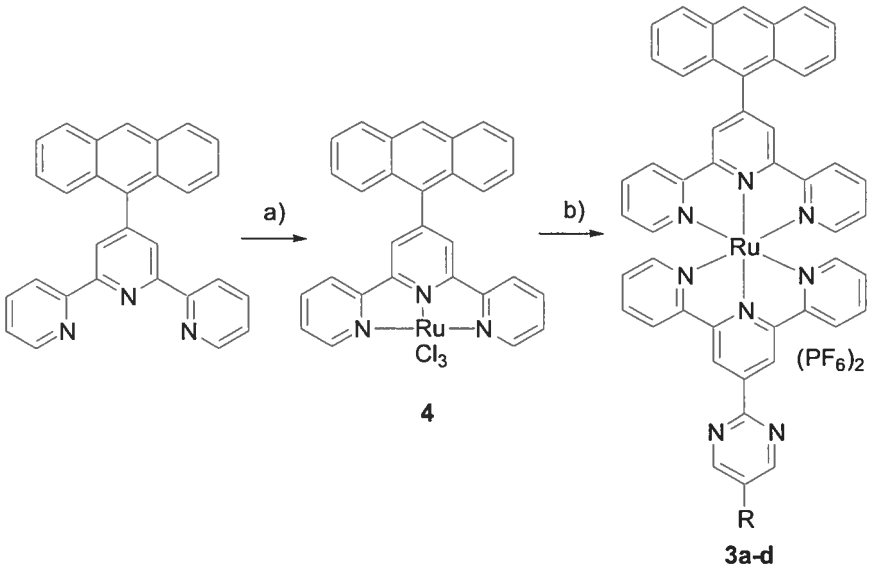

Scheme 3.2 Synthesis of the ruthenium complexes **3a-d** (**3a**, R = H; **3b**, R = Cl; **3c**, R = phenyl; **3d**, R = *p*-bromophenyl). Reagents and conditions: (a) $RuCl_3$ xH_2O, excess LiCl, DMF, reflux, 8 h; (b) tpy-pm-R **2a-d**, $AgNO_3$, DMF, reflux, 2-3 h.

3.2.2 NMR spectroscopy

The newly synthesized complexes **3a-e** have been characterized by the ^1H and ^{13}C NMR spectroscopy (**Figure 3.1**). The ^1H NMR spectroscopic data of complex **3a-e** in CD_3CN are compiled in **Table 3.1**. The assignments of the ^1H NMR signals were assisted by two-dimensional COSY spectra.

Through the comparison of the ^1H NMR spectra of newly synthesized complexes **3a-d**, we note that the anthryl fragment in these complexes is kept independent from the R-pm-tpy ligand. Another interesting point is that upon coordination of the ligands with the ruthenium cation, the changes of the chemical shift on the ligand are quite significant, showing the electronic and conformational changes induced by coordination to the metal

ion. For example, the $H_{3',5'}$ signals in Cl-m-tpy ligand shift around 0.29 ppm downfield (**Table 3.1**), which can be justified by the hydrogen bonding with nitrogen lone pair in pyrimidine rings.[11] Dramatic chemical shift change is seen on the $H_{6,6''}$ protons in the side pyridine rings between the free ligands and the complexes. The $H_{6,6''}$ shifts significantly upfield (1.1 ppm). From the crystal structure of the complexes (**Figure 3.2** and **Figure 3.3**), $H_{6,6''}$ protons are located in the anisotropically shielding zone produced by the ring current of the pyridine rings from the other ligand.[13] A similar, but weaker result is observed for $H_{5,5''}$, which is slightly shielded and has the lowest chemical shift. Surprisingly, $H_{3',5'}$ shows little shift (0.29 ppm). This is presumably due to the opposite effects of conformational change (downfield) and newly produced H···H steric hindrance (upfield) during coordination, which offsets each other.

Table 3.1 Chemical shifts of ^{1}H NMR signals of complexes **3a-f** and ligand **2a**.[a]

Complex	t3,3"	T3,3"	t4,4"	T4,4"	t5,5"	T5,5"	t6,6"	T6,6"	t3',5'	T3',5'	A10	A4,5	A1,8	A2,3,6,7	P4,6	R
3a	8.76	8.44	8.05	7.89	7.37	7.18	7.68	7.49	9.74	8.94	8.90	8.32	8.19	7.68	9.18	7.68(P5)
3b	8.76	8.45	8.05	7.89	7.38	7.19	7.69	7.49	9.70	8.95	8.90	8.32	8.20	7.69	9.19	---
3c	8.80	8.45	8.06	7.90	7.38	7.20	7.68	7.52	9.80	8.96	8.92	8.33	8.20	7.68	9.46	7.98, 7.68
3d	8.79	8.47	8.07	7.88	7.40	7.22	7.70	7.55	9.79	8.96	8.90	8.32	8.22	7.70	9.42	7.88
3e	8.46	8.56	7.88	7.98	7.19	7.33	7.42	7.65	8.80	8.91	8.89	8.31	8.18	7.65		
3f[b]		8.48		7.93		7.32		7.68		8.96	8.91	8.31	8.20	7.68		
2b	8.74		8.01		7.50		8.79		9.41						9.02	
5b[c]	8.69	8.51	7.96	7.93	7.21	7.15	7.39	7.40	9.63	8.78					9.15	

[a] Spectra were recorded in CD_3CN at r.t. at 400 MHz. T-signals from tpy moiety in an-tpy ligand, t-signals from tpy moity in R-pm-tpy ligand (from tpy moiety for **3e**), A-signals from anthryl moiety, P-pyrimidyl signals, R-other signals from R. See **Chart 3.1** for naming scheme. [b] **3f** = $Ru(tpy\text{-}an)_2^{2+}$, data from ref. 9a. [c] **5b** = [(Cl-pm-tpy)Ru(tpy)]$(PF_6)_2$, data from reference 5e.

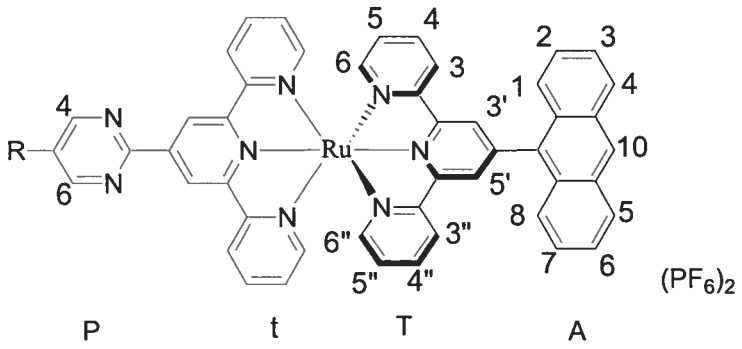

Chart 3.1 Numbering scheme for complexes [(an-tpy)Ru(tpy-pm-R)]$(PF_6)_2$ **3a-d**. The prefixes P, t, T and A represent pyrimidyl, tpy of R-pm-tpy, tpy of an-tpy and anthryl moieties, respectively.

The proton signals from anthracene moieties in this new series of complexes are nearly the same as those in the reference complex **3e** (**Table 3.1**), indicating that the chemical environments of the anthracene groups in these complexes are nearly the same. The pyrimidyl substituent on the other side tpy ligand has no effect on the anthracene group, which is perpendicular to the tpy (*c.f.* crystal structure).

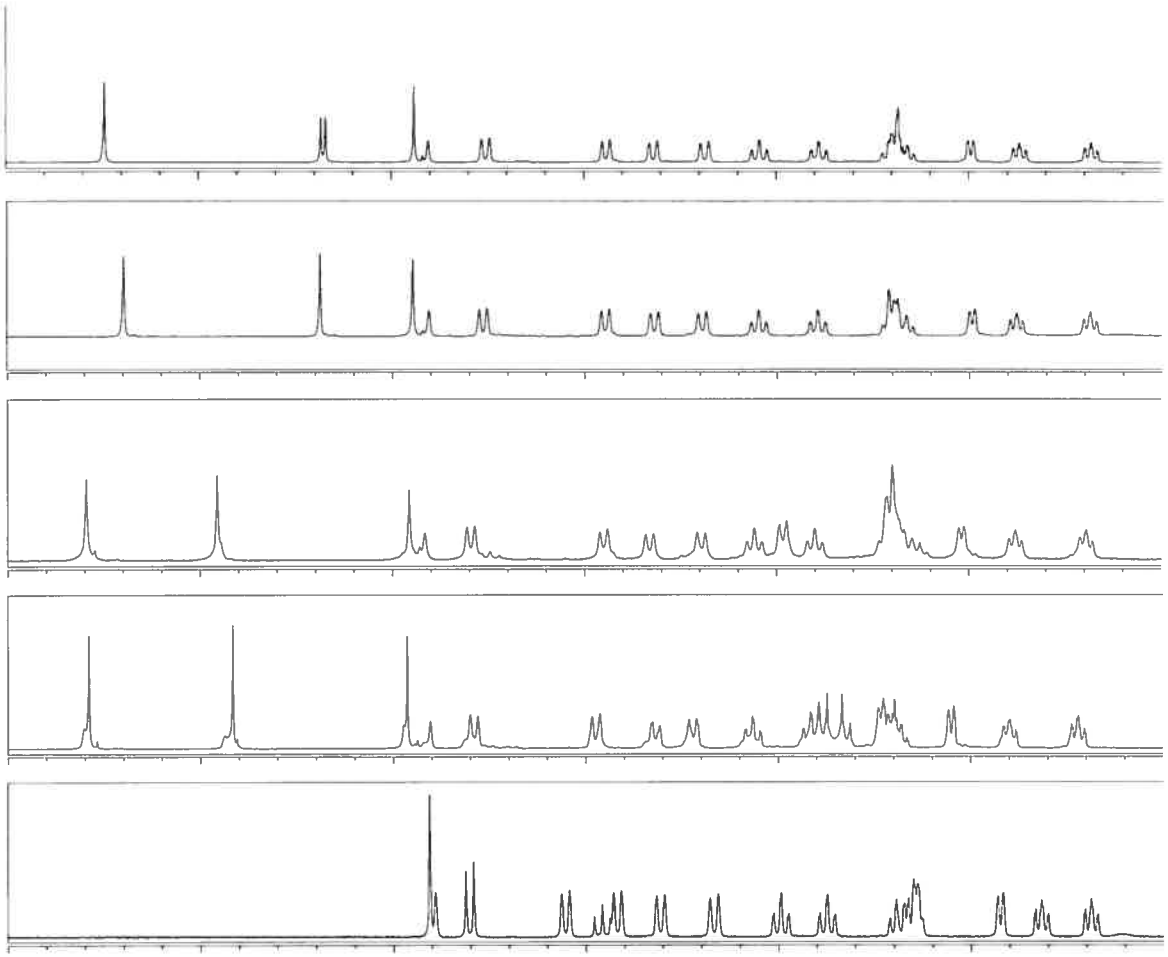

Figure 3.1 ^{1}H NMR spectra of complexes **3a-e** (from top to bottom) between 10.0 ppm and 7.0 ppm. Spectra were recorded in CD_3CN at r.t. on a Bruker AV400 spectrometer at 400 MHz. See **Table 3.1** for assignments.

3.2.3 Crystal structure determination

The ORTEP diagrams of the cation of complexes **3b** and **3d**[§] are showed in **Figure 3.2** and **Figure 3.3**, respectively, while selected bond parameters are listed in **Table 3.2**.

Table 3.2 Selected bond lengths (Å) and angles (°) for complexes **3b** and **3d**.

3b			
Ru – N214	2.071(7)	N214 – Ru – N28	79.6(3)
Ru – N28	1.978(7)	N214 – Ru – N21	158.1(3)
Ru – N21	2.060(7)	N28 – Ru – N21	78.5(3)
Ru – N11	2.074(8)	N11 – Ru – N18	78.9(3)
Ru – N18	1.970(8)	N11 – Ru – N114	158.8(3)
Ru – N114	2.091(8)	N18 – Ru – N114	79.9(3)
Cl12 – C47	1.753(11)	N28 – Ru – N18	178.1(3)
3d			
Ru – N1	2.070(4)	N1 – Ru – N2	79.3(2)
Ru – N2	1.947(5)	N1 – Ru – N3	157.7(2)
Ru – N3	2.079(4)	N2 – Ru – N3	78.5(2)
Ru – N4	2.080(4)	N4 – Ru – N5	78.5(2)
Ru – N5	1.933(4)	N4 – Ru – N6	157.8(2)
Ru – N6	2.085(4)	N5 – Ru – N6	79.3(2)
C52 – Br	1.871(8)	N2 – Ru – N5	179.2(2)

The R_1 factor and wR_2 of the single crystal structure determination of complex **3b** is 0.1359 and 0.4025, although there is no disorder in the single molecules. The unsatisfied refinement of the structure is probably due to the quality of the crystals.

The Ru-to-N bond lengths and internal pyridine angles in complexes **3b** and **3d** are similar to those found in Ru(II) complexes of modified tpy-like tridentate ligands.[8] The 9-anthryl subunit in **3b** and **3d** lies at a 76.8° and an 82.3° angle, respectively, to the N1-N3 terpyridine plane which diminishes its conjugation to the pyrimidyl-tpy unit (**Figure 3.2** and **Figure 3.3**), which allowing the subunits to maintain their independent properties in the complexes. The pyrimidyl group lies virtually co-planar to the N4-N6 terpyridine (7.7° and 6.2° angles, respectively), whereas the 5-pyrimidyl substituted *p*-bromophenyl group in **3d** is twisted at a 27.3° angle with respect to the pyrimidine (**Figure 3.3**). The co-planar nature of the pyrimidine-tpy sub-unit favors π-conjugation and is crucial for the enhanced photophysical properties of these complexes (*cf.*, photophysics).

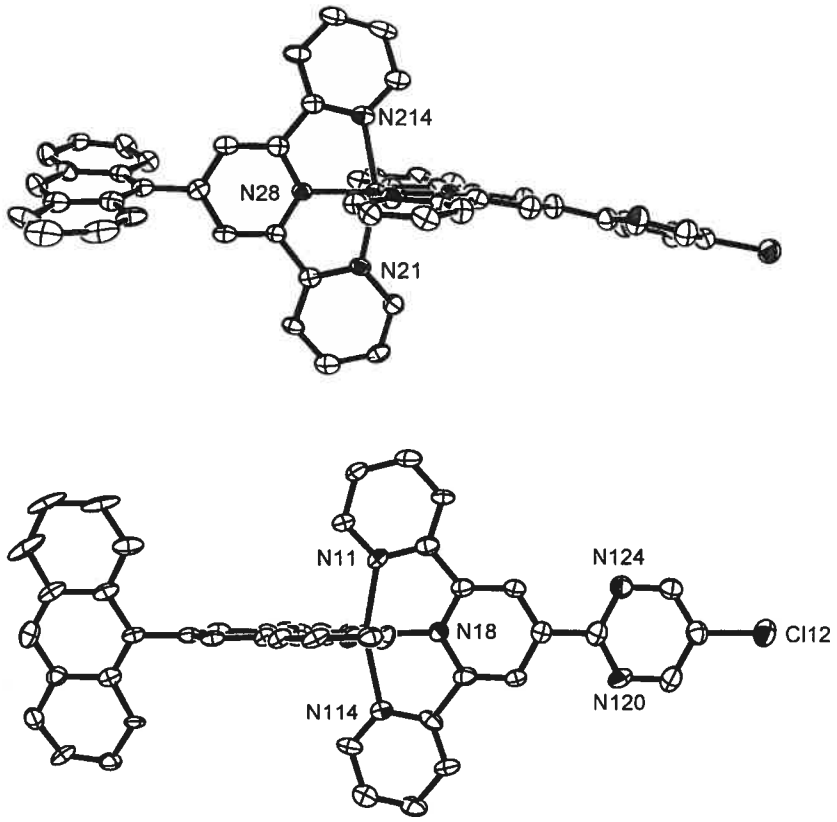

Figure 3.2 ORTEP plots of the X-ray crystal structure of complex **3b** exposing the an-tpy ligand (top) and, after a 90° rotation, the 5-Cl-pyrimid-2-yl ligand (bottom). Thermal ellipsoids are set at 30% probability with hydrogen atoms and counteranions omitted for clarity.

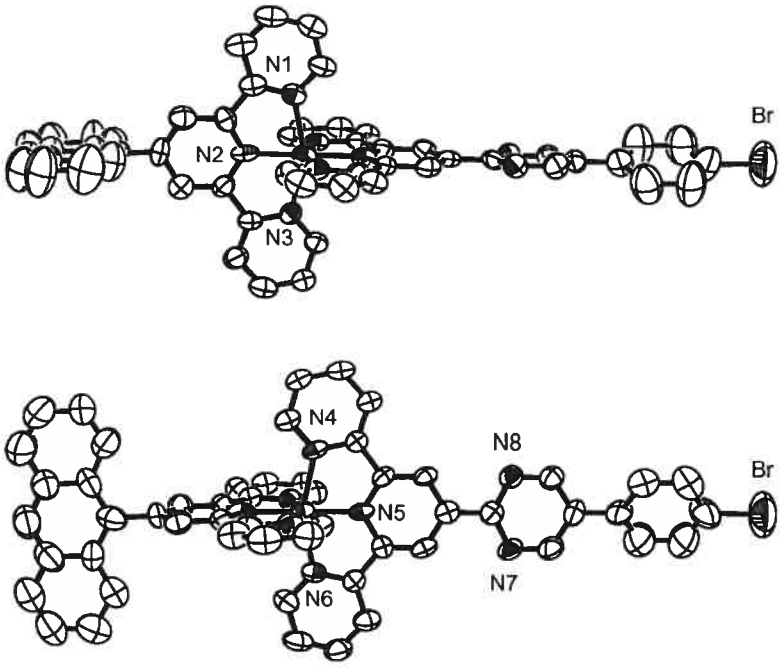

Figure 3.3 ORTEP plots of the X-ray crystal structure of complex **3d** exposing the an-tpy ligand (top) and, after a 90° rotation, the 5-(*p*-bromophenyl)pyrimid-2-yl ligand (bottom). Thermal ellipsoids are set at 30% probability with hydrogen atoms and counteranions omitted for clarity.

3.2.4 Electrochemistry

The electrochemical data of complexes **3a-e** are listed in **Table 3.3**. The redox potentials of each new complexes are similar to that of $Ru(tpy)_2^{2+}$ with a single one-electron metal-based oxidation and a series of ligand-based reductions, of which the first reduction process is reversible. The oxidation potentials have slightly shifted to more positive potentials by 25-50 mV compared with reference complex **3e**, (+1.30 V vs SCE), due to the greater stablization of the metal-based orbitals by the pyrimidyl-tpy

substituents. The 9-anthryl group has little electronic effect on the complexes as the redox potentials of **3a-d** are nearly the same as those of their non-anthryl counterparts, ([(tpy)Ru(tpy-pm)] $(PF_6)_2$ (**5a**).[5e]

Table 3.3 Cyclic voltammetric potentials of complexes **3a-e** at r.t. in Ar-purged acetonitrile (0.1 M Bu_4NPF_6) at a platinum electrode. [a]

Comp	$E_{1/2}$/V (ΔE_p/mV)					
	Oxidation	Reduction				
3a	+1.33 (70)	-1.09 (60)	-1.46 (70)	-1.72	-1.88	
3b	+1.32 (80)	-1.10 (70)	-1.45	-1.75	-1.88	-2.05
3c	+1.36 (90)	-1.19 (60)	-1.53		-1.89	
3d	+1.34 (80)	-1.11(70)	-1.43			
3e	+1.30 (70)	-1.31 (70)	-1.95			
5a[b]	+1.32 (80)	-1.13 (70)	-1.48 (80)			

[a] Scan rate 100 mV s^{-1}. $E_{1/2}$ = ½ (E_{pa} + E_{pc}), where E_{pa} and E_{pc} are the anodic and cathodic peak potential respectively. $\Delta E_p = E_{pa} - E_{pc}$. Irreversible process if no ΔE_p presented. Reference electrode, SCE. Potentials are corrected by internal reference to ferrocene. [b] From reference 5e.

3.2.5 Spectroscopic properties

The newly synthesized complexes **3a-e** were characterized by UV-vis spectroscopy in deaerated acetonitrile at r.t..

The absorption spectra of complexes **3a-e** are showed in **Figure 3.4** and the absorption data are compiled in **Table 3.4**. In the UV region, the spectra are dominated by the π-π* transitions of the tpy and anthracene moities. In the visible region, the spin-allowed ^{1}MLCT bands of complexes **3a-d** have shifted to lower energy as compared to that of complex **3e** due to the extended delocalization of the pyrimidyl-tpy moiety. The absorption spectra of complexes **3a-d** are similar to the sum of the spectra of ruthenium pyrimidyl-tpy moieties and anthracene, indicating that the 9-anthryl group contributes independently to the electronic spectra of the complex.

Table 3.4 Electronic absorption spectra for complexes **3a-e**.[a]

Complex	λ_{max}/nm ($\varepsilon/10^3$ M^{-1} cm^{-1})			
3a	490 (18.9)	309 (37.5)	275 (55.0)	254 (116.0)
3b	492 (35.7)	308 (71.0)	276 (110.2)	254 (220.0)
3c	494 (15.3)	309 (33.8)	276 (31.9)	254 (65.0)
3d	494 (23.7)	309 (51.2)	275 (47.4)	254 (120.6)
3e	482 (11.0)	308 (41.3)	270 (37.8)	254 (104.6)

[a] Data was collected in deaerated spectroscopic quality acetonitrile at 298 K.

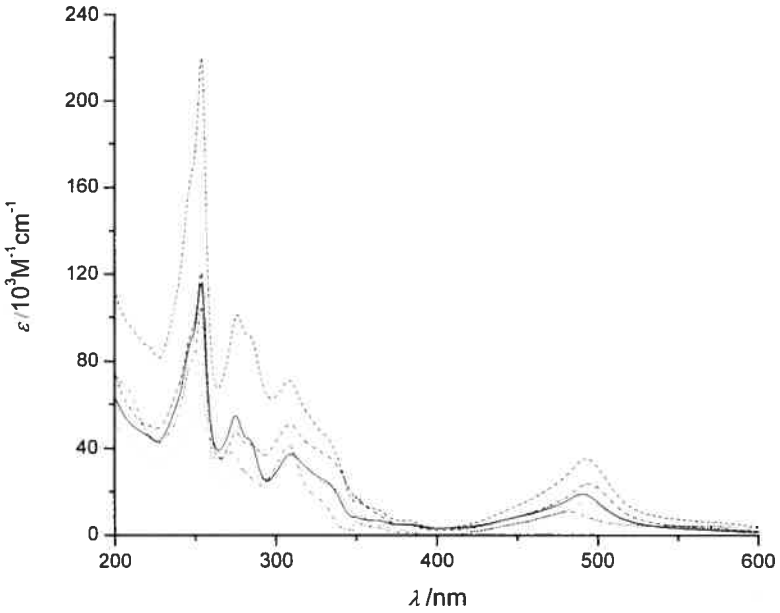

Figure 3.4 Electronic absorption spectra for **3a** (solid line), **3b** (dashed line), **3c** (dotted line), **3d** (intermittent line) and **3e** (double intermittent line). The spectra were recorded at room temperature in argon-purged acetonitrile.

3.2.6 Photoluminescence measurements

At room temperature, the emission spectra of new complexes are typical of MLCT emitters. The luminescence data collected in **Table 3.5** confirm our interpretation by showing that the introduction of the two independent chromophores significantly enhances the lifetime as compared to complex **3e**, in which the ^{3}MLCT luminescence has been totally quenched by the ^{3}An state, as well as to complex $[(tpy)Ru(tpy\text{-}pm\text{-}R)](PF_6)_2$ **5a**, in which multichromophoric behaviour cannot be obtained.

The emission data (**Table 3.5**) clearly showed that in all the complexes **3a-d** the energy level of the emitting ^{3}MLCT state has been lowered to a region comparable to that of the non-emissive anthracene triplet state (^{3}An) (E^{00}=1.85eV, 671 nm)[12] definitely not involved in the tpy-Pm-R ligands. The ^{3}MLCT state of complexes **3a-d** is therefore close enough in energy to the ^{3}An state to make equilibration between the two states possible, thus accounting for the enhancement of the excited state lifetimes of the new complexes (**Table 3.5**). As expected, the emission spectra of complexes **3a-d** exhibit biexponential decay (**Table 3.5**). The first shorter lifetime is attributed to the decay of the initially formed ^{3}MLCT state. The second lifetime results from the equilibration between the emitting ^{3}MLCT level and the ^{3}An state. The experimental results at 77 K (in particular, lifetimes and emission spectra) allow the low temperature emission to be attributed to the anthracene triplet. The additional increases in the luminescence lifetimes of the new species are necessarily related to the presence of the anthracene triplet not involved in ^{3}MLCT emitting state.

Table 3.5 Luminescence data of complexes **3a-e**.

Complex	298 K[a]	
	λ_{max}/nm	τ/ns (contribution)
3a	669	>1000
3b	680	10(5%), 698(95%)
3c	670	25(20%), 1052(80%)
3d	670	28(10%), 1040(90%)
3e	-----	-----
5a	675	8

[a] In deaerated acetonitrile.

3.3 Conclusions

A new series of r.t. luminescent $Ru(tpy)_2^{2+}$ species have been designed and synthesized, incorporating a pyrimid-2-yl-tpy subunit for extended electron delocalization and an independent organic chromophore, 9-anthryl subunit, as an energy reservoir for the emissive ^{3}MLCT state. Importantly, prolonged luminescence lifetimes via excited-state equilibration have been obtained by grafting the excited-state storage element onto a ligand which does not act as the acceptor ligand of the ^{3}MLCT emitting level. Separation of the two chromophoric subunits onto different ligands greatly simplifies the synthetic procedure while maintaining long-lived excited state lifetimes at r.t.. This approach enables the design and synthesis of the ruthenium terpyridine moiety and the organic chromophore subunit independently and can open the way to a new class of compounds with predetermined photophysical properties.

3.4 Experimental

3.4.1 General methods

All reactions were performed under a dry argon atmosphere using standard Schlenk techniques. Solvents for the reaction were pre-dried using Solvent Purification System. All chemicals, except where stated otherwise, were purchased from Sigma-Aldrich and used as received.

Nuclear magnetic resonance (NMR) spectra were recorded in $CDCl_3$ or CD_3CN at room temperature (r.t.) on a Bruker AV400 spectrometer at 400 MHz for ^1H NMR and at 100 MHz for ^{13}C NMR. Chemical shifts are reported in part per million (ppm) relative to residual solvents proton (7.23 ppm for chloroform-d and 1.93 ppm for acetonitrile-d_3) and the carbon resonance of the solvents. Melting points were measured on an Electrothermal Mel-Temp 1101D without correction. Fast-atom bombardment (FAB, positive mode) spectra were recorded on a ZAB-HF-VB-analytical apparatus in an *m*-nitrobenzylalcohol (*m*-NBA) matrix and Ar atoms were used for the bombardment (8 KeV). ESI-MS and MALDI-TOF MS were done by the Mass Spectrometry Facility at Université de Montréal. Microanalysis was done in the Elemental Analysis Laboratory, Université de Montréal. Column chromatography was performed on Kiesegel 60 (230-400 mesh) silica gel. Routine absorption spectra and emission spectra were measured in deaerated acetonitrile at r.t. on a Cary 500i UV-Vis-NIR Spectrophotometer and a Cary Eclipse Fluorescence Spectrophotometer, respectively. Electrochemistry data were collected in deaerated acetonitrile with 0.1 M $^nBu_4NPF_6$ on a BAS CV-50W Voltammetric Analyzer. Redox potentials were corrected by the internal reference ferrocence (395 mV vs SCE).

3.4.2 X-Ray crystallography

The solid-state structures of the complexes **3b** and **3d** were determined by X-ray crystallography. Recrystallization of **3b** and **3d** from acetonitrile solution, respectively, by slow diffusion of diethyl ether vapor provided dark-red single crystal suitable for X-ray crystallography. Crystal parameters and details of the data collection and refinement for **3b** and **3d** are given in **Table 3.6**.

Table 3.6 Crystallography data for complexes **3b** and **3d**.

Complex	**3b**	**3d**
Molecular formula	$C_{48}H_{31}ClN_8Ru(PF_6)_2$	$C_{54}H_{35}BrN_8Ru(PF_6)_2$
M	1146.27	1266.82
Crystal system	triclinic	monoclinic
a/Å	10.4037(6)	25.1776 (18)
b/Å	12.2062(7)	11.4829 (8)
c/Å	21.9324(12)	23.2866 (15)
α/°	80.801(3)	90
β/°	85.840(3)	104.716 (3)
γ/°	80.360(3)	90
U/Å^3	2719.5(3)	6511.6 (8)
Space group	P-1	P21/c
Z	2	4
Dc/Mg m^{-3}	1.400	1.292
μ/mm^{-1}	4.059	3.765
Temperature/K	100(2)	220 (2)
R1	0.1359	0.0550
wR2	0.4025	0.0992

3.4.3 Ligands synthesis

An-tpy ligand was prepared following literature method[9a] or as we reported recently.[9b] Vinamidium hexaflurophosphate salts **1a-d** were prepared following literature method.[10] Ligands **2a-d** were synthesized by following a general procedure outlined below for **2a**.[11]

4'-(Pyrimid-2-yl)-2,2':6',2"-terpyridine (**2a**)

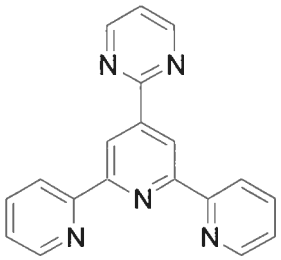

Vinamidine salt **1a** (0.160 g, 0.71 mmol), 4'-terpyridylamidine hydrochloride (0.205 g, 0.66 mmol) and sodium methoxide (0.042 g, 0.78 mmol) were heated at reflux overnight in dry methanol (30 mL). The mixture was filtered, washed with chilled methanol (2×5 mL) and dried in vacuum to obtain a white crystalline product (0.108 g, 0.35 mmol, 53%). mp 287.5-288.5 °C (methanol). ^{1}H NMR (400 MHz, $CDCl_3$) δ 9.42 (s, 2H, $H_{3',5'}$), 8.89 (d, J = 4.9 Hz, 2H, $H_{P4,6}$), 8.74 (d, J = 4.9 Hz, 2H, $H_{6,6''}$), 8.63 (d, J = 7.9 Hz, 2H, $H_{3,3''}$), 7.84 (t, J = 7.7 Hz, 2H, $H_{4,4''}$), 7.38 (t, J = 7.5 Hz, 2H, $H_{5,5''}$), 7.29 (t, J = 4.8 Hz, 1H, H_{P5}). ^{13}C NMR (100 MHz, $CDCl_3$) δ 163.2, 157.5, 156.5, 156.2, 149.4, 147.2, 136.9, 123.9, 121.3, 120.6, 119.7. Anal. Calcd for $C_{19}H_{13}N_5$: C, 73.30; H, 4.21; N, 22.49. Found: C, 73.36; H, 4.13; N, 22.61.

4'-(5-Chloro-pyrimid-2-yl)-2,2':6',2"-terpyridine (**2b**)

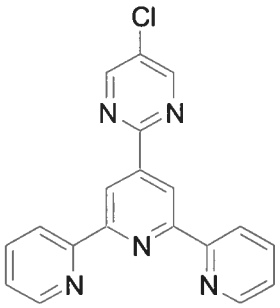

Yield 76%. mp 231.5-233 °C (methanol). ^{1}H NMR (400 MHz, $CDCl_3$) δ 9.40 (s, 2H, H $_{3',5'}$), 8.84 (s, 2H, H $_{P\,4,6}$), 8.75 (d, J = 4.1 Hz, 2H, H $_{6,6''}$), 8.65 (d, J = 7.9 Hz, 2H, H $_{3,3''}$), 7.86 (t, J = 7.8 Hz, 2H, H $_{4,4''}$), 7.34 (t, J = 7.3 Hz, 2H, H $_{5,5''}$). ^{1}H NMR (400 MHz, CD_3CN) δ 9.41 (s, 2H, H $_{3',5'}$), 9.02 (s, 2H, H $_{P\,4,6}$), 8.79 (d, J = 4.2 Hz, 2H, H $_{6,6''}$), 8.74 (d, J = 7.9 Hz, 2H, H $_{3,3''}$), 8.01 (td, J^t = 7.8 Hz, J^d = 1.8 Hz, 2H, H $_{4,4''}$), 7.50 (td, J^t = 7.7, J^d = 1.8 Hz, 2H, H $_{5,5''}$). ^{13}C NMR (100 MHz, $CDCl_3$) δ 161.0, 156.6, 156.0, 156.0, 149.4, 145.9, 136.9, 131.0, 124.0, 121.3, 119.5. Anal. Calcd for $C_{19}H_{12}ClN_5$: C, 66.00; H, 3.50; N, 20.25. Found: C, 66.14; H, 3.45; N, 20.43.

4'-(5-Phenyl-pyrimid-2-yl)-2,2':6',2"-terpyridine (**2c**)

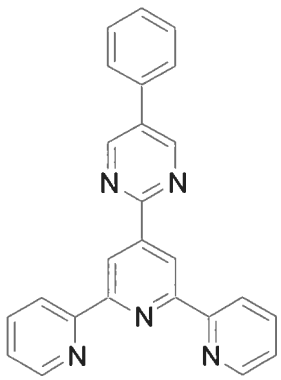

Yield 85%. mp 246-247 °C (methanol). ^{1}H NMR (400 MHz, $CDCl_3$) δ 9.49 (s, 2H, $H_{3',5'}$), 9.10 (s, 2H, $H_{P\,4,6}$), 8.76 (d, J = 4.0 Hz, 2H, $H_{6,6''}$), 8.66 (d, J = 8.0 Hz, 2H, $H_{3,3''}$), 7.87(t, J = 7.7 Hz, 2H, $H_{4,4''}$), 7.65 (d, J = 7.0 Hz, 2H, $H_{Ph\,3,5}$), 7.51 (m, 3H, $H_{Ph\,2,4,6}$), 7.34 (t, J = 7.4Hz, 2H, $H_{5,5''}$). ^{13}C NMR (100 MHz, $CDCl_3$) δ 161.9, 156.5, 156.2, 155.4, 149.4, 146.9, 136.8, 134.4, 133.2, 129.5, 129.1, 127.1, 123.9, 121.3, 119.6. Anal. Calcd for $C_{25}H_{17}N_5$: C, 77.50; H, 4.42; N, 18.08. Found: C, 77.31; H, 4.40; N, 18.17.

4'-(5-*p*-Bromo-phenyl-pyrimid-2-yl)-2,2':6',2"-terpyridine (**2d**)

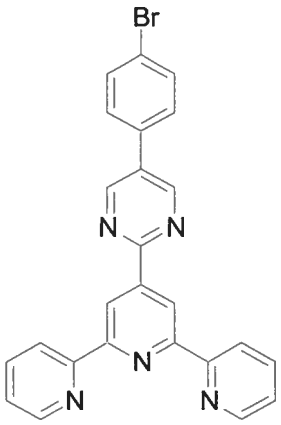

Yield 58%. mp 251-252 °C (methanol). ^{1}H NMR (400 MHz, $CDCl_3$) δ 9.53 (s, 2H, $H_{3',5'}$), 9.11 (s, 2H, $H_{P\,4,6}$), 8.82 (d, J = 4.0 Hz, 2H, $H_{6,6''}$), 8.73 (d, J = 8.0 Hz, 2H, $H_{3,3''}$), 7.94 (t, J = 7.7 Hz, 2H, $H_{4,4''}$), 7.70 (d, J =7.0 Hz, 2H, $H_{Ph\,3,5}$), 7.56 (d, J = 7.1 Hz, 2H, $H_{Ph\,2,6}$), 7.41 (t, J = 7.4 Hz, 2H, $H_{5,5''}$). ^{13}C NMR (100 MHz, $CDCl_3$) δ 162.1, 156.7, 156.3, 155.5, 149.6, 146.9, 144.4, 136.8, 133.2, 129.5, 129.5, 128.3 123.9, 121.4, 119.7. Anal. Calcd for $C_{25}H_{16}BrN_5$: C, 64.39; H, 3.46; N, 15.02. Found: C, 64.24; H, 3.42; N, 15.14.

3.4.4 Metal complexes preparation

Reference complex **5a-e** were prepared as we reported previously.[5e]

(An-tpy)$RuCl_3$ (**4**)

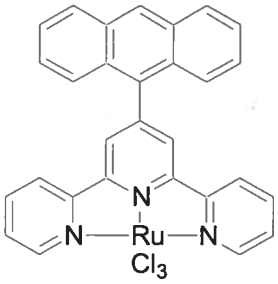

Ligand an-tpy (0.41g, 1.0 mmol), ruthenium trichloride hydrate (0.23g, 1.0 mmol) and lithium chloride (0.20g, 5.0 mmol) were heated at reflux in anhydrous DMF (50 mL) for 8 h. Then the solution was cooled down and the solvent was removed under reduced pressure. The residue was sonicated in ethanol (50 mL) for 30 minutes. Filtration through celite gave pure product (0.52g, 0.84 mmol, 84%). FAB-MS: 616.5 $[M]^+$, 581.5 $[M-Cl]^+$, 546.6 $[M-2Cl]^+$, 510.6 [M-3Cl]+. Anal. Calc. for $C_{19}H_{15}N_5O$ (**4**·H_2O): C, 54.86; H, 3.33; N, 6.62. Found: C, 54.33; H, 3.37; N, 6.98.

[(An-tpy)Ru(**2a**)]$(PF_6)_2$ (**3a**)

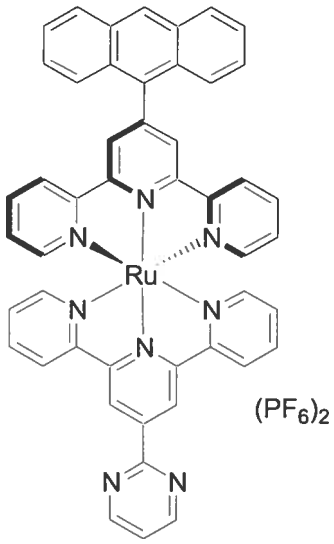

All the complexes **3a-d** were synthesized by following a general procedure outlined below for **3a**. Complex **4** (0.039g, 0.063 mmol), 4'-(pyrimid-2-yl)-terpyridine (0.031 g, 0.080 mmol) and silver nitrate (0.032 g, 0.19 mmol) were heated at reflux in anhydrous DMF (20 mL) for 2 h. The mixture was filtered through celite and the filtrate was evaporated to dryness. The residue was then chromatographed on a silica gel column with 7:1 acetonitrile and saturated aqueous KNO_3. Counteranion exchange with NH_4PF_6 gave pure red product (0.054 g, 0.045 mmol, 72%). Care was taken in order to avoid full laboratory light over the reaction vessel. Purification was accomplished in dim light. ^{1}H NMR (400 MHz, CD_3CN): δ 9.74 (s, 2H), 9.18 (d, J = 4.9 Hz, 2H), 8.94 (s, 2H), 8.90 (s, 1H), 8.76 (d, J = 8.1 Hz, 2H), 8.44 (d, J = 8.0 Hz, 2H), 8.32 (d, J = 8.3 Hz, 2H), 8.19 (d, J = 8.5 Hz, 2H), 8.05 (t, J = 7.9 Hz, 2H), 7.89 (t, J = 8.0 Hz, 2H), 7.68 (m, 7H), 7.49 (d, J = 5.5 Hz, 2H), 7.37 (t, J = 6.5 Hz, 2H), 7.18 (t, J = 6.5 Hz, 2H). ^{13}C NMR (100 MHz, CD_3CN): δ 161.5, 158.8, 158.5, 158.4, 156.4, 155.8, 153.3, 153.1, 147.8, 145.3, 138.7, 138.6, 132.4, 131.8, 130.3, 129.4, 129.3, 128.2, 127.9, 127.4, 126.9, 126.5, 126.3, 125.2, 125.1, 122.4, 122.0. ESI-MS: 411.1 ($[M-2PF_6]^{2+}$, 100%); 967.1, ($[M-PF_6]^+$, 42%). Calc.

for $C_{48}H_{32}N_8Ru$ $(M\text{-}2PF_6)^{2+}$, 411.0891; observed, 411.0890. Calc. for $C_{48}H_{32}N_8RuPF_6$ $(M\text{-}PF_6)^+$, 967.1429; observed, 967.1420. Anal. Calc. for $C_{48}H_{32}N_8RuP_2F_{12}$: C, 51.85; H, 2.90; N, 10.08. Found: C, 38.42; H, 2.53; N, 6.47.

[(An-tpy)Ru(**2b**)]$(PF_6)_2$ (**3b**)

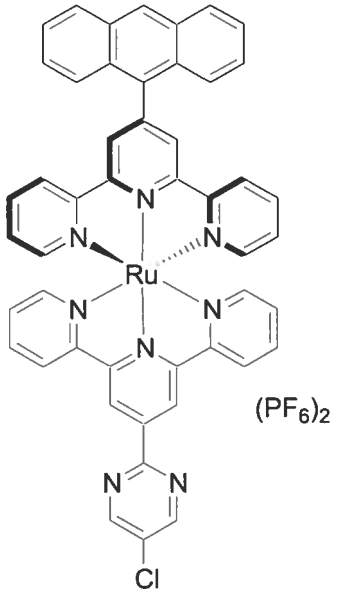

Yield 82%. ^{1}H NMR (400 MHz, CD_3CN): δ 9.70 (s, 2H), 9.19 (s, 2H), 8.95 (s, 2H), 8.90 (s, 1H), 8.76 (d, J = 8.1 Hz, 2H), 8.45 (d, J = 8.0 Hz, 2H), 8.32 (d, J = 8.3 Hz, 2H), 8.20 (d, J = 8.5 Hz, 2H), 8.05 (t, J = 7.9 Hz, 2H), 7.89 (t, J = 8.0 Hz, 2H), 7.69 (m, 6H), 7.49 (d, J = 5.5 Hz, 2H), 7.38 (t, J = 6.5 Hz, 2H), 7.19 (t, J = 6.5 Hz, 2H). ^{13}C NMR (100 MHz, CD_3CN): δ 159.5, 158.5, 158.3, 157.3, 156.5, 155.7, 153.3, 153.1, 147.8, 143.9, 138.7, 138.6, 132.5, 132.4, 131.8, 130.3, 129.3, 129.2, 128.2, 127.9, 127.4, 126.9, 126.5, 126.3, 125.3, 125.2, 122.0. ESI-MS: 428.1 ($[M\text{-}2PF_6]^{2+}$, 100%); 1001.3 ($[M\text{-}PF_6]^+$, 21%). Calc. for $C_{48}H_{31}N_8RuCl$ $(M\text{-}2PF_6)^{2+}$, 428.0696; observed, 428.0695. Calc. for

$C_{48}H_{31}N_8RuClPF_6$ $(M\text{-}PF_6)^+$, 1001.1040; observed, 1001.1033. Anal. Calc. for $C_{48}H_{31}N_8RuClP_2F_{12}$: C, 50.29; H, 2.73; N, 9.78. Found: C, 50.13; H, 2.56; N, 9.64.

[(An-tpy)Ru(**2c**)]$(PF_6)_2$ (**3c**)

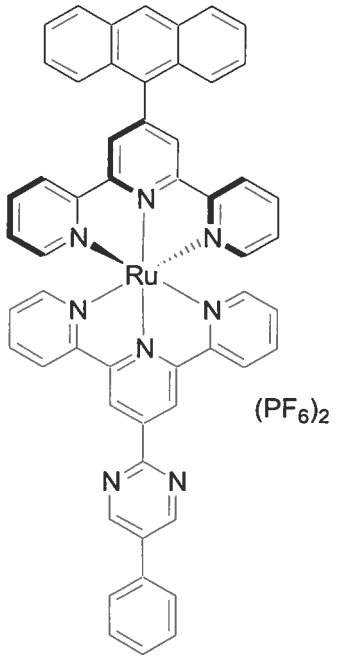

Yiled 72%. ^{1}H NMR (400 MHz, CD_3CN) δ 9.80 (s, 2H), 9.46 (s, 2H), 8.96 (s, 2H), 8.92 (s, 1H), 8.80 (d, J = 7.8 Hz, 2H), 8.45 (d, J = 8.0 Hz, 2H), 8.33 (d, J = 8.2 Hz, 2H), 8.20 (d, J = 8.5 Hz, 2H), 8.06 (t, J = 7.8 Hz, 2H), 7.98 (d, J = 7.4 Hz, 2H), 7.90 (t, J = 7.7 Hz, 2H), 7.68 (m, 9H), 7.52 (d, J = 5.4 Hz, 2H), 7.38 (t, J = 6.2 Hz, 2H), 7.20 (t, J = 6.4 Hz, 2H). ^{13}C NMR (100 MHz, CD_3CN) δ 160.1, 158.6, 158.4, 156.5, 156.4, 155.8, 153.3, 153.1, 147.7, 144.8, 138.7, 138.6, 134.3, 134.2, 131.8, 130.3, 130.0, 129.3, 128.2, 128.0, 127.7, 127.4, 126.9, 126.5, 126.4, 132.5, 129.3, 128.1, 125.3, 125.2, 121.9. ESI-MS: 449.0 ($[M\text{-}2PF_6]^{2+}$, 86%), 1043.4 ($[M\text{-}PF_6]^+$, 100%). Calc. for $C_{54}H_{36}N_8Ru$ $(M\text{-}2PF_6)^{2+}$,

449.1048; observed, 449.1040. Calc. for $C_{54}H_{36}N_8RuPF_6$ $(M\text{-}PF_6)^+$, 1043.1742; observed, 1043.1738. Anal. Calc. for $C_{54}H_{36}N_8RuP_2F_{12}$: C, 54.60; H, 3.05; N, 9.43. Found: C, 54.45; H, 2.84; N, 9.81.

[(An-tpy)Ru(**2d**)]$(PF_6)_2$ (**3d**)

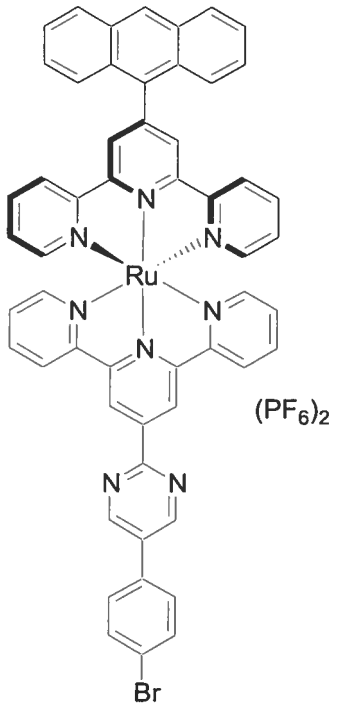

Yield 70%. ^{1}H NMR (400 MHz, CD_3CN) δ 9.79 (s, 2H), 9.42 (s, 2H), 8.96 (s, 2H), 8.90 (s, 1H), 8.79 (d, J = 8.0 Hz, 2H), 8.47 (d, J = 8.1 Hz, 2H), 8.32 (d, J = 7.1 Hz, 2H), 8.22 (d, J = 8.1 Hz, 2H, H), 8.07 (t, J = 7.8 Hz, 2H), 7.88 (m, 6H), 7.70 (m, 6H), 7.55 (d, J = 5.7 Hz, 2H), 7.40 (t, J = 6.6 Hz, 2H), 7.22 (t, J = 6.6 Hz, 2H). ^{13}C NMR (100 MHz, CD_3CN) δ 160.4, 158.5, 158.4, 156.4, 156.4, 155.8, 153.3, 153.1, 147.8, 144.7, 138.7, 138.6, 133.4, 133.2, 133.0, 132.5, 131.8, 130.3, 129.6, 129.4, 129.3, 128.2, 128.0, 127.4, 127.0, 126.5, 126.4, 125.3, 125.2, 123.9, 121.9. ESI-MS: 488.9 ($[M\text{-}2PF_6+H]^{2+}$, 100%).

Calc. for $C_{54}H_{35}N_8RuBr$ $(M\text{-}2PF_6)^{2+}$, 488.0601; observed, 488.0602. Calc. for $C_{54}H_{35}N_8RuBrPF_6$ $(M\text{-}PF_6)^+$, 1121.0847; observed, 1121.0852. Anal. Calc. for $C_{54}H_{35}N_8RuBrP_2F_{12}$: C, 51.20; H, 2.78; N, 8.85. Found: C, 61.41; H, 5.75; N, 6.51.

[(An-tpy)Ru(tpy)]$(PF_6)_2$ (**3e**)

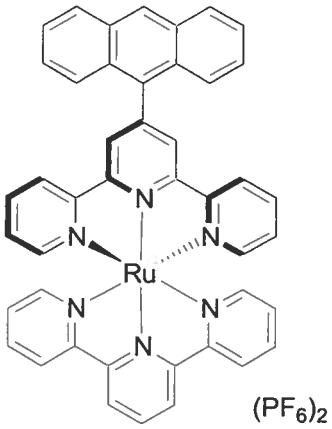

Complex **3e** was prepared from ruthenium tpy trichloride and an-tpy ligand following the general procedure for **3a**. Yield 84%. ^{1}H NMR (400 MHz, CD_3CN): δ 8.91 (s, 2H), 8.89 (s,1 H), 8.80 (d, J = 8.1 Hz, 2 H), 8.56 (d, J = 8.3 Hz, 2H), 8.46 (t, J = 8.1 Hz, 1 H), 8.42 (d, J = 8.2 Hz, 2H), 8.31 (d, J = 8.2 Hz, 2H), 8.18 (d, J = 8.2 Hz, 2H), 7.98 (t, J = 7.9 Hz, 2H), 7.88 (t, J = 7.9 Hz, 2H), 7.65 (m, 6H), 7.42 (d, J = 5.6 Hz, 2H), 7.33 (t, J = 6.6 Hz, 2H), 7.19 (t, J = 6.6 Hz, 2H). ^{13}C NMR (100 MHz, CD_3CN): δ 158.6, 158.4, 156.0, 155.8, 153.3, 153.0, 147.3, 138.6, 138.4, 136.3, 132.5, 131.8, 130.2, 129.3, 129.2, 128.0, 127.9, 127.4, 126.8, 126.5, 126.3, 125.1, 124.8, 124.2. ESI-MS: 372.1 ($[M\text{-}2PF_6]^{2+}$, 100%); 889.1 ($[M\text{-}PF_6]^+$, 72%). Calc. for $C_{44}H_{30}N_6Ru$ $(M\text{-}2PF_6)^{2+}$, 372.0782; observed, 372.0730. Calc. for $C_{44}H_{30}N_6RuPF_6$ $(M\text{-}PF_6)^+$, 889.1211; observed, 889.1195. Anal.

Calc. for $C_{44}H_{30}N_6RuP_2F_{12}$: C, 51.12; H, 2.93; N, 8.13. Found: C, 49.99; H, 2.99; N, 8.08.

3.5 References

* Part of this work has been published as a communication: J. Wang, G. S. Hanan, F. Loiseau, S. Campagna *Chem. Commun.* **2004**, 2068.

§ CCDC 235987. See http://www.rsc.org/suppdata/cc/b4/b405619a/ for crystallographic data for **3d** in .cif or other electronic format.

1 (a) J. P. Sauvage, J. P. Collin, J. C. Chambron, S. Guillerez, C. Coudret, V. Balzani, F. Barigelletti, L. De Cola, L. Flamigni *Chem. Rev.* **1994**, *94*, 993. (b) M. Maestri, N. Armaroli, V. Balzani, E. C. Constable, A. M. Cargill Thompson *Inorg. Chem.* **1995**, *34*, 2759. (c) F. Barigelletti, L. Flamigni *Chem. Soc. Rev.* **2000**, *29*, 1. (d) A. El-ghayoury, A. Harriman, A. Khatyr, R. Ziessel *Angew. Chem. Int. Ed.* **2000**, *39*, 185. (e) S. Encinas, L. Flamigni, F. Barigelletti, E. C. Constable, C. E. Housecroft, E. R. Schofield, E. Figgemeier, D. Fenske, M. Neuburger, J. G. Vos, M. Zehnder *Chem. Eur. J.* **2002**, *8*, 137. (f) E. Baranff, J.-P. Collin, L. Flamigni, J.-P. Sauvage *Chem. Soc. Rev.* **2004**, *33*, 147.

2 (a) V. Balzani, A. Juris, M. Venturi, S. Campagna, S. Serroni *Chem. Rev.* **1996**, *96*, 956., and refs. therein. (b) A. Hagfeldt, M. Graetzel *Acc. Chem. Res.* **2000**, *33*, 269. (c) L. Sun, L. Hammarström, B. Akermark, S. Styring *Chem. Soc. Rev.* **2001**, *30*, 36. (d) R. Ballardini, V. Balzani, A. Credi, M. T. Gandolfi, M. Venturi *Acc. Chem. Res.* **2001**, *34*, 445. (e) D. Pomeranc, V. Heitz, J.-C. Chambron, J.-P. Sauvage *J. Am. Chem. Soc.* **2001**, *123*, 12215. (f) C. J. Kleverlaan, M. T. Indelli, C. A. Bignozzi, L. Pavanin, F. Scandola, G. M. Hasselman, T. J. Meyer *J. Am.*

Chem. Soc. **2002**, *122*, 2840. (g) G. Benkö, J. Kallioinen, J. E. I. Korppi-Tommola, A. P. Yartsev, V. Sundström *J. Am. Chem. Soc.* **2002**, *124*, 489.

3 (a) T. J. Meyer *Pure Appl. Chem.* **1986**, *58*, 1193. (b) A. Juris, V. Balzani, F. Barigelletti, S. Campagna, P. Belser, A. von Zelewsky *Coord. Chem. Rev.* **1988**, *84*, 85., and refs. therein.

4 (a) M. Beley, J.-P. Collin, R. Louis, B. Metz, J.-P. Sauvage *J. Am. Chem. Soc.* **1991**, *113*, 851. (b) J.-P. Collin, M. Beley, J.-P. Sauvage, F. Barigelletti *Inorg. Chim. Acta.* **1991**, *186*, 91. (c) M. Beley, J.-P. Collin, J.-P. Sauvage *Inorg. Chem.* **1993**, *32*, 4539. (d) E. C. Constable, A. M. W. Cargill Thompson, J. Cherryman, T. Liddiment *Inorg. Chim. Acta* **1995**, *235*, 165.

5 (a) E. C. Constable, A. M. W. Cargill Thompson, N. Ararmoli, V. Balzani, M. Maestri *Polyhedron* **1992**, *11*, 2707. (b) M. T. Indelli, C. A. Bignozzi, F. Scandola, J.-P. Collin *Inorg. Chem.* **1998**, *37*, 6084. (c) M. Maestri, N. Armaroli, V. Balzani, E. C. Constable, A. M. W. Cargill Thompson *Inorg. Chem.* **1995**, *34*, 2759. (d) F. Barigelletti, L. Flamigni, M. Guardigli, A. Juris, M. Beley, S. Chodorowski-Kimmes, J.-P. Collin, J.-P. Sauvage *Inorg. Chem.* **1996**, *35*, 136. (e) Y.-Q. Fang, N. J. Taylor, G. S. Hanan, F. Loiseau, R. Passalacqua, S. Campagna, H. Nierengarten, A. van Dorsselaer *J. Am. Chem. Soc.* **2002**, *124*, 7912. (f) J. Wang, Y.-Q. Fang, G. S. Hanan, F. Loiseau, S. Campagna *Inorg. Chem.* **2005**, *44*, 5.

6 (a) L. Hammarström, F. Barigelletti, L. Flamigni, M. T. Indelli, N. Armaroli, G. Calogero, M. Guardigli, A. Sour, J.-P. Collin, J.-P. Sauvage *J. Phys. Chem. A*

1997, *101*, 9061. (b) L. M. Vogler, K. J. Brewer *Inorg. Chem.* **1996**, *35*, 818. c) A. Harriman, R. Ziessel *Chem. Commun.* **1996**, 1707. (c) A. C. Benniston, A. Harriman, V. Grosshenny, R. Ziessel *New J. Chem.* **1997**, *21*, 405. (d) A. El-ghayoury, A. Harriman, A. Khatyr, R. Ziessel *J. Phys. Chem. A* **2000**, *107*, 1512.

7 (a) W. E. Ford, M. A. J. Rodgers *J. Phys. Chem.* **1992**, *96*, 2917. (b) G. J. Wilson, A. Launikonis, W. H. Sasse, A. W.-H. Mau *J. Phys. Chem. A* **1997**, *101*, 4860. (c) J. A. Simon, S. L. Curry, R. H. Schmehl, T. R. Schatz, P. Piotrowiak, X. Jin, R. P. Thummel *J. Am. Chem. Soc.* **1997**, *119*, 11012. (d) D. S. Tyson, C. R. Luman, X. Zhou, F. N. Castellano *Inorg. Chem.* **2001**, *40*, 4063. (e) B. Maubert, N. D. McClenaghan, M. T. Indelli, S. Campagna *J. Phys. Chem. A* **2003**, *107*, 447. (f) R. Passalacqua, F. Loiseau, S. Campagna, Y.-Q. Fang, G. S. Hanan *Angew. Chem. Int. Ed.* **2003**, *42*, 1608. (g) J. Wang, G. S. Hanan, F. Loiseau, S. Campagna *Chem. Commun.* **2004**, 2068. (h) N. D. McClenaghan, Y. Leydet, B. Maubert, M. T. Indelli, S. Campagna *Coord. Chem. Rev.* **2005**, in press.

8 (a) G. S. Hanan, C. R. Arana, J.-M. Lehn, D. Fense *Angew. Chem. Int. Ed. Engl.* **1995**, *34*, 1122. (b) G. S. Hanan, C. R. Arana, J.-M. Lehn, D. Fense *Chem. Eur. J.* **1996**, *2*, 1292.

9 (a) G. Albano, V. Balzani, E. C. Constable, M. Mastri,D. R. Smith *Inorg. Chim. Acta* **1998**, *277*, 225. (b) J. Wang, G. S. Hanan *Synlett* **2005**, in press.

10 I. W. Davies, J.-F. Marcoux, J. Wu, M. Palucki, E. G. Corley, M. A. Robbins, N. Tsou, R. G. Ball, P. Dormer, R. D. Larsen, P. J. Reider *J. Org. Chem.* **2000**, *65*, 4571.

11 Y.-Q. Fang *Master's thesis.* Department of Chemistry, University of Waterloo, Canada. **2002**.

12 S. L. Murov, I. Carmichael, G. L. Hug, In: *Handbook of Photochemistry*, Marcel Dekker, New York, **1993**.

13 A similar effect was reported previously: R. P. Thummel, Y. Jahng, *Inorg. Chem.* **1986**, *25*, 2527.

Chapter 4

Synthesis and Properties of the Elusive Cyano-complexes: Facile Palladium-Catalyzed Cyanation on the Ru(II) Terpyridine Complexes*

4.1 Introduction

Since the tridentate ligand 2,2':6',2"-terpyridine (tpy) was first prepared over 70 years ago,[1] the coordination chemistry of tpy based ligands has been widely studied.[2] Areas of the research include the application of tpy complexes as protein labels,[3] reagents for enantioselective synthesis,[4] modifiers for porphyrins,[5] catechols,[6] and macrocycles,[7] in solar energy devices based on modified nanocrystalline TiO_2 surface[8] and in supramolecular chemistry to build up the linear multinuclear assemblies for energy and/or electron transfer process at molecular level.[9]

Ru(II) complexes based on polypyridyl ligands have rich photophysical properties.[2f] Indeed, ruthenium(II) polypyridyl complexes play outstanding roles in fields connected to solar energy conversion and the storage of light and/or electronic information at the molecular level. The Ru(II) complexes based on the 2,2'-bipyridine ligand are most commonly used due to their favorable photophysical properties, which have relative long room temperature (rt) excited state lifetimes ($Ru(bpy)_3^{2+}$, $\tau = 1$ μs).[10] However, the chirality inherent to the Ru(II) bpy complex hindered their application in linear assemblies for vectorial energy and/or electron transfer. These problems, inherent to the $Ru(bpy)_3^{2+}$ structural motif, can indeed be overcome by the use of tridentate tpy-

type polypyridine ligands.[11] The chemical modification on the 4'-position of tpy ligand will maintain the *C2* axe in the complex, which can make the synthesis and purification of a linear arrangement easier. However, $Ru(tpy)_2^{2+}$ and derivatives have far less useful photophysical properties than $Ru(bpy)_3^{2+}$, essentially due to a short excited-state lifetime (<250 ps) at room temperature.[2f] These unfavorable photophysical properties are due to proximity (in energy) between the lowest-lying triplet metal-to-ligand charge transfer (^{3}MLCT) and metal-centered (^{3}MC) states, with the latter governing the excited-state decay dynamics by thermally-activated surface crossing.

Approaches to extend the excited state lifetime of $Ru(tpy)_2^{2+}$ complexes have mainly focused on: (1) the manipulation of the energy of the emitting ^{3}MLCT, including cyclometalating ligands,[12] electron-donating (D) and -accepting (A) substituents (**Figure 4.1**),[13] σ-donor lgands[14] and π-delocalization[15]; (2) the introduction of secondary organic chromophores (OC) to develop the energy equilibrium between ^{3}MLCT and ^{3}OC state.[16]

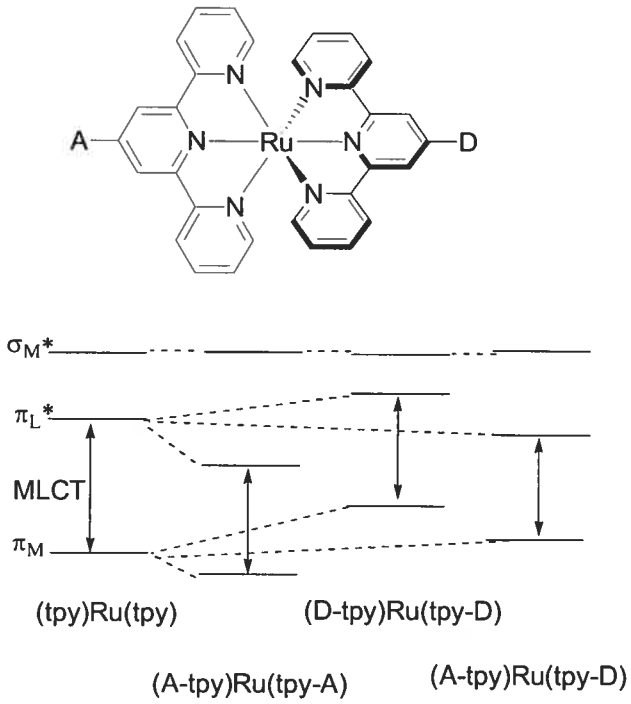

Figure 4.1 Energy diagram of the frontier orbitals (HOMO (π_M), LUMO (π_L*) and (σ_M*) of $Ru(tpy)_2^{2+}$ complexes effected by electron accepting and donating substituents (A = electron accepting substituent, D = electron donating substituent).[13c]

For the strategy based on electron withdrawing and/or donor substituents, electron withdrawing substituents stabilize the LUMO π* ligand orbital more than the HOMO $\pi(t_{2g})$ metal orbital without interfering with the anti-bonding σ* orbital, thereby increasing the energy gap between ^{3}MLCT and ^{3}MC excited state and minimizing the thermally-activated surface crossing which dominates the ^{3}MLCT deactivation processes. It has been shown that 4'-sulfonyl-tpy based complexes have proponged r.t. lifetimes ($[(MeSO_2\text{-tpy})_2Ru](PF_6)_2$, 25.0 ns; $[(MeSO_2\text{-tpy})Ru(tpy\text{-}OH)](PF_6)_2$, 50.0 ns).[13c] This approach featured facile synthesis of the ligands and their complexes. In addition, mono-exponential decay of the excited-state renders them relatively easier to study as compared

to bichromophoric systems with non-emissive triplet organic states. Thus, the synthetic procedure for the synthesis of polynuclear arrays based on 4'-substituted tpy is greatly simplified.

We envisioned that coordination of 4'-cyano-tpy with a Ru(II) center should provide a very large effect on the energy state and increase the energy gap between ^{3}MLCT and ^{3}MC state, thereby prolonging the rt lifetime of the complexes. Moreover, due to the strong coordination capacity of the cyano group, the metal complexes containing cyano groups can act as building blocks to build up linear polymetallic units.[17] Katz has reported a new mononuclear complex ($[Ru(bpy)_2(5\text{-}CNphen)]^{2+}$, bpy = 2,2'-bipyridine; 5-CNphen = 5-cyano-1,10-phenanthroline) as a precursor for polynuclear molecular entities that may engage in light-induced electron-transfer processes.[17b] In particular, 5-cyano-1,10-phenanthroline can bridge two ruthenium atoms to build mixed-valent di-ruthenium system ($[Ru^{II}(bpy)_2(5\text{-}CNphen)Ru^{III}(NH_3)_5](PF_6)_5$, **Figure 4.2**) with a slight electronic coupling at a considerable distance. The redox asymmetry and the moderate reorganization energy results in a charge recombination process close to the barrierless region. The mixed-valent system described in the work is thus a good model for testing current electron-transfer theories (**Scheme 4.1**).

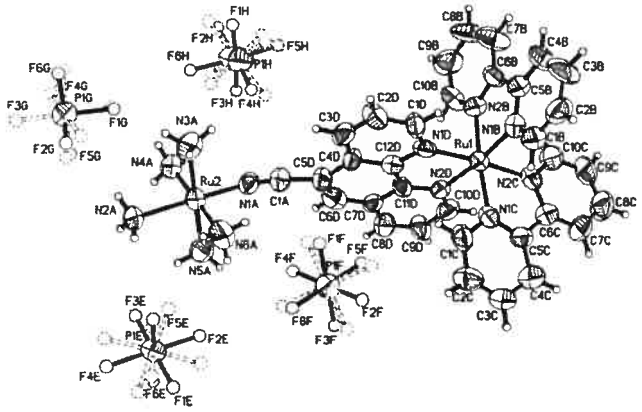

Figure 4.2 A recent example of di-ruthenium system, which has a slight electronic coupling, using 5-cyano-1,10-phenanthroline ligand as the bridging ligands.[17b]

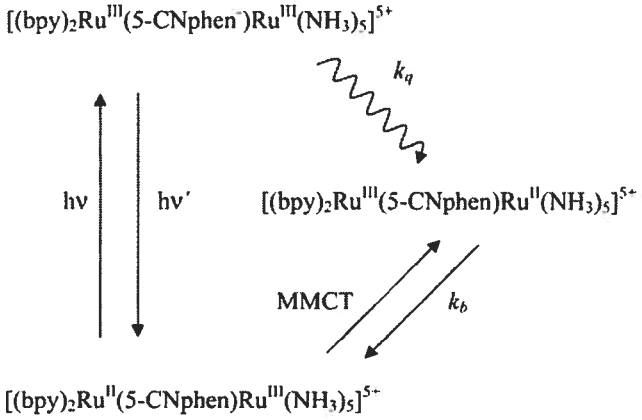

Scheme 4.1 Possible intramolecular electron-transfer processes taking place after light excitation of the mixed-valent Ru(II)-Ru(III) dimer.[17b]

However, the efficient way to introduce the cyano groups onto an activated position (which has direct interaction with metal center) of the ligands upon coordination to the metal center has not been published previously. A synthetic approach to introduce the cyano group(s) into the Ru(II) complexes was developed using an efficient palladium-

catalyzed cyanation reaction[18] on the complexes based on the "chemistry-on-the-complex" concept.[19]

4.2 Results and Discussion

4.2.1 Synthesis

Originally, the synthetic method of 4'-cyano-tpy ligand (NC-tpy) was developed through sequential reactions (**Scheme 4.2**).[20] However, this long sequence suffered from (1) low overall yield; (2) the emission of highly toxic methylthiol; (3) inefficient cyanation with high load of potassium cyanide.

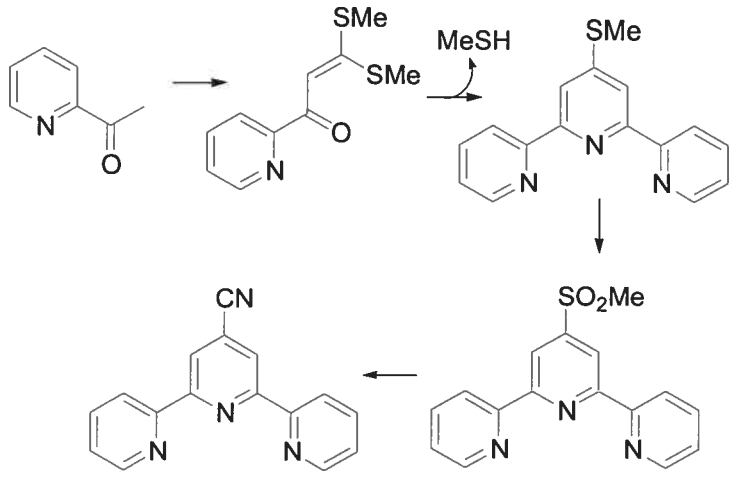

Scheme 4.2 Original synthesis of 4'-cyano-2,2':6',2"-terpyridine ligand.[20]

The optimization of the synthesis of NC-tpy started with 4'-chloro-2,2':6',2"-terpyridine ligand (Cl-tpy), which was used as the substrate for the transition-metal catalyzed cyanation reaction. Cl-tpy is commercially available from Sigma-Aldrich or is easily synthesized in 50 mmol scale following reported methods.[21] After surveying the efficient cyanation conditions, the reaction conditions reported by Jin and Confalone[22] seemed promising with very high yields. The palladium(0)-catalyzed cyanation reaction

on Cl-tpy proceeded smoothly to give 95% yield of NC-tpy under modified conditions (0.6 equiv. $Zn(CN)_2$, 2 mol% $Pd_2(dba)_3$, 4 mol% dppf, 12 mol% Zn dust (325 mesh) in DMA at 120°C for 6 h, **Scheme 4.3**). This improvement features (1) high efficiency and high yield; (2) low catalyst load (2 mol% Pd(0)); (3) less toxicity $Zn(CN)_2$ as cyanation reagent; (4) column free purification; (5) short reaction time.

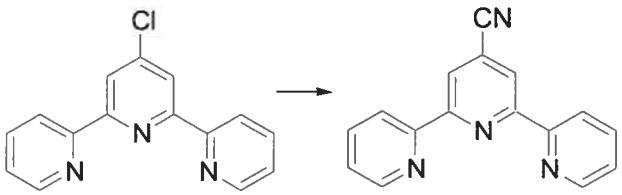

Scheme 4.3 Synthesis of 4'-cyano-2,2':6',2"-terpyridine through palladium(0)-catalyzed cyanation of 4'-chloro-2,2':6',2"-terpyridine. Reagents and conditions: 0.6 equiv. $Zn(CN)_2$, 1 mol% $Pd_2(dba)_3$, 2 mol% dppf, 6 mol% Zn dust (325 mesh) in DMA at 120°C for 6 h.

With the facile approach to NC-tpy in hand, the incorporation of NC-tpy ligand into Ru(II) complexes was then attempted. Our initial approach to the Ru(II) complexes with cyano group(s) adopted the classical way to synthesis the complex from 4'-cyano-tpy ligand (**Scheme 4.4**). Various complexation conditions have been surveyed to find a convenient way to synthesize the elusive cyano complexes. However, the complexation starting from 4'-cyano-tpy ligand always ended up with carboximide complexes, which resulted from the attack of the cyano group by nucleophiles (trace H_2O, MeOH or EtOH) under the relatively harsh reaction conditions for the synthesis of Ru(II) complexes of 4'-

cyano-tpy. The strong activation of the cyano group to nuclear attack upon coordination with the Ru(II) metal center has kept these complexes veiled.

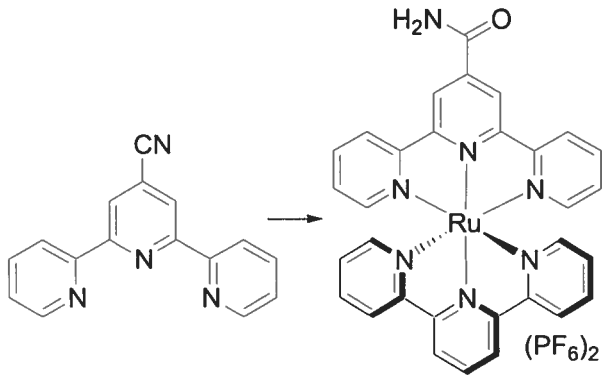

Scheme 4.4 Classical approach to the Ru(II) 4'-cyano-2,2':6',2"-terpyridine complex. Reagent and conditions: 1.0 equiv. $Ru(tpy)Cl_3$, 3.0 equiv. $AgNO_3$, MeOH or EtOH or DMF, reflux, 2-16 h.

In order to bypass the possible destruction of the cyano group upon coordination, we turned our focus onto the "chemistry-on the-complex" concept through the transition metal catalyzed cyanation on the Ru(II) complexes. In order to elucidate this methodology to perform the cyanation on the complexes, we first choose two Ru(II) terpyridine complexes, homoleptic **1a** and hetereoleptic **1b** (**Scheme 4.5**), as our starting materials. After several unsuccessful attempts to perform Ni(0) catalyzed cyanation[23] (1.0 equiv. KCN, 10mol % $Ni(PPh_3)_2Br$, 10mol % Zn, 20 mol% PPh_3, DMF or acetonitrile, 60°C) on these complexes, we turned to perform Pd(0) catalyzed-cyanation on the complexes.[22] Then we applied slightly modified conditions to complexes **1a** and **1b** (**Scheme 4.5**). Reaction of the heteroleptic complex **1a** with 0.6 equiv. $Zn(CN)_2$, 5 mol% $Pd_2(dba)_3$, 10 mol% dppf, 30 mol% Zn dust (325 mesh) in DMA at 120°C for 6 h

afforded cyano-complex **2a** quantitively. For the homoleptic complex **1b**, modification of the stoichemistry of the reagents and longer reaction time gave out the same full conversion to homoleptic cyano-complex **2b**. The full conversion of the chloride to the cyanide was secured by the strong activation effect from the Ru(II) cations.

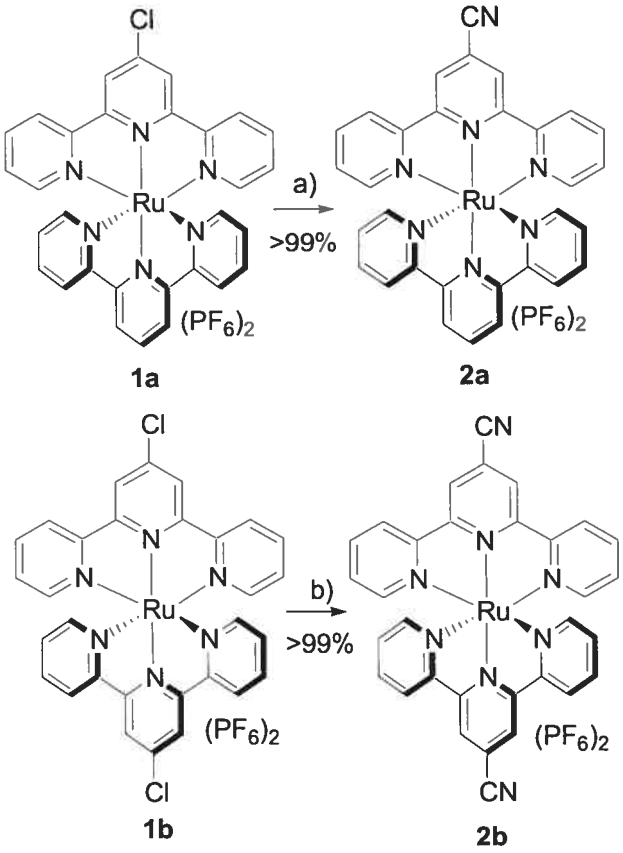

Scheme 4.5 Palladium-catalyzed cyanation of Ru(II) complexes of 4'-chloro-2,2':6',2"-terpyridine. Reagents and conditions: a) 0.6 equiv. $Zn(CN)_2$, 5 mol% $Pd_2(dba)_3$, 10 mol% dppf, 30 mol% Zn dust (325 mesh), DMA, 120°C, 6 h; b) 1.2 equiv. $Zn(CN)_2$, 5 mol% $Pd_2(dba)_3$, 10 mol% dppf, 30 mol% Zn dust (325 mesh), DMA, 120°C, 12 h.

With the satisfactory results from the Pd(0)-catalyzed cyanation of complexes **1a** and **1b**, we then applied the optimized reaction conditions (1.2 equiv. $Zn(CN)_2$, 10 mol% $Pd_2(dba)_3$, 20 mol% dppf, 60 mol% Zn dust (325 mesh), DMA, 120°C, 12 h.) to the other substrates, complexes **1c-d** (**Scheme 4.6**). For the complexes **1c-d**, the reactions under the optimized conditions have yielded nearly full conversion of the starting materials (more than 90% isolated yields). The optimized conditions for the cyanation of Ru(II) complexes are extremely powerful, even the nonactivated bromide **1d** was obtained in quantitative yield, despite the distant separation from Ru(II) center.

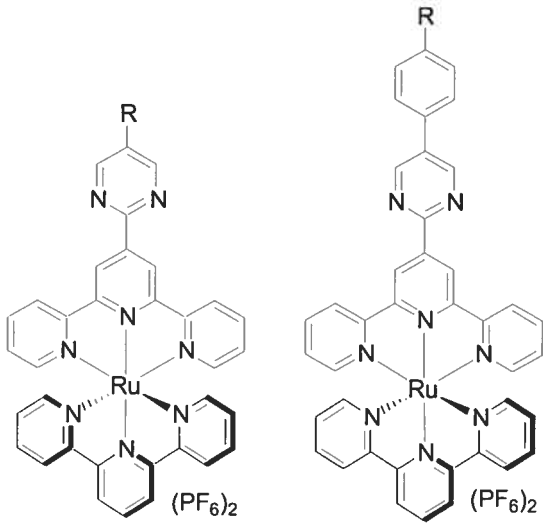

1c R = Cl
2c R = CN

1d R = Br
2d R = CN

Scheme 4.6 Palladium catalyzed cyanation on Ru(II) complexes **1c-d**. Reagents and conditions: 0.6 equiv. $Zn(CN)_2$, 5 mol% $Pd_2(dba)_3$, 10 mol% dppf, 30 mol% Zn dust (325 mesh), DMA, 120°C, 6 h.

4.2.2 NMR spectroscopy

The newly synthesized complexes **2a-d** have been verified by ^{1}H and ^{13}C NMR spectroscopy. The ^{1}H NMR spectroscopic data of complexes **2a-d** in CD_3CN are compiled in **Table 4.1**.

Table 4.1 ^{1}H NMR data of complexes **1a-d** and complexes **2a-d** with $Ru(tpy)_2^{2+}$ as reference.[a]

Complex	chemical shifts δ / ppm												
	3,3"	4,4"	5,5"	6,6"	3',5'	3,3"	4,4"	5,5"	6,6"	3',5'	4'	Pm	Ph
3[b]	8.48	7.91	7.15	7.33	8.74						8.40		
1a	8.46	7.92	7.16	7.34	8.82	8.46	7.89	7.12	7.33	8.72	8.40		
2a	8.52	8.00	7.26	7.42	9.06	8.50	7.93	7.16	7.29	8.78	8.49		
1b	8.50	7.97	7.21	7.41	8.87								
2b	8.53	8.00	7.33	7.58	9.02								
1c	8.69	7.96	7.21	7.40	9.63	8.51	7.93	7.15	7.40	8.78	8.45		
2c	8.72	7.98	7.24	7.41	9.70	8.51	7.98	7.15	7.41	8.80	8.48	9.46	
1d	8.69	7.94	7.19	7.40	9.70	8.49	7.94	7.15	7.37	8.75	8.43	9.37	7.94
2d	8.74	8.01	7.23	7.44	9.75	8.53	8.01	7.17	7.41	8.80	8.47	9.46	8.11 8.01

[a] All the spectra were collected in CD_3CN at r.t. at 400 MHz. The assignments of the ^{1}H NMR signals were assisted by two-dimensional COSY spectra. The proton signals from the tpy moieties are underlined. [b] Data from ref. 1g, **3** = $Ru(tpy)_2^{2+}$

Through the comparison of the ^{1}H NMR spectra of newly synthesized complexes **2a-d** with their respective starting materials **1a-d**, we noted that the introduction of a cyano group onto the ligands through the Pd(0)-catalyzed cyanation reaction has greatly

changed the chemical environments of the neighbouring protons. The proton chemical shift of the rings to which the cyano groups were attached have been deshielded with about 0.1-0.3 ppm due to the electron withdrawing effects of cyano groups. In the case of complexes **2a-b**, even the proton signals from the tpy moieties have been shifted to lower field due to the direct connection of the cyano groups. Due to the coplanarity of the pyrimidine ring in complex **2c**, the cyano groups still have a notable effect to the chemical environments of tpy moieties with a slight deshielding effect in the NMR spectra. It is noteworthy that the strong effect from the cyano group can be seen in complex **2d**, in which the cyano group is separated from (tpy)Ru(tpy-pm)$^{2+}$ moiety with nonplanar phenyl linker. The long distance electron withdrawing effect is crucial to the photophysical properties (*c.f.* photophysical data) due to the strong electron withdrawing effect of the cyano group, which can increase the energy gap between ^{3}MC and ^{3}MLCT and in turn prolong the lifetimes as well as increase the quantum yields.

4.2.3 Crystal structure determination

The solid-state structures of the complexes **2c** was determined by X-ray crystallography. Recrystallization of **2c** from acetonitrile solution through slowly dispersed diethyl ether vapor provided dark-red single crystal suitable for X-ray crystallography. Crystal parameters and details of the data collection and refinement are given in **Table 4.2**. The ORTEP diagrams of the cation of complexes **2c** is showed in **Figure 4.3**. Selected bond lengths and angles are given in **Table 4.3**.

The Ru-to-N bond lengths and internal pyridine angles are similar to those found in the parent systems.[24] The pyrimidyl group lies virtually co-planar to the N4-N6

terpyridine (2.0° torsion angle, **Figure 4.3**). Due to the co-planarity of the pyrimidine ring to the tpy moiety, the strong electron withdrawing effect from the cyano group can extend to the tpy moiety through the conjugation. The co-planar nature of the pyrimidine-tpy sub-unit favours π-conjugation and is crucial for the enhanced photophysical properties of these complexes (*c.f.*, photophysics).

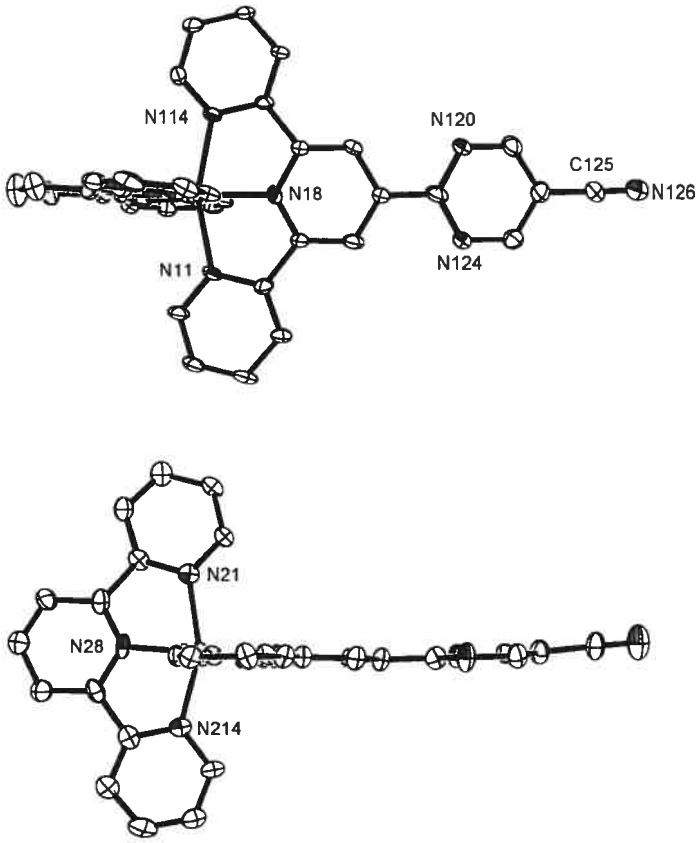

Figure 4.3 ORTEP plots of the X-ray crystal structure of complex **2c** exposing the tpy-pm-CN ligand (top) and, after a 90° rotation, the tpy ligand (bottom). Thermal ellipsoids are set at 30% probability with hydrogen atoms and counteranions omitted for clarity.

The bond length and bond angle of the cyano group are of a typical triple bond (N9 - C35, 1.11 Å). The N9 - C35 - C33 angle is 177.5°, a nearly perfect linear C-C≡N bond, which also confirmed the introduction of the elusive cyano group onto the complex **2c**.

Table 4.2 Crystallography data for complexes **2c**.

Complex	**2c**
Molecular formula	$C_{35}H_{23}N_9Ru$
M	670.69
Crystal system	Triclinic
a/Å	8.6272(4)
b/Å	8.8957(3)
c/ Å	28.2782(11)
α/°	81.425(2)
β/°	86.118(2)
γ/°	86.135(2)
U/Å^3	2137.29(15)
Space group	P-1
Z	2
Dc/Mg m^{-3}	1.042
μ/mm^{-1}	3.202
Temperature/K	100 (2) K
R1	0.0996
wR2	0.2812

Table 4.3 Selected bond lengths (Å) and angles (°) in complexes **2c**.

bond lengths (Å)			bond angles (°)			
Ru	N21	2.068(7)	N21	Ru	N28	77.7(3)
Ru	N28	1.996(6)	N21	Ru	N214	157.8(3)
Ru	N214	2.037(7)	N28	Ru	N214	80.2(3)
Ru	N114	2.083(6)	N28	Ru	N18	178.7(3)
Ru	N18	1.993(6)	N114	Ru	N18	79.0(3)
Ru	N11	2.066(6)	N114	Ru	N11	158.0(3)
N126	C125	1.106(12)	N18	Ru	N11	79.2(3)
			N126	C125	C122	177.5(1)

4.2.4 Electrochemistry

Electrochemical data also showed that the introduction of the cyano into the complexes destabilized the Ru(III) state and increased the potential of the Ru(II)/Ru(III) couple (**Table 4.4**).

The half wave potentials of metal-centered oxidation of **2a** and **2b** have increased by more than 80 mV compared to $Ru(tpy)_2^{2+}$ (**3**). The ligand-centered reductions are facilitated as a result of the electron withdrawing nature of the cyano group.

The shifts of half wave potentials of metal-centered oxidation of **2c** and **2d** are nearly the same as that of **3**, in accordance with the effects in Ru(II) 5-R-pyrimid-2-yl-tpy complexes.[20] The first and the second one-electron reductions are assigned to the R-pm-tpy ligand and tpy ligand, respectively. The ligand-centered reductions of **2c** and **2d** shifted to more positive values as the combined results of the electron-withdrawing cyano group and π-accepting ability of pyrimidine. It is noteworthy that the strong electron-

withdrawing effect from the cyano group on the reduction potential of complex **2d** diminishes when cyano group and $(tpyRu(tpy\text{-}pm)^{2+}$ moiety is separated by a phenyl spacer.

Table 4.4 Electrochemical data of complexes **2a-d**.[a]

complex	E_{ox}/V (ΔE_p/mV)	E_{red}/V (ΔE_p/mV)
1a	+1.33 (70)	-1.16 (65), -1.46 (80)
2a	+1.42 (64)	-1.15 (70), -1.44 (70), -1.81 (60)
1b	+1.40 (70)	-1.27 (65), -1.46 (80)
2b	+1.49 (65)	-0.88 (70), -1.15 (ir), -1.63 (ir)
1c	+1.33 (90)	-1.09 (60), -1.46 (70), -1.73 (ir)
2c	+1.34 (75)	-0.92 (70), -1.34 (70), -1.60 (80)
1d	+1.30 (80)	-1.11 (70), -1.46 (80), -1.79 (90)
2d	+1.30 (90)	-1.07 (70), -1.42 (70), -1.59 (ir)
3[b]	+1.32	-1.27, -1.52

[a] V vs SHE. Data were collected in Ar purged acetonitrile at rt with 0.1 M supporting electrolyte, Bu_4NPF_6. Working electrode, platinum wire. Redox potentials were corrected by internal reference to ferrocence (395 mV vs SCE). [b] **3** = $Ru(tpy)_2^{2+}$, data from ref. 1g.

4.2.5 Absorption and emission measurements

The absorption spectra of the new species are dominated by spin-allowed MLCT bands in the visible region (**Table 4.5**). The absorption and emission spectra of complex **2b** are showed in **Figure 4.4**. We noted that the cyano-substitution on the 4'-position or on the conjugated pyrimidyl has an strong electron withdrawing effect on the metal

center. The ^{1}MLCT bands of **2a** and **2b** (**Figure 4.4** and **Figure 4.5**) have red-shifted to 489 nm and 505 nm, respectively. Compared with that of $[Ru(tpy)_2](PF_6)_2$ (**4**) at 476 nm, the introduction of cyano group on the 4'-position of the tpy moiety has lowered the ^{1}MLCT state. In complex **2d**, the phenyl spacer between the cyano group and conjugated system diminishes the electron withdrawing effect on the metal center, presenting only a 2 nm red-shift compared to the (Ph-pm-tpy)Ru(tpy)$(PF_6)_2$[5d] moiety. In order to lower ^{1}MLCT energy state as well as ^{3}MLCT energy state, directly connection of the cyano group with MLCT emitting state is needed.

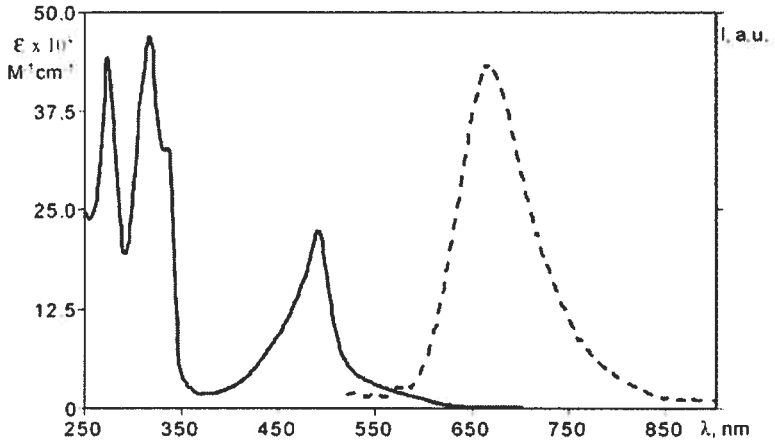

Figure 4.4 Absorption (-) and emission (- - -) spectra of **2b** in acetonitrile solution.

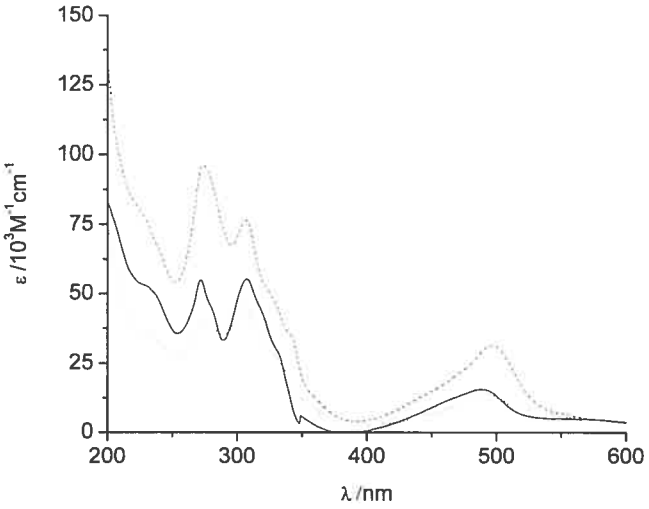

Figure 4.5 UV-vis spectra of complex **2a** (solid line), **2c** (dashed line) and **2d** (dotted line) in acetonitrile solution.

Table 4.5 Absorption spectra data of complexes **2a-d**.[a]

complex	λ_{max}/nm ($\varepsilon/10^3$ $M^{-1}cm^{-1}$)
5 (NC-tpy)	336 (6.9)
1a	478 (14.5)
2a	489 (15.7), 307 (55.4), 272 (55.2)
1b[c]	480 (16.0)
2b	490 (22.4),
1c[b]	487 (23.7)
2c	497 (31.3), 307 (76.5), 274 (96.3)
1d[b]	489 (24.4)
2d	491 (14.1), 307 (44.7), 273 (40.2)
3[c]	474 (10.4)

[a] Data were collected in deaerated acetonitrile at rt. [b] Data from ref. 13e. [c] **3** = $Ru(tpy)_2^{2+}$, Data from ref. 1g.

Luminescence data of the newly synthesized complexes **2a-d** are compiled in **Table 4.6**. The rt emission spectra showed that the energy of the ^{3}MLCT state is also lowered with the introduction of a cyano group. The corresponding emission maxima (λ_{max}) for **2a** and **2b** (see **Figure 4.4**) have red-shifted to 701 and 680 nm, respectively, due to the greater lowering of the ligand-based LUMO energy (π^*_L) over the metal-based HOMO energy (π_M). Since the introduction of the cyano group has less effect on the metal-based orbitals, the energy gap between ^{3}MC and ^{3}MLCT increases. As a consequence, the efficiency of the thermally activated surface crossing process from the ^{3}MLCT state to the ^{3}MC state decreases, thus prolonging the rt luminescence lifetime and significantly increasing quantum yields.

Table 4.6 Luminescence data of complexes **2a-d**.

complex	emission 298 K[a]		
	λ_{max}/nm	τ/ns	Φ
5 (NC-tpy)	353	1.2	3×10^{-4}
1a	651	0.7	4×10^{-5}
2a	701	75	2×10^{-3}
1b[b]	653	0.2	$\leq 1 \times 10^{-5}$
2b	680	50	2×10^{-3}
1c[d]	684	21	2.4×10^{-4}
2c	713	200	8.9×10^{-4}
3[c]	629	<0.25	$\leq 1 \times 10^{-6}$

[a] Data were collected in deaerated acetonitrile. [b] Data from ref. 13e. [c] **3** = $Ru(tpy)_2^{2+}$, data from ref. 1g.

4.3 Conclusion

A highly efficient palladium-catalyzed reaction to introduce cyano group(s) onto transition metal complexes, which are inaccessible from a traditional way, was developed. The introduction of the strongly electron withdrawing cyano group(s) onto the 4'-position of the $Ru(tpy)_2^{2+}$ moieties has profound influence on their redox potentials and photophysical properties. Lifetime measurements have shown that the introduction of cyano group(s) has greatly increased their rt lifetimes. The substitution of the cyano group on $Ru(tpy)_2^{2+}$ causes dramatic changes to its photophysical properties. Prolonged rt excited-state lifetimes compared to the prototype $Ru(tpy)_2^{2+}$ species are achieved, due to the increased energy gap between ^{3}MLCT and ^{3}MC states induced by the electron-withdrawing cyano group. The luminescence quantum yields are also significantly increased.

4.4 Experimental

4.4.1 General methods

All reactions were performed under a dry argon atmosphere using standard Schlenk techniques. Solvents for the reaction were pre-dried using Pure-Solv Solvent Purification System (Innovative Technology Inc.). All chemicals were purchased from Sigma-Aldrich and used as received.

Nuclear magnetic resonance (NMR) spectra were recorded at room temperature (r.t.) on a Bruker AC-400 spectrometer at 400 MHz for ^{1}H NMR and at 100 MHz for ^{13}C NMR. Chemical shifts are reported in part per million (ppm) relative to residual solvents (1.94 ppm for acetonitrile-d_3) and the carbon resonance of the solvents. ESI-MS was done by the Mass Spectrometry Facility at Université de Montréal. Routine absorption spectra and emission spectra were measured in argon-purged acetonitrile at r.t. on a Cary 500i UV-vis-NIR Spectrophotometer and a Cary Eclipse Fluorescence Spectrophotometer, respectively. Electrochemical data were collected in Ar-purged acetonitrile with 1.0 M $^{n}Bu_4NPF_6$ on a BAS CV-50W Voltammetric Analyzer. Redox potentials were corrected by internal reference to ferrocence (395 mV vs SCE).

4.4.2 Materials

$RuCl_3 \cdot 3H_2O$ was purchased from Precious Metal Online (PMO). Cl-tpy was prepared by the modified literature methods.[22] All other chemicals were purchased from Sigma-Aldrich and were used as received. [(4'-Cl-tpy)Ru(tpy)]$(PF_6)_2$ (**1a**), [(4'-Cl-tpy)$_2$Ru]$(PF_6)_2$ (**1b**) were prepared by the literature methods.[13c] [(5-Cl-pyrimid-2-yl-

tpy)Ru(tpy)]$(PF_6)_2$ (**1c**), [(5-*p*-bromophenylpyrimid-2-yl-tpy)Ru(tpy)]$(PF_6)_2$ (**1d**) was prepared as previous reported.[20]

4.4.3 Syntheses

Ligands:

3-step synthesis of 4'-chloro-2,2':6',2''-terpyridine (**4**, Cl-tpy)

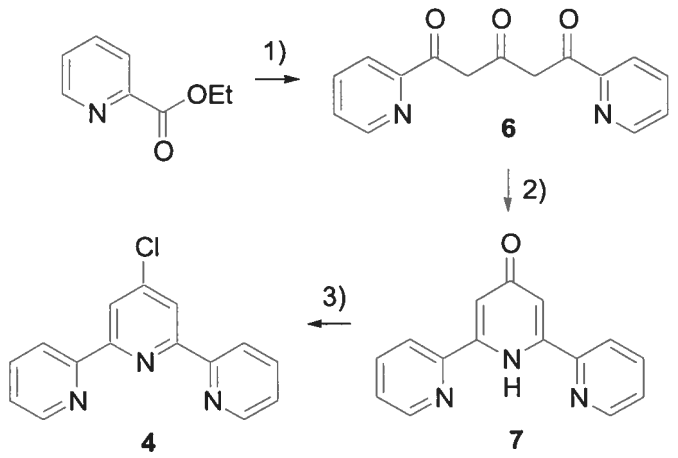

1) Synthesis of 1,5-di-2-pyridylpentane-1,3,5-trione (**6**):

A solution of acetone (2.90 g, 50 mmol) and ethyl picolinate (22.7 g, 150 mmol) in dry THF (100 mL) was added dropwise to a suspension of NaH (6.0 g × 60%, 150 mmol) in dry THF (150 mL) under reflux in an argon atmosphere over 4 h. After an additional reflux for 2 h, the THF was removed under reduced pressure and the remaining orange paste was carefully treated with H_2O (Caution!). The resultant orange solution was filtered through celite and the filtrate was neutralized by the addition of acetic acid. The yellow precipitate was collected and washed thoroughly with H_2O, followed by drying

under vacuum to yield trione **6** (~ 10 g, 37 mmol, 74%). Trione **6** holds water tenaciously and wet trione **6** can be used in the next step without compromise of the yield.

2) Synthesis of 2,6-*bis*(2'-pyridyl)-4-pyridone (**7**):

Trione **6** (~ 10 g, 37 mmol) and ammonium acetate (35.8 g, excess) were added to absolute EtOH (300 mL) and the mixture was heated at reflux for 6 h. The EtOH solution was concentrated to 50 mL and cooled down to ambient temperature. The resultant white precipitate was collected by filtration and washed with diethyl ether (10 mL × 2), followed by drying under vacuum to yield pyridone **7** (9.11 g, 36.5 mmol, 98%).

3) Synthesis of 4'-chloro-2,2':6',2''-terpyridine (**4**):

A mixture of pyridone **7** (9.11 g, 36.5 mmol) and PCl_5 in $POCl_3$ (200 mL) was heated at reflux for 12 h, after which time the solvent was distilled off. The concentrated solution (~ 30 mL) was treated cautiously with H_2O (Caution!) and the resultant acidic solution was neutralized cautiously with NaOH (s) (Caution!). The resultant white suspension was extracted with $CHCl_3$ (50 mL × 5) and the combined organic phases were washed with H_2O, dried on Na_2SO_4 (s) and filtered through celite. Removal of the solvent yielded brown residue, which was recrystallized from MeOH to yield Cl-tpy **4** (5.08 g, 19.0 mmol). The MeOH filtrate was concentrated to yield another crop of **4** (1.71 g, 6.4 mmol). Combined **4** (25.4 mmol) yields, 69%. Overall yield from acetone, 51%. All the characterizations were identical with those reported previously.[22]

Synthesis of 4'-cyano-2,2':6',2''-terpyridine (**5**, NC-tpy):

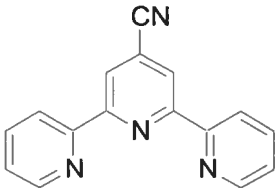

A flame-dried 100 mL round-bottomed flask was charged with Ar. Then Cl-tpy **4** (2.67 g, 10 mmol), $Zn(CN)_2$ (0.70 g, 6.0 mmol), $Pd_2(dba)_3$ (0.20 g, 0.20 mmol), dppf (0.12 g, 0.40 mmol) and Zn dust (325 mesh, 0.078 g, 1.2 mmol) were added into the flask, which was evacuated and recharged with Ar. Then DMA (40 ml) was added and the resultant mixture was heated up to 120°C with stirring for 6 h. After cooling down to ambient temperature, H_2O (200 mL) was added and the suspension was extracted with $CHCl_3$ (30 mL × 5). The combined organic phases were washed with H_2O, dried on Na_2SO_4 (s) and decolored by filtering through alumina (30 g). Removal of the solvent yielded pale-yellow residue, which was recrystallized from EtOH to yield NC-tpy **5** (2.46 g, 9.5 mmol, 95%). All the characterizations were identical with those reported previously.[20]

General procedure for the preparation of heteroleptic complexes 2a, 2c and 2e.

$[(NC\text{-}tpy)Ru(tpy)](PF_6)_2$ (**2a**)

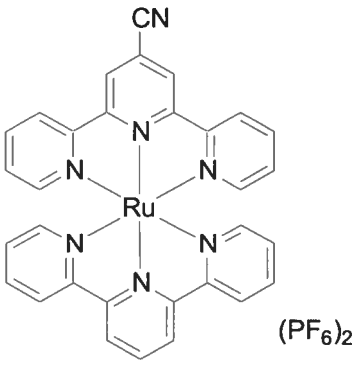

A flame-dried 25 mL round-bottomed flask was charged with Ar. Then $[(4'\text{-}Cl\text{-}tpy)Ru(tpy)](PF_6)_2$ (236 mg, 0.26 mmol), $Zn(CN)_2$ (18.4 mg, 0.16 mmol), $Pd_2(dba)_3$ (10.8

mg, 0.011 mmol), dppf (11.5 mg, 0.022 mmol) and Zn dust (325 mesh, 2.1 mg, 0.032 mmol) were added into the flask, which was evacuated and recharged with Ar. Then DMA (10 ml) was added and the resultant mixture was heated up to 120°C with stirring for 6 h. After cooling down to ambient temperature, the reaction mixture was filtered through celite and the solvent in the filtrate was removed under reduced pressure. The resultant residue was redisolved in 5 ml acetonitrile and the red solution was loaded onto a small silica gel column (3.0×11.8 cm), which was eluted by 7:1 CH_3CN/KNO_3 (aq., saturated). The red band was collected and counter-anion exchanged with NH_4PF_6. Recrystallization of the acetonitrile solution from diethyl ether yielded dark-red product **2a** (232 mg, 0.26 mol, isolated yield > 99%). ^{1}H NMR (400 MHz, CD_3CN): δ 9.06 (s, 2H, H $_{3',5'}$), 8.78 (d, J = 8.2 Hz, 2H, H $_{3',5'}$), 8.52 (d, J = 8.6 Hz, 4H, H $_{3,3''}$), 8.50 (d, J = 8.2 Hz, 2H, $H_{3,3''}$), 8.49 (t, J = 8.2 Hz, 1H, $H_{4'}$), 8.00 (t, J = 7.9 Hz, 2H, $H_{4,4''}$), 7.93 (t, J = 8.0 Hz, 2H, $H_{4,4''}$), 7.42 (d, J = 5.6 Hz, 2H, $H_{6,6''}$), 7.29 (d, J = 5.6 Hz, 2H, $H_{6,6''}$), 7.26 (t, J = 6.2 Hz, 2H, $H_{5,5''}$), 7.16 (t, J = 6.5 Hz, 2H, $H_{5,5''}$). ^{13}C NMR (100 MHz, CD_3CN): δ 158.1, 153.2, 153.1, 152.9, 144.3, 138.9, 138.8, 138.6, 128.6, 127.9, 127.8, 126.0, 125.4, 125.1, 124.4. ESI-MS: 296.5 ($[M-2PF_6]^{2+}$, 100%), 737.9 ($[M-PF_6]^+$, 37%).

$[(NC\text{-}pm\text{-}tpy)Ru(tpy)](PF_6)_2$ (**2c**)

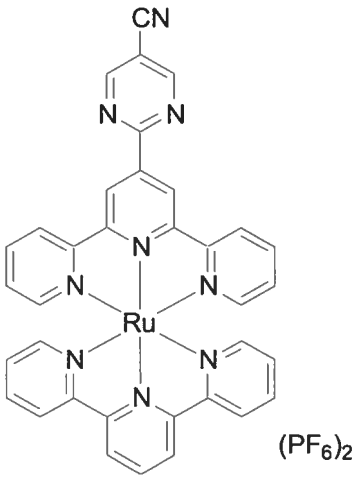

Isolated yield, 95%. ^{1}H NMR (400 MHz, CD_3CN): δ 9.70 (s, 2H, H $_{3',5'}$), 9.46 (s, 2H, H $_{Pm\ 4,6}$), 8.80 (d, J = 8.2 Hz, 2H, H $_{3',5'}$), 8.72 (d, J = 8.0 Hz, 2H, H $_{3,3''}$), 8.51 (d, J = 8.1 Hz, 2H, H $_{3,3''}$), 8.48 (t, J = 8.2 Hz, 1H, H $_{4'}$), 7.98 (m, 4H, H$_{4,4'',4,4''}$), 7.41 (dd, J = 5.7 Hz, 2H, H $_{6,6'',6,6''}$, 4H), 7.24 (t, J = 7.6 Hz, 2H, H $_{5,5''}$), 7.15 (t, J = 7.7 Hz, 2H, H $_{5,5''}$). ^{13}C NMR (100 MHz, CD_3CN): δ 162.6, 161.4, 157.9, 157.8, 156.3, 155.0, 152.7, 152.5, 142.5, 138.4, 138.3, 136.5, 127.8, 127.5, 125.0, 124.6, 123.9, 122.1, 114.9, 109.4. ESI-MS: 335.7 ($[M-2PF_6]^{2+}$, 79%), 815.9 ($[M-PF_6]^{+}$, 100%).

[(NC-ph-pm-tpy)Ru(tpy)]$(PF_6)_2$ (**2d**)

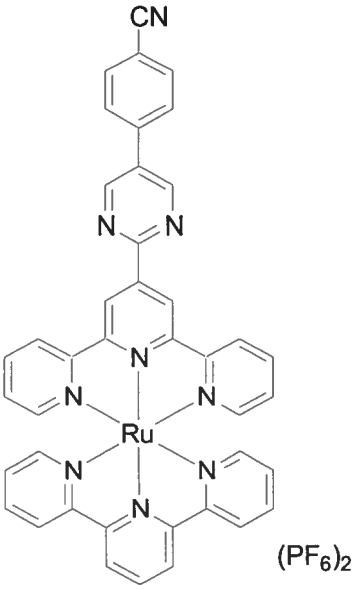

Isolated yield 98%. ^{1}H NMR (400 MHz, CD_3CN): δ 9.75 (s, 2H, $H_{3',5'}$), 9.46 (s, 2H, $H_{Pm4,6}$), 8.80 (d, J = 8.1 Hz, 2H, $H_{3',5'}$), 8.74 (d, J = 8.0 Hz, 2H, $H_{3,3''}$), 8.53 (d, J = 8.1 Hz, 2H, $H_{3,3''}$), 8.47 (t, J = 8.2 Hz, 1H, $H_{4'}$), 8.11 (d, J = 8.5 Hz, 2H, $H_{Ph3,5}$), 8.01 (m, 6H, $H_{4,4'',4,4'',Ph2,6}$), 7.44 (d, J = 5.6 Hz, 2H, $H_{6,6''}$), 7.41 (d, J = 5.6 Hz, 2H, $H_{6,6''}$), 7.23 (t, J = 6.6 Hz, 2H, $H_{5,5''}$), 7.17 (t, J = 6.6 Hz, 2H, $H_{5,5''}$). ^{13}C NMR (100 MHz, CD_3CN): δ 158.3, 156.9, 155.5, 153.0, 152.9, 142.0, 138.7, 138.6, 133.7, 128.7, 128.5, 128.3, 128.1, 127.9, 125.3, 124.9, 124.8, 124.2, 121.9. ESI-MS: 374.1 ($[M-2PF_6]^{2+}$, 100%), 892.9 ($[M-PF_6]^+$, 33%).

$[(NC\text{-}tpy)_2Ru](PF_6)_2$ (**2b**)

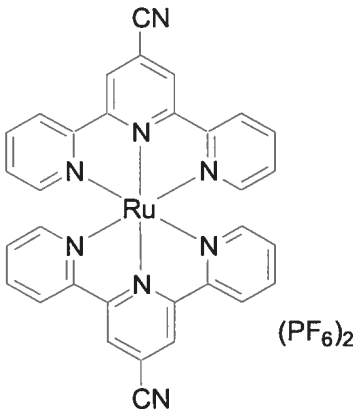

A flame-dried 25 mL round-bottomed flask was charged with Ar. Then [(4'-Cl-tpy)$_2$Ru](PF$_6$)$_2$ (21.5 mg, 0.023mmol), Zn(CN)$_2$ (3.24 mg, 0.028 mmol), Pd$_2$(dba)$_3$ (2.4 mg, 0.0023 mmol), dppf (2.6 mg, 0.0046 mmol) and Zn dust (325 mesh, 0.5 mg, 0.077 mmol) were added into the flask, which was evacuated and recharged with Ar. Then DMA (10 ml) was added and the resultant mixture was heated up to 120°C with stirring for 12 h. After cooling down to ambient temperature, the reaction mixture was filtered through celite and the solvent in the filtrate was removed under reduced pressure. The resultant residue was redisolved in 5 ml acetonitrile and the red solution was loaded onto a small silica gel column (3.0×12.5 cm), which was eluted by 7:1 CH_3CN/KNO_3 (aq., saturated). The red band was collected and counteranion exchanged with NH_4PF_6. Recrystallization of the acetonitrile solution from diethyl ether yielded dark-red product **2b** (20.5 mg, 0.023 mol, isolated yield 99%). ^{1}H NMR (400 MHz, CD_3CN): δ 9.02 (s, 4H, $H_{3',5'}$), 8.53 (d, J = 8.5 Hz, 4H, $H_{3,3''}$), 8.00 (t, J = 7.9 Hz, 4H, $H_{4,4''}$), 7.58 (d, J = 5.6 Hz, 4H, $H_{6,6''}$), 7.33 (t, J = 5.6 Hz, 4H, $H_{5,5''}$). ^{13}C NMR can not be obtained due to the poor solubility in acetonitrile. ESI-MS: 309.1 ([M-2PF$_6$]$^{2+}$, 100%), 764.9 ([M-PF$_6$]$^+$, 34%).

4.5 Reference

* Part of this work has been published as a communication: Wang, J.; Fang, Y.-Q.; Hanan, G. S.; Loiseau, F.; Campagna, S. *Inorg. Chem.* **2005**, *44*, 5.

1 Morgan, G. T.; Burstall, F. H. *J. Chem. Soc.* **1932**, 20.

2 (a) Balzani, V.; Barigelletti, F.; Belser, P.; Bernhard, S.; De Cola, L.; Flamigni, L. *J. Phys. Chem.* **1996**, *100*, 16786. (b) Constable, E. C. Prog. *Inorg. Chem.* **1994**, *42*, 67. (c) Chodorowski-Kimmes, S.; Beley, M.; Collin, J.-P.; Sauvage, J.-P. *Tetrahedron Lett.* **1996**, *37*, 2963. (d) Cargill Thompson, A. M. W. *Coord. Chem. Rev.* **1997**, *160*, 1. (e) Constable, E. C.; Davies, J. E.; Phillips, D.; Raithby, P. R. *Polyhedron* **1998**, *17*, 3989. (f) Sauvage, J.-P.; Collin, J.-P.; Chambron, J.-C.; Guillerez, S. Coudret, C.; Balzani, V.; Barigelletti, F.; De Cola, L.; Flamigni, L. *Chem. Rev.* **1994**, *94*, 993. (g) Constable, E. C.; Cargill Thompson, A. M. W.; Tocher, D. A.; Daniels, M. A. M. *New J. Chem.* **1992**, *16*, 855.

3 Mukkala, M.; Helenius, M.; Hemmila, I.; Kankare, J.; Takalo, H. *Helv. Chim. Acta* **1993**, *76*, 1361.

4 (a) Chelucci, G. *Synth. Commun.* **1993**, *23*, 1897. (b) Chelucci, G.; Saba, A.; Vignola, D.; Solinas, C. *Tetrahedron* **2001**, *57*, 1099.

5 (a) Collin, J.-P.; Heitz, V.; Sauvage, J.-P. *Tetrahedron Lett.* **1991**, *32*, 5977. (b) Chambron, J. C.; Collin, J.-P.; Dalbavie, J.-O.; Dietrich-Buchecker, C. O.; Heitz, V.; Odobel, F.; Solladié, N.; Sauvage, J.-P. *Coord. Chem. Rev.* **1998**, *178*, 1299. (c) Collin, J.-P.; Harriman, A.; Heitz, V.; Odobel, F.; Sauvage, J.-P. *Coord. Chem. Rev.* **1996**, *148*, 63. (d) Kimura, M.; Hamakawa, T.; Hanabusa, K.; Shirai, H.; Kobayashi, N. *Inorg. Chem.* **2001**, *40*, 4775. (e) Flamigni, L.; Barigelletti, F.;

Armaroli, N.; Ventura, B.; Collin, J.-P.; Sauvage, J.-P.; Williams, J. A. G. *Inorg. Chem.* **1999**, *38*, 661. (f) Collin, J.-P.; Harriman, A.; Heitz, V.; Odobel, F.; Sauvage, J.-P. *J. Am. Chem. Soc.* **1994**, *116*, 5679.

6 (a) Whittle, B.; Everest, N. S.; Howard C.; Ward, M. D. *Inorg. Chem.* **1995**, 34, 2025. (b) Storrier, G. D.; Takad, K.; Abruna, H. D. *Inorg. Chem.* **1999**, 38, 559.

7 (a) Tsukube, H.; Hamada, T.; Tanaka, T.; Uenishi, J. *Inorg. Chim. Acta* **1993**, *214*, 1. (b) Loiseau, F.; Di Petrio, C.; Serroni, S.; Campagna, S.; Licciardello, A.; Manfredi, A.; Pozzi, G.; Quici, S. *Inorg. Chem.* **2001**, *40*, 6901. (c) Haider, J. M.; Chavarot, M.; Weidner, S.; Sadler, I.; Williams, R. M.; De Cola, L.; Pikramenou, Z. *Inorg. Chem.* **2001**, *40*, 3912.

8 (a) Pechy, P.; Rotzinger, F. P.; Nazeeruddin, M. K.; Kohle, O.; Zakeeruddin, S. M.; Humphry-Baker, R.; Grätzel, M. *J. Chem. Soc., Chem. Commun.* **1995**, 65. (b) Liang, Y. W.; Schmehl R. H. *J. Chem. Soc., Chem. Commun.* **1995**, 1007. (c) Rice, C. R.; Ward, M. D.; Nazeeruddin, M. K.; Grätzel, M. *New J. Chem.* **2000**, *24*, 651. (d) Islam, A.; Sugihara, H.; Arakawa, H. J. *Photochem. Photobiol. A: Chem.* **2003**, *158*, 131. (e) Bauer, C.; Boschloo, G.; Mukhtar, E.; Hagfeldt, A. *J. Phys. Chem. B* **2002**, *106*, 12693.

9 (a) Zeng, F.; Zimmerman, S. C. *Chem. Rev.* **1997**, *97*, 1681. (b) Constable, E. C.; Housecroft, C. E.; Neuburger, M.; Schneider, A. G.; Springler, B.; Zehnder, M. *Inorg. Chim. Acta* **2000**, *300*, 49. (c) Flamigni, L.; Barigelletti, F.; Armaroli, N.; Collin, J.-P.; Dixon, I. M.; Sauvage, J.-P.; Gareth Williams, J. A. *Coord. Chem. Rev.* **1999**, *190*, 671. (d) Collin, J. P.; Gillerez, S.; Sauvage, J.-P.; Barigelletti, F.; Flamigni, L.; De Cola, L.; Balzani, V. *Coord. Chem. Rev.* **1991**, *111*, 291. (e)

Johansson, O.; Borgstrom, M.; Lomoth, R.; Palmblad, M.; Bergquist, J.; Hammarström, L.; Sun, L.; Åkermark, B. *Inorg. Chem.* **2003**, *42*, 2908. (f) Collin, J.-P.; Dietrich-Buchecker, C.; Gavina, P.; Jimenez-Molero, M. C.; Sauvage, J.-P. *Acc. Chem. Res.* **2001**, *34*, 477.

10 Juris, A., Balzani, V.; Barigelletti, F.; Campagna, S.; Belser, P.; von Zelewsky, A. *Coord. Chem. Rev.* **1998**, *84*, 85.

11 Sauvage, J.-P.; Collin, J.-P.; Chambron, J.-C.; Guillerez, S.; Coudret, C.; Balzani, V.; Barigelletti, F.; De Cola L.; Flamigni, L. *Chem. Rev.* **1994**, *94*, 993.

12 (a) Constable, E. C.; Cargill Thompson, A. M. W.; Cherryman J.; Liddiment, T. *Inorg. Chim. Acta* **1995**, *235*, 165. (b) Collin, J.-P.; Beley, M.; Sauvage, J.-P.; Barigelletti, F. *Inorg. Chim. Acta* **1991**, *186*, 91. (c) Beley, M.; Chodorowski, S.; Collin, J.-P.; Sauvage, J.-P.; Flamigni, L.; Barigelletti, F. *Inorg. Chem.* **1994**, *33*, 2543.

13 (a) Constable, E. C.; Cargill Thompson, A. M. W.; Ararmoli, N.; Balzani, V.; Maestri, M. *Polyhedron* **1992**, *11*, 2707. (b) Indelli, M. T.; Bignozzi, C. A.; Scandola, F.; Collin, J.-P. *Inorg. Chem.* **1998**, *37*, 6084. (c) Maestri, M.; Armaroli, N.; Balzani, V.; Constable, E. C.; Cargill Thompson, A. M. W. *Inorg. Chem.* **1995**, *34*, 2759. (d) Barigelletti, F.; Flamigni, L.; Guardigli, M.; Juris, A.; Beley, M.; Chodorowski-Kimmes, S.; Collin, J.-P.; Sauvage, J.-P. *Inorg. Chem.* **1996**, *35*, 136. (e) Fang, Y.-Q.; Taylor, N. J.; Hanan, G. S.; Loiseau, F.; Passalacqua, R.; Campagna, S.; Nierengarten, H.; van Dorsselaer, A. *J. Am. Chem. Soc.* **2002**, *124*, 7912.

14 (a) Duati, M.; Fanni, S.; Vos, J. G. *Inorg. Chem. Commun.* **2000**, *3*, 68. (b) Duati, M.; Tasca, S.; Lynch, F. C.; Bohlen, H.; Vos, J. G.; Stagni, S; Ward, M. D. *Inorg. Chem.* **2003**, *42*, 8377. (c) Indelli, M. T.; Bagnozzi, C. A.; Scandola, F.; Collin, J.-P. *Inorg. Chem.* **1998**, *37*, 6084.

15 (a) Hammarström, L.; Barigelletti, F.; Flamigni, L.; Indelli, M. T.; Armaroli, N.; Calogero, G.; Guardigli, M.; Sour, A.; Collin, J.-P.; Sauvage, J.-P. *J. Phys. Chem. A* **1997**, *101*, 9061. (b) Vogler, L. M.; Brewer, K. J. *Inorg. Chem.* **1996**, *35*, 818.

16 (a) Ford, W. E.; Rodgers, M. A. J. *J. Phys. Chem.* **1992**, *96*, 2917. (b) Wilson, G. J.; Launikonis, A.; Sasse, W. H.; Mau, A. W.-H. *J. Phys. Chem. A* **1997**, *101*, 4860. (c) Simon, J. A.; Curry, S. L.; Schmehl, R. H.; Schatz, T. R.; Piotrowiak, P.; Jin, X.; Thummel, R. P. *J. Am. Chem. Soc.* **1997**, *119*, 11012. (d) Tyson, D. S.; Luman, C. R.; Zhou, X.; Castellano, F. N. *Inorg. Chem.* **2001**, *40*, 4063. (e) Maubert, B.; McClenaghan, N. D.; Indelli, M. T.; Campagna, S. *J. Phys. Chem. A* **2003**, *107*, 447. (f) Passalacqua, R.; Loiseau, F.; Campagna, S.; Fang, Y.-Q.; Hanan, G. S. *Angew. Chem. Int. Ed.* **2003**, *42*, 1608. (g) Wang, J.; Hanan, G. S.; Loiseau, F.; Campagna, S. *Chem. Commun.* **2004**, 2068.

17 (a) Bignozzi, C. A.; Schoonover, J. R.; Scandola, F. *Prog. Inorg. Chem.* **1997**, *44*, 1 and references therein; (b) Mellace, M. G.; Fagalde, F.; Katz, N. E.; Crivelli, I. G.; Delgadillo, A.; Leiva, A. M.; Loeb, B.; Garland, M. T.; Baggio R. *Inorg. Chem.* **2004**, *43*, 1100.

18 Recent review: Sundermeier, M.; Zapf, A.; Beller, M. *Euro. J. Inorg. Chem.* **2003**, 3513.

19 (a) Chodorowski, S.; Beley, M.; Collin, J.-P.; Sauvage, J.-P. *Tetrahedron Lett.* **1996**, *37*, 2963. (b) Tzalis, D.; Tor, Y. *Chem. Commun.* **1996**, 1043. (c) Hissler, M.; Ziessel, R. *New J. Chem.* **1997**, *21*, 843. (d) Coudret, C.; Fraysse, S.; Launay, J.-P. *Chem. Commun.* **1998**, 663. (e) Osawa, M.; Hoshino, M.; Horiuchi, S.; Wakatsuki, Y. *Organometallics* **1999**, *18*, 112. (f) Kelch, S.; Rehahn, M. *Macromolecules* **1999**, *32*, 5818. (g) Storrier, G. D.; Colbran, S. B. *Inorg. Chim. Acta* **1999**, *284*, 76. (h) Aspley, C. J.; Gareth Williams, J. A. *New J. Chem.* **2001**, *25*, 1136. (i) Harriman, A.; Hissler, M.; Khatyr, A.; Ziessel, R. *Eur. J. Inorg. Chem.* **2003**, 955.

20 Fang Y.-Q. Master's Thesis, Department of Chemistry, University of Waterloo, Canada. **2002**.

21 Jin, F.; Confalone, P. N. *Tetrahedron Lett.* **2000**, *41*, 3271.

22 (a) Potts, K. T.; Konwar, D. *J. Org. Chem.* **1991**, *56*, 4815. (b) Constable, E. C.; Ward, M. D. *J. Chem. Soc., Dalton Trans.* **1990**, 1405.

23 (a) Takagi, K.; Okmoto, T.; Sakakibara, Y.; Ohno, A.; Oka, S.; Hayama, N. *Bull. Chem. Soc. Jpn.* **1975**, *48*, 3298. (b) Sakakibar, Y.; Okuda, F.; Shimobayashi, A.; Kirino, K.; Sakai, M.; Uchino, N.; Takagi, K. *Bull. Chem. Soc. Jpn.* **1988**, *61*, 1985.

24 Lashgari, K.; Kritikos, M.; Norrestam, R.; Norrby, T. *Acta Crystallogr. Sect. C* **1999**, *C55*, 64.

Chapter 5

Synthesis of 2,6-*bis*(5'-Substituted-pyrimid-2'-yl)pyridine Ligands and Their Ruthenium(II) Complexes

Abstract

A convergent and efficient synthetic approach to a new family of ligands **1a-c**, 2,6-*bis*(5'-R-pyrimyd-2'-yl)pyridine (Rbppy, R = H, **1a**; Cl, **1b**; Ph, **1c**), was developed. The two peripheral pyrimidine rings were constructed from 2,6-pyridine-*bis*amidinium dichloride (**6**) and 2-substituted-*N,N'*-(dimethylamino)trimethinium hexaflurophosphate in the presence of NaOMe. Application of these ligands to the coordination sphere of Ru(II) metal center led to a new series of Ru(II) complexes **2a-c** and **3a-c**. The solid state structures of ligand **1a**, complexes **2a-b** and **3b** were characterized by single crystal X-ray diffraction. The UV-vis and electrochemical results indicated that the Rbppy ligands act as electron deficient ligands, whose low energy ligand-based π_L^* orbital stabilizes the metal-based π_M orbital.

5.1 Introduction

The tridentate ligand 2,2':6',2"-terpyridine (tpy) was first prepared over 70 years ago[1] and since then the coordination chemistry of tpy-based ligands has been widely studied.[2] Several areas of the research have evolved for the application of tpy complexes: as protein labels;[3] as reagents for enantioselective synthesis;[4] as modifiers for porphyrins,[5] catechols,[6] and macrocycles;[7] and in solar energy devices based on nanocrystalline TiO_2 surfaces.[8] They have also been used in supramolecular chemistry to build up linear multinuclear assemblies for energy and/or electron transfer processes at the molecular level.[9]

Considering the importance of tpy in coordination chemistry, one of its main areas of research has been concerned with the syntheses of tpy and its analogues. Several different tridentate tpy analogues have been reported (**Chart 5.1**): 1) 2,4-*bis*(pyrid-2'-yl)triazines (**A**);[10] 2) 6-phenyl-2,2'-bipyrdines (**B**);[11] 3) 1,3-di(pyrid-2'-yl)benzene (**C**);[12] 4) 6-(2'-picolyl)-2,2'-bipyridine (**D**);[13] 5) 2,6-*bis*(pyrimid-4'-yl)pyridines (**E**);[14] 6) 2,6-*bis*(pyrimid-2'-yl)pyridine (**F**).[15] The main strategy has been to keep the tridentate coordination ability while exploring the electronic properties of the ligands by introducing electron rich C donors (cyclometallated **B**[11], **C**[12]), or electron deficient donors (**A**[10], **E**[14], **F**[15]). An alternative strategy has been to relieve the steric strain around the metal center in order to increase ligand field strength of the ligand (**D**[13]). The coordination chemistry of these tpy analogues with a variety of transition metals has been extensively explored in the area of supermolecules, catalysts and polymers. Some of the experiments showed that the substitution of tpy with these analogues in $M(tpy)_m^{n+}$ complexes can give rise to a variety of novel or improved properties.[10-13]

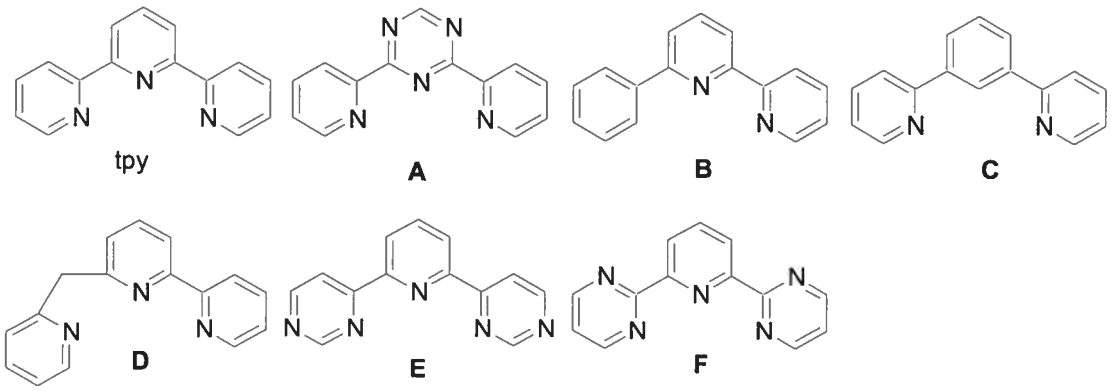

Chart 5.1 Tridentate ligands: 2,2':6':2"-terpyridine (tpy) and tpy analogues **A-F**.

2,6-*bis*(Pyrimid-2'-yl)pyridine (bppy) and its palladium complexes have been reported previously.[15] The palladium complexes with this novel tridentate nitrogen ligand display dynamic behavior due to the exchange of the coordinated and uncoordinated pyrimidyl nitrogen atoms (**Figure 5.1**). Methyl- and acyl-palladium complexes containing the novel tridentate nitrogen ligand, bppy, show dynamic behaviour due to exchange of the pyrimidyl nitrogen atoms. The mechanism of this process involves nitrogen dissociation, which may be initiated by chloride, solvent or CO coordination, subsequent rotation about the C-C bond and reformation of the nitrogen–palladium bond (**Figure 5.1**).[15]

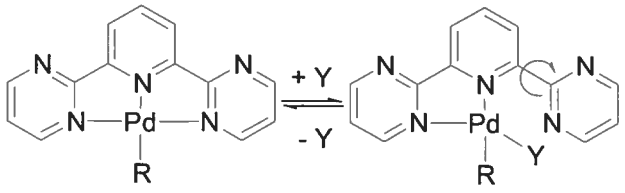

Figure 5.1 Dynamic behavior of [bppy]PdR complexes. R = Me, Y = Cl-, solvent or CO.[15]

Due to the myriad applications of luminescent Ru(II) tpy complexes,[16-17] the exploration of new types of tridentate ligands and their Ru(II) complexes play a key role in our research. First, since the bppy can initiate dynamic behavior at a metal center, we envision that the bppy ligand could have the same dynamic behavior while coordinated to a Ru(II) center, which could introduce a binding site for H_2O in its potential oxidative or reductive cleaving into O_2 and H_2, respectively. Secondly, the initial synthesis of the bppy ligand followed a classic two-step approach to tpy ligand (**Scheme 5.1**), which features harsh conditions and low overall yield in the formation of the central pyridine ring. Based on our research on the construction of the pyrimidine ring on the 4'-position of the tpy ligand,[18] we proposed to synthesize the bppy ligand in the other direction, namely construction of the pyrimidine rings from amidinium chloride and vinamidium hexaflurophosphate salt. The new approach should have better yields, mild conditions and be convergent in order to introduce the different substituents onto the 5-position of the pyrimidine rings.

In this chapter, we report the syntheses of a new family of Rbppy ligands and their applications in Ru(II) chemistry.

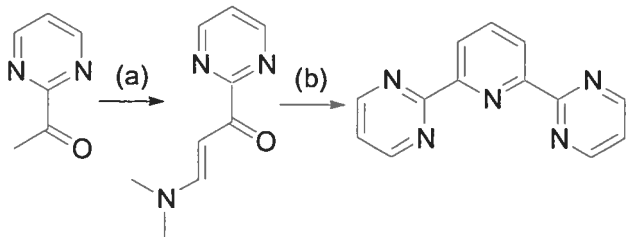

Scheme 5.1 Reported synthesis of bppy ligand. Reagents and conditions: (a) $Me_2NCH(OMe)_2$, toluene, reflux, 92%. (b) KO^tBu, 2-acetylpyridine, THF, rt; NH_4OAc, acetic acid, reflux, 23%.[15]

5.2 Results and Discussion

5.2.1 Syntheses

The new approach to the bppy ligands with a variety of substituents in the 5-position of the pyrimidine rings started from 2,6-pyridine-*bis*amidinium dichloride (**6**),[21] which is easily accessible from commercial available 2,6-dicyanopyridine (**Scheme 5.2**). The condensation reaction of **6** with 2-substituted-*N,N'*-(dimethylamino)trimethinium hexaflurophosphate in the presence of NaOMe formed the two pyrimidine rings to give ligands **1a-c**. The overall yields, higher than the reported approach, ranged from 48% to 52% with the different substituents. All the Rbppy ligands were characterized by ^{1}H NMR spectroscopy (**Table 5.1**), ESI-MS, MALDI-TOF MS and elemental analysis.

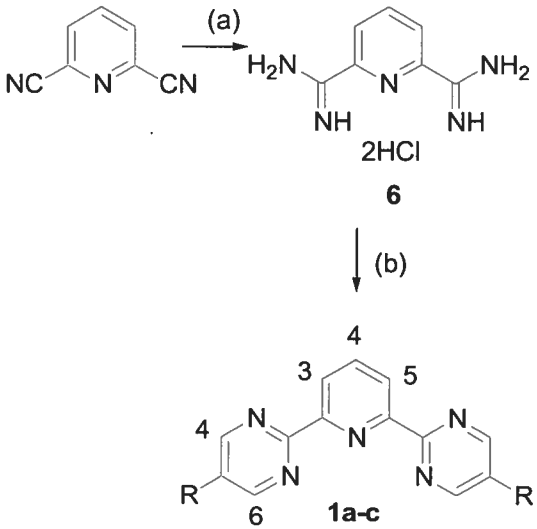

Scheme 5.2 Syntheses of 2,6-*bis*(5'-R-pyrimid-2'-yl)pyridine ligands Rbppy **1a-c**. Reagents and conditions: (a) (i) NaOMe, MeOH, r.t., 24 h; (ii) NH_4Cl, MeOH, r.t., 48 h, 73% over two steps. (b) NaOMe, vinamidium PF_6 salt, MeOH, reflux, 16 h. R = H, **1a**, 66%; Cl, **1b**, 68%; Ph, **1c**, 70%.

The Ru(II) complexes with Rbppy ligand were synthesized through a classic approach. The addition of two equivalent of the Rbppy ligands **1a-c**, respectively, to $RuCl_3 \cdot xH_2O$ with a dechlorinating reagent, $AgNO_3$, led to the formation of the homoleptic complexes **2a-c**, which were purified by silica chromatography followed by the counteranion metathesis (**Scheme 5.3**). For ligands **1a** and **1c**, the coordination to the Ru(II) center proceeded smoothly to give the homoleptic complexes as the only product. However, for ligand **1b**, Clbppy, the complexation reaction yielded complex **2b'** as the major product (**Figure 5.2**) with homoleptic complex **2b** as minor product. The reluctance of ligand **1b** to coordinate to the Ru(II) center may come from the strong electron withdrawing effect of the chloride, which removes electron density away from the nitrogen atoms in the pyrimidine ring, which in turn weakens its coordination capacity to the metal center.

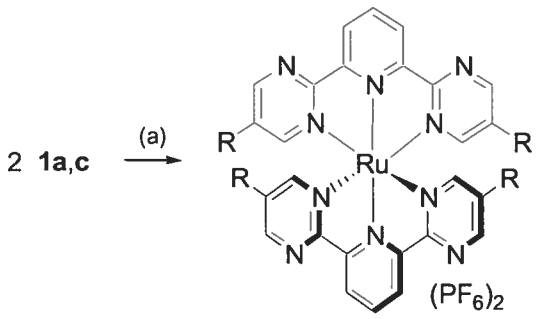

2a,c

Scheme 5.3 Syntheses of $[(Rbppy)_2Ru](PF_6)_2$ complexes **2a-c** (R = H, **2a**; phenyl, **2c**). Reagents and conditions: (a) $RuCl_3 \cdot xH_2O$, 3.0 equiv. $AgNO_3$, EtOH, reflux, 2-4 h.

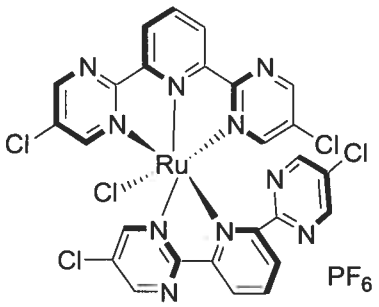

Figure 5.2 Proposed structure of complex **2b'**.

The heteroleptic Ru(II) complexes **3a-c** were also synthesized from the complexation of the Rbppy ligands with (tpy)$RuCl_3$ under standard reaction conditions (**Scheme 5.4**). The ligands **1a-c** can be easily converted to their corresponding heteroleptic complexes and the partially coordinated product has not been noticed in the complexation leading to the heteroleptic complexes.

All the complexes were confirmed by ^1H NMR (**Table 5.2**), ESI-MS and MALDI-TOF MS.

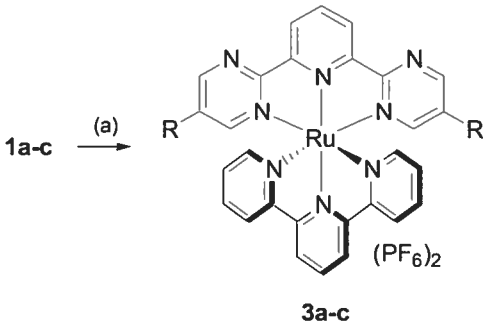

Scheme 5.4 Syntheses of heteroleptic (Rbbpy)Ru(tpy)[$(PF_6)_2$] complexes **3a-c** (R = H, **3a**; Cl, **3b**; phenyl, **3c**). Reagents and conditions: (a) Ru(tpy)Cl_3, 3.0 equiv. $AgNO_3$, EtOH, reflux, 2-4 h.

5.2.2 NMR spectroscopy

The newly synthesized ligands **1a-c** and complexes **2a-c**, **3a-c** have been characterized by ^{1}H and ^{13}C NMR spectroscopy. The ^{1}H NMR spectroscopic data of ligands **1a-c** in $CDCl_3$ are compiled in **Table 5.1**. The ^{1}H NMR spectroscopic data of complexes **2a-c** and **3a-c** in CD_3CN are compiled in **Table 5.2**. The assignments of the ^{1}H NMR signals were according to the specific coupling constants from pyridine ring and pyrimidine rings.

Compared with the ligand tpy, the ligands **1a-c**, which have their CH group in tpy substituted with nitrogen atoms, display large chemical shifts in their ^{1}H NMR spectra, indicating that the pyrimidine rings have an important effect on the electronics of the ligands. The ^{1}H NMR signals from the central pyridine have shifted to lower field and are deshielded 0.12–0.23 ppm for $H_{Py\,3,\,5}$ and 0.07–0.13 ppm for $H_{Py\,4}$ by the nitrogen lone pairs of the neighboring pyrimidine rings. It is noteworthy that the biggest shifts come from ligand **1c**, which has phenyl substituents on the 5-position of the pyrimidine rings, which lead to further deshielding. The ^{1}H NMR signals from the peripheral pyrimidine rings have the same trend and shift to lower field compared with those from the tpy peripheral pyridine rings. The overall effects of the pyrimidine rings in the newly synthesized ligand **1a-c** are the increase electron delocalization produced by the coplanar pyrimidine rings.

Table 5.1 ^{1}H NMR resonances for ligands **1a-c**.[a]

Solvent	Cpd	Py 3,5	Py 4	Pm 4,6	R groups[b]
$CDCl_3$	**1a**	8.60	8.06	8.94	7.32
	1b	8.60	8.06	8.91	---
	1c	8.71	8.12	9.21	7.71, 7.60-7.49
CD_3CN	**1a**	8.59	8.13	8.99	7.48
	1b	8.59	8.15	8.99	---
	1c	8.68	8.18	9.27	7.85, 7.64-7.53

[a] See **Scheme 5.2** for ^{1}H assignments. [b] In ligand **1a**, R = H; ligand **1b**, R = Cl; ligand **1c**, R = Ph.

Through the comparison of the ^{1}H NMR spectra of the newly synthesized complexes, we note that upon coordination of the ligands with the ruthenium cation, the changes of the chemical shift on the ligand are quite significant, showing the electronic and conformational changes induced by coordination to the metal ion. Comparison between the chemical shift of the ligands and the complexes gives some interesting information. Upon coordination, the proton signals $H_{Py\,3,5}$ and $H_{Py\,4}$, from the pyridine ring have all shifted to lower field with about 0.40 ppm, indicating the protons have been more deshielded when coordinated to the Ru(II) center. The chemical shifts of $H_{Pm\,4}$ on coordination are nearly the same as those of free ligands. However, the $H_{Pm\,6}$ shifted about 1.20 ppm (1.50 ppm for complexes **2c** and **3c** due to extra shielding effect from phenyl ring current) due to strong shielding effects from the pyrimidine rings on the other orthogonal ligand.[22]

In the heteroleptic complexes **3a-c**, when tpys are used as support ligands on the other side, all the proton signals from the Rbppy ligands have the same trend. Compared

with their homoleptic counterparts **2a-c**, the protons in the Rbppy ligands have shifted slightly to higher field due to the better electron-donating ability of tpy ligand

Table 5.2 ^{1}H NMR resonances for complexes.[a]

Cpd	3, 3''	4, 4''	5, 5''	6, 6''	3', 5'	Py 3,5	Py 4	Pm 4	Pm 6	R	R'
2a						9.00	8.54	8.88	7.74	7.23	
2b						8.98	8.56	8.92	7.76	---	
2c						9.03	8.56	9.14	7.85	7.46-7.44	
3a	8.50	7.95	7.18	7.38	8.75	9.00	8.51	8.86	7.71	7.18	8.45
3b	8.52	7.98	7.21	7.36	8.76	8.99	8.52	8.87	7.73	---	8.48
3c	8.49	7.94	7.21	7.42	8.75	9.03	8.53	9.11	7.74	7.46-7.40	8.44
4[b]	8.51	7.92	7.17	7.35	8.76		8.42				

[a] In CD_3CN at r.t., see reaction schemes for ^{1}H assignments. In complexes **3a-c**, R'=H $_{T4'}$.

[b] **4** = $Ru(tpy)_2^{2+}$, from ref. 16o.

5.2.3 Solid state structure

Colorless single crystals of ligand **1a** suitable for X-ray crystallography were grown from MeOH/H_2O (1:1) solution by slowly evaporation of MeOH. The single crystal structure of ligand **1a** is shown in **Figure 5.3**.

Solid structure of ligand **1a** has one mirror plane, crossing the C7-N3 atoms and perpendicular to the plane created by the molecule. Interestingly, the single crystal of ligand **1a** incorporated H_2O molecules in it with 1:2 ratio of **1a**:H_2O. The three dimensional structure of **1a**·2H_2O was showed in **Figure 5.4**. The ligand molecules are

stacked in a zigzag mode along the Z-axis, while the two molecules of H_2O are heterogeneous. One of the two H_2O molecules is coplanar to **1a** with two H-bonding with N1 and N4 atoms. The other one, perpendicular to the plane of **1a**, extends along Z-axis through intramolecular H-bonding between O_a and H_b (**Figure 5.4**). The H-bonding network is build up through N···H–O–H···O···H–O-H interactions. Since this interesting host-guest interaction could have the potential application in the storage of hydrides, other X-ray crystallography studies towards ligands **1a-c** are still under way.

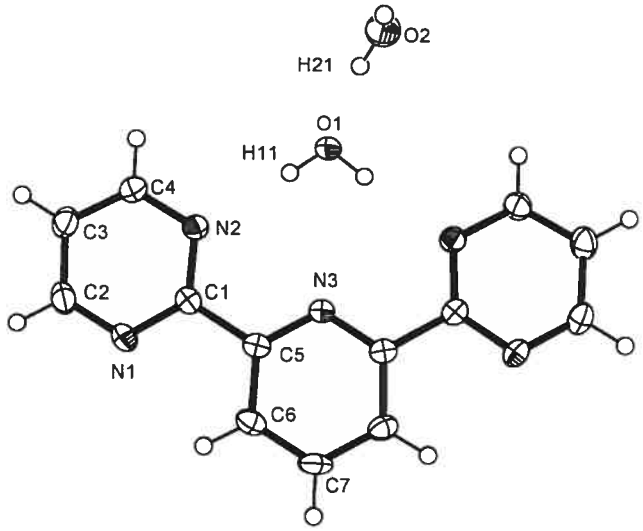

Figure 5.3 ORTEP plot of the X-ray crystal structure of **1a**·2H_2O with atom labelling. Thermal ellipsoids are set at 50% probability. H-bonding distances: N2-H11, 1.99 Å; O1-H21, 1.94 Å. See Appendix A2 for crystal data.

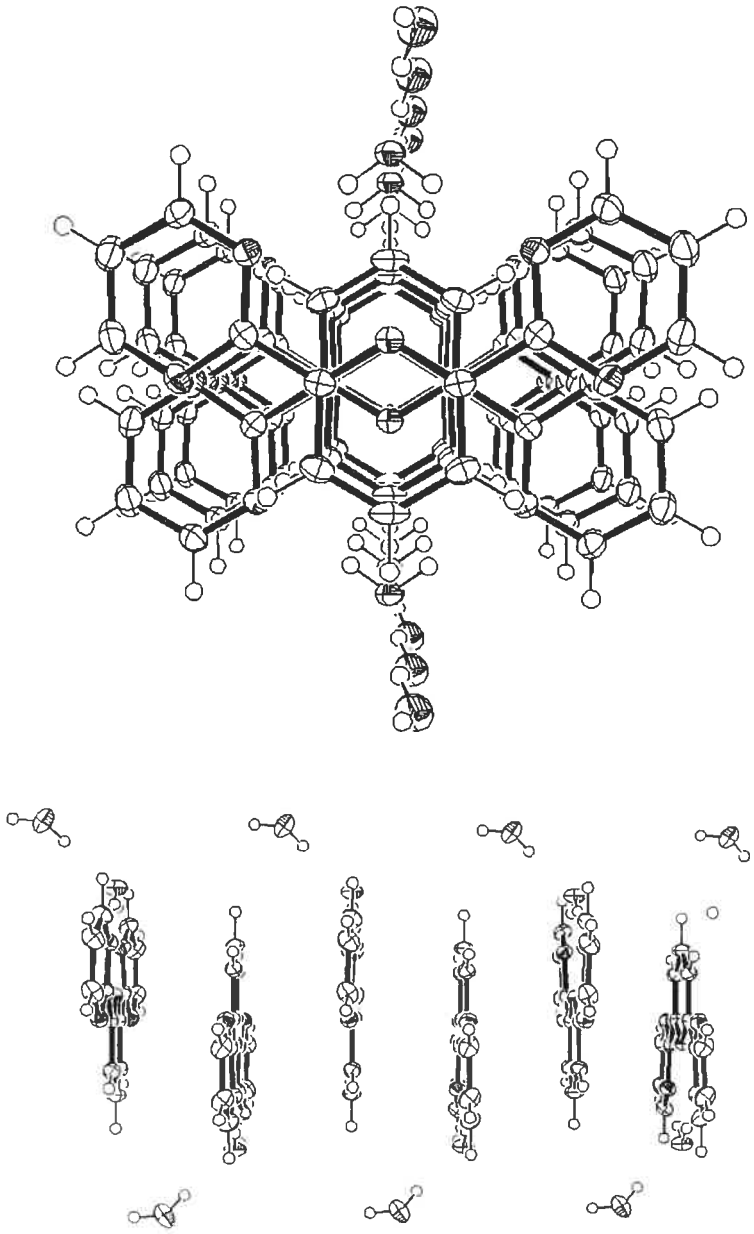

Figure 5.4 ORTEP plots of the three dimensional structure of **1a**·$2H_2O$ viewed from Z-axis (top) and viewed along Z-axis (bottom). Thermal ellipsoids are set at 50% probability.

Red single crystals of complexes **2a**, **2b** and **3b** suitable for X-ray crystallography were grown from the acetonitrile solution by slow diffusion of diethyl ether, respectively. The single crystal structures of complexes **2a**, **2b** and **3b** are showed in **Figure 5.5**, **Figure 5.6** and **Figure 5.7**, respectively, with selected bond lengths and bond angles in **Table 5.3**.

The solid state structures of complexes **2a-b** and **3b** all adopt symmetric distorted octahedral configurations. The Ru – N bond lengths and internal bond angles (**Table 5.3**) are similar to those found in other Ru(II) polypyridine complexes.[19] The N1-N4 bite angles in complexes **2a**, **2b** and **3b** are 157.1°, 157.0° and 158.8°, respectively. All the bite angles are smaller than that of $Ru(tpy)_2^{2+}$ prototype (168.3°), indicating that the complexes are more distorted from idealized octahedral configurations which account for the weak ligand field strength of Rbppy ligands. It is noteworthy that each unit cell in single crystal of complex **3b** has an unusual *Z* number, 16, indicating molecules have an unusual stacking mode. Further research concerning on this stacking mode is still under way to clarified the effect.

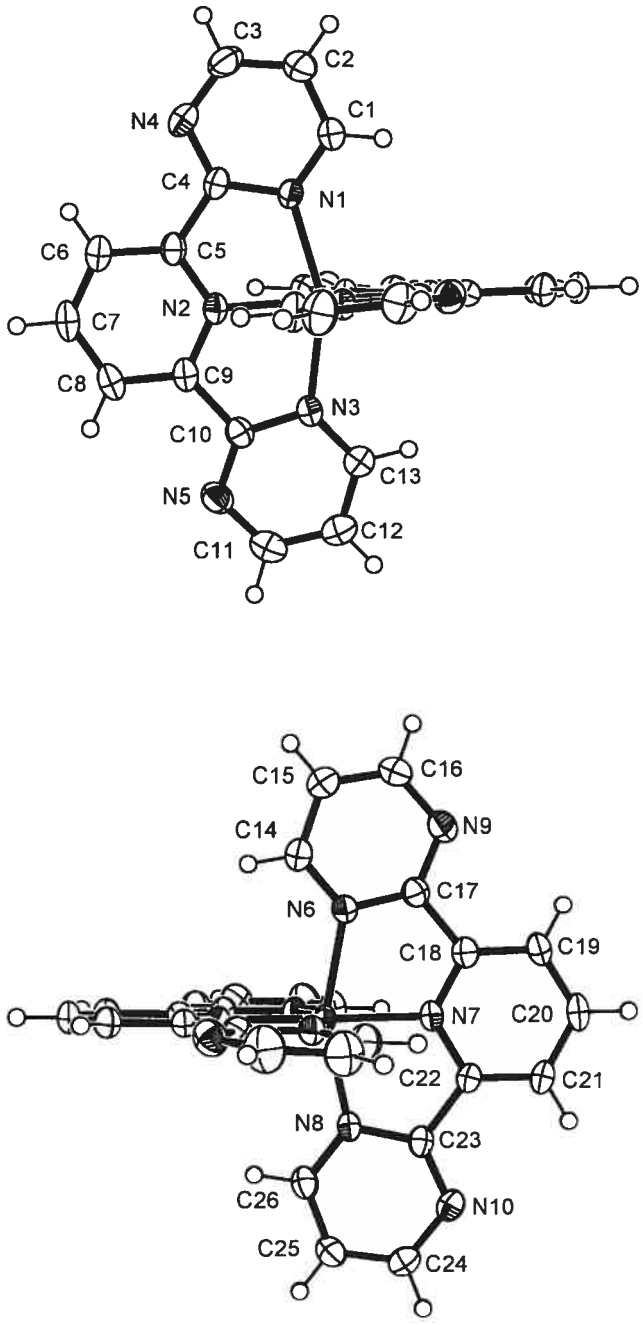

Figure 5.5 ORTEP plot of the X-ray crystal structure of complex **2a** with atom labelling. Thermal ellipsoids are set at 50% probability with the counteranions and solvent have been omitted for clarity.

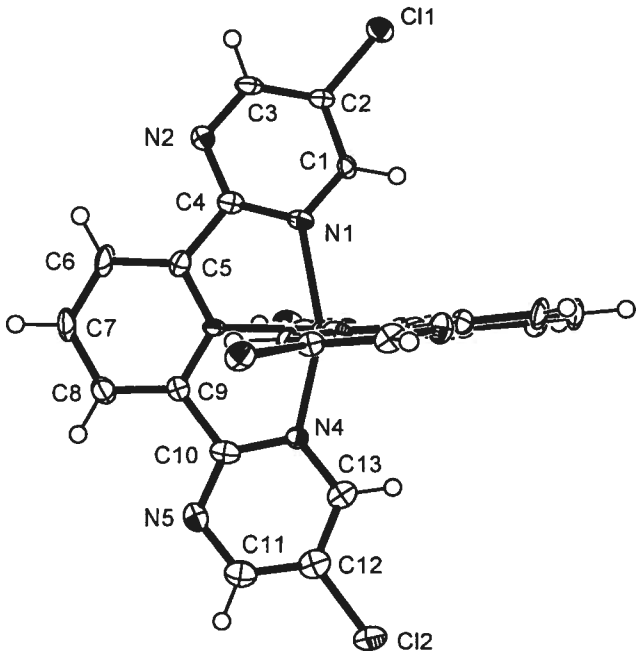

Figure 5.6 ORTEP plot of the X-ray crystal structure of complex **2b** with atom labelling. Thermal ellipsoids are set at 50% probability with the counteranions and solvent have been omitted for clarity.

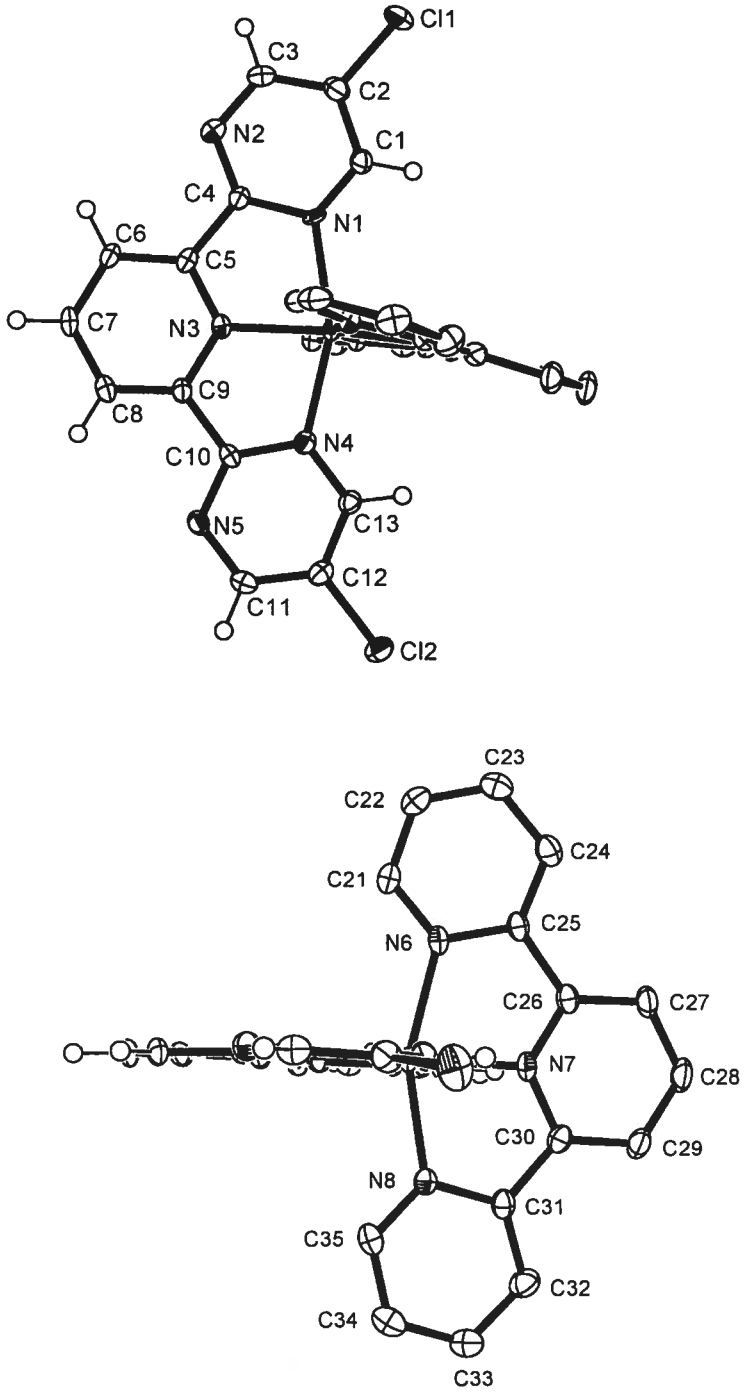

Figure 5.7 ORTEP plots of the X-ray crystal structure of complex **3b** exposing the Clppy ligand (top) and, after a 90° rotation, the tpy ligand (bottom). Thermal ellipsoids are set at 50% probability with tpy hydrogen atoms and counteranions omitted for clarity.

Table. 5.3 Selected bond lengths (Å) and bond angles (°) for complexes **2a-b** and **3b**.

Bond distances (Å) for **2a**	Bond distances (Å) for **2b**	Bond distances (Å) for**3b**
Ru N1 2.074(3)		Ru N1 2.087(2)
Ru N2 1.980(3)	Ru N1 2.074(8)	Ru N3 1.979(2)
Ru N3 2.080(3)	Ru N3 1.988(7)	Ru N4 2.068(2)
Ru N6 2.082(3)	Ru N4 2.087(8)	Ru N6 2.084(3)
Ru N7 1.982(3)	Cl1 C2 1.728(9)	Ru N7 2.000(2)
Ru N8 2.065(3)	Cl2 C12 1.722(11)	Ru N8 2.067(3)
		Cl1 C2 1.722(3)
		Cl2 C12 1.719(3)
Bond angles (°) for **2a**	Bond angles (°) for **2b**	Bond angles (°) for **2b**
N1 Ru N2 78.40(11)		N1 Ru N3 79.51(9)
N1 Ru N3 157.10(11)	N1 Ru N3 78.3(3)	N1 Ru N4 158.80(8)
N2 Ru N3 78.76(11)	N1 Ru N4 157.0(3)	N3 Ru N4 79.30(9)
N2 Ru N7 178.49(10)	N3 Ru N4 78.80(3)	N3 Ru N8 175.32(11)
N6 Ru N7 78.51(11)	N3 Ru N8 176.27(3)	N6 Ru N7 78.70(11)
N6 Ru N8 157.23(10)	C13 N4 C10 117.33(3)	N6 Ru N8 157.63(9)
N7 Ru N8 78.73(11)	C10 N5 C11 116.52(3)	N7 Ru N8 79.00(12)
		C13 N4 C10 116.4(2)
		C10 N5 C11 117.3(2)

5.2.4 Electrochemistry

The electrochemistry of the newly synthesized Ru(II) Rbppy complexes was examined to obtain a quantitative effect of the Rbppy ligands on the energy state of the complexes. The electrochemical data were obtained and compiled in **Table 5.4**. The oxidation processes in all of the complexes are metal centered, whereas reduction processes are ligand centered, which are very typical for ruthenium polypyridyl complexes.

Compared with the oxidation potential of $Ru(tpy)_2^{2+}$, the substitution of tpy with Rbppy have shifted the oxidation potentials of complexes **2a-c** and **3a-c** to more positive

values (harder to oxidize) due to the greater π-accepting character of the Rbppy ligands as compared to tpy. The Rbppy-based reduction potentials have also shifted to more positive value (easier to reduce), indicating the lowering effect of the ligand-based π* orbitals.

Comparing the homoleptic complexes **2a-c** with the heteroleptic complexes **3a-c**, the same effect exists since the tpy ligand is a better electron donor than are Rbppy ligands.

As far as the substituents are concerned, their electronic properties have quite a strong effect on the HOMO orbital and the oxidation potentials related to the bppy moieties, as compared to their effect on the metal center. Electron withdrawing chloride substituents in complexes **2b** and **3b** showed the largest inductive effect on the metal-based oxidation process as well as the ligand-based reduction processes.

Table 5.4 Half-wave potentials for Ru(II) complexes **2a-c**, **3a-c**.[a]

cmpd	$E_{1/2}$(oxidn)	$E_{1/2}$(redn)	
2a	1.53(84)	-1.04(56)	-1.26(ir)
2b	1.68(82)	-0.96(36)	-1.15(ir)
2c	1.54(76)	-0.96(68)	-1.15(ir)
3a	1.40(70)	-1.13(76)	-1.49(ir)
3b	1.54(70)	-1.03(80)	-1.42(ir)
3c	1.41(66)	-1.04(ir)	-1.41(ir), -1.62(ir)
4[b]	1.32	-1.27	-1.52

[a] Potentials are in volts vs SCE for acetonitrile solutions, 0.1 M in TBAP at r.t. at a sweep rate of 100 mV/s. The difference between cathodic and anodic peak potentials (mV) is given in parentheses. ir = irreversible. [b] **4** = $Ru(tpy)_2^{2+}$, data from ref. 16o.

5.2.5 UV-vis spectroscopy

The UV-vis absorption spectra of ligands **1a-c** (**Figure 5.8**, **Table 5.5**) are dominated by π-π^* and n-π^* transitions. The lowest π-π^* transition energy absorption bands of ligands **1a-c** appeared below 277 nm, lower than that of the analogous tpy ligand (279.5 nm in CH_2Cl_2), indicating the substitution of CH with nitrogen atom in these new family of ligands stabilize the 2,6-*bis*(pyrimid-2'-yl)-pyridine-based π_{1a} orbital to a greater extent than the 2,6-*bis*(pyrimid-2'-yl)pyridine-based π^*_{1a} orbital. The $\pi \rightarrow \pi^*$ absorption band of ligand **1b** has a red-shifted compared to the absorption band of ligand **1a**, due to the fact that chloro substituents stabilize the π^* orbital to a greater extent than

π orbital. Ligand **1c**, which has two phenyl substituents, has two $\pi \rightarrow \pi^*$ transitions. The higher energy transition can be assigned to the transition from low-lying π_{ph} orbital to 2,6-*bis*(pyrimid-2'-yl)pyridine-based π^*_{1a} orbital, while the other one to the $\pi_{1a} \rightarrow \pi^*_{1a}$ transition. The phenyl substituents in ligand **1c**, which has the lowest $\pi_{1a} \rightarrow \pi^*_{1a}$ transition energy, stabilize the π^*_{1a} to the greatest extent in the newly synthesized ligand **1a-c** due to their strong π-accepting ability.

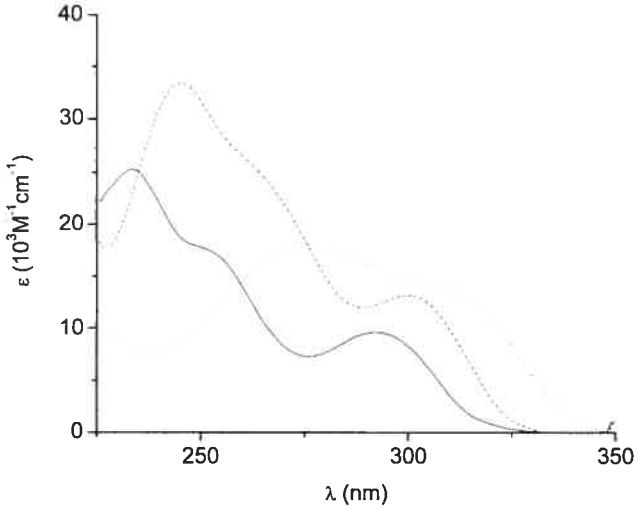

Figure 5.8 Absorption spectra of ligands **1a** (solid line), **1b** (dashed line) and **1c** (dotted line) in CH_2Cl_2 at room temperature.

Table 5.5 Absorption spectra data of ligands **1a-c**.[a]

ligand	λ (nm); ε ($10^3 M^{-1}cm^{-1}$)	
	$\pi \rightarrow \pi^*$	$n \rightarrow \pi^*$
1a	233 (25.3)	292 (9.57)
1b	245 (33.4)	300 (13.1)
1c	225 (11.7), 277 (18.0)[b]	312 (13.4)
tpy[c]	280 (20.0)	

[a] In CH_2Cl_2 at room temperature. [b] $\pi_{ph} \rightarrow \pi^*_{1a}$ and $\pi_{1a} \rightarrow \pi^*_{1a}$, respectively. [c] From ref 20.

The absorption spectra of homoleptic complexes **2a-c** and heteroleptic complexes **3a-c** are shown in **Figure 5.9** and **Figure 5.10**, respectively, with the data compiled in **Table 5.6**. Since the ligands Rbppy have a better stabilization effect on metal-based π_M orbitals than the tpy ligand. The ^{1}MLCT bands of the homoleptic complexes **2a-c** are shifted to higher energy compared with $Ru(tpy)_2^{2+}$ (**4**). The ^{1}MLCT bands of the heteroleptic complexes **3a-c** are shifted to higher energy compared with their homoleptic counterparts, due to the better electron donating ability of the tpy ligand.

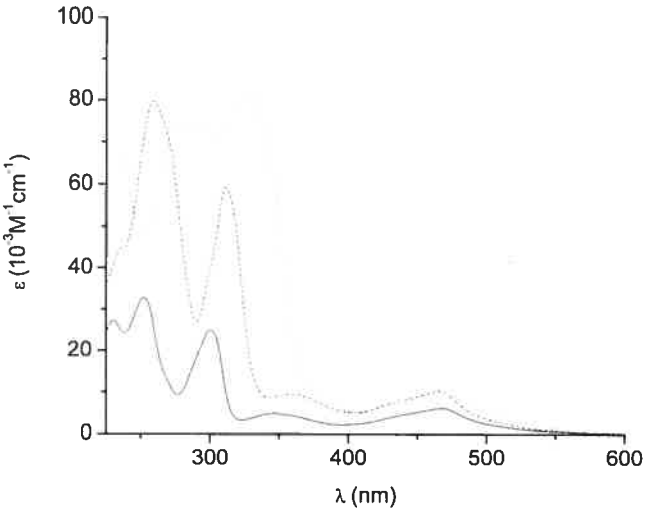

Figure 5.9 Absorption spectra of complexes **2a** (solid line), **2b** (dashed line) and **2c** (dotted line) in CH_3CN at room temperature.

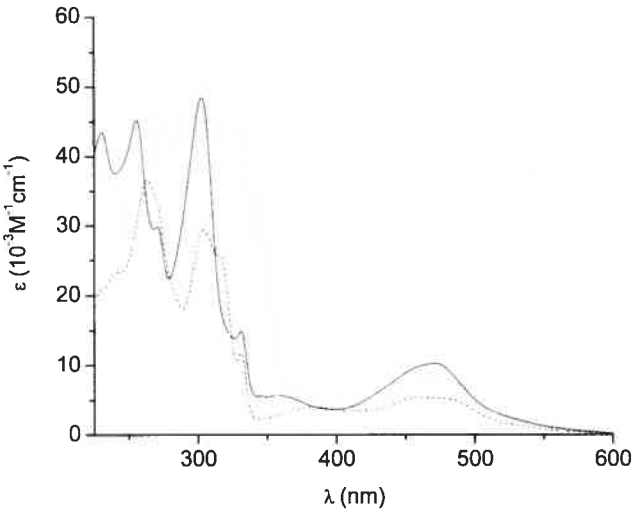

Figure 5.10 Absorption spectra of complexes **3a** (solid line), **3b** (dashed line) and **3c** (dotted line) in CH_3CN at room temperature.

The substituents on the pyrimidine rings in Rbppy ligands have very little effect on the ^{1}MLCT of the complexes, since the substituents have the same effect on the metal-based π_M orbital and ligand-based π_L^*.

Table 5.6 Absorption spectra data of complexes **2a-c**, **3a-c**.[a]

cpd	Absorption
	λ_{max}, nm (ε, $10^3 M^{-1}cm^{-1}$)
2a	468 (6.24), 347 (5.03), 300 (24.9), 252 (32.6), 230 (27.2)
2b	466 (10.3), 359 (9.43), 311 (59.3), 259 (79.8)
2c	474 (8.67), 328 (81.8), 278 (74.3), 232 (65.6)
3a	471 (10.3), 356 (5.63), 331 (15.0), 303 (48.5), 271 (29.9), 256 (45.3), 231 (43.5)
3b	469 (5.33), 382 (4.02), 331 (11.8), 304 (29.4), 263 (36.5), 243 (23.3)
3c	474 (8.08), 373 (5.79), 331 (43.9), 302 (50.7), 272 (47.3), 231 (38.2)
4[b]	474(10.4)

[a] Collected in acetonitrile at room temperature. [b] **4** = $Ru(tpy)_2^{2+}$, from ref. (16o).

5.3 Conclusion

A new synthetic approach to the tridentate ligands, 2,6-*bis*(5'-R-pyrimyd-2'-yl)pyridine (R = H, **1a**; Cl, **1b**; Ph, **1c**.), was developed. Application of these ligands to the coordination sphere of Ru(II) led to a new family of Ru(II) complexes **2a-c** and **3a-c**. The single crystal structural data of complexes **2a-b** and **3b** showed that the complexes adopted more distorted octahedral configurations which result in the weak ligand field strength of Rbppy ligands. The coordination of Rbppy ligands to the Ru(II) metal center has lowered (stabilized) the metal-based π_M orbital and ligand-based π_L^*. Better stabilization effects were observed on metal-based π_M orbital in homoleptic complexes **2a-c**. In heteroleptic complexes **3a-c**, the stabilization effects were in the same extent that the ^{1}MLCT bands were kept nearly the same as that in $Ru(tpy)_2^{2+}$.

5.4 Experimental Section

5.4.1 General methods

All reactions were performed under a dry argon atmosphere using standard Schlenk techniques. Solvents for the reaction were pre-dried using Pure-Solv Solvent Purification System (Innovative Technology Inc.). All chemicals were purchased from Sigma-Aldrich and used as received.

Nuclear magnetic resonance (NMR) spectra were recorded at room temperature (r.t.) on a Bruker AC-400 spectrometer at 400 MHz for ^{1}H NMR and at 100 MHz for ^{13}C NMR. Chemical shifts are reported in part per million (ppm) relative to residual solvents (2.50 ppm for DMSO-d_6, 7.26 ppm for chloroform-d and 1.94 ppm for acetonitrile-d_3) and the carbon resonance of the solvents. Melting points were measured on a Mel-Temp 1101D (Electrothermal, USA) without correction. ESI-MS and MALDI-TOF MS were done by the Mass Spectrometry Facility at Université de Montréal. Elemental analyses were done in the Elemental Analyses Lab in Département de chimie, Université de Montréal. Routine absorption spectra and emission spectra were measured in argon-purged acetonitrile at r.t. on a Cary 500i UV-vis-NIR Spectrophotometer and a Cary Eclipse Fluorescence Spectrophotometer, respectively. Electrochemical data were collected in Ar-purged acetonitrile with 1.0 M $^{n}Bu_4NPF_6$ on a BAS CV-50W Voltammetric Analyzer. Redox potentials were corrected by internal reference to ferrocence (395 mV vs SCE).

5.4.2 X-Ray crystallography

The solid-state structures of the complexes **2a-b** and **3b** were determined by X-ray crystallography. Recrystallization of **2a-b** and **3b** from acetonitrile solution, respectively, by slow diffusion of diethyl ether vapor provided dark-red single crystals suitable for single crystal X-ray diffraction. Crystal parameters and details of the data collection and refinement for **2a-b** and **3b** are given in **Table 5.7**.

Table 5.7 Crystallography data for complexes **2a-b** and **3b**.[a]

Complex	**2a**	**2b**	**3b**
Molecular formula	$C_{26}H_{18}F_{12}N_{10}P_2Ru\cdot 2.5(C_2H_3N)$	$C_{26}H_{14}Cl_4F_{12}N_{10}P_2Ru\cdot 2(C_2H_3N)\cdot 2(H_2O)$	$C_{28}H_{18}C_{12}N_8Ru\cdot 2(PF_6)\cdot 2(C_2H_3N)$
M	964.15	1117.42	1010.52
Crystal system	triclinic	monoclinlic	orthorhombic
a/Å	12.9633(18)	11.877(3)	16.3846(2)
b/Å	14.844(2)	10.666(2)	62.8985(8)
c/Å	19.220(3)	17.361(3)	14.5581(2)
α/°	87.483(3)	90	90
β/°	88.590(2)	119.990(11)	90
γ/°	78.648(2)	90	90
U/Å^3	3622.1(9)	1904.8(7)	15003.1(3)
Space group	P-1	P2/c	Fdd2
Z	4	2	16
Dc/Mg m^{-3}	1.768	1.948	1.790
μ/mm^{-1}	0.629	0.887	6.435
Temperature/K	125(2)	125(2)	100(2)
R1	0.0464	0.1066	0.277
wR2	0.1158	0.2791	0.0685

[a] Radiation sources for the structure determination of complexes **2a-b** were Mo source.

5.4.3 Syntheses of Ligands 1a-c

2,6- pyridine-bisamidine · 2HCl (**6**)[21]:

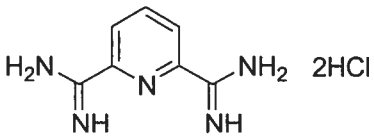

2,6-Pyridinedicarbonitrile (0.39 g, 3.0 mmol) and MeONa (0.42 g, 7.8 mmol) were added to anhydrous MeOH (25 mL) and the solution was stirred at room temperature for 24 h. Solid NH_4Cl (0.80 g, 15 mmol) was added and the mixture was stirred at room temperature for 48 h. Diethyl ether (200 mL) was added to the mixture and the resultant white solid was collected by filtration, washed with diethyl ether (10 mL × 3) and dried under vacuum to give **6**[21] (0.53 g, 2.2 mmol, 73%). ^{1}H NMR (DMSO-d_6, 400 MHz): δ 9.11 (s, br, 4H, H $_{N-H}$), 8.91 (d, J = 7.9 Hz, 2H, H $_{Py\,3,5}$), 8.53 (t, J = 7.9 Hz, 1H, H $_{Py\,4}$). ^{13}C NMR (DMSO-d_6, 100 MHz): δ 161.4, 144.9, 141.6, 128.2. ESI-MS: 237.1, $[M+H]^+$.

Ligands **1a-c**: General procedure for the synthesis of ligands **1a-c**.

2,6-*bis*(pyrimid-2'-yl)pyridine (**1a**):

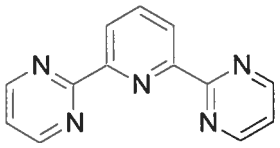

Compound **6** (0.47 g, 2.0 mmol), MeONa (0.27 g, 5.0 mmol) and vinamidine hexaflurophophate salt (1.24 g, 4.0 mmol) were added into anhydrous MeOH (25 mL) and the resultant mixture was heated at reflux for 16 h. The solvent was removed under reduced pressure and the residue was extracted with CH_2Cl_2 (15 mL × 3). The combined organic phases were washed with H_2O and the solvent was removed under reduced

pressure. Recrystallization of the residue from $CHCl_3$/MeOH afforded colorless crystalline product (0.31 g, 1.32 mmol, 66%). mp: 222.8-223.1. ^{1}H NMR ($CDCl_3$, 400 MHz): δ 8.94 (d, J = 4.9 Hz, 4H, H $_{Pm\,4,\,6}$), 8.60 (d, J = 7.8 Hz, 2H, H $_{Py\,3,\,5}$), 8.06 (t, J = 7.8 Hz, 1H, H $_{Py\,4}$), 7.32 (t, J = 4.9 Hz, 2H, H $_{Pm\,5}$). ^{1}H NMR (CD_3CN, 400 MHz): δ 8.99 (d, J = 4.9 Hz, 4H, H $_{Pm\,4,\,6}$), 8.59 (d, J = 7.9 Hz, 2H, H $_{Py\,3,\,5}$), 8.13 (t, J = 7.9 Hz, 1H, H $_{Py\,4}$), 7.48 (t, J = 4.9 Hz, 2H, H $_{Pm\,5}$). ^{13}C NMR ($CDCl_3$, 100 MHz): δ 164.1, 158.1, 155.6, 138.4, 125.1, 120.8. ESI-MS: 236.2 ($[M+H]^+$, 100%). Calculated for $C_{13}H_9N_5$, 236.0931, $[M+H]^+$; found, 236.0933. Calc. for $C_{13}H_9N_5$: C, 66.37; H, 3.86; N, 29.77. Found: C, 65.40; H, 3.73; N, 29.49.

2,6-*bis*(5'-chloro-pyrimid-2'-yl)pyridine (**1b**):

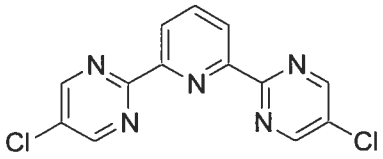

Yield, 68%. mp: 220.3-221.2. ^{1}H NMR ($CDCl_3$, 400 MHz): δ 8.91 (s, 4H, H $_{Pm4,\,6}$), 8.60 (d, J = 7.9 Hz, 2H, H $_{Py\,3,\,5}$), 8.08 (t, J = 7.9 Hz, 1H, H $_{Py\,4}$). ^{1}H NMR (CD_3CN, 400 MHz): δ 8.99 (s, 4H, H $_{Pm4,\,6}$), 8.59 (d, J = 7.9 Hz, 2H, H $_{Py\,3,\,5}$), 8.15 (t, J = 7.9 Hz, 1H, H $_{Py\,4}$). ^{13}C NMR ($CDCl_3$, 100 MHz): δ 161.7, 156.7, 154.7, 138.6, 131.4, 125.4. ESI-MS: 304.2 ($[M]^+$, 100%). Calculated for $C_{13}H_7Cl_2N_5$, 304.0154, $[M+H]^+$; found, 304.0151. Calc. for $C_{13}H_7Cl_2N_5$: C, 51.34; H, 2.32; N, 23.03. Found: C, 53.47; H, 2.18; N, 20.58.

2,6-*bis*(5'-phenyl-pyrimid-2'-yl)pyridine (**1c**):

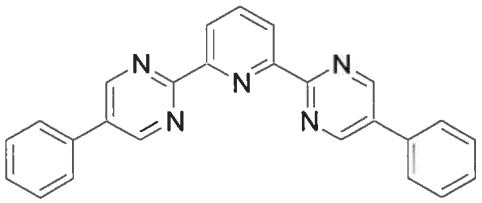

Yield, 70%. mp: 234.1-234.7. ^{1}H NMR ($CDCl_3$, 400 MHz): δ 9.21 (s, 4H, H $_{Pm\ 4,6}$), 8.71 (d, J = 7.8 Hz, 2H, H $_{Py\ 3,5}$), 8.12 (t, J = 7.8 Hz, 1H, H $_{Py\ 4}$), 7.71 (d, J = 8.2 Hz, 4H, H $_{Ph\ 2,6}$), 7.60-7.49 (m, 6H, H $_{Ph\ 3,4,5}$). ^{1}H NMR (CD_3CN, 400 MHz): δ 9.27 (s, 4H, H $_{Pm\ 4,6}$), 8.68 (d, J = 7.9 Hz, 2H, H $_{Py\ 3,5}$), 8.18 (t, J = 7.9 Hz, 1H, H $_{Py\ 4}$), 7.85 (d, J = 7.2 Hz, 4H, H $_{Ph\ 2,6}$), 7.64-7.53 (m, 6H, H $_{Ph\ 3,4,5}$). ^{13}C NMR ($CDCl_3$, 100 MHz): δ 162.0, 155.3, 154.6, 137.7, 133.9, 132.6, 129.1, 128.7, 126.6, 124.3. ESI-MS: 388.3 ($[M+H]^+$, 100%). Calculated for $C_{25}H_{17}N_5$, 388.1556, $[M+H]^+$; found, 388.1567. Calc. for $C_{25}H_{17}N_5$: C, 77.50; H, 4.42; N, 18.08. Found: C, 65.09; H, 4.15; N, 15.01.

5.4.4 Synthesis of complexes 2a-c and 3a-c

Complexes **2a-c**: General procedure for homoleptic complexes **2a-c**.

Bis[2,6-*bis*(pyrimid-2'-yl)pyridine] ruthenium(II) hexaflurophosphate (**2a**):

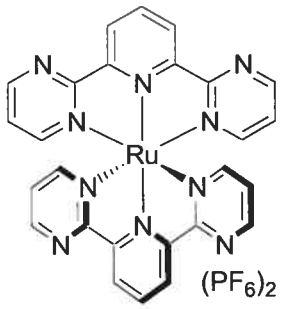

Ligand 2,6-bis(pyrimyd-2yl)pyridine (2a, 94 mg, 0.40 mmol), ruthenium trichloride hydrate (45 mg, 0.20 mmol) and silver nitrate (102 mg, 0.60 mmol) were heated to reflux in anhydrous ethanol (20 mL) for 12 h. The mixture was filtered through celite and the

filtrate was evaporated to dryness under reduced pressure. The residue was then chromatographed on a silica gel column with 7:1 acetonitrile and saturated aqueous KNO_3 as eluent. Anion exchange with NH_4PF_6 gave pure product **3a** (0.113 g, 66 %). ^{1}H NMR (CD_3CN, 400 MHz): δ 9.00 (d, J = 8.1 Hz, 4H, H $_{Py\,3,5}$), 8.88 (dd, J = 4.7, 1.0 Hz, 4H, H $_{Pm\,4}$), 8.54 (t, J = 8.1 Hz, 2H, H $_{Py\,4}$), 7.74 (dd, J = 5.7, 1.1 Hz, 4H, H $_{Pm\,6}$), 7.23 (t, J = 5.3, 4H, H $_{Pm\,5}$). ^{13}C NMR (CD_3CN, 100 MHz): δ 164.9, 160.9, 157.5, 154.1, 137.0, 127.2, 122.5. ESI-MS: 285.8 ($[M-2PF_6]^{2+}$, 100%); 716.2 ($[M-PF_6]^+$, 48%). Calculated for $C_{26}H_{18}N_{10}RuP_2F_{12}$, 717.0401, $[M-PF_6]^+$; found, 717.0396.

Bis[2,6-*bis*(5'-chloro-pyrimid-2'-yl)pyridine] ruthenium(II) hexaflurophosphate (**2b**):

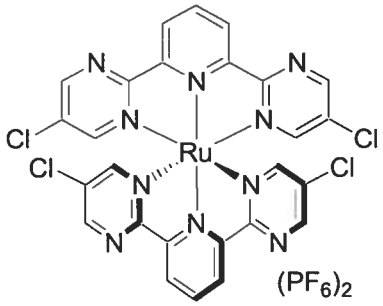

Yield, 20 %. ^{1}H NMR (CD_3CN, 400 MHz): δ 8.98 (d, J = 8.1 Hz, 4H, H $_{Py\,3,5}$), 8.92 (d, J = 2.4 Hz, 4H, H $_{Pm\,4}$), 8.56 (t, J = 7.9 Hz, 2H, H $_{Py\,4}$), 7.76 (d, J = 2.4 Hz, 4H, H $_{Pm\,6}$). ^{13}C NMR (CD_3CN, 100 MHz): δ 163.8, 160.7, 157.1, 154.4, 138.5, 132.2, 128.6. ESI-MS: 355.0 ($[M-2PF_6]^{2+}$, 100%); 854.9 ($[M-PF_6]^+$, 17%). Calculated for $C_{26}H_{14}Cl_4N_{10}RuP_2F_{12}$, 852.8842, $[M-PF_6]^+$; found, 852.8837.

Unknown complex **2b'**: Proposed structure.

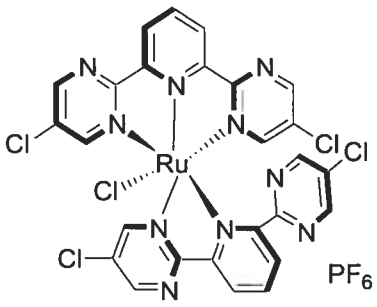

Yield, 76%. ^{1}H NMR (CD_3CN, 400 MHz): δ 10.18 (d, J = 2.7 Hz, 1H), 9.30 (d, J = 2.7 Hz, 1H), 8.93 (d, J = 2.6 Hz, 2H), 8.92 (d, J = 7.9 Hz, 1H), 8.42 (d, J = 8.0 Hz, 2H), 8.35 (s, 2H), 8.25 (d, J = 2.6 Hz, 2H), 8.08-8.00 (m, 2H), 7.23 (dd, J = 7.7, 1.5 Hz, 1H). ^{13}C NMR (CD_3CN, 100 MHz): δ 163.7, 163.1, 160.0, 158.6, 156.3, 156.2, 155.8, 155.7, 155.6, 153.6, 138.1, 137.7, 134.2, 132.1, 131.4, 131.2, 128.8, 127.9, 126.5, 125.3. ESI-MS: 355.1 ($[M-PF_6-Cl]^{2+}$, 7%); 744.9 ($[M-PF_6]^{+}$, 100%). Calculated for $C_{26}H_{14}Cl_5N_{10}RuPF_6$, 742.8890, $[M-PF_6]^{+}$; found, 742.8884.

Bis[2,6-*bis*(5'-chloro-pyrimid-2'-yl)pyridine] ruthenium(II) hexaflurophosphate (**2c**):

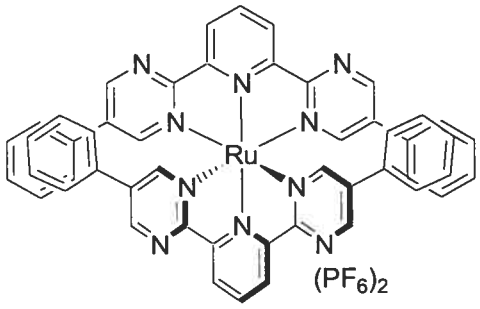

Yield, 68%. ^{1}H NMR (CD_3CN, 400 MHz): δ 9.14 (d, J = 2.5 Hz, 4H, $H_{Pm\,4}$), 9.03 (d, J = 8.1 Hz, 4H, $H_{Py\,3,5}$), 8.56 (t, J = 8.1 Hz, 2H, $H_{Py\,4}$), 7.85 (d, J = 2.6 Hz, $H_{Pm\,6}$), 7.46-7.44 (m, 10H, H_{Ph}). ^{13}C NMR (CD_3CN, 100 MHz): δ 163.4, 158.0, 155.1, 154.1, 137.0, 135.0, 131.3, 129.7, 129.0, 127.2, 127.1. ESI-MS: 438.1 ($[M-2PF_6]^{2+}$, 100%); 1021.2 ($[M-PF_6]^{+}$, 46%). Calculated for $C_{50}H_{34}N_{10}RuP_2F_{12}$, 1021.1653, $[M-PF_6]^{+}$; found,

1021.1648.

Complexes **3a-c**: General procedure for heteroleptic complexes **3a-c**.

[2,6-*bis*(pyrimid-2'-yl)pyridine](2,2':6',2"-terpyridine) ruthenium(II) hexaflurophosphate (**3a**):

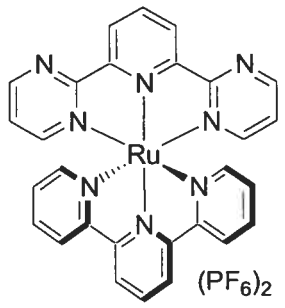

Ligand 2,6-bis(pyrimyd-2yl)pyridine (1a, 56 mg, 0.24 mmol), ruthenium terpyridine trichloride (110 mg, 0.25 mmol) and silver nitrate (0.128 g, 0.75 mmol) were heated to reflux in anhydrous DMF (15 mL) for 4 h. The mixture was filtered through celite and the filtrate was evaporated to dryness under reduced pressure. The residue was then chromatographed on a silica gel column with 7:1 acetonitrile and saturated aqueous KNO_3. Anion exchange with NH_4PF_6 gave pure product (0.132 g, 64 %). ^{1}H NMR (CD_3CN, 400 MHz): δ 9.00 (d, J = 8.0 Hz, 2H, H $_{Py\,3,\,5}$), 8.86 (dd, J = 4.8, 2.1 Hz, 2H, H $_{Pm\,4}$), 8.75 (d, J = 8.2 Hz, 2H, H $_{3',\,5'}$), 8.53–8.45 (m, 4H, H $_{3,\,3'',\,4',\,Py\,4}$), 7.95 (td, J^t = 7.9 Hz, J^d = 1.5 Hz, 2H, H $_{4,\,4''}$), 7.71 (dd, J = 5.8, 2.0 Hz, 2H, H $_{Pm\,6}$), 7.38 (d, J = 4.8 Hz, 2H, H $_{6,\,6''}$), 7.23 – 7.17 (m, 4H, H $_{5,\,5'',\,Pm\,5}$). ^{13}C NMR (CD_3CN, 100 MHz): δ 165.0, 160.0, 157.5, 157.2, 155.0, 154.0, 152.9, 138.0, 136.3, 136.2, 127.2, 127.1, 124.0, 123.4, 122.5. ESI-MS: 285.4 ($[M\text{-}2PF_6]^{2+}$, 100%); 715.0 ($[M\text{-}PF_6]^+$, 67%). Calculated for $C_{28}H_{20}N_8RuP_2F_{12}$, 715.0496, $[M\text{-}PF_6]^+$; found, 715.0491.

[2,6-*bis*(5-chloro-pyrimid-2-yl)pyridine](2,2':6',2"-terpyridine) ruthenium(II) hexaflurophosphate (**3b**):

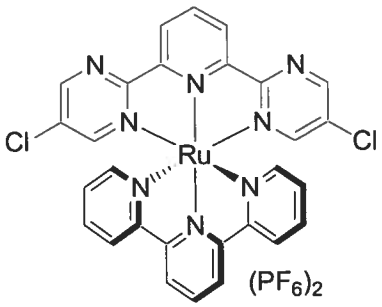

Yield, 65%. ^{1}H NMR (CD_3CN, 400 MHz): δ 8.99 (d, J = 8.1 Hz, 2H, H $_{Py\ 3,5}$), 8.87 (d, J = 2.6 Hz, 2H, H $_{Pm\ 4}$), 8.76 (d, J = 8.2 Hz, 2H, H $_{3',5'}$), 8.53-8.45 (m, 4H, H $_{3,3'',4',Py\ 4}$), 7.98 (td, J^t = 7.9 Hz, J^d = 1.5 Hz, 2H, H $_{4,4''}$), 7.73 (d, J = 2.6 Hz, 2H, H $_{Pm\ 6}$), 7.36 (dd, J = 5.6, 0.6 Hz, 2H, H $_{6,6''}$), 7.21 (td, J^t = 6.6 Hz, J^d = 1.3 Hz, 2H, H $_{5,5''}$). ^{13}C NMR (CD_3CN, 100 MHz): δ 162.9, 158.6, 157.7, 156.0, 155.1, 153.4, 153.2, 138.2, 136.8, 136.3, 131.6, 127.3, 127.1, 124.2, 123.8. ESI-MS: 319.0 ($[M-2PF_6]^{2+}$, 100%); 783.0 ($[M-PF_6]^{+}$, 56%). Calculated for $C_{28}H_{18}N_8Cl_2RuP_2F_{12}$, 782.9711, $[M-PF_6]^{+}$; found, 782.9705.

[2,6-*bis*(5-phenyl-pyrimid-2-yl)pyridine](2,2':6',2"-terpyridine) ruthenium(II) hexaflurophosphate (**3c**):

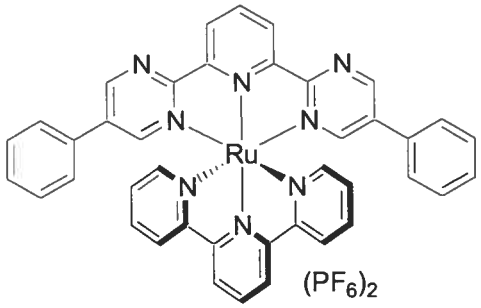

Yield, 62%. ^{1}H NMR (CD_3CN, 400 MHz): δ 9.11 (d, J = 2.6 Hz, 2H, H $_{Pm\ 4}$), 9.03 (d, J = 8.1 Hz, 2H, H $_{Py\ 3,5}$), 8.75 (d, J = 8.2 Hz, 2H, H $_{3',5'}$), 8.53 (t, J = 8.0 Hz, 1H, H $_{Py\ 4}$), 8.49

(d, J = 7.8 Hz, 2H, H $_{3, 3''}$), 8.44 (t, J = 8.2 Hz, 1H, H $_{4'}$), 7.94 (td, J^t = 7.9 Hz, J^d = 1.5 Hz, 2H, H $_{4, 4''}$), 7.74 (d, J = 2.6 Hz, 2H, H $_{Pm\,6}$), 7.46-7.40 (m, 12H, H $_{6, 6'', Ph\,2, 3, 4, 5, 6}$), 7.21 (td, J^t = 6.7 Hz, J^d = 1.4 Hz, 2H, H $_{5, 5''}$). ^{13}C NMR (CD_3CN, 100 MHz): δ 164.0, 158.5, 157.7, 155.9, 155.8, 154.6, 153.5, 138.7, 137.0, 136.9, 135.9, 132.1, 130.5, 129.7, 127.9, 127.8, 127.6, 125.1, 124.5. ESI-MS: 361.4 ($[M-2PF_6]^{2+}$, 100%); 867.0 ($[M-PF_6]^+$, 99%). Calculated for $C_{40}H_{28}N_8RuP_2F_{12}$, 867.1122, $[M-PF_6]^+$; found, 867.1117.

5.5 References

1. G. T. Morgan, F. H. Burstall. J. Chem. Soc. 20 (1932).

2. (*a*) V. Balzani, F. Barigelletti, P. Belser, S. Bernhard, L. De Cola, L. Flamigni. J. Phys. Chem. **100**, 16786 (1996). (*b*) E. C. Constable. Prog. Inorg. Chem. **42**, 67 (1994). (*c*) S. Chodorowski-Kimmes, M. Beley, J.-P. Collin, J.-P. Sauvage. Tetrahedron Lett. **37**, 2963 (1996). (*d*) A. M. W. Cargill Thompson. Coord. Chem. Rev. **160**, 1 (1997). (*e*) E. C. Constable, J. E. Davies, D. Phillips, P. R. Raithby. Polyhedron **17**, 3989 (1998). (*f*) J.-P. Sauvage, J.-P. Collin, J.-C. Chambron, S. Guillerez, C. Coudret, V. Balzani, F. Barigelletti, L. De Cola, L. Flamigni. Chem. Rev. **94**, 993 (1994).

3. M. Mukkala, M. Helenius, I. Hemmila, J. Kankare, H. Takalo. Helv. Chim. Acta **76**, 1361 (1993).

4. (*a*) G. Chelucci. Synth. Commun. **23**, 1897 (1993). (*b*) G. Chelucci, A. Saba, D. Vignola, C. Solinas. Tetrahedron **57**, 1099 (2001).

5. (*a*) J.-P. Collin, V. Heitz, J.-P. Sauvage. Tetrahedron Lett. **32**, 5977 (1991). (*b*) J. C. Chambron, J.-P. Collin, J.-O. Dalbavie, C. O. Dietrich-Buchecker, V. Heitz, F. Odobel, N. Solladié, J.-P. Sauvage. Coord. Chem. Rev. **178**, 1299 (1998). (*c*) J.-P. Collin, A. Harriman, V. Heitz, F. Odobel, J.-P. Sauvage. Coord. Chem. Rev. **148**, 63 (1996). (*d*) M. Kimura, T. Hamakawa, K. Hanabusa, H. Shirai, N. Kobayashi. Inorg. Chem. **40**, 4775 (2001). (*e*) L. Flamigni, F. Barigelletti, N. Armaroli, B. Ventura, J.-P. Collin, J.-P. Sauvage, J. A. G. Williams. Inorg. Chem. **38**, 661 (1999). (*f*) J.-P. Collin, A. Harriman, V. Heitz, F. Odobel, J.-P. Sauvage. J. Am. Chem. Soc. **116**, 5679 (1994).

6. (*a*) B. Whittle, N. S. Everest, C. Howard M. D. Ward. Inorg. Chem. **34**, 2025 (1995). (*b*) G. D. Storrier, K. Takad, H. D. Abruna. Inorg. Chem. **38**, 559 (1999).

7. (*a*) H. Tsukube, T. Hamada, T. Tanaka, J. Uenishi. Inorg. Chim. Acta **214**, 1 (1993). (*b*) F. Loiseau, C. Di Petrio, S. Serroni, S. Campagna A. Licciardello, A. Manfredi, G. Pozzi, S. Quici. Inorg. Chem. **40**, 6901 (2001). (*c*) J. M. Haider, M. Chavarot, S. Weidner, I. Sadler, R. M. Williams, L. De Cola, Z. Pikramenou. Inorg. Chem. **40**, 3912 (2001).

8. (*a*) P. Pechy, F. P. Rotzinger, M. K. Nazeeruddin, O. Kohle, S. M. Zakeeruddin, R. Humphry-Baker, M. Grätzel. J. Chem. Soc., Chem. Commun. 65 (1995). (*b*) Y. W. Liang, R. H. Schmehl. J. Chem. Soc., Chem. Commun. 1007 (1995). (*c*) C. R. Rice, M. D. Ward, M. K. Nazeeruddin, M. Grätzel. New J. Chem. **24**, 651 (2000). (*d*) A. Islam, H. Sugihara, H. Arakawa. J. Photochem. Photobiol. A: Chem. **158**, 131 (2003). (*e*) C. Bauer, G. Boschloo, E. Mukhtar, A. Hagfeldt. J. Phys. Chem. B **106**, 12693 (2002).

9. (*a*) F. Zeng, S. C. Zimmerman. Chem. Rev. **97**, 1681 (1997). (*b*) E. C. Constable, C. E. Housecroft, M. Neuburger, A. G. Schneider, B. Springler, M. Zehnder. Inorg. Chim. Acta **300**, 49 (2000). (*c*) L. Flamigni, F. Barigelletti, N. Armaroli, J.-P. Collin, I. M. Dixon, J.-P. Sauvage, J. A. Gareth Williams. Coord. Chem. Rev. **190**, 671 (1999). (*d*) J. P. Collin, S. Gillerez, J.-P. Sauvage, F. Barigelletti, L. Flamigni, L. De Cola, V. Balzani. Coord. Chem. Rev. **111**, 291 (1991). (*e*) O. Johansson, M. Borgstrom, R. Lomoth, M. Palmblad, J. Bergquist, L. Hammarström, L. Sun, B. Åkermark. Inorg. Chem. **42**, 2908 (2003). (*f*) J.-P. Collin, C. Dietrich-Buchecker, P. Gavina, M. C. Jimenez-Molero, J.-P. Sauvage.

Acc. Chem. Res. **34**, 477 (2001).

10. M. I. J. Polson, E. A. Medlycott, G. S. Hanan, L. Mikelsons, N. J. Taylor, M. Watanabe, Y. Tanaka, F. Loiseau, R. Passalacqua, S. Campagna. Chem. Eur. J. **10**, 3640 (2004).

11. (*a*) E. C. Constable, R. P. G. Henney, T. A. Leese, D. A. Tocher. J. Chem. Soc., Dalton Trans. **2**, 443 (1990). (*b*) J.-P. Collin, M. Beley, J.-P. Sauvage, F. Barigelletti. Inorg. Chim. Acta **186**, 91 (1991).

12. (*a*) M. Beley, J.-P. Collin, R. Louis, B. Metz, J.-P. Sauvage. J. Am. Chem. Soc. **113**, 8521 (1991). (*b*) D. J. Cardenas, A. M. Echavarren, M. C. Ramirez de Arellano. Organometallics **18**, 3337 (1999). (*c*) J. A. G. Williams, A. Beeby, E. S. Davies, J. A. Weinstein, C. Wilson. Inorg. Chem. **42**, 8609 (2003).

13. (*a*) H. Wolpher, O. Johansson, M. Abrahamsson, M. Kritikos, L. Sun, B. Akermark. Inorg. Chem. Commun. **7**, 337 (2004). (*b*) M. Abrahamsson, H. Wolpher, O. Johansson, J. Larsson, M. Kritikos, L. Eriksson, P.-O. Norrby, L. Sun, B. Akermark, L. Hammarström. Inorg. Chem. **44**, 3215 (2005).

14. E. Bejan, H. A. Haddou, J. C. Daran, G. G. A. Balavoine. Synthesis **8**, 1012 (1996).

15. J. H. Groen, P. W. N. M. van Leeuwen, K. Vrieze. J. Chem. Soc., Dalton Trans. **1**, 113 (1998).

16. (*a*) E.C. Constable. Prog. Inorg. Chem. Vol. **42**, Wiley, New York 67 (1994). (*b*) E. M. Kober, J. L. Marshall, W. J. Dressick, B. P. Sullivan, J. V. Caspar and T. J. Meyer. Inorg. Chem. **24**, 2755 (1985). (*c*) C. R. Hecker, A. K. I. Gushurst and D. R. McMillin. Inorg. Chem. **30**, 538 (1991). (*d*) E. Amouyal, M. Mouallem-Bahout

and G. Calzaferri. J. Phys. Chem. **95**, 7641 (1991). (*e*) C. R. Arana and H. D. Abruña. Inorg. Chem. **32**, 194 (1993). (*f*) J.-P. Collin, S. Guillerez, J.-P. Sauvage, F. Barigelletti, L. De Cola, L. Flamigni and V. Balzani. Inorg. Chem. **30**, 4230 (1991). (*g*) J.-P. Collin, S. Guillerez, J.-P. Sauvage, F. Barigelletti, L. De Cola, L. Flamigni and V. Balzani. Inorg. Chem. **31**, 4112 (1992). (*h*) V. Grosshenny and R. Ziessel. J. Chem. Soc., Dalton Trans. 817 (1993). (*i*) V. Grosshenny and R. Ziessel. J. Organomet. Chem. **19**, 453 (1993). (*j*) A. Harriman and R. Ziessel. Chem. Commun. 1707 (1996). (*k*) F. Barigelletti, L. Flamigni, V. Balzani, J.-P. Collin, J.-P. Sauvage, A. Sour, E. C. Constable and A. M. W. Cargill Thompson. J. Chem. Soc., Chem. Commun. 942 (1993). (*l*) F. Barigelletti, L. Flamigni, V. Balzani, J.-P. Collin, J.-P. Sauvage, A. Sour, E. C. Constable and A. M. W. Cargill Thompson. J. Am. Chem. Soc. **116**, 7692 (1994). (*m*) F. Barigelletti, L. Flamigni, V. Balzani, J.-P. Collin, J.-P. Sauvage and A. Sour. New J. Chem. **19**, 793 (1995). (*n*) J.-P. Sauvage, J.-P. Collin, J.-C. Chambron, S. Guillerez, C. Coudret, V. Balzani, F. Barigelletti, L. De Cola and L. Flamigni. Chem. Rev. **94**, 993 (1994). (*o*) M. Maestri, N. Armaroli, V. Balzani, E. C. Constable and A. M. W. Cargill Thompson. Inorg. Chem. **34**, 2759 (1995). (*p*) J. Wang, G. S. Hanan, F. Loiseau, R. Passalacqua, S. Campagna. Inorg. Chem. **44**, 5 (2005). (*q*) E. A. Medlycott,G. S. Hanan. Chem. Soc. Rev. **34**, 133 (2005).

17 (*a*)A. Juris, V. Balzani, F. Barigelletti, S. Campagna, P. Belser, and A. Von Zelewsky. Coord. Chem. Rev. **84**, 85 (1988); (*b*) J. A. Treadway, B. Loeb, R. Lopez, P. A. Anderson, F. R. Keene and T. J. Meyer. Inorg. Chem. **35**, 2242 (1996); (*c*) X.-Y. Xian, A. Del Guerzo and R. H. Schemehl. J. Photochem.

Photobiol., C 5, 55 (2004); (*d*) E. Baranoff, J.-P. Collin, L. Flamigni and J.-P. Sauvage. Chem. Soc. Rev. **33**, 147 (2004).

18 Y.-Q. Fang, A. J. Taylor, G. S. Hanan, F. Loiseau, R. Passalacqua, S. Campagna, H. Nierengarten, A. Van Dorsselaer. J. Am. Chem. Soc. **124**, 7912 (2002).

19 (*a*) E. C. Constable, A. M. W. Cargill Thompson, D. A. Tocher, M. A. M. Daniels. New J. Chem. **16**, 855 (1992). (*b*) S. Pyo, E. Perez-Cordero, S. G. Bott, L. Echegoyen. Inorg. Chem. **38**, 3337 (1999). (*c*) G. S. Hanan, C. R. Arana, J.-M. Lehn, D. Fense. Angew. Chem. Int. Ed. Engl. **34**, 1122 (1995). (*d*) G. S. Hanan, C. R. Arana, J.-M. Lehn, D. Fense. Chem. Eur. J. **2**, 1292 (1996). (*e*) K. Lashgari, M. Kritikos, R. Norrestam, T. Norrby. Acta Crystallogr. Sect. C **C55**, 64 (1999).

20 T. Mutai, J.-D. Cheon, S. Arita and K. Araki. J. Chem. Soc., Perkin Trans. 2 1045 (2001).

21 H. Takalo, V. M. Mukkala. PCT Int. Appl. 78. WO 9311433 A1 19930610 (1993).

22 A similar effect was reported previously: R. P. Thummel, Y. Jahng. Inorg. Chem. **25**, 2527 (1986).

Chapter 6

A Facile Route to Sterically Hindered and Non-hindered 4'-Aryl-2,2':6',2''-Terpyridines

---

Article

Jianhua Wang, Garry S. Hanan

SynLett. **2005**, *8*, 1251-1254.

Abstract

A facile one-pot synthesis of 4'-aryl-2,2':6',2"-terpyridines from aryl aldehydes and 2-acetylpyridine is presented. The synthesis of terpyridines incorporating sterically hindered aryl groups, such as the 9-anthryl group, can also be readily synthesized using this method.

Key words

nitrogen ligands, heterocycles, substituted terpyridines, one-pot reactions

6.1 Introduction

Transition metal complexes of polypyridyl ligands have long been a target in coordination chemistry due to their potential utility in a range of applications, such as luminescent chemosensors, photocatalysts, components of devices for the conversion of light into electrical energy, and new electroluminescent materials.[1-3] The prototypical 2,2'-bipyridine (bpy) and 2,2':6',2"-terpyridine (tpy) ligands have been employed in a large number of these studies, usually binding as bidentate and tridentate ligands, respectively. The advantage of the latter ligand is that structurally simple achiral bis-tpy complexes are obtained with octahedrally coordinating metal ions, which can in turn be used to build up stereochemically discrete polynuclear arrays, as opposed to the racemic mixtures derived from bpy. Moreover, the achirality of tpy complexes is retained upon the chemical modification of the tpy by introducing functional groups into its 4'-position, which necessarily arranges them in a *trans* configuration along a *C2* axis.

Introducing aryl substituents at the 4'-position of tpy can also have a profound influence on the photophysical properties of bis-tpy metal complexes and this effect has been investigated in some detail.[4] More recently, the photophysical properties of uncomplexed terpyridines have also begun to attract interest due to their potential application in photophysical devices.[5-8] Strategies for the incorporation of aryl substituents into the 4'-position of the terpyridine core are of considerable interest with respect to many of the applications discussed above.

The classical approach to 4'-aryl-tpy are based on the synthesis of a pyridine, involving the condensation of two equivalents of 2-acetylpyridine with the appropriate aryl aldehyde, with formation of the central pyridine ring from the reaction of the

diketone intermediate with ammonia (or a source thereof) at elevated temperatures.[9] A number of variations have been reported, some involving isolation of the intermediate enone or diketone, others employing mild or solvent-free conditions for parts of the synthesis, but almost all relying on a common step in which the central pyridine ring is formed.[10] In particular, the approach involving the reaction of 2-pyridyl enaminone and 2-acetylpyridine with a strong base, tBuOK, has been widely employed for the synthesis of the parent tpy ligand. Distinctly different synthetic approaches, in which all three pyridine rings are present in the starting materials, include the reaction of 2,2'-bipyridine with 2-pyridyl-lithiums, the Stille coupling of 2,6-dibromopyridines with 2-trialkylstannyl pyridines,[11] and the Suzuki cross-coupling of 4'-bromo-tpy with aryl-boronic acid/ester.[12] However, these approaches feature relatively long reaction times, harsh conditions and the necessity to purify the products by column chromatography. As part of our research with Ru(II) complexes of tridentate tpy ligands, a mild and efficient synthesis of a variety of 4'-aryl-tpy ligands was required.[13] Herein we report the facile one-step synthesis of a variety of tpy-based ligands with aromatic substituents in their 4'-position, which greatly improves the one-pot synthesis for 4'-aryl-tpy ligands previously reported.[14]

6.2 Results and discussion

Our optimization of the one-step reaction started from readily available aryl aldehydes[15] and 2-acetylpyridine (**Scheme 6.1**). The reaction conditions and yields of the various ligands are gathered in **Table 6.1**. The enolate of 2-acetylpyridine can be generated by KOH under mild conditions. The following aldol condensation and Michael addition proceeded smoothly at room temperature. The soluble diketone intermediate was then allowed to form the central pyridine ring with an aqueous ammonia nitrogen source. The synthesis of the phenyl-based tpy ligands, **1-9**, was very straightforward using these mild conditions. Typically, the ligands precipitated from the reaction mixture as finely dispersed solids, which were easily separated by filtration. For **4**, after 24 h reaction, the ligand was separated from the reaction mixture by acidification with AcOH, extraction with DCM and recrystallization from EtOH.

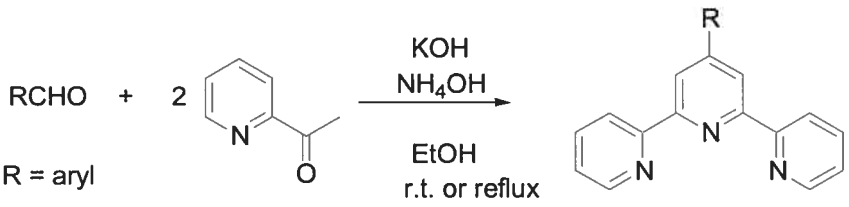

Scheme 6.1 Facile one-pot synthesis of 4'-aryl-2,2':6',2"-terpyridine.

The encouraging results for the synthesis of ligands **1-9** led us to apply these mild conditions to introduce organic chromophores into the tpy moiety, which is a critical step to prolong the r.t. luminescence lifetime of $Ru(tpy)_2^{2+}$ complexes by the bichromophore approach.[16] The 4'-biphenyl and 1-naphthyl groups were introduced into 4'-position of tpy to give ligand **10** and **11** by stirring at r.t. for 4 h. However, the synthesis of ligand **12**

with the bulkier 9-anthryl group was problematic due to the insolubility of the intermediate, 2-(1-(9-anthryl)-3-oxo-3-prop-2-enyl] pyridine, in EtOH. Treatment of the same starting materials at reflux kept the enone intermediate in solution leading to a one-step synthesis of 4'-(9-anthryl)-tpy. It is noteworthy that this is the first example of a one-step synthesis of tpy-based ligands with bulky substituents in the 4'-position.

To survey the scope of the reaction conditions for heteroatom aromatic aldehydes, the 2-furyl-tpy (**13**) and 4-pyridyl-tpy (**14**) were also synthesized in moderate yield.

Table 6.1 Reaction conditions and yields of 4'-aryl-2,2':6',2"-terpyridines compared with the methods previously reported.[a]

Ligand, R	Rxn time, h; Yield (%)[b]	Yield, %;[c] (steps[d])
1 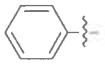	2; (53)	<5; (4)[6]e
2 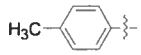	2; (49)	19; (4)[5], 46; (1)[13]
3 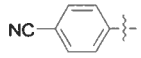	4; (42)	36; (5)[6]e
4 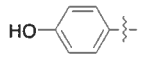	12; (43)	40; (2)[17]
5 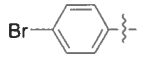	2; (56)	70; (2)[5]
6 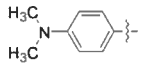	12; (25)	17; (4)[5], 29; (4)[6]e
7 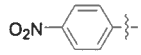	4; (51)	65; (2)[5], 34; (5)[6]e
8 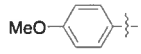	12; (20)	20; (4)[5]
9 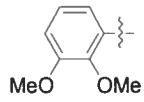	24; (27)	new
10 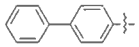	4; (48)	42; (1)[6]f
11 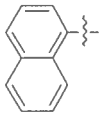	4; (32)	no yield available[18]
12 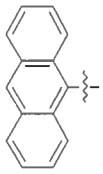	24[g]; (27)	59; (2)[4c]
13 	4; (24)	69; (2)[19]
14 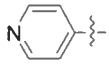	4; (42)	69; (2)[20]

[a] Reaction condition: 1.0 equiv. aryl aldehyde, 2.0 equiv. 2-acetyl pyridine, 2.0 equiv. KOH, 2.5 equiv. $NH_3 \cdot H_2O$, EtOH, rt.

[b] Isolated yield of first crop of precipitate in our work.

[c] Isolated overall yields as previously reported.

d Number of reaction steps from commercial available starting materials.

[e] In ref.[6], from 4'-TfO-2,2':6',2"-terpyridine (TfO-tpy, 45% overall yield over 3 steps) or 4'-bromo-2,2':6',2"-terpyridine (45% overall yield over 4 steps).

[f] Starting from 4'-*p*-bromophenyl-2,2':6',2"-terpyridine.

[g] Reaction condition: 1.0 equiv. 9-anthryl aldehyde, 2.0 equiv. 2-acetyl pyridine, 2.5 equiv. $NH_3 \cdot H_2O$, EtOH, reflux, 24 h.

6.3 Conclusion

In conclusion, we have developed mild reaction conditions for the synthesis of 4'-aryl and 4'-heteroaryl substituted tpys. These reaction conditions are compatible with various functional groups and provide an efficient route to tridentate 2,2':6',2''-terpyridine-based ligands.

6.4 Experimental

6.4.1 General methods

Nuclear magnetic resonance (NMR) spectra were recorded at room temperature (r.t.) on a Bruker AV400 spectrometer at 400 MHz for ^{1}H NMR and at 100 MHz for ^{13}C NMR. Chemical shifts are reported in part per million (ppm) relative to residual protonated solvents and the carbon resonance of the solvents. Fast-atom bombardment (FAB, positive mode) spectra were recorded on a ZAB-HF-VB-analytical apparatus in an *m*-nitrobenzylalcohol (*m*-NBA) matrix and Ar atoms were used for the bombardment (8 KeV). Microanalysis was done in the Microanalysis Laboratory, Universite de Montreal.

6.4.2 Materials

All chemicals were purchased from Sigma-Aldrich, AnaChemia and BDH and were used as received. Solvents for reaction were purchased from Fisher and used as received.

6.4.3 Ligands: General method for 1-11, 13-14:

4'-phenyl-2,2':6',2"-terpyridine (1)

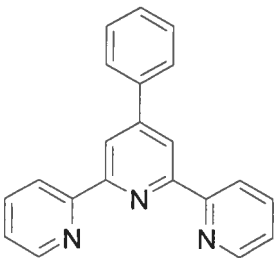

2-Acetylpyridine (4.84 g, 40 mmol) was added into a solution of benzaldehyde (2.12 g, 20 mmol) in ethanol (100 mL). KOH pellet (3.08 g, 85%, 40 mmol) and aqueous ammonium (58 mL, 29.3%, 50 mmol) were then added to the solution. The solution was stirred at room temperature for 2 h. The pale-green solid was collected by filtration, washed with ethanol (10 mL × 3). Recrystallization from $CHCl_3$/MeOH afforded white crystalline solid (3.24 g, 10.5 mmol, 53%): ^{1}H NMR ($CDCl_3$, 400 MHz): δ 8.76 (s, 2H, H $_{3',5'}$), 8.74 (d, J = 6.5 Hz, 2H, H $_{6,6''}$), 8.68 (d, J = 8.0, 2H, H $_{3,3''}$), 7.92 (d, J = 6.9 Hz, 2H, H $_{Ph\,2,6}$), 7.90 (t, J = 7.5 Hz, 2H, H $_{4,4''}$), 7.52 (t, J = 6.9 Hz, 2H, H $_{Ph\,3,5}$), 7.46 (t, J = 6.9 Hz, 1H, H $_{Ph\,4}$), 7.37 (dd, J = 7.5, 5.0 Hz, 2H, H $_{5,5''}$). ^{13}C NMR ($CDCl_3$, 100 MHz): δ 156.5, 156.2, 150.8, 149.4, 138.8, 137.4, 129.5, 129.3, 127.8, 124.3, 121.9, 119.4. Anal. Calcd. for $C_{21}H_{15}N_3$: C, 81.53; H, 4.89; N, 13.58. Found: C, 81.15; H, 4.98; N, 13.50.

4'-*p*-Tolyl-2,2':6',2"-terpyridine (2)

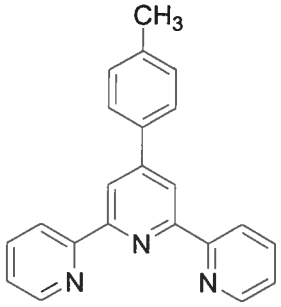

^{1}H NMR ($CDCl_3$, 400 MHz): δ 8.76 (s, br, 4H, H $_{3',5',6,6''}$) δ 8.70 (d, J = 8.0 Hz, 2H, H $_{3,3''}$), 7.90 (td, J = 7.9, 1.7 Hz, 2H, H $_{4,4''}$), 7.85 (d, J = 7.9 Hz, 2H, H $_{Ph\,2,6}$), 7.39-7.32 (m, 4H, H $_{5,5'',Ph\,3,5}$), 2.46 (s, 3H, H $_{CH3}$). ^{13}C NMR ($CDCl_3$, 100 MHz): δ 156.8, 156.3, 150.6, 149.5, 139.5, 137.3, 135.9, 130.1, 127.6, 124.2, 121.8, 119.1, 21.7. Anal. Calcd. for $C_{22}H_{17}N_3$: C, 81.71; H, 5.30; N, 12.99. Found: C, 81.79; H, 5.35; N, 13.19.

***p*-Cyanophenyl-2,2':6',2"-terpyridine (3)**

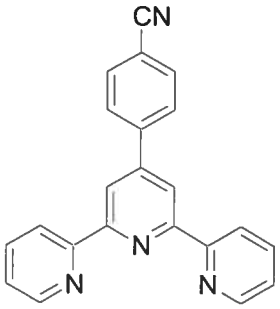

Yield, 42%. ^{1}H NMR ($CDCl_3$, 400 MHz): δ 8.74 (s, 2H, H $_{3',5'}$), 8.73 (d, J = 5.1 Hz, 2H, H $_{6,6"}$), 8.00 (d, J = 8.6 Hz, 2H, H $_{Ph\,2,6}$), 7.90 (td, J = 7.5, 2.0 Hz, 2H, H $_{4,4"}$), 7.82 (d, J = 9.9 Hz, 2H, H $_{Ph\,3,5}$), 7.32 (ddd, J = 6.0, 5.0, 1.5 Hz, 2H, H $_{5,5"}$). ^{13}C NMR ($CDCl_3$, 100 MHz): δ 156.3, 155.7, 148.3, 143.2, 137.1, 132.6, 128.0, 124.1, 121.4, 118.8, 118.6, 112.6. FAB-MS: 334.3, $[M]^+$.

***p*-Hydroxyphenyl-2,2':6',2"-terpyridine (4)**

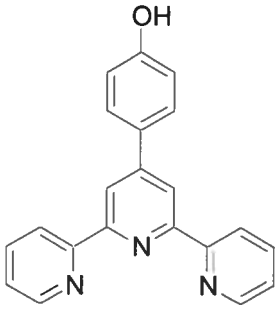

Yield, 43%. ^{1}H NMR (DMSO-d_6, 400 MHz): δ 8.75 (d, J = 5.5 Hz, 2H, H $_{6,6"}$), 8.65(m, 4H, H $_{3',5',3,3"}$), 8.02(t, J = 7.5 Hz, 2H, H $_{4,4"}$), 7.80(d, J = 8.5 Hz, 2H, H $_{Ph\,2,6}$), 7.52(dd, J = 6.0, 4.8 Hz, 2H, H $_{5,5"}$), 6.95 (d, J = 8.6 Hz, 2H, H $_{Ph\,3,5}$). ^{13}C NMR (DMSO-d_6, 100 MHz): δ 158.9, 155.5, 155.2, 149.3, 137.4, 128.2, 127.9, 124.4, 120.9, 117.1, 116.2. FAB-MS: 325.2, $[M]^+$.

***p*-bromophenyl-2,2':6',2"-terpyridine (5)**

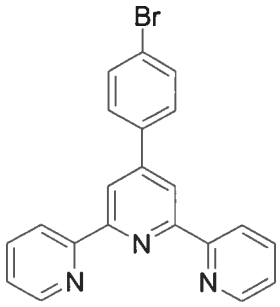

Yield, 56%. ^{1}H NMR ($CDCl_3$, 400 MHz): δ 8.76 (ddd, J = 4.8, 1.5, 0.8 Hz, 2H, H $_{6,6"}$), 8.72 (s, 2H, H $_{3',5'}$), 8.69 (d, J = 7.9 Hz, 2H, H $_{3,3"}$), 7.91 (td, J = 7.8, 1.8 Hz, H $_{4,4"}$), 7.80 (dt, J = 8.6, 2.2 Hz, 2H, H $_{Ph\,2,6}$), 7.56 (dt, J = 8.6, 2.2 Hz, 2H, H $_{Ph\,3,5}$), 7.39 (ddd, J = 6.7, 5.2, 1.1 Hz, 2H, H $_{5,5"}$). ^{13}C NMR ($CDCl_3$, 100 MHz): δ 156.0, 149.6, 149.1, 138.0, 137.5, 132.6, 131.9, 131.4, 129.4, 124.5, 122.1, 119.3. FAB-MS: 388.2 $[M+1]^+$.

***p*-(*N,N*-dimethylaminophenyl) -2,2':6',2"-terpyridine (6)**

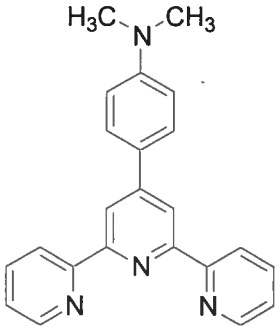

Yield, 25%. ^{1}H NMR ($CDCl_3$, 400 MHz): δ 8.76 (d, J = 4.3 Hz, 2H, H $_{6,6"}$), 8.74 (s, 2H, H $_{3',5'}$), 8.69 (d, J = 8.0 Hz, 2H, H $_{3,3"}$), 7.89–7.87 (m, 4H, H $_{4,4",\,Ph\,2,6}$), 7.36 (td, J = 5.1, 1.4 Hz, 2H, H $_{5,5"}$), 6.84 (d, J = 8.8 Hz, 2H, H $_{Ph\,3,5}$), 3.05 (s, 6H, H $_{N\text{-}CH3}$), ^{13}C NMR ($CDCl_3$, 100 MHz): δ 156.3, 155.3, 151.1, 150.1, 148.8, 137.2, 128.1, 125.0, 123.7, 121.5, 117.7, 112.4, 40.4. FAB-MS: 352.2, $[M]^+$. Anal. Calcd. for $C_{23}H_{20}N_4$:C, 78.38; H, 5.72; N, 15.90. Found: C, 77.71; H, 5.88; 15.50.

***p*-nitrophenyl-2,2':6',2"-terpyridine (7)**

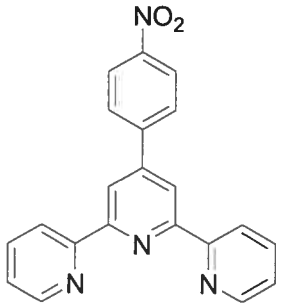

Yield, 51%. ^{1}H NMR ($CDCl_3$, 400 MHz): δ 8.76 (s, 2H, H $_{3',5'}$), 8.73 (dd, J = 4.8, 1.6 Hz, 2H, H $_{6,6''}$), 8.68 (d, J = 7.9 Hz, 2H, H $_{3,3''}$), 8.35 (d, J = 8.8 Hz, 2H, H $_{Ph\ 2,6}$), 8.04 (d, J = 8.8 Hz, 2H, H $_{Ph\ 3,5}$), 7.91 (dd, J = 7.8, 7.7 Hz, 2H, H $_{4,4''}$), 7.39 (dd, J = 7.4, 4.8 Hz, 2H, H $_{5,5''}$). ^{13}C NMR ($CDCl_3$, 100 MHz): δ 156.6, 155.9, 151.3, 150.3, 149.2, 137.1, 128.2, 125.8, 124.2, 121.4, 117.8, 118.9. FAB-MS: 355.4, $[M+1]^+$.

***p*-methoxyphenyl-2,2':6',2"-terpyridine (8)**

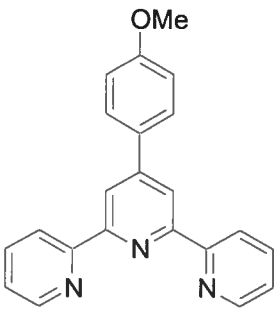

Yield: 20%, ^{1}H NMR ($CDCl_3$, 400 MHz): δ 8.71 (d, J = 5.5 Hz, 2H, H $_{6,6''}$), 8.69 (s, 2H, H $_{3',5'}$), 8.65 (d, J = 7.6 Hz, 2H, H $_{3,3''}$), 7.84–7.87 (m, 4H, H $_{4,4'',\ Ph\ 2,6}$), 7.33 (ddd, J = 7.5, 5.0, 1.0 Hz, 2H, H $_{5,5''}$), 7.01 (d, J = 7.9 Hz, 2H, H $_{Ph\ 3,5}$), 3.87 (s, 3H, H $_{O\text{-}CH3}$). ^{13}C NMR ($CDCl_3$, 100 MHz): δ 160.1, 156.0, 155.4, 149.4, 148.7, 136.5, 130.3, 128.2, 123.4,

121.0, 117.9, 113.9, 55.0. FAB-MS: 339.7, $[M]^+$. Anal. Calcd. for $C_{22}H_{17}N_3O$: C, 77.86; H, 5.05; N, 12.38. Found: C, 77.08; H, 5.09; N, 12.42.

4'-(2,3-dimethoxyphenyl)-2,2':6',2"-terpyridine (9)

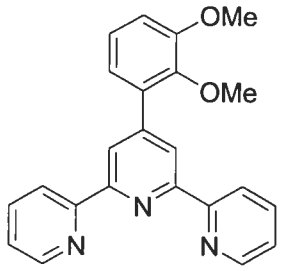

Yield, 27%. ^{1}H NMR ($CDCl_3$, 400 MHz): δ 8.72 (dt, J = 6.7, 0.7 Hz, 2H, H $_{6,6"}$), 8.70 (s, 2H, H $_{3',5'}$), 8.68 (d, J = 8.0 Hz, 2H, H $_{3,3"}$), 7.88 (td, J = 7.7, 1.7 Hz, 2H, H $_{4,4"}$), 7.34 (ddd, J = 7.4, 4.8, 0.8 Hz, 2H, H $_{5,5"}$), 7.18-7.16 (m, 2H, H $_{Ph\,5,6}$), 7.02 (m, 1H, H $_{Ph\,4}$), 3.95 (s, 3H, H $_{CH3}$), 3.73 (s, 3H, H $_{CH3}$). ^{13}C NMR ($CDCl_3$, 100 MHz): δ 156.8, 155.8, 153.5, 149.6, 148.7, 147.3, 137.2, 134.2, 124.6, 124.1, 122.8, 122.0, 121.7, 113.3, 61.5, 56.4. FAB-MS: 370.4, $[M+1]^+$. Anal. Calcd. for $C_{23}H_{19}N_3O_2$: C, 74.78; H, 5.18; N, 11.37. Found: C, 74.26; H, 5.15; N, 11.09.

4'-(4-diphenyl)-2,2':6',2"-terpyridine (10)

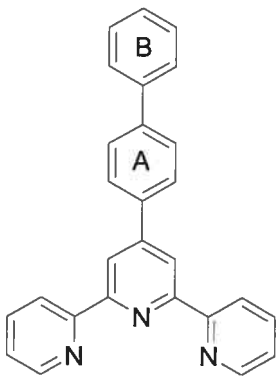

Yield, 48%. ^{1}H NMR ($CDCl_3$, 400 MHz): δ 8.80 (s, 2H, H $_{3',5'}$), 8.74 (d, J = 4.1 Hz, 2H, H $_{6,6''}$), 8.69 (d, J = 7.9 Hz, 2H, H $_{3,3''}$), 8.01 (d, J = 8.4 Hz, 2H, H $_{A\,2,6}$), 7.89 (td, J = 7.6, 1.7 Hz, H $_{4,4''}$), 7.75 (d, J = 8.4 Hz, 2H, H $_{A\,3,5}$), 7.68 (d, J = 7.4 Hz, 2H, H $_{B\,2,6}$), 7.49 (t, J = 7.5 Hz, 2H, H $_{B\,3,5}$), 7.39 (t, J = 7.5 Hz, 1H, H $_{B\,4}$), 7.37 (dd, J = 6.6, 4.5 Hz, 2H, H $_{5,5''}$). ^{13}C NMR ($CDCl_3$, 100 MHz): δ 156.6, 156.3, 150.1, 149.5, 142.2, 140.8, 137.6, 137.2, 129.7, 129.2, 128.1, 128.0, 127.5, 124.2, 121.7, 119.1. FAB-MS: 385.8, $[M]^+$.

4'-(1-naphthyl)-2,2':6',2"-terpyridine (11)

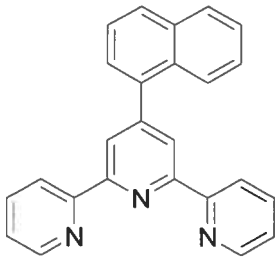

Yield, 32%. ^{1}H NMR ($CDCl_3$, 400 MHz): δ 8.76 (d, J = 7.8 Hz, 2H, H $_{3,3''}$), 8.71 (d, J = 3.7 Hz, 2H, H $_{6,6''}$), 8.68 (s, 2H, H $_{3',5'}$), 8.01-7.90 (m, 5H, H $_{4,4'',nap}$), 7.63-7.49 (m, 4H, H $_{nap}$), 7.37 (t, J = 5.6 Hz, 2H, H $_{5,5''}$). ^{13}C NMR (CD_3Cl, 400 MHz): δ 156.7, 155.9, 151.3, 149.6, 138.4, 137.3, 134.1, 131.4, 129.1, 128.8, 127.5, 127.0, 126.4, 126.0, 125.7, 124.3, 122.8, 121.8. FAB-MS: 359.1, $[M]^+$. Anal. Calcd. for $C_{25}H_{17}N_3$: C, 83.54; H, 4.77; N, 11.69. Found: C, 83.27; H, 4.79; N, 11.61.

4'-(9-anthryl)-2,2':6',2"-terpyridine (12)

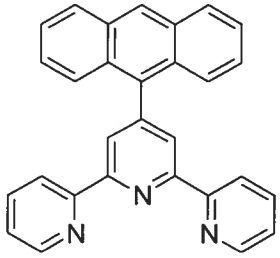

2-Acetylpyridine (0.61 g, 5.0 mmol) was added into a solution of 9-anthraldehyde (0.52 g, 2.5 mmol) in ethanol (25 mL). KOH pellet (0.39 g, 85%, 5.0 mmol) and aqueous ammonium (7.5 mL, 29.3%, 6.3 mmol) were then added to the solution. The solution was heated to reflux for 24 h. After cooling down to ambient temperature, the solution was evaporated to dryness under reduced pressure. Recrystallization of the residue from $CHCl_3$/MeOH afforded yellow crystalline solid (0.28 g, 0.68 mmol, 27%) ^{1}H NMR ($CDCl_3$, 400 MHz): δ 8.82 (d, J = 7.9 Hz, 2H, H $_{3, 3''}$), 8.66 (d, J = 0.3 Hz, 2H, H $_{6, 6''}$), 8.63 (s, 2H, H $_{3', 5'}$), 8.57 (s, 1H, H $_{An\ 10}$), 8.09 (d, J = 8.7 Hz, 2H, H $_{An\ 1, 8}$), 7.95 (t, J = 7.5 Hz, 2H, H $_{4, 4''}$), 7.73 (d, J = 8.7 Hz, 2H, H $_{An\ 2, 7}$), 7.49 (t, J = 7.2 Hz, 2H, H $_{An\ 3, 6}$), 7.39-7.36 (m, 4H, H $_{5, 5'', An\ 4, 5}$). ^{13}C NMR (CD_3Cl, 400 MHz): δ 156.5, 156.0, 150.0, 149.6, 137.4, 134.7, 131.6, 129.9, 128.8, 127.8, 126.8, 126.3, 125.6, 124.3, 124.3, 121.9. FAB-MS: 409.5, $[M]^+$. Anal. Calcd. for $C_{29}H_{19}N_3$: C, 85.06; H, 4.68; N, 10.26. Found: C, 85.27; H, 4.65; N, 10.08.

4'-(2-furyl)-2,2':6',2"-terpyridine (13)

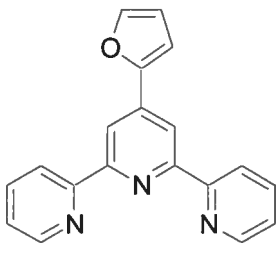

Yield, 24%. ^{1}H NMR ($CDCl_3$, 400 MHz): δ 8.77 (dt, J = 4.0, 0.8 Hz, 2H, H $_{6,6''}$), 8.74 (s, 2H, H $_{3',5'}$), 8.66 (d, J = 8.0 Hz, 2H, H $_{3,3''}$), 7.89 (td, J = 7.7, 0.7 Hz, 2H, H $_{4,4''}$), 7.61 (d, J = 0.9 Hz, 1H, H $_{Fu\,3}$), 7.37 (ddd, J = 7.4, 4.8, 1.0 Hz, 2H, H $_{5,5''}$), 7.14 (dd, J = 3.2, 0.4 Hz, 1H, H $_{Fu\,5}$), 6.59 (dd, J = 3.4, 0.7 Hz, 1H, H $_{Fu\,4}$). ^{13}C NMR (CD_3Cl, 400 MHz): δ 156.5, 156.3, 152.3, 149.5, 144.0, 139.9, 137.2, 124.2, 121.6, 115.5, 112.5, 109.5. FAB-MS: 300.1, $[M+1]^+$.

4'-(4-pyridyl)-2,2':6',2"-terpyridine (14)

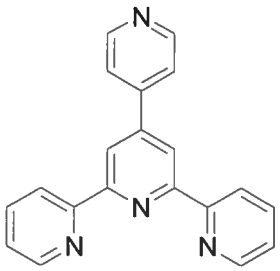

Yield, 42%. ^{1}H NMR (400 MHz, $CDCl_3$): δ 8.87 (s, 2H, H $_{3',5'}$), 8.83 (d, J = 6.3 Hz, 2H, H $_{6,6''}$), 8.78 (d, J = 4.8 Hz, 2H, H $_{Py\,2,6}$), 8.73 (d, J = 8.0 Hz, 2H, H $_{3,3''}$), 8.01 (d, J = 6.4 Hz, 2H, H $_{Py\,3,5}$), 7.96 (t, J = 7.7 Hz, 2H H $_{4,4''}$), 7.45 (t, J = 7.2 Hz, 2H, H $_{5,5''}$). ^{13}C NMR (100 MHz, $CDCl_3$): δ 156.7, 155.6, 149.4, 148.7, 147.0, 137.9, 124.8, 122.9, 122.0, 119.3. FAB-MS: 311.2, $[M+1]^+$. Anal. Calcd. for $C_{20}H_{14}N_4$: C, 77.40; H, 4.55; N, 18.05. Found: C, 77.68; H, 4.49; N, 17.68.

6.5 Reference

1 (a) Demas, J. M.; DeGra, B. A. Coord. *Chem. Rev.* **2001**, *211*, 317; (b) for a recent example: Kimura, M.; Takahashi, A.; Sakata, T.; Tsukahara, K. *Bull. Chem. Soc. Jpn.* **1998**, *71*, 1839; (c) Péchy, P.; Rotzinger, F. P.; Nazeeruddin, M. K.; Kohle, O.; Zakeeruddin, S. M.; Humphry-Baker, R.; Grätzel,M. *J. Chem. Soc., Chem. Commun.* **1995**, 65. (d) Baldo, M. A.; Thompson, M. E.; Forrest, S. R. *Nature* **2000**, *403*, 750; (e) Ziessel, R. J. *Inclusion Phenom. Macrocyclic Chem.* **1999**, *35*, 369.

2 Constable, E. C.; Cargill Thompson, A. M. W.; Tocher, D. A.; Daniels, M. A. M. *New J. Chem.* **1992**, *16*, 855.

3 Sauvage, J.-P.; Collin, J.-P.; Chambron, J.-C.; Guillerez, S.; Coudret, C.; Balzani, V.; Barigelletti, F.; De Cola, L.; Flamigni, L. *Chem. Rev.* **1994**, *94*, 993.

4 (a) Maestri, M.; Armaroli, N.; Balzani, V.; Constable, E. C.; Cargill Thompson, A. M. W. Inorg. Chem. 1995, 34, 2759; (b) Hammarström, L.; Barigelletti, F.; Flamigni, L.; Indelli, M. T.; Armaroli, N.; Calogero, G.; Guardigli, M.; Sour, A.; Collin, J.-P.; Sauvage, J.-P. *J. Phys. Chem. A* **1997**, *101*, 9061; (c) Albano, G.; Balzani, V.; Constable, E. C.; Maestri, M.; Smith, D. R. *Inorg. Chim. Acta* **1998**, *277*, 225.

5 Mutai, T.; Cheon, J.-D.; Arita, S.; Araki, K. *J. Chem. Soc., Perkin Trans. 2* **2001**, 1045.

6 Goodall, W.; Williams, J. A. G. *Chem. Commun.* **2001**, 2514.

7 Roberto, D.; Tessore, F.; Ugo, R.; Bruni, S.; Manfredi, A.; Quici, S. *Chem. Commun.* **2002**, 846.

8 Alcock, N. W.; Barker, P. R.; Haider, J. M.; Hannon, M. J.; Painting, C. L.; Pikramenou, Z.; Plummer, E. A.; Rissanen, K.; Saarenketo, P. *J. Chem. Soc., Dalton Trans.* **2000**, 1447.

9 A comprehensive review of methods up to 1995 is provided by: Cargill Thompson, A. M. W. *Coord. Chem. Rev.* **1997**, 160, 1.

10 (a) Kröhnke, F. *Synthesis* **1976**, 1. (b) Constable, E. C.; Ward, M. D.; Corr, S. *Inorg. Chim. Acta* **1988**, *141*, 201; (c) Frank, R. L.; Riener, E. F. *J. Am. Chem. Soc.* **1950**, *72*, 4182; (d) Korall, P.; Börje, A.; Norrby, P.-O.; Åkermark, B. *Acta Chem. Scand.* **1997**, *51*, 760; (e) Cave, G. W. V.; Raston, C. L. *Chem. Commun.* **2000**, 2199.

11 (a) Cardenas; D. J.; Sauvage, J.-P. *Synlett* **1996**, 916; (b) Hanan, G. S.; Schubert, U. S.; Volkmer, D.; Riviere, E.; Lehn, J.-M.; Kyritsakas, N.; Fisher, J. *Can. J. Chem.* **1997**, *75*, 169; (c) Fallahpour, R.-A.; Neuberger, M.; Zehnder, M. *New J. Chem.* **1999**, *23*, 53; (d) Fallahpour, R.-A. *Eur. J. Inorg. Chem.* **1998**, 1205.

12 Goodall, W.; Wild, K.; Arm, K. J.; Williams, J. A. G. *J. Chem. Soc., Pekins Trans. 2* **2002**, 1669.

13 During the preparation of this paper, a similar approach to synthesize 4'-p-tolyl-2,2':6',2"-terpyridine was reported: Vaduvescu, S.; Potvin, P. G. *Eur. J. Inorg. Chem.* **2004**, 1763.

14 Collin, J. P.; Guillerez, S.; Sauvage, J. P.; Barigelletti, F.; De Cola, L.; Flamigni, L.; Balzani, V. *Inorg. Chem.* **1991**, *30*, 4230.

15 Most of the starting aryl aldehydes were purchased from Aldrich. Aldehydes that were not commercial available were synthesized from the corresponding aryl bromides by lithiation and then formylation with dimethylformamide.

16 Wang, J.; Hanan, G. S.; Loiseau, F.; Campagna, S. *Chem. Commun.* **2004**, 2068.

17 Yoo, D.-W.; Yoo, S.-K.; Kim, C.; Lee, J.-K. *J. Chem. Soc., Dalton Trans.* **2002**, 3931.

18 Michalec, J. F.; Bejune, S. A.; Cuttell, D. G.; Summerton, G. C.; Gertenbach, J. A.; Field, J. S.; Haines, R. J.; McMillin, D. R. *Inorg. Chem.* **2001**, *40*, 2193.

19 Husson, J.; Beley, M.; Kirsch, G. *Tetrahedron Lett.* **2003**, *44*, 1767.

20 Persaud, L.; Barbiero, G. *Can. J. Chem.* **1991**, *69*, 315.

Chapter 7

Conclusions and Future Proposals

7.1 Conclusions

In conclusion, we have optimized the photophysical properties of Ru(II) polypyridyl complexes based on separated approaches.

In **Chapter 2**, the multi-chromophoric approach has been demonstrated as an efficient approach to delay ^{3}MLCT decay and to prolong the rt lifetimes of the complexes. The "chemistry-on-the-complex" approach to deliberately design the ligands on complexes has been shown as a powerful way to introduce the new functionalities onto the complexes and as the only efficient way to obtain the desired compound. The optimization of the syntheses of the multi-chromophoric species has been realized in the work depicted in **Chapter 3**. The independent chromophore approach can also initiate the multi-chromophoric behaviour even the two equilibrating triplet states have been separated more than one nanometer. Since this method gives separated chromophores on different ligands, it may allow special design of the Ru(II) tpy moiety and the organic chromophore, and could result in compounds with specific photophysical properties.

The palladium(0)-catalyzed cyanation reactions on the complexes have successfully introduced the complexation-sensitive cyano group(s) into $Ru(tpy)_2^{2+}$ moieties (**Chapter 4**). It is noteworthy that the introduction of strongly electron-withdrawing cyano group into the complexes has significantly enhanced their

photophysical properties. Through this approach, the excited state lifetime of [(NC-tpy)Ru(tpy)]$^{2+}$ has been increased to 75 ns with highest quantum yield. The advantage of cyanation on the complexes method is that it could offer an alternative way to afford sensitive functionalities, which could not be obtained in a classical way, onto the metal complexes. The efficient incorporation of cyano group has opened the gate to the polymetallic array using the cyano group as the bridging ligand.

For the ligand design and synthetic method exploration in **Chapter 5**, we have efficiently and convergently synthesized a new family of ligands, Rbppy using a pyrimidine-ring formation reaction. The application of these newly synthesized ligands to Ru(II) coordination chemistry has proved their strong π-accepting nature. The facile one-pot syntheses of 4'-aryl-tpy ligands in **Chapter 6** is a great optimization of the synthetic methods reported previously. In this one-pot synthesis of tpy ligands, a variety of functionalities can endure the mild conditions we adopted and a variety of 4'-aryl-tpy ligands can be afforded with reasonable yields and column-free purifications.

However, there is no limit for scientific research. The optimization of the photophysical properties of Ru(II) complexes for the practical application is still under way. Some of the promising and challenging research directions will be presented as future proposals for incoming researchers.

7.2 Future proposals

7.2.1 Tridentate ligands:

Based on the previously reported results and the research carried on during my master's studies, the ligands shown in **Chart 7.1** could serve as target ligands for application in Ru(II) polypyridyl complexes to get the optimized photophysical properties.

Since Chung and coworkers reported the longest rt excited state lifetime of Ru(II) complexes with tridentate carbene ligands,[1] the exploration of new carbene ligands with different conformation and electronic properties should be one of the concerns in our research. The proposed carbene ligands (**A** in **Chart 7.1**) could also act as the building block to form supermolecular structures such as grids and helice.

The ligands **B** in Chart 7.1 are proposed because of their strongly electron withdrawing abilities. Previous work showed that the 4'-cyano-tpy ligand on the Ru(II) complexes can significantly increase the rt excited state lifetime with relatively high quantum yield.[2] The incorporation of 4,4',4"-trichloro-tpy ligand[3] and 4,4',4"-tricyano-tpy ligand into Ru(II) coordination sphere should give the best ever result in the electron withdrawing approach to enhance its photophysical properties.

Constructing the polymetallic arrays with bridging ligands with phenyl spacer has a problem: the non-coplanar phenyl ring diminishes the electronic interaction of metal cations.[4] Ligand **C** in Chart 7.1 have the 1,2,4,5-tetrazine as the spacers, which are coplanar to the peripheral binding site (4-pyridine or tpy) due to the existence of H-bonds between the nitrogen atoms in tetrazine and neighbouring hydrogens.[5] The synthesis of **C** and their incorporation into metal complexes can produce bimetallic complexes with direct electronic interactions.

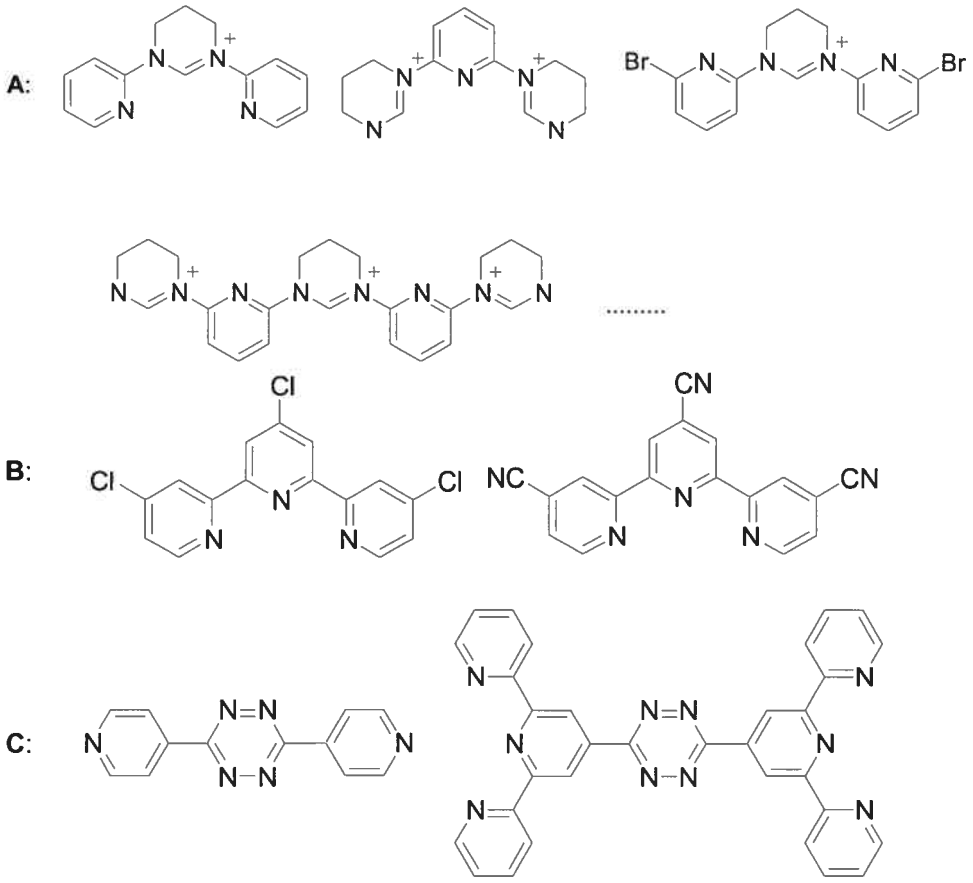

Chart 7.1 Proposed target ligands for ligand approach in coordination chemistry.

7.2.2 Complexes:

We have synthesized a new family of tridentate ligands, 2,6-*bis*(5'-R-pyrimyd-2'-yl)pyridine (Rbppy, R = H, Cl, Ph), in the previous work.[6] However, the complexes obtained from the application of the ligands to the Ru(II) chemistry were non-luminescent, sine the ^{3}MC state is too close to the ^{3}MLCT state because of the weak ligand field strength of Rbppy ligands.[7] The application of these ligands to other transition metals, such as platinum, iridium, osmium, through metal approach should

obtain some promising results. The complexes obtained should have novel photophysical properties, as well as potential dynamic behavior.

Another potential area in Ru(II) chemistry towards the rt emitter is the expansion of the multi-chromophoric approach. S. Buchwald, one of the pioneers in transition metal catalyzed cross-coupling reaction, has recently reported a series of new ligands for sterically hindered substrates in Suzuki-Miyaura coupling reaction.[8] The ligand, 2-(2',6'-dimethoxybiphenyl)dicyclohexylphosphine, has been demonstrated to be the most powerful one so far for this type of reactions. The application of this ligand as well as the reported reaction conditions in our systems should be promising, since one of the challenges we met in the synthesis of multi-chromophoric species is the incorporation of sterically bulky 9-anthryl group into tpy-containing ligands or complexes.[9] The cross coupling reaction could open the door to the multi-chromophoric species with heterogeneous energy storage elements.

7.2.3 Synthetic methodology:

Since the adoption of conjugated pyrimidine to enhance the photophysical properties of Ru(II) complexes,[10] the synthesis of oligo-2,5-pyrimidines is important in our pursuit to improve the rt luminescence properties of the Ru(II) complexes. The syntheses of oligo-2,5-pyrimidines have been reported previously.[11] However, the incorporation of the oligo-2,5-pyrimidines into tpy ligand is challenging. I have tried several methods to approach the oligo-2,5-pyrimidines (**Scheme 7.1**). In approach **A**, one of the problems I met is the deliberate choice of solvents for the reaction as well as the following purification. Switch to the standard reaction conditions for the conversion of

methyl to vinamidinium perchlorate also failed (approach **B**). Approach **B** should have the priority in the attempt to synthesize the oligo-2,5-pyrimidine, since the instalment of the tpy ligand can be put in the final stage, which, in turn, facilitates the purification for the poor solubility of tpy ligands in alcohol solvents (MeOH, EtOH).

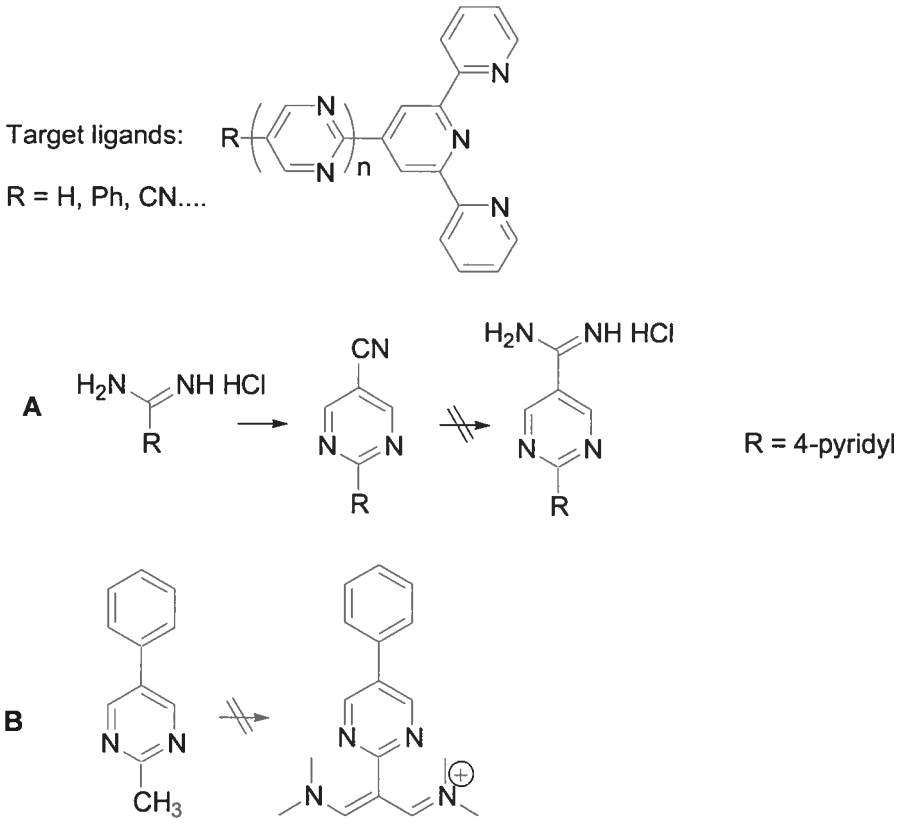

Scheme 7.1 Target ligand, 4'-(oligo-2,5-pyrimidine)-tpy ligand with unsuccessful attempts to synthesize oligo-2,5-pyrimidine.

With the successful exploration of the synthesis of oligo-2,5-pyrimidine in hand, the incorporation of oligo-2,5-pyrimidine into tpy ligands through pyrimidine-ring forming reaction or transition-metal catalyst cross coupling[12] reaction could be promising

if combine with all the previous research work, such as head-to-head 5,5'-bipyrimidine bridged ligand[9b] and pm-pm-tpy ligand.[10]

7.3 References and Notes

1 Son, S. U.; Park, K. H.; Lee, Y.-S.; Kim, B. Y.; Choi, C. H.; Lah, M. S.; Jang, Y. H.; Jang, D.-J.; Chung, Y. K. *Inorg. Chem.* **2004**, *43*, 6896.

2 Wang, J.; Fang, Y.-Q.; Hanan, G. S.; Loiseau, F.; Campagna, S. *Inorg. Chem.* **2005**, *44*, 5.

3 (a) Wieprecht, T.; Xia, J.; Heinz, U.; Dannacher, J.; Schlingloff, G. *J. Mol. Cat. A: Chemical* **2003**, *203*, 113. (b) Hobert, S. E.; Carney, J. T.; Cummings, S. D. *Inorg. Chim. Acta* **2001**, *318*, 89.

4 Vaduvescu, S.; Potvin, P. G. *Eur. J. Inorg. Chem.* **2004**, 1763.

5 Wang, J. Lab notebooks. Attempts to synthesize the 1,2,4,5-tetrazine bridged ligands, unpublished data.

6 See **Chapter 5** for details.

7 Wang J.; Medlycott, E. A.; Hanan, G. S.; Udachin, C. A. *Can. J. Chem.* **2005**, manuscript in preparation.

8 Barder, T. E.; Walker, S. D.; Martinelli, J. R.; Buchwald, S. L. *J. Am. Chem. Soc.* **2005**, *127*, 4685.

9 (a) Passalacqua, R.; Loiseau, F.; Campagna, S.; Fang, Y.-Q.; Hanan, G. S. *Angew. Chem. Int. Ed.* **2003**, *42*, 1608. (b) Wang, J.; Fang Y.-Q.; Bourget-Merle, L.; Polson, M. I. J.; Hanan, G. S.; Passalacqua, R.; Loiseau, F.; Campagna, S. *Chem. Eur. J.* **2005**, manuscript in preparation.

10 Fang Y.-Q.; Taylor, A. J.; Hanan, G. S.; Loiseau, F.; Passalacqua, R.; Campagna, S.; Nierengarten, H.; Van Dorsselaer, A. *J. Am. Chem. Soc.* **2002**, *124*, 7912.

11 Gompper, R.; Mair, H. J.; Polborn, K. *Synthesis* **1997**, *6*, 696.

12 Fang, Y.-Q. Master's thesis. Department of Chemistry, University of Waterloo, Canada. **2002**, p111.

Appendix

A1 Papers published during Master's studies.

A1-1. Wang, J.; Hanan, G. S.; Loiseau, F.; Campagna, S. *Chem. Commun.* **2004**, 2068.

A1-2. Wang, J.; Fang, Y.-Q.; Hanan, G. S.; Loiseau, F.; Campagna, S. *Inorg. Chem.* **2005**, *44*, 5.

A1-3. Wang, J.; Hanan, G. S. *Synlett* **2005**, *8*, 1251.

A2 Supplementary data of single crystal structures.

A2-1 Complex **3a** in **Chapter 2**.

A2-2Complex **3b** in **Chapter 2**.

A2-3 Complex **3b** in **Chapter 3**.

A2-4 Complex **3d** in **Chapter 3**.

A2-5 Complex **2c** in **Chapter 4**.

A2-6 Ligand **1a** in **Chapter 5**.

A2-7 Complex **2a** in **Chapter 5**.

A2-8 Complex **2b** in **Chapter 5**.

A2-9 Complex **3b** in **Chapter 5**.

COMMUNICATION

ChemComm
www.rsc.org/chemcomm

Prolonged luminescence lifetimes of Ru(II) complexes *via* the multichromophore approach: the excited-state storage element can be on a ligand not involved in the MLCT emitting state†

Jianhua Wang,[a] Garry S. Hanan,*[a] Frédérique Loiseau[b] and Sebastiano Campagna*[b]

[a] *Département de chimie, Université de Montréal, Montréal, Québec, Canada H3T 1J4. Fax: +1 514 343 7586; Tel: +1 514 343 7056; E-mail:* [redacted]

[b] *Dipartimento di Chimica Inorganica, Chimica Analitica e Chimica Fisica, Università di Messina, 98166 Messina, Italy. E-mail: photochem@chem.unime.it; Fax: +39 090-393756*

Received (in Columbia, MO, USA) 16th April 2004, Accepted 30th June 2004
First published as an Advance Article on the web 13th August 2004

A novel series of ruthenium terpyridine complexes with bichromophoric units separated by more than 1 nm display an extraordinary enhancement of their luminescence lifetimes when compared to the parent $Ru(tpy)_2^{2+}$ chromophore (tpy = 2,2′:6′,2″-terpyridine).

Ruthenium complexes based on the bidentate ligand 2,2′-bipyridine (bpy) have been incorporated into several different types of photoactive devices due to their outstanding photophysical properties.[1] One of the few drawbacks of the $Ru(bpy)_3^{2+}$ chromophore is its chirality, which generates diastereomers when light-harvesting polymetallic complexes are applied in a device.[2] The $Ru(tpy)_2^{2+}$ chromophore, on the other hand, is achiral when substituted in the 4′-position and has recently been used to build up multinuclear complexes structures.[3] To be applied in a practical device, however, it would be convenient if these complexes had relatively long-lived excited states at room temperaure (r.t.). As the parent $Ru(tpy)_2^{2+}$ chromophore has a very short excited-state lifetime at r.t. (<250 ps),[4] several attempts have been made to prolong the r.t. luminescence lifetime of the $Ru(tpy)_2^{2+}$ moieties.[5–7]

We have previously reported that Ru(II) complexes of a tpy with a coplanar pyrimidine and a 9-anthryl chromophore have greatly increased luminescence lifetimes due to the bichromophoric effect, in which the triplet metal-to-ligand charge-transfer state (^{3}MLCT) is in equilibrium with the anthracene triplet state (^{3}An), which acts as an excited-state storage element.[7] In all cases in which bichromophoric states are known for Ru(II) polypyridine complexes, the organic chromophore used as the energy storage element is incorporated into the polypyridine ligand which is directly involved in the ^{3}MLCT emitting state.[8] These complexes display exceptional properties, however, their syntheses also depend on several sequential reactions in order to incorporate the two chromophores into the same ligand. Herein we report on a new series of Ru(tpy)-type complexes in which the excited-state storage element (an anthryl subunit) is linked to a ligand which is not involved in the ^{3}MLCT emitting level, and demonstrate that the multichromophoric approach is still effective in spite of the large (nanometric) spatial separation between the subunits.

In order to simplify the synthetic procedure, we connected the 9-anthryl chromophore directly into the 4′-position of the tpy moiety (Chart 1).† Although 4′-(9-anthryl)-2,2′:6′,2″-tpy (An-tpy) complexes of Ru(II) are non-emissive due to energy transfer from the ^{3}MLCT of $Ru(tpy)_2^{2+}$ to the non-emissive triplet anthracene state (^{3}An),[9] we reasoned that lowering the ^{3}MLCT state of $Ru(tpy)_2^{2+}$ by way of a 2-pyrimidyl substituent could initiate bichromophoric behaviour.

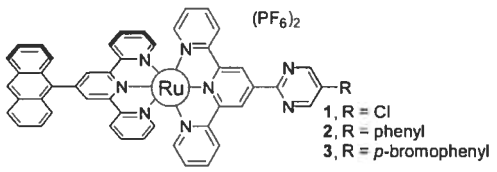

Chart 1 Ruthenium(II) complexes **1–3**.

† Electronic supplementary information (ESI) available: experimental details. See http://www.rsc.org/suppdata/cc/b4/b405619a/

Red single crystals of **3** suitable for X-ray crystallography were grown from an acetonitrile solution by diffusion of diethylether (Fig. 1).‡ The Ru–N bond lengths and internal pyridine angles are similar to those found in other Ru(II) polypyridine complexes. The 9-anthryl subunit lies at an 82.3° angle to the N1–N3 terpyridine plane which diminishes conjugation (Fig. 1), thus allowing the subunits to maintain their independent properties in the complexes. The pyrimidyl group lies virtually coplanar to the N4–N6 terpyridine (6.2° angle), whereas the 5-pyrimidyl substituted *p*-bromophenyl group is twisted at a 27.3° angle with respect to the pyrimidine (Fig. 1). The coplanar nature of the pyrimidine–terpyridine sub-unit favours π-conjugation and is crucial for the enhanced photophysical properties of these complexes (*cf.*, photophysics).

The electrochemistry of complexes **1–3** is similar to that of $Ru(tpy)_2^{2+}$ with a single one-electron metal-based oxidation (+1.32, +1.35 and +1.34 V *vs.* SCE for **1–3**, respectively), and a series of ligand-based reductions, of which the first reduction process is reversible (−1.10 V, −1.19 V and −1.10 V *vs.* SCE, respectively). The oxidation potentials have shifted to more positive potentials by 25–50 mV compared with reference complex **4**, $[(An\text{-}tpy)Ru(tpy)](PF_6)_2$ (+1.30 V *vs.* SCE), due to the greater stablization of the metal-based orbitals by the pyrimidyl-tpy substituents. The 9-anthryl group has little electronic effect on the complexes as the redox potentials of **1** are nearly the same as those

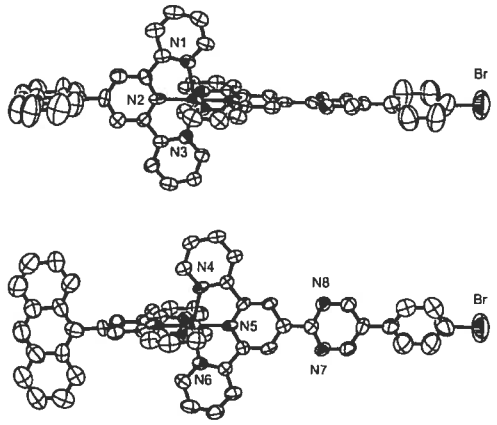

Fig. 1 Two ORTEP plots of the X-ray crystal structure of complex **3** exposing the An-tpy ligand (top) and, after a 90° rotation, the R-pm-tpy ligand (R-pm-tpy = 4′-(5-R-pyrimid-2-yl)-tpy, with R = *p*-bromophenyl) (bottom). Thermal ellipsoids are set at 30% probability with hydrogen atoms and counteranions omitted for clarity.

DOI: 10.1039/b405619a

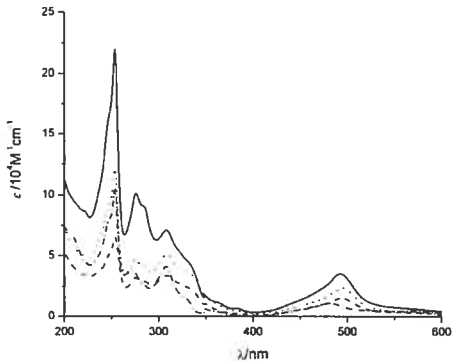

Fig. 2 Electronic absorption spectra for **1** (solid line), **2** (dashed line), **3** (dotted line) and **4** (intermittent line). The spectra were recorded at room temperature in argon purged acetonitrile.

Table 1 Spectroscopic data for **1–5** in deaerated CH_3CN solution

	Absorption	Luminescence 298 K	
Complex	λ/nm (ε/mol^{-1}L^{-1}cm^{-1})	λ_{max}/nm	τ/ns (% contribution)
1	492 (35700)	680	10 (5%); 698 (95%)
2	494 (15300)	670	25 (20%); 1052 (80%)
3	494 (23700)	670	28 (10%); 1040 (90%)
4	482 (11000)	—	—
5[a]	487 (23700)	684	21

[a] Data from ref. 10.

of **5** ([(tpy)Ru(Cl-pm-tpy)] $(PF_6)_2$ (E_{ox} = +1.33 V and E_{red} = −1.09 V *vs.* SCE) (Cl-pm-tpy = 4′-(5-chloro-pyrimid-2-yl)-tpy).

The absorption spectra and spectroscopic data of complexes **1–4** are showed in Fig. 2 and Table 1 respectively. In the UV region, the spectra are dominated by the π–π* transitions of the tpy and anthracene moities. In the visible region, the ^{1}MLCT bands of complexes **1–3** have shifted to lower energy as compared to that of complex **4** due to the extended delocalization of the pyrimidyl-tpy moiety, as expected.[10] The absorption spectra of complexes **1–3** are similar to the sum of the spectra of ruthenium pyrimidyl-tpy moieties and anthracene, indicating that the 9-anthryl group contributes independently to the electronic spectra of the complex.

The emission data clearly show that in all the new complexes the energy level of the emitting ^{3}MLCT state has been lowered to a region comparable to the energy level of the non-emissive anthracene triplet state (^{3}An) ($E^{(0)}$ = 1.85 eV, 671 nm),[11] and definitely involves the tpy-pm-R ligands (Table 1).[10] The ^{3}MLCT state of complexes **1**, **2** and **3** is therefore close enough in energy to the ^{3}An state to make equilibration between the two states possible, thus accounting for the enhancement of the excited state lifetime of the new complexes (Table 1).

The luminescence data collected in Table 1 confirm our interpretation, by showing that the introduction of the two independent chromophores significantly enhances the lifetime as compared to complex **4**, in which the ^{3}MLCT luminescence has been totally quenched by the ^{3}An state, as well as compared to complex **5**, in which multichromophoric behaviour cannot be obtained. As expected,[7] the emission spectra of complexes **1–3** exhibit biexponential decay (Table 1). The first shorter lifetime is attributed to the decay of the initially formed ^{3}MLCT. The second lifetime results from the equilibration between the emitting ^{3}MLCT level and the ^{3}An state.

In conclusion, we have designed and synthesized a new series of r.t. luminescent $Ru(tpy)_2^{2+}$ species incorporating a 2-pyrimidyl-tpy subunit for extended electron delocalization and an independent organic chromophore, a 9-anthryl subunit, as an energy reservoir for the emissive ^{3}MLCT state. Importantly, prolonged luminescence lifetimes *via* excited-state equilibration have been obtained for the first time by grafting the excited-state storage element onto a ligand which does not act as the acceptor ligand of the ^{3}MLCT emitting level. Separation of the two chromophoric subunits onto different ligands greatly simplifies the synthetic procedure while maintaining long-lived excited states at r.t. This approach enables the design and synthesis of the ruthenium terpyridine moiety and the organic chromophore subunit independently and can open the way to a new class of compounds with predetermined photophysical properties. Further work is in progress to fully characterize the excited-state and redox properties of the complexes.

This work was supported by NSERC (Canada), the Université de Montréal, and MIUR (Italy). E. Medlycott and F. Bélanger-Gariépy are thanked for the X-ray structural analysis of **3**.

Notes and references

‡ CCDC 235987. See http://www.rsc.org/suppdata/cc/b4/b405619a/ for crystallographic data for **3** in .cif or other electronic format.

1 V. Balzani and F. Scandola, *Supramolecular Photochemistry*, Ellis Horwood, Chichester, UK, 1991.
2 V. Balzani, A. Juris, M. Venturi, S. Campagna, G. Denti and S. Serroni, *Chem. Rev.*, 1996, **96**, 759.
3 J. P. Sauvage, J. P. Collin, J. C. Chambron, S. Guillerez, C. Coudret, V. Balzani, F. Barigelletti, L. DeCola and L. Flamigni, *Chem. Rev.*, 1994, **94**, 993.
4 J. R. Winkler, T. L. Netzel, C. Creutz and N. Sutin, *J. Am. Chem. Soc.*, 1987, **109**, 2381.
5 M. Maestri, N. Armanoli, V. Balzani, E. C. Constable and A. M. W. C. Thompson, *Inorg. Chem.*, 1995, **34**, 2759.
6 (*a*) M. Beley, J. P. Collin, R. Louis, B. Metz and J. P. Sauvage, *J. Am. Chem. Soc.*, 1991, **113**, 8521; (*b*) E. C. Constable, A. M. W. C. Thompson and S. Greulich, *J. Chem. Soc., Chem. Commun.*, 1993, 1444.
7 R. Passalacqua, F. Loiseau, S. Campagna, Y.-Q. Fang and G. S. Hanan, *Angew. Chem., Int. Ed.*, 2003, **42**, 1608.
8 D. S. Tyson, C. R. Luman, X. Zhou and F. N. Castellano, *Inorg. Chem.*, 2001, **40**, 4063 and refs therein.
9 G. Albano, V. Balzani, E. C. Constable, M. Maestri and D. R. Smith, *Inorg. Chim. Acta*, 1998, **277**, 225.
10 Y.-Q. Fang, N. J. Taylor, G. S. Hanan, F. Loiseau, R. Passalacqua, S. Campagna, H. Nierengarten and A. Van Dorsselaer, *J. Am. Chem. Soc.*, 2002, **124**, 7912.
11 S. L. Murov, I. Carmicheal and G. L. Hug, *Handbook of Photochemistry*, Marcel Dekker, New York, 1993.

Inorg. Chem. 2005, 44, 5–7

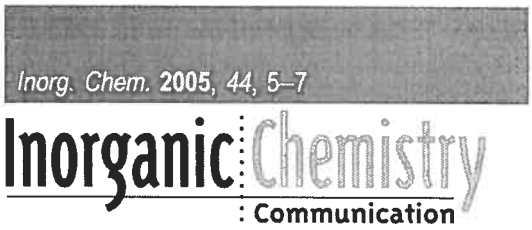

Synthesis and Properties of the Elusive Ruthenium(II) Complexes of 4′-Cyano-2,2′:6′,2″-terpyridine

Jianhua Wang,[†] Yuan-Qing Fang,[‡] Garry S. Hanan,*[,†] Frédérique Loiseau,[§] and Sebastiano Campagna*[,§]

Département de Chimie, Université de Montréal, Montréal, Québec, Canada H3T 1J4, Department of Chemistry, University of Waterloo, Waterloo, Ontario, Canada N2L 3G1, and Dipartimento di Chimica Inorganica, Chimica Analitica e Chimica Fisica, Università di Messina, 98166 Messina, Italy

Received August 12, 2004

The heteroleptic and homoleptic ruthenium(II) complexes of 4′-cyano-2,2′:6′,2″-terpyridine are synthesized by palladium catalyzed cyanation of the corresponding Ru(II) complexes of 4′-chloro-2,2′:6′,2″-terpyridine. The introduction of the strongly electron-withdrawing cyano group into the $Ru(tpy)_2^{2+}$ moiety dramatically changes its photophysical and redox properties as well as prolongs its room temperature excited-state lifetime.

In the last two decades, ruthenium(II) complexes have become widely studied within the field of inorganic chemistry.[1] Indeed, Ru(II) polypyridine complexes play outstanding roles in fields connected to solar energy conversion and the storage of light and/or electronic information at the molecular level.[2] The prototype of this class of compounds, $[Ru(bpy)_3]^{2+}$ (bpy = 2,2′-bipyridine), has been one of the most studied metal-containing species.[2a,3] However, compared with achiral $Ru(tpy)_2^{2+}$ complexes based on the tridentate polypyridyl ligand 2,2′:6′,2″-terpyridine (tpy), $[Ru(bpy)_3]^{2+}$ has two main structural disadvantages: the Δ and Λ enantiomers of $[Ru(bpy)_3]^{2+}$ give rise to many diastereomers in polynuclear complexes and Ru(II) complexes of monosubstituted bpy ligands are mixtures of *fac* and *mer* isomers. These problems, inherent to the $[Ru(bpy)_3]^{2+}$ structural motif, can be overcome by the use of tridentate, tpy-type polypyridyl ligands. However, $[Ru(tpy)_2]^{2+}$ and its derivatives have far less useful photophysical properties as compared to $[Ru(bpy)_3]^{2+}$. This is essentially due to a shorter excited-state lifetime (<250 ps) at room temperature (rt) resulting from the population of a nonemissive metal-centered triplet (^{3}MC) state from the potentially emissive metal-to-ligand charge transfer (^{3}MLCT) state.[4] Nevertheless, this shortcoming may be overcome if new ligands are designed which enhance the rt luminescence lifetimes of Ru(II) complexes of tridentate ligands.[5]

Several strategies have been employed to prolong the rt excited-state lifetime of ruthenium(II) complexes with tridentate polypyridyl ligands, including the use of (a) electron withdrawing and/or donor substituents on tpy,[1d] (b) cyclometalating ligands,[1e] (c) ligands with extended acceptor orbitals,[1c] and (d) bichromophoric complexes.[6]

The first strategy was based on the introduction of electron-withdrawing and/or donor substituents into the 4′-position

* To whom correspondence should be addressed. E-mail: [redacted] (G.S.H.); photochem@chem.unime.it (S.C.).
† Université de Montréal.
‡ University of Waterloo.
§ Università di Messina.

(1) (a) Encinas, S.; Flamigni, L.; Barigelletti, F.; Constable, E. C.; Housecroft, C. E.; Schofield, E. R.; Figgemeier, E.; Fenske, D.; Neuburger, M.; Vos, J. G.; Zehnder, M. *Chem. Eur. J.* **2002**, *8*, 137. (b) Barigelletti, F.; Flamigni, L. *Chem. Soc. Rev.* **2000**, *29*, 1. (c) Hissler, M.; Ziessel, R. *New J. Chem.* **1997**, *21*, 843. (d) Maestri, M.; Armaroli, N.; Balzani, V.; Constable, E. C.; Cargill Thompson, A. M. W. *Inorg. Chem.* **1995**, *34*, 2759. (e) Sauvage, J. P.; Collin, J. P.; Chambron, J. C.; Guillerez, S.; Coudret, C.; Balzani, V.; Barigelletti, F.; De Cola, L.; Flamigni, L. *Chem. Rev.* **1994**, *94*, 993. (f) Constable, E. C.; Thompson, A. M. W.; Tocher, D. A.; Daniels, M. A. M. *New J. Chem.*, **1992**, *16*, 855.

(2) (a) Balzani, V.; Juris, A.; Venturi, M.; Campagna, S.; Serroni, S. *Chem. Rev.* **1996**, *96*, 956 and references therein. (b) Hagfeldt, A.; Graetzel, M. *Acc. Chem. Res.* **2000**, *33*, 269. (c) Sun, L.; Hammarström, L.; Akermark, B.; Styring, S. *Chem. Soc. Rev.* **2001**, *30*, 36. (d) Ballardini, R.; Balzani, V.; Credi, A.; Gandolfi, M. T.; Venturi, M. *Acc. Chem. Res.* **2001**, *34*, 445. (e) Pomerane, D. Heitz, V.; Chambron, J.-C.; Sauvage, J.-P. *J. Am. Chem. Soc.* **2001**, *123*, 12215. (f) Kleverlaan, C. J.; Indelli, M. T.; Bignozzi, C. A.; Pavanin, L.; Scandola, F.; Hasselman, G. M.; Meyer, T. J. *J. Am. Chem. Soc.* **2002**, *122*, 2840. (g) Benkö, G.; Kallioinen, J.; Korppi-Tommola, J. E. I.; Yartsev, A. P.; Sundström, V. *J. Am. Chem. Soc.* **2002**, *124*, 489.

(3) (a) Meyer, T. J. *Pure Appl. Chem.* **1986**, *58*, 1193. (b) Juris, A.; Balzani, V.; Barigelletti, F.; Campagna, S.; Belser, P.; von Zelewsky, A. *Coord. Chem. Rev.* **1988**, *84*, 85 and references therein.

(4) These unfavorable photophysical properties are due to proximity (in energy) between the lowest-lying MLCT and metal-centered (MC) states, with the latter governing the excited-state decay dynamics by thermally activated surface crossing. This topic has been definitely clarified and is reported in detail in several reviews [refs 1e, 2a, 3a,b].

(5) Medlycott, E. A.; Hanan, G. S. *Chem. Soc. Rev.*, in press.

(6) (a) Harriman, A.; Ziessel, R. *Chem. Commun.* **1996**, 1707. (b) Benniston, A. C.; Harriman, A.; Grosshenny, V.; Ziessel, R. *New J. Chem.* **1997**, *21*, 405. (c) El-ghayoury, A.; Harriman, A.; Khatyr, A.; Ziessel, R. *J. Phys. Chem. A* **2000**, *107*, 1512. (d) Fang, Y.-Q.; Taylor, N. J.; Hanan, G. S.; Loiseau, F.; Passalacqua, R.; Campagna, S.; Nierengarten, H.; Van Dorsselaer, A. *J. Am. Chem. Soc.* **2002**, *124*, 7912. (e) Passalacqua, R.; Loiseau, F.; Campagna, S.; Fang, Y.-Q.; Hanan, G. S. *Angew. Chem., Int. Ed.* **2003**, *42*, 1608.

10.1021/ic048891p CCC: $30.25
Published on Web 12/10/2004

of tpy. The electron-withdrawing substituents stabilize the LUMO π^* ligand orbital more than the HOMO $\pi(t_{2g})$ metal orbital, thereby increasing the energy gap between ^{3}MLCT and ^{3}MC excited state and minimizing the thermally activated surface crossing which dominates the MLCT deactivation process.[4] It has been shown that 4′-(methyl-sulfonyl)-tpy based complexes have prolonged rt luminescence lifetimes ([(MeSO$_2$-tpy)$_2$Ru](PF$_6$)$_2$, 25.0 ns; [(MeSO$_2$-tpy)Ru(tpy-OH)](PF$_6$)$_2$, 50.0 ns) due to the strong electron-withdrawing ability of the methyl-sulfonyl group.[1d] One of the advantages of this strategy is the facile synthesis of the ligands and their complexes; thus, the synthetic procedure for building up the polynuclear arrays based on 4′-substituted tpy should be simplified. In addition, monoexponential decay of the excited state renders these complexes relatively easy to study as compared to bichromophoric systems based on an equilibrium between a nonemissive triplet organic state and the ^{3}MLCT state of the metal complex, which on the other side does not allow an increase in luminescence quantum yields.[5] In this context, we envisioned that coordination of 4′-cyano-tpy with a Ru(II) center should provide a very large effect on the ligand-based LUMO and increase the energy gap between the ^{3}MLCT and ^{3}MC states, thereby prolonging the rt luminescence lifetime (and increasing quantum yields) of the complexes. Moreover, cyano-complexes can act as building blocks to build up linear polymetallic units due to the strong coordination capacity of the cyano group.[7] However, until now no successful synthesis of the 4′-cyano-tpy Ru(II) complexes has been reported. Herein we report the synthesis of the heteroleptic and homoleptic Ru(II) complexes of 4′-cyano-tpy and the effect that the cyano group has on their photophysical and redox properties.

The difficulty in the preparation of Ru(II) complexes of 4′-cyano-tpy results from the activation of the cyano group toward nucleophilic attack by the electron withdrawing Ru(II) metal center. In order to bypass the possible destruction of the cyano group, we shifted our focus toward a "chemistry-on-the-complex" approach,[8] that is, the transition-metal catalyzed cyanation of appropriately functionalized Ru(II) complexes.

In order to elucidate the methodology for cyanation on the complex, we chose two Ru(II) terpyridine complexes, **1** and **2**, as our starting materials (Scheme 1). After several unsuccessful attempts to perform Ni(0) catalyzed cyanation of **1** and **2** (1.0 equiv of KCN, 10 mol % Ni(PPh$_3$)$_2$Br, 10 mol % Zn, 20 mol % PPh$_3$, DMF, or acetonitrile, 60 °C),[9] we turned to the Pd(0)-catalyzed-cyanation of the

Scheme 1. Palladium-Catalyzed Cyanation of Ru(II) Complexes of 4′-Chloro-tpy[a]

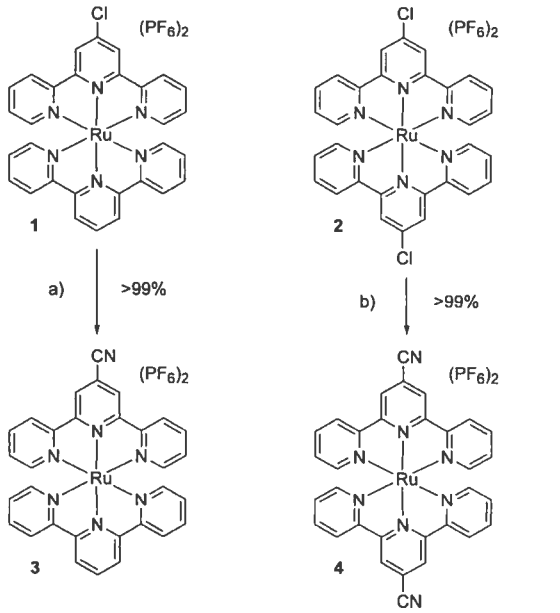

[a] Reagents and conditions: (a) 0.6 equiv Zn(CN)$_2$, 5 mol % Pd$_2$(dba)$_3$, 10 mol % dppf, 30 mol % Zn dust (325 mesh), DMA, 120 °C, 6 h; (b) 1.2 equiv Zn(CN)$_2$, 10 mol % Pd$_2$(dba)$_3$, 20 mol % dppf, 60 mol % Zn dust (325 mesh), DMA, 120 °C, 12 h.

complexes. Previously reported reaction conditions for purely organic systems seemed promising with very high yields.[10] We applied slightly modified conditions to complexes **1** and **2** in order to synthesize cyano complexes **3** and **4** (Scheme 1).

The reaction of heteroleptic complex **1** with 0.6 equiv of Zn(CN)$_2$, 5 mol % Pd$_2$(dba)$_3$, 10 mol % dppf, and 30 mol % Zn dust (325 mesh) in DMA at 120 °C for 6 h afforded cyano-complex **3** quantitatively. For homoleptic complex **2**, modification of the stoichiometry of the reagents and a longer reaction time afforded the same full conversion to homoleptic complex **4**. The full conversion of the 4′-chloro-tpy complexes to the cyano-complexes was secured by the strongly activating Ru(II) cations.

The electrochemical data indicates that the introduction of the cyano group into the Ru(tpy)$_2^{2+}$ moiety stabilizes the metal center as it is more difficult to oxidize (Table 1). The half-wave potentials of metal-centered oxidation of **3** and **4** have increased by more than 80 mV compared to Ru(tpy)$_2^{2+}$ (**5**). In addition, the ligand-centered reductions are facilitated as a result of the electron-withdrawing nature of the cyano group.

The absorption spectra of the new species (see Figure 1) are dominated by spin-allowed ^{1}MLCT bands in the visible region. We note that the cyano-substitution on the 4′-position of tpy has an strong electron-withdrawing effect on the tpy ligand, and, consequently, the metal center. The ^{1}MLCT

(7) (a) Bignozzi, C. A.; Schoonover, J. R.; Scandola, F. *Prog. Inorg. Chem.* **1997**, *44*, 1 and references therein. (b) Mellace, M. G.; Fagalde, F.; Katz, N. E.; Crivelli, I. G.; Delgadillo, A.; Leiva, A. M.; Loeb, B.; Garland, M. T.; Baggio, R. *Inorg. Chem.* **2004**, *43*, 1100.

(8) (a) Beley, M.; Collin, J.-P.; Louis, R.; Metz; B. Sauvage, J.-P. *J. Am. Chem. Soc.*, **1991**, *113*, 8521. (b) Constable, E. C.; Cargill Thompson, A. M. W.; Greulich, S. *J. Chem. Soc., Chem. Commun.*, **1993**, 1444. (c) Campagna, S.; Denti, G.; Serroni, S.; Juris, A.; Venturi, M.; Ricevuto, V.; Balzani, V. *Chem. Eur. J.* **1995**, *1*, 211. (d) Johansson, K. O.; Lotoski, J. A.; Tong, C.; Hanan, G. S. *Chem. Commun.* **2000**, 819. (e) Loiseau, F.; Passalaqua, R.; Campagna, S.; Polson, M. I. J.; Fang, Y.-Q.; Hanan, G. S. *Photochem. Photobiol. Sci.* **2002**, *1*, 982. (f) Fang, Y.-Q.; Polson, M. I. J.; Hanan, G. S. *Inorg. Chem.* **2003**, *42*, 5.

(9) (a) Takagi, K.; Okmoto, T.; Sakakibara, Y.; Ohno, A.; Oka, S.; Hayama, N. *Bull. Chem. Soc. Jpn.* **1975**, *48*, 3298. (b) Sakakibar, Y.; Okuda, F.; Shimobayashi, A.; Kirino, K.; Sakai, M.; Uchino, N.; Takagi, K. *Bull. Chem. Soc. Jpn.* **1988**, *61*, 1985.

(10) Jin, F.; Confalone, P. N. *Tetrahedron Lett.* **2000**, *41*, 3271.

Table 1. Electrochemical Potential Data[a]

complex	E_{ox}/V	E_{red}/V
1[b]	1.33	−1.16, −1.46
2[b]	1.40	−1.27, −1.46
3	1.42 (64)	−1.15 (70), −1.44 (70), −1.81 (60)
4	1.49 (65)	−0.88 (70), −1.15 (ir), −1.63 (ir)
5[b]	1.32	−1.27, −1.52

[a] V vs SCE. Data were collected in deaerated acetonitrile with 0.1 M supporting electrolyte, Bu_4NPF_6. Working electrode, platinum wire. Redox potentials were corrected by internal reference to ferrocene. [b] Data from ref 1f; **5** = $Ru(tpy)_2^{2+}$.

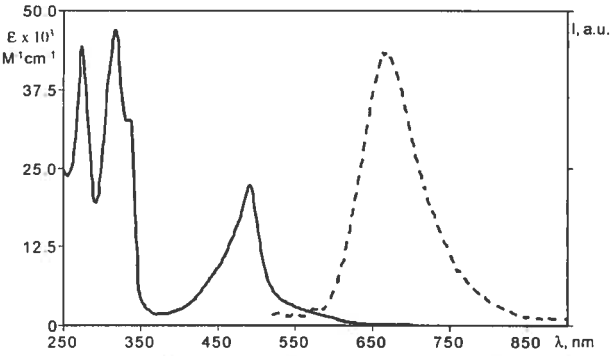

Figure 1. Absorption (—) and emission (- - -) spectra of **4** in acetonitrile solution.

bands of **3** and **4** have red-shifted (to 489 and 490 nm, respectively) as compared to their counterparts in **1** and **2** (Table 2). The introduction of the cyano group on the 4′-position of tpy lowers the energy of ^{1}MLCT state significantly as compared to **5**.

The rt emission spectra showed that the energy of the ^{3}MLCT state was also lowered with the introduction of cyano group. The corresponding emission maxima (λ_{max}) for **3** and **4** (see Figure 1) have red-shifted compared to **5** to 701 and 680 nm, respectively, due to the greater lowering of the ligand-based LUMO energy (π^*_L) over the metal-based HOMO energy (π_M). Since the introduction of the cyano group has less effect on the metal-based orbitals, the energy gap between ^{3}MC and ^{3}MLCT increases. As a consequence, the efficiency of the thermally activated surface crossing process from the ^{3}MLCT state to the ^{3}MC state decreases, thus prolonging the rt luminescence lifetime and significantly increasing quantum yields.

Table 2. Absorption Spectra and Luminescence Data[a]

compd	abs 298 K λ/nm ($\epsilon/10^3$ M^{-1} cm^{-1})	em 298 K λ_{max}/nm	τ/ns	Φ
4′-cyano-tpy	336 (6.9)	353	1.2	3×10^{-4}
1	478 (14.5)	651	0.7	4×10^{-5}
2[b]	480 (16.0)	653	0.2	$\leq 1 \times 10^{-5}$
3	489 (15.7)	701	75	2×10^{-3}
4	490 (22.4)	680	50	2×10^{-3}
5[b]	474 (10.4)	629	<0.25	$\leq 1 \times 10^{-6}$

[a] Data were collected in deaerated acetonitrile. [b] Data from ref 1d; **5** = $Ru(tpy)_2^{2+}$.

In conclusion, we have introduced a cyano group onto the 4′-position of $Ru(tpy)_2^{2+}$ complexes via a palladium-catalyzed cyanation reaction. This approach enables the synthesis of Ru(II) complexes of 4′-cyano-tpy from the corresponding 4′-chloro-tpy complexes. The substitution of the cyano group on $Ru(tpy)_2^{2+}$ causes dramatic changes to its photophysical properties. Prolonged rt excited-state lifetimes and significantly higher luminescence quantum yields compared to the prototype $Ru(tpy)_2^{2+}$ species are achieved, due to the increased energy gap between ^{3}MLCT and ^{3}MC states induced by the electron-withdrawing cyano group. Intensive work on the generality of this cyanation methodology and full characterization of new Ru(II) species will be described at a later date.

Acknowledgment. This work was financially supported by NSERC (Canada), the Université de Montréal, and MIUR (Italy).

Supporting Information Available: Experimental details for the synthesis of **3** and **4**. This material is available free of charge via the Internet at http://pubs.acs.org.

IC048891P

A Facile Route to Sterically Hindered and Non-Hindered 4′-Aryl-2,2′:6′,2″-Terpyridines

Jianhua Wang, Garry S. Hanan*

Département de Chimie, Université de Montréal, Montreal, Québec H3T 1J4, Canada
Fax +1(514)3437586; E-mail: [redacted]

Received 11 February 2005

Abstract: A facile one-pot synthesis of 4′-aryl-2,2′:6′,2″-terpyridines from aryl aldehydes and 2-acetylpyridine is presented. The synthesis of terpyridines incorporating sterically hindered aryl groups, such as the 9-anthryl group, can also be readily synthesized using this method.

Key words: nitrogen ligands, heterocycles, substituted terpyridines, one-pot reactions

Transition metal complexes of polypyridyl ligands have long been a target in coordination chemistry due to their potential utility in a range of applications, such as luminescent chemosensors, photocatalysts, components of devices for the conversion of light into electrical energy, and new electroluminescent materials.[1–3] The prototypical 2,2′-bipyridine (bpy) and 2,2′:6′,2″-terpyridine (tpy) ligands have been employed in a large number of these studies, usually binding as bidentate and tridentate ligands, respectively. The advantage of the latter ligand is that structurally simple achiral bis-tpy complexes are obtained with octahedrally coordinating metal ions, which can in turn be used to build up stereochemically discrete polynuclear arrays, as opposed to the racemic mixtures derived from bpy. Moreover, the achirality of tpy complexes is retained upon the chemical modification of the tpy by introducing functional groups into its 4′-position, which necessarily arranges them in a *trans* configuration along a C2 axis.

Introducing aryl substituents at the 4′-position of tpy can also have a profound influence on the photophysical properties of bis-tpy metal complexes and this effect has been investigated in some detail.[4] More recently, the photophysical properties of uncomplexed terpyridines have also begun to attract interest due to their potential application in photophysical devices.[5–8] Strategies for the incorporation of aryl substituents into the 4′-position of the terpyridine core are of considerable interest with respect to many of the applications discussed above.

The classical approach to 4′-aryl-tpy are based on the synthesis of a pyridine, involving the condensation of two equivalents of 2-acetylpyridine with the appropriate aryl aldehyde, with formation of the central pyridine ring from the reaction of the diketone intermediate with ammonia (or a source thereof) at elevated temperatures.[9] A number of variations have been reported, some involving isolation of the intermediate enone or diketone, others employing mild or solvent-free conditions for parts of the synthesis, but almost all relying on a common step in which the central pyridine ring is formed.[10] In particular, the approach involving the reaction of 2-pyridyl enaminone and 2-acetylpyridine with a strong base, *t*-BuOK, has been widely employed for the synthesis of the parent tpy ligand. Distinctly different synthetic approaches, in which all three pyridine rings are present in the starting materials, include the reaction of 2,2′-bipyridine with 2-pyridyl-lithiums, the Stille coupling of 2,6-dibromopyridines with 2-trialkylstannyl pyridines,[11] and the Suzuki cross-coupling of 4′-bromo-tpy with aryl-boronic acid/ester.[12] However, these approaches feature relatively long reaction times, harsh conditions and the necessity to purify the products by column chromatography. As part of our research with Ru(II) complexes of tridentate tpy ligands, a mild and efficient synthesis of a variety of 4′-aryl-tpy ligands was required.[13] Herein we report the facile one-step synthesis of a variety of tpy-based ligands with aromatic substituents in their 4′-position, which greatly improves the one-pot synthesis for 4′-aryl-tpy ligands previously reported.[14]

Our optimization of the one-step reaction started from readily available aryl aldehydes[15] and 2-acetylpyridine (Scheme 1). The reaction conditions and yields of the various ligands are gathered in Table 1. The enolate of 2-acetylpyridine can be generated by KOH under mild conditions. The following aldol condensation and Michael addition proceeded smoothly at room temperature. The soluble diketone intermediate was then allowed to form the central pyridine ring with an aqueous ammonia nitrogen source. The synthesis of the phenyl-based tpy ligands, **1**–**9**, was very straightforward using these mild conditions. Typically, the ligands precipitated from the reaction mixture as finely dispersed solids, which were easily separated by filtration. For **4**, after 24 hours reaction, the ligand was separated from the reaction mixture by acidification with AcOH, extraction with CH_2Cl_2 and recrystallization from EtOH.

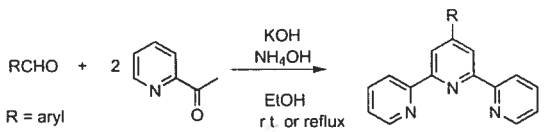

Scheme 1 Facile one-pot synthesis of 4′-aryl-2,2′:6′,2″-terpyridine

SYNLETT 2005, No. 8, pp 1251–1254
Advanced online publication: 21.04.2005
DOI: 10.1055/s-2005-868481; Art ID: S01605ST

Table 1 Reaction Conditions and One-Step Yields of 4′-Aryl-2,2′:6′,2″-terpyridines as Compared with Previously Reported Methods[a]

Ligand	R	Reaction time (h), yield (%)[b]	Reported yield (%),[c] (steps)[d]
1		2, (53)	<5, (4)[6e]
2	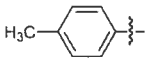	2, (49)	19, (4)[5]; 46 (1)[13]
3	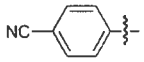	4, (42)	36, (5)[6e]
4	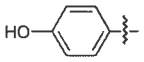	12, (43)	40, (2)[17]
5	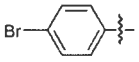	2, (56)	70, (2)[5]
6	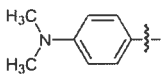	12, (25)	17, (4)[5]; 29, (4)[6e]
7	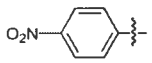	4, (51)	65, (2)[5]; 34, (5)[6e]
8	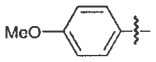	12, (20)	20, (4)[5]
9	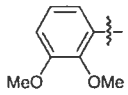	24, (27)	New
10	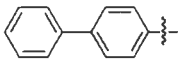	4, (48)	42, (1)[6f]
11	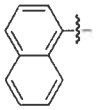	4, (32)	No yield available[18]
12	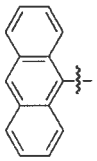	24,[g] (27)	59, (2)[4c]
13		4, (24)	69, (2)[19]
14	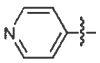	4, (42)	69, (2)[20]

[a] Reaction conditions: 1.0 equiv aryl aldehyde, 2.0 equiv 2-acetyl pyridine, 2.0 equiv KOH, 2.5 equiv NH_4OH, EtOH, r.t.
[b] Isolated yield of first crop of precipitate in our work.
[c] Isolated overall yields as previously reported.
[d] Number of reaction steps from commercially available starting materials.
[e] In ref.[6], from 4′-TfO-2,2′:6′,2″-terpyridine (TfO-tpy, 45% overall yield over 3 steps) or 4′-bromo-2,2′:6′,2″-terpyridine (45% overall yield over 4 steps).
[f] Starting from 4′-*p*-bromophenyl-2,2′:6′,2″-terpyridine.
[g] Reaction conditions: 1.0 equiv 9-anthryl aldehyde, 2.0 equiv 2-acetyl pyridine, 2.0 equiv KOH, 2.5 equiv NH_4OH, EtOH, reflux, 24 h.

The encouraging results for the synthesis of ligands **1**–**9** led us to apply these mild conditions to introduce organic chromophores into the tpy moiety, which is a critical step to prolong the room temperature luminescence lifetime of $Ru(tpy)_2^{2+}$ complexes by the bichromophore approach.[16] The 4′-biphenyl and 1-naphthyl groups were introduced into 4′-position of tpy to give ligand **10** and **11** by stirring at room temperature for four hours. However, the syn-

thesis of ligand **12** with the bulkier 9-anthryl group was problematic due to the insolubility of the intermediate, 2-[1-(9-anthryl)-3-oxo-3-prop-2-enyl] pyridine, in EtOH. Treatment of the same starting materials at reflux kept the enone intermediate in solution leading to a one-step synthesis of 4′-(9-anthryl)-tpy. It is noteworthy that this is the first example of a one-step synthesis of tpy-based ligands with bulky substituents in the 4′-position.

To survey the scope of the reaction conditions for heteroatom aromatic aldehydes, the 2-furyl-tpy (**13**) and 4-pyridyl-tpy (**14**) were also synthesized in moderate yield.

In conclusion, we have developed mild reaction conditions for the synthesis of 4′-aryl and 4′-heteroaryl substituted tpys. These reaction conditions are compatible with various functional groups and provide an efficient route to tridentate 2,2′:6′,2″-terpyridine-based ligands.

Representative Procedure for Ligands 1–11, 13–16
Synthesis of 1

2-Acetylpyridine (4.84 g, 40 mmol) was added into a solution of benzaldehyde (2.12 g, 20 mmol) in EtOH (100 mL). KOH pellets (3.08 g, 85%, 40 mmol) and aq NH_3 (58 mL, 29.3%, 50 mmol) were then added to the solution. The solution was stirred at r.t. for 4 h. The off-white solid was collected by filtration and washed with EtOH (3 × 10 mL). Recrystallization from $CHCl_3$–MeOH afforded white crystalline solid **1** (3.24 g, 10.5 mmol, 53%). ^{1}H NMR (400 MHz, $CDCl_3$): δ = 8.76 (s, 2 H, $H_{3',5'}$), 8.74 (d, J = 6.5 Hz, 2 H, $H_{6,6''}$), 8.68 (d, J = 8.0 Hz, 2 H, $H_{3,3''}$), 7.92 (d, J = 6.9 Hz, 2 H, H_{Ph}), 7.90 (t, J = 7.5 Hz, 2 H, $H_{4,4''}$), 7.52 (t, J = 6.9 Hz, 2 H, $H_{Ph2,6}$), 7.46 (t, J = 6.9 Hz, 1 H, $H_{Ph3,5}$), 7.37 (dd, J = 7.5, 5.0 Hz, 2 H, $H_{5,5''}$). ^{13}C NMR (100 MHz, $CDCl_3$): δ = 156.5, 156.2, 150.8, 149.4, 138.8, 137.4, 129.5, 129.3, 127.8, 124.3, 121.9, 119.4. Anal. Calcd for $C_{21}H_{15}N_3$: C, 81.53; H, 4.89; N, 13.58. Found: C, 81.15; H, 4.98; N, 13.50.

4′-(2,3-Dimethoxyphenyl)-2,2′:6′,2″-terpyridine (9)

Yield 27%. ^{1}H NMR (400 MHz, $CDCl_3$): δ = 8.72 (dt, J = 6.7, 0.7 Hz, 2 H, $H_{6,6''}$), 8.70 (s, 2 H, $H_{3',5'}$), 8.68 (d, J = 8.0 Hz, 2 H, $H_{3,3''}$), 7.88 (td, J = 7.7, 1.7 Hz, 2 H, $H_{4,4''}$), 7.34 (ddd, J = 7.4, 4.8, 0.8 Hz, 2 H, $H_{5,5''}$), 7.18–7.16 (m, 2 H, $H_{Ph5,6}$), 7.02 (m, 1 H, H_{Ph4}), 3.95 (s, 3 H, H_{CH3}), 3.73 (s, 3 H, H_{CH3}). ^{13}C NMR (100 MHz, $CDCl_3$): δ = 156.8, 155.8, 153.5, 149.6, 148.7, 147.3, 137.2, 134.2, 124.6, 124.1, 122.8, 122.0, 121.7, 113.3, 61.5, 56.4. FAB-MS: 370.4 $[M + 1]^+$. Anal. Calcd for $C_{23}H_{19}N_3O_2$: C, 74.78; H, 5.18; N, 11.37. Found: C, 74.26; H, 5.15; N, 11.09.

4′-(1-Naphthyl)-2,2′:6′,2″-terpyridine (11)

Yield 32%. ^{1}H NMR (400 MHz, $CDCl_3$): δ = 8.76 (d, J = 7.8 Hz, 2 H, $H_{3,3''}$), 8.71 (d, J = 3.7 Hz, 2 H, $H_{6,6''}$), 8.68 (s, 2 H, $H_{3',5'}$), 8.01–7.90 (m, 5 H, $H_{4,4'',nap}$), 7.63–7.49 (m, 4 H, H_{nap}), 7.37 (t, J = 5.6 Hz, 2 H, $H_{5,5''}$). ^{13}C NMR (100 MHz, CD_3Cl): δ = 156.7, 155.9, 151.3, 149.6, 138.4, 137.3, 134.1, 131.4, 129.1, 128.8, 127.5, 127.0, 126.4, 126.0, 125.7, 124.3, 122.8, 121.8. FAB-MS: 359.1 $[M]^+$. Anal. Calcd for $C_{25}H_{17}N_3$: C, 83.54; H, 4.77; N, 11.69. Found: C, 83.27; H, 4.79; N, 11.61.

4′-(9-Anthryl)-2,2′:6′,2″-terpyridine (12)
Ligand 12

2-Acetylpyridine (0.61 g, 5.0 mmol) was added into a solution of 9-anthraldehyde (0.52 g, 2.5 mmol) in EtOH (25 mL). KOH pellets (0.39 g, 85%, 5.0 mmol) and aq NH_3 (7.5 mL, 29.3%, 6.3 mmol) were then added to the solution. The solution was heated at reflux for 24 h. After cooling down to ambient temperature, the solution was evaporated to dryness under reduced pressure. Recrystallization of the residue from $CHCl_3$–MeOH afforded a yellow crystalline solid (0.28 g, 0.68 mmol, 27%). ^{1}H NMR (400 MHz, $CDCl_3$): δ = 8.82 (d, J = 7.9 Hz, 2 H, $H_{3,3''}$), 8.66 (d, J = 0.3 Hz, 2 H, $H_{6,6''}$), 8.63 (s, 2 H, $H_{3',5'}$), 8.57 (s, 1 H, H_{An10}), 8.09 (d, J = 8.7 Hz, 2 H, $H_{An1,8}$), 7.95 (t, J = 7.5 Hz, 2 H, $H_{4,4''}$), 7.73 (d, J = 8.7 Hz, 2 H, $H_{An2,7}$), 7.49 (t, J = 7.2 Hz, 2 H, $H_{An3,6}$), 7.39–7.36 (m, 4 H, $H_{5,5'',An4,5}$). ^{13}C NMR (100 MHz, CD_3Cl): δ = 156.5, 156.0, 150.0, 149.6, 137.4, 134.7, 131.6, 129.9, 128.8, 127.8, 126.8, 126.3, 125.6, 124.3, 124.3, 121.9. FAB-MS: 409.5 $[M]^+$. Anal. Calcd for $C_{29}H_{19}N_3$: C, 85.06; H, 4.68; N, 10.26. Found: C, 85.27; H, 4.65; N, 10.08.

Acknowledgment

The authors thank the Natural Sciences and Engineering Research Council (NSERC) of Canada and the Université de Montréal for financial support.

References

(1) (a) Demas, J. M.; DeGra, B. A. *Coord. Chem. Rev.* **2001**, *211*, 317. (b) For a recent example: Kimura, M.; Takahashi, A.; Sakata, T.; Tsukahara, K. *Bull. Chem. Soc. Jpn.* **1998**, *71*, 1839. (c) Péchy, P.; Rotzinger, F. P.; Nazeeruddin, M. K.; Kohle, O.; Zakeeruddin, S. M.; Humphry-Baker, R.; Grätzel, M. *J. Chem. Soc., Chem. Commun.* **1995**, 65. (d) Baldo, M. A.; Thompson, M. E.; Forrest, S. R. *Nature* **2000**, *403*, 750. (e) Ziessel, R. J. *Inclusion Phenom. Macrocyclic Chem.* **1999**, *35*, 369.

(2) Constable, E. C.; Cargill Thompson, A. M. W.; Tocher, D. A.; Daniels, M. A. M. *New J. Chem.* **1992**, *16*, 855.

(3) Sauvage, J.-P.; Collin, J.-P.; Chambron, J.-C.; Guillerez, S.; Coudret, C.; Balzani, V.; Barigelletti, F.; De Cola, L.; Flamigni, L. *Chem. Rev.* **1994**, *94*, 993.

(4) (a) Maestri, M.; Armaroli, N.; Balzani, V.; Constable, E. C.; Cargill Thompson, A. M. W. *Inorg. Chem.* **1995**, *34*, 2759. (b) Hammarström, L.; Barigelletti, F.; Flamigni, L.; Indelli, M. T.; Armaroli, N.; Calogero, G.; Guardigli, M.; Sour, A.; Collin, J.-P.; Sauvage, J.-P. *J. Phys. Chem. A* **1997**, *101*, 9061. (c) Albano, G., Balzani, V.; Constable, E. C.; Maestri, M.; Smith, D. R. *Inorg. Chim. Acta* **1998**, *277*, 225.

(5) Mutai, T.; Cheon, J.-D.; Arita, S.; Araki, K. *J. Chem. Soc., Perkin Trans. 2* **2001**, 1045.

(6) Goodall, W.; Williams, J. A. G. *Chem. Commun.* **2001**, 2514.

(7) Roberto, D.; Tessore, F.; Ugo, R.; Bruni, S.; Manfredi, A.; Quici, S. *Chem. Commun.* **2002**, 846.

(8) Alcock, N. W.; Barker, P. R.; Haider, J. M.; Hannon, M. J.; Painting, C. L.; Pikramenou, Z.; Plummer, E. A.; Rissanen, K.; Saarenketo, P. *J. Chem. Soc., Dalton Trans.* **2000**, 1447.

(9) A comprehensive review of methods up to 1995 is provided by: Cargill Thompson, A. M. W. *Coord. Chem. Rev.* **1997**, *160*, 1.

(10) (a) Kröhnke, F. *Synthesis* **1976**, 1. (b) Constable, E. C.; Ward, M. D.; Corr, S. *Inorg. Chim. Acta* **1988**, *141*, 201. (c) Frank, R. L.; Riener, E. F. *J. Am. Chem. Soc.* **1950**, *72*, 4182. (d) Korall, P.; Börje, A.; Norrby, P.-O.; Åkermark, B. *Acta Chem. Scand.* **1997**, *51*, 760. (e) Cave, G. W. V.; Raston, C. L. *Chem. Commun.* **2000**, 2199.

(11) (a) Cardenas, D. J.; Sauvage, J.-P. *Synlett* **1996**, 916. (b) Hanan, G. S.; Schubert, U. S.; Volkmer, D.; Riviere, E.; Lehn, J.-M.; Kyritsakas, N.; Fisher, J. *Can. J. Chem.* **1997**, *75*, 169. (c) Fallahpour, R.-A.; Neuberger, M.; Zehnder, M. *New J. Chem.* **1999**, *23*, 53. (d) Fallahpour, R.-A. *Eur. J. Inorg. Chem.* **1998**, 1205.

(12) Goodall, W.; Wild, K.; Arm, K. J.; Williams, J. A. G. *J. Chem. Soc., Perkin Trans. 2* **2002**, 1669.
(13) During the preparation of this paper, a similar approach to synthesize 4′-*p*-tolyl-2,2′:6′,2″-terpyridine was reported: Vaduvescu, S.; Potvin, P. G. *Eur. J. Inorg. Chem.* **2004**, 1763.
(14) Collin, J.-P.; Guillerez, S.; Sauvage, J.-P.; Barigelletti, F.; De Cola, L.; Flamigni, L.; Balzani, V. *Inorg. Chem.* **1991**, *30*, 4230.
(15) Most of the starting aryl aldehydes were purchased from Aldrich. Aldehydes that were not commercial available were synthesized from the corresponding aryl bromides by lithiation and then formylation with dimethylformamide.
(16) Wang, J.; Hanan, G. S.; Loiseau, F.; Campagna, S. *Chem. Commun.* **2004**, 2068.
(17) Yoo, D.-W.; Yoo, S.-K.; Kim, C.; Lee, J.-K. *J. Chem. Soc., Dalton Trans.* **2002**, 3931.
(18) Michalec, J. F.; Bejune, S. A.; Cuttell, D. G.; Summerton, G. C.; Gertenbach, J. A.; Field, J. S.; Haines, R. J.; McMillin, D. R. *Inorg. Chem.* **2001**, *40*, 2193.
(19) Husson, J.; Beley, M.; Kirsch, G. *Tetrahedron Lett.* **2003**, *44*, 1767.
(20) Persaud, L.; Barbiero, G. *Can. J. Chem.* **1991**, *69*, 315.

A2-1 Supplementary data of single crystal structure of complexes **3a** in **Chapter 2**.

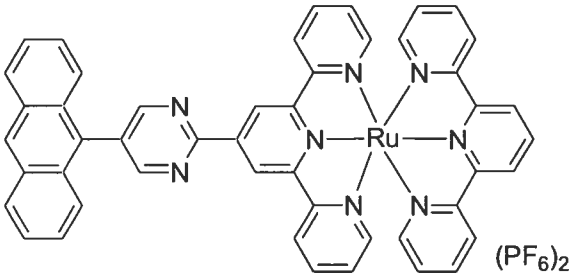

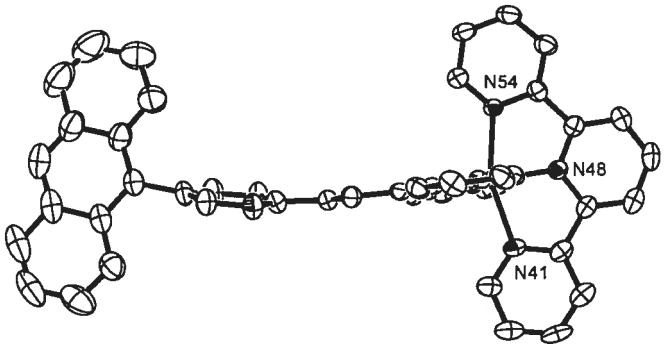

Acta Cryst. (2002). C**00**, 000–000

Structure of gary11

GARRY HANAN AND FRANCINE BÉLANGER-GARIÉPY

Département de Chimie, Université de Montréal. C.P. 6128. Succ. Centre-ville. Montréal. Québec. Canada H3C 3J7. E-mail: [redacted]

Abstract

The crystal stucture of the title compound, recrystallized from ...

Comment

comment

Experimental

Small details about the preparation of the compound.

Crystal data

$C_{18}H_{32}N_8RU.2(F_6P).C_2H_3N$
$M_r = 1152.88$
Monoclinic
$P2_1$
$a = 8.96320\,(10)$ Å
$b = 8.76480\,(10)$ Å
$c = 30.6115\,(4)$ Å
$\beta = 92.1247\,(8)°$
$V = 2403.21\,(5)$ Å^3
$Z = 2$
$D_x = 1.593$ Mg m^{-3}
D_m not measured
Cu $K\alpha$ radiation
$\lambda = 1.54178$ Å

Cell parameters from 8042 reflections
$\theta = 2.89–72.65°$
$\mu = 4.104$ mm^{-1}
$T = 220\,(2)$ K
Block
Red
0.46 × 0.25 × 0.15 mm
Crystal source: synthesized by the authors. See text

Data collection

Bruker AXS Smart 2K/Platform diffractometer

ω scans

Absorption correction:
multi-scan Sadabs (Sheldrick,1996)

$T_{min} = 0.4500$, $T_{max} = 0.6500$

29130 measured reflections

8123 independent reflections

7427 reflections with
>2sigma(I)

$R_{int} = 0.040$

$\theta_{max} = 72.86°$

$h = -11 \rightarrow 11$

$k = -9 \rightarrow 10$

$l = -37 \rightarrow 37$

232 standard reflections

every ? reflections

intensity decay: none

Refinement

Refinement on F^2

$R[F^2 > 2\sigma(F^2)] = 0.0401$

$wR(F^2) = 0.0973$

$S = 1.004$

8123 reflections

668 parameters

H-atom parameters constrained

$w=1/[\sigma^2(F_o^2) + (0.0678P)^2 + 0.0000P]$
where $P = (F_o^2 + 2F_c^2)/3$

$(\Delta/\sigma)_{max} = 0.001$

$\Delta\rho_{max} = 0.712$ e Å^{-3}

$\Delta\rho_{min} = -0.352$ e Å^{-3}

Extinction correction: none

Scattering factors from *International Tables for Crystallography* (Vol. C)

Absolute structure: Flack H D (1983), *Acta Cryst.* A39, 876-881

Flack parameter = −0.013 (7)

Table 1. *Selected geometric parameters (Å, °)*

Ru—N8	1.978 (3)	C9—C13	1.462 (6)
Ru—N18	1.981 (3)	C10—C11	1.392 (7)
Ru—N11	2.069 (3)	C11—C12	1.389 (7)
Ru—N14	2.081 (3)	C11—C19	1.484 (5)
Ru—N1	2.084 (3)	C13—N14	1.369 (5)
Ru—N51	2.093 (3)	C13—C18	1.391 (6)
N1—C2	1.328 (5)	N14—C15	1.341 (5)
N1—C6	1.367 (5)	C15—C16	1.382 (6)
C2—C3	1.385 (6)	C16—C17	1.379 (6)
C3—C4	1.382 (6)	C17—C18	1.373 (7)
C4—C5	1.379 (7)	C19—N20	1.320 (7)
C5—C6	1.386 (6)	C19—N24	1.345 (7)
C6—C7	1.467 (6)	N20—C21	1.339 (6)
C7—N8	1.362 (6)	C21—C22	1.375 (7)
C7—C12	1.382 (5)	C22—C23	1.386 (6)
N8—C9	1.344 (6)	C22—C25	1.487 (6)
C9—C10	1.392 (5)	C23—N24	1.327 (5)

Supplementary data

The tables of data shown below are not normally printed in *Acta Cryst. Section C* but the data will be available electronically *via* the online contents pages at

http://journals.iucr.org/c/journalhomepage.html

Table *S*1. *Fractional atomic coordinates and equivalent isotropic displacement parameters (Å²)*

$$U_{\rm eq} = (1/3)\Sigma_i\Sigma_j U^{ij} a^i a^j \mathbf{a}_i.\mathbf{a}_j.$$

	x	y	z	$U_{\rm eq}$
Ru	0.69083 (3)	0.15050 (4)	**0.168202** (8)	0.02668 (7)
N1	0.7738 (3)	0.3644 (4)	0.18633 (10)	0.0287 (7)
C2	0.8376 (4)	0.4671 (5)	0.16114 (14)	0.0362 (9)
H2	0.8451	0.4459	0.1312	0.043
C3	0.8937 (5)	0.6041 (5)	0.17719 (15)	0.0421 (11)
H3	0.9396	0.6737	0.1586	0.051
C4	0.8809 (5)	0.6369 (7)	0.22104 (14)	0.0435 (10)
H4	0.9168	0.7298	0.2326	0.052
C5	0.8147 (5)	0.5314 (5)	0.24758 (14)	0.0389 (9)
H5	0.8054	0.5517	0.2775	0.047
C6	0.7620 (4)	0.3954 (5)	0.22981 (12)	0.0303 (8)
C7	0.6944 (4)	0.2749 (5)	0.25582 (13)	0.0307 (8)
N8	0.6542 (3)	0.1504 (6)	0.23152 (8)	0.0271 (5)
C9	0.5891 (4)	0.0282 (5)	0.24930 (12)	0.0299 (8)
C10	0.5582 (5)	0.0275 (5)	0.29351 (13)	0.0339 (9)
H10	0.5126	−0.0576	0.3061	0.041
C11	0.5956 (4)	0.1546 (8)	0.31890 (11)	0.0339 (7)
C12	0.6647 (5)	0.2784 (5)	0.29980 (13)	0.0346 (9)
H12	0.6913	0.3642	0.3168	0.042
C13	0.5590 (4)	−0.0945 (5)	0.21785 (13)	0.0309 (8)
N14	0.5992 (3)	−0.0655 (4)	0.17594 (10)	0.0284 (7)
C15	0.5783 (4)	−0.1751 (5)	0.14579 (14)	0.0344 (9)
H15	0.6078	−0.1562	0.1171	0.041
C16	0.5152 (5)	−0.3147 (5)	0.15503 (15)	0.0423 (12)
H16	0.5029	−0.3896	0.1332	0.051
C17	0.4706 (4)	−0.3419 (8)	0.19696 (13)	0.0428 (8)
H17	0.4245	−0.4348	0.2038	0.051
C18	0.4937 (5)	−0.2328 (5)	0.22867 (14)	0.0378 (9)
H18	0.4656	−0.2514	0.2575	0.045
C19	0.5517 (4)	0.1609 (8)	0.36516 (12)	0.0395 (8)
N20	0.4639 (5)	0.0507 (5)	0.37850 (12)	0.0500 (10)
C21	0.4129 (6)	0.0679 (6)	0.41876 (16)	0.0524 (13)
H21	0.3535	−0.0102	0.4300	0.063
C22	0.4425 (5)	0.1935 (5)	0.44456 (14)	0.0425 (12)
C23	0.5438 (5)	0.2957 (6)	0.42793 (14)	0.0441 (11)
H23	0.5748	0.3787	0.4455	0.053
N24	0.5993 (4)	0.2827 (5)	0.38851 (12)	0.0435 (9)
C25	0.3658 (6)	0.2194 (6)	0.48617 (15)	0.0476 (11)
C26	0.4446 (6)	0.1979 (5)	0.52635 (15)	0.0506 (13)
C27	0.5955 (6)	0.1524 (10)	0.52993 (16)	0.0617 (12)
H27	0.6491	0.1364	0.5045	0.074
C28	0.6645 (9)	0.1313 (9)	0.5701 (2)	0.084 (2)
H28	0.7655	0.1022	0.5719	0.101
C29	0.5875 (9)	0.1523 (11)	0.60835 (17)	0.0850 (19)
H29	0.6368	0.1359	0.6356	0.102
C30	0.4434 (10)	0.1960 (7)	0.60681 (19)	0.081 (2)
H30	0.3939	0.2088	0.6331	0.097
C31	0.3638 (8)	0.2233 (7)	0.56632 (17)	0.0628 (15)
C32	0.2181 (8)	0.2707 (8)	0.5636 (2)	0.0741 (19)
H32	0.1680	0.2867	0.5896	0.089
C33	0.1425 (7)	0.2956 (8)	0.5247 (2)	0.0707 (17)

C34	−0.0075 (10)	0.3485 (12)	0.5217 (3)	0.102 (3)
H34	−0.0580	0.3654	0.5476	0.122
C35	−0.0796 (8)	0.3753 (12)	0.4833 (4)	0.110 (3)
H35	−0.1778	0.4131	0.4830	0.132
C36	−0.0114 (8)	0.3480 (10)	0.4439 (3)	0.092 (2)
H36	−0.0638	0.3653	0.4172	0.111
C37	0.1326 (7)	0.2957 (8)	0.4445 (2)	0.0685 (16)
H37	0.1779	0.2775	0.4178	0.082
C38	0.2166 (6)	0.2676 (7)	0.48455 (18)	0.0548 (13)
N41	0.9057 (4)	0.0646 (4)	0.16744 (12)	0.0329 (7)
C42	0.9950 (5)	0.0305 (6)	0.20213 (16)	0.0427 (10)
H42	0.9606	0.0489	0.2303	0.051
C43	1.1367 (5)	−0.0314 (6)	0.19799 (19)	0.0533 (13)
H43	1.1980	−0.0530	0.2228	0.064
C44	1.1848 (5)	−0.0602 (7)	0.1564 (2)	0.0575 (15)
H44	1.2781	−0.1065	0.1527	0.069
C45	1.0967 (5)	−0.0211 (6)	0.12088 (18)	0.0490 (12)
H45	1.1306	−0.0375	0.0926	0.059
C46	0.9560 (4)	0.0433 (5)	0.12654 (15)	0.0360 (9)
C47	0.8556 (5)	0.0926 (5)	0.09049 (14)	0.0347 (9)
N48	0.7249 (3)	0.1472 (6)	0.10455 (9)	0.0299 (6)
C49	0.6160 (4)	0.1983 (4)	0.07654 (13)	0.0334 (9)
C50	0.6387 (5)	0.1962 (5)	0.03206 (14)	0.0421 (11)
H50	0.5644	0.2321	0.0122	0.051
C51	0.7724 (5)	0.1404 (9)	0.01725 (13)	0.0492 (11)
H51	0.7889	0.1386	−0.0129	0.059
C52	0.8815 (5)	0.0873 (6)	0.04640 (15)	0.0446 (11)
H52	0.9718	0.0484	0.0364	0.054
C53	0.4835 (4)	0.2531 (5)	0.09864 (13)	0.0331 (9)
N54	0.4891 (3)	0.2402 (4)	0.14298 (10)	0.0278 (7)
C55	0.3713 (5)	0.2840 (5)	0.16518 (14)	0.0343 (9)
H55	0.3743	0.2719	0.1957	0.041
C56	0.2447 (5)	0.3465 (6)	0.14504 (16)	0.0412 (11)
H56	0.1641	0.3779	0.1617	0.049
C57	0.2385 (5)	0.3622 (6)	0.10010 (16)	0.0449 (11)
H57	0.1536	0.4040	0.0857	0.054
C58	0.3596 (5)	0.3151 (5)	0.07652 (15)	0.0411 (10)
H58	0.3578	0.3251	0.0459	0.049
P1	0.78459 (12)	0.6433 (2)	0.03999 (3)	0.0407 (2)
F11	0.6580 (3)	0.7718 (4)	0.03506 (10)	0.0571 (8)
F12	0.8475 (3)	0.7267 (4)	0.08318 (10)	0.0595 (8)
F13	0.9102 (4)	0.5151 (4)	0.04580 (13)	0.0770 (10)
F14	0.7207 (5)	0.5602 (4)	−0.00293 (10)	0.0750 (10)
F15	0.6765 (4)	0.5448 (4)	0.06906 (10)	0.0648 (8)
F16	0.8894 (4)	0.7448 (4)	0.01105 (12)	0.0757 (11)
P2	0.20643 (16)	0.3805 (2)	0.28880 (4)	0.0602 (4)
F21	0.0507 (4)	0.3027 (7)	0.29438 (17)	0.1180 (18)
F22	0.2581 (5)	0.3344 (5)	0.33653 (11)	0.0839 (12)
F23	0.3632 (4)	0.4570 (7)	0.28222 (17)	0.124 (2)
F24	0.1574 (5)	0.4264 (7)	0.24030 (11)	0.1156 (19)
F25	0.1397 (6)	0.5353 (6)	0.30485 (15)	0.1135 (17)
F26	0.2720 (5)	0.2241 (6)	0.27176 (14)	0.1104 (16)
C100	1.1147 (15)	0.953 (2)	0.3443 (4)	0.221 (9)
H10A	1.1584	0.8758	0.3635	0.331
H10B	1.0979	1.0455	0.3609	0.331
H10C	1.1823	0.9749	0.3211	0.331
C101	0.9749 (9)	0.8987 (10)	0.3257 (2)	0.091 (2)
N102	0.8743 (8)	0.8525 (9)	0.3110 (2)	0.105 (2)

Table *S2*. *Anisotropic displacement parameters* (Å^2)

	U_{11}	U_{22}	U_{33}	U_{12}	U_{13}	U_{23}
Ru	0.02428 (12)	0.02904 (13)	0.02666 (12)	0.00088 (15)	0.00034 (8)	−0.00020 (16)
N1	0.0274 (16)	0.0285 (18)	0.0297 (16)	−0.0008 (13)	−0.0049 (13)	0.0021 (13)
C2	0.029 (2)	0.044 (3)	0.035 (2)	0.0000 (17)	−0.0038 (16)	0.0069 (18)

A2-2 Supplementary data of single crystal structure of complexes **3b** in **Chapter 2**.

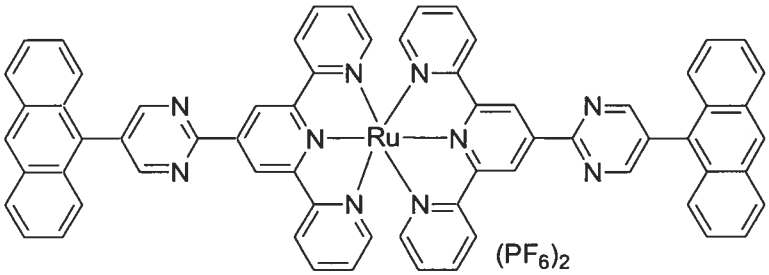

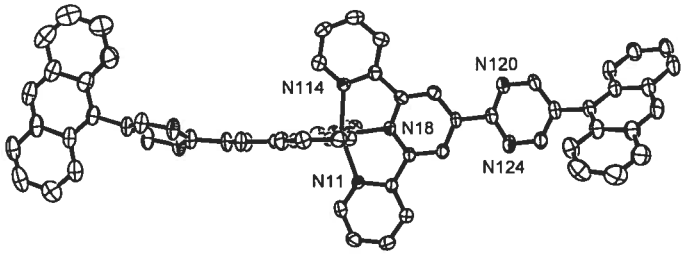

Acta Cryst. (2002). C**00**, 000–000

Structure of gary12

GARRY HANAN AND FRANCINE BÉLANGER-GARIÉPY

Département de Chimie, Université de Montréal. C.P. 6128, Succ. Centre-ville, Montréal, Québec, Canada H3C 3J7. E-mail: [redacted]

Abstract

The crystal stucture of the title compound, recrystallized from ...

Comment

comment

Experimental

Small details about the preparation of the compound.

Crystal data

$C_{66}H_{12}N_{10}Ru.2(F_6P).2(C_2H_3N)$
$M_r = 1448.21$
Monoclinic
Cc
$a = 13.1378\,(2)$ Å
$b = 12.1410\,(2)$ Å
$c = 39.3588\,(6)$ Å
$\beta = 92.4490\,(10)°$
$V = 6272.23\,(17)$ Å^3
$Z = 4$
$D_x = 1.534$ Mg m^{-3}
D_m not measured
Cu $K\alpha$ radiation
$\lambda = 1.54178$ Å

Cell parameters from 7613 reflections
$\theta = 3.37$–$72.92°$
$\mu = 3.293$ mm^{-1}
$T = 220\,(2)$ K
Block
Orange
0.28 × 0.20 × 0.14 mm
Crystal source: synthesized by the authors. See text

Data collection

Bruker AXS Smart 2K/Platform diffractometer

ω scans

Absorption correction:
multi-scan Sadabs (Sheldrick,1996)

$T_{min} = 0.2900$, $T_{max} = 0.8500$

75410 measured reflections

10112 independent reflections

9468 reflections with
>2sigma(I)

$R_{int} = 0.077$

$\theta_{max} = 72.92°$

$h = -15 \rightarrow 12$

$k = -15 \rightarrow 15$

$l = -48 \rightarrow 48$

282 standard reflections

every ? reflections

intensity decay: none

Refinement

Refinement on F^2

$R[F^2 > 2\sigma(F^2)] = 0.0493$

$wR(F^2) = 0.1224$

$S = 1.013$

10112 reflections

876 parameters

H-atom parameters constrained

w=$1/[\sigma^2(F_o^2) + (0.0874P)^2]$
where $P = (F_o^2 + 2F_c^2)/3$

$(\Delta/\sigma)_{max} = 0.001$

$\Delta\rho_{max} = 1.600$ e Å^{-3}

$\Delta\rho_{min} = -0.971$ e Å^{-3}

Extinction correction: none

Scattering factors from *International Tables for Crystallography* (Vol. C)

Absolute structure: Flack H D (1983), *Acta Cryst.* A39, 876-881

Flack parameter = 0.014 (6)

Table 1. *Selected geometric parameters (Å, °)*

Ru—N28	1.981 (5)	C19—C113	1.456 (6)
Ru—N18	1.993 (4)	C110—C111	1.403 (7)
Ru—N111	2.064 (4)	C111—C112	1.400 (6)
Ru—N11	2.070 (3)	C111—C119	1.483 (5)
Ru—N211	2.086 (4)	C113—N114	1.370 (6)
Ru—N21	2.087 (4)	C113—C118	1.388 (6)
N11—C12	1.340 (6)	N114—C115	1.336 (6)
N11—C16	1.381 (5)	C115—C116	1.378 (7)
C12—C13	1.385 (7)	C116—C117	1.380 (9)
C13—C14	1.382 (7)	C117—C118	1.382 (7)
C14—C15	1.387 (7)	C119—N120	1.336 (6)
C15—C16	1.381 (6)	C119—N121	1.340 (6)
C16—C17	1.478 (6)	N120—C121	1.336 (6)
C17—N18	1.349 (6)	C121—C122	1.384 (7)
C17—C112	1.376 (6)	C122—C123	1.391 (7)
N18—C19	1.360 (6)	C122—C125	1.477 (6)
C19—C110	1.361 (6)	C123—N121	1.330 (6)

Supplementary data

The tables of data shown below are not normally printed in *Acta Cryst. Section C* but the data will be available electronically *via* the online contents pages at

http://journals.iucr.org/c/journalhomepage.html

Table *S*1. *Fractional atomic coordinates and equivalent isotropic displacement parameters (Å²)*

$$U_{\rm eq} = (1/3)\Sigma_i\Sigma_j U^{ij} a^i a^j \mathbf{a}_i.\mathbf{a}_j.$$

	x	y	z	$U_{\rm eq}$
Ru	**−0.009895** (17)	0.57642 (2)	**0.934661** (9)	0.02674 (9)
N11	−0.0691 (3)	0.4200 (3)	0.92671 (9)	0.0272 (7)
C12	−0.1122 (4)	0.3541 (4)	0.94928 (11)	0.0372 (10)
H12	−0.1174	0.3799	0.9717	0.045
C13	−0.1496 (4)	0.2500 (4)	0.94156 (13)	0.0415 (11)
H13	−0.1789	0.2062	0.9582	0.050
C14	−0.1426 (5)	0.2124 (4)	0.90859 (14)	0.0445 (12)
H14	−0.1659	0.1415	0.9026	0.053
C15	−0.1009 (4)	0.2798 (4)	0.88435 (12)	0.0391 (11)
H15	−0.0975	0.2557	0.8617	0.047
C16	−0.0644 (3)	0.3826 (4)	0.89370 (11)	0.0298 (9)
C17	−0.0169 (3)	0.4604 (4)	0.87022 (11)	0.0293 (8)
N18	0.0097 (3)	0.5569 (3)	0.88509 (10)	0.0277 (8)
C19	0.0562 (4)	0.6387 (4)	0.86793 (12)	0.0295 (9)
C110	0.0758 (4)	0.6237 (4)	0.83450 (12)	0.0323 (10)
H110	0.1056	0.6809	0.8223	0.039
C111	0.0518 (4)	0.5237 (4)	0.81815 (10)	0.0310 (9)
C112	0.0027 (4)	0.4423 (4)	0.83663 (11)	0.0317 (9)
H112	−0.0167	0.3756	0.8261	0.038
C113	0.0791 (3)	0.7341 (4)	0.88936 (11)	0.0314 (9)
N114	0.0543 (3)	0.7259 (3)	0.92271 (9)	0.0303 (8)
C115	0.0740 (4)	0.8113 (4)	0.94338 (12)	0.0399 (11)
H115	0.0578	0.8050	0.9663	0.048
C116	0.1169 (5)	0.9082 (4)	0.93268 (15)	0.0489 (14)
H116	0.1286	0.9669	0.9479	0.059
C117	0.1423 (5)	0.9169 (4)	0.89913 (17)	0.0523 (15)
H117	0.1720	0.9819	0.8912	0.063
C118	0.1237 (4)	0.8293 (4)	0.87731 (13)	0.0411 (11)
H118	0.1411	0.8342	0.8544	0.049
C119	0.0838 (4)	0.5007 (4)	0.78318 (11)	0.0328 (9)
N120	0.1307 (3)	0.5815 (3)	0.76695 (10)	0.0356 (9)
C121	0.1738 (4)	0.5517 (4)	0.73823 (11)	0.0372 (10)
H121	0.2084	0.6059	0.7262	0.045
C122	0.1705 (4)	0.4460 (4)	0.72512 (11)	0.0351 (10)
C123	0.1101 (4)	0.3736 (4)	0.74281 (11)	0.0383 (10)
H123	0.0983	0.3032	0.7335	0.046
N124	0.0680 (3)	0.3975 (4)	0.77203 (10)	0.0395 (9)
C125	0.2268 (4)	0.4079 (4)	0.69562 (12)	0.0353 (10)
C126	0.2148 (4)	0.4606 (4)	0.66367 (11)	0.0364 (10)
C127	0.1458 (4)	0.5502 (4)	0.65735 (13)	0.0428 (11)
H127	0.1059	0.5753	0.6750	0.051
C128	0.1365 (5)	0.5999 (5)	0.62643 (14)	0.0489 (14)
H128	0.0888	0.6568	0.6227	0.059
C129	0.1990 (5)	0.5660 (5)	0.59952 (13)	0.0503 (14)
H129	0.1952	0.6033	0.5786	0.060
C130	0.2635 (5)	0.4805 (5)	0.60428 (12)	0.0490 (13)
H130	0.3037	0.4584	0.5863	0.059
C131	0.2726 (4)	0.4220 (4)	0.63592 (12)	0.0411 (12)
C132	0.3289 (4)	0.3266 (5)	0.63936 (12)	0.0448 (12)
H132	0.3620	0.2988	0.6205	0.054
C133	0.3380 (4)	0.2701 (5)	0.67027 (13)	0.0426 (11)

C134	0.3937 (5)	0.1690 (5)	0.67400 (17)	0.0554 (14)
H134	0.4215	0.1367	0.6548	0.066
C135	0.4069 (5)	0.1192 (6)	0.7044 (2)	0.0644 (17)
H135	0.4408	0.0511	0.7061	0.077
C136	0.3697 (5)	0.1698 (6)	0.73401 (18)	0.0630 (17)
H136	0.3845	0.1383	0.7555	0.076
C137	0.3132 (4)	0.2630 (5)	0.73157 (13)	0.0490 (14)
H137	0.2885	0.2945	0.7514	0.059
C138	0.2904 (4)	0.3145 (4)	0.69955 (12)	0.0414 (11)
N21	0.1317 (3)	0.5210 (3)	0.95372 (9)	0.0285 (7)
C22	0.2090 (4)	0.4823 (3)	0.93637 (11)	0.0320 (9)
H22	0.1994	0.4729	0.9128	0.038
C23	0.3034 (4)	0.4551 (4)	0.95155 (13)	0.0393 (11)
H23	0.3558	0.4267	0.9386	0.047
C24	0.3179 (4)	0.4712 (4)	0.98628 (13)	0.0407 (11)
H24	0.3812	0.4553	0.9972	0.049
C25	0.2385 (4)	0.5110 (4)	1.00468 (12)	0.0395 (10)
H25	0.2473	0.5215	1.0283	0.047
C26	0.1454 (4)	0.5353 (4)	0.98819 (11)	0.0330 (9)
C27	0.0570 (4)	0.5787 (3)	1.00522 (11)	0.0314 (9)
N28	−0.0247 (4)	0.5972 (3)	0.98413 (12)	0.0324 (9)
C29	−0.1131 (4)	0.6368 (4)	0.99550 (11)	0.0313 (10)
C210	−0.1226 (4)	0.6602 (5)	1.02960 (12)	0.0404 (12)
H210	−0.1846	0.6857	1.0377	0.048
C211	−0.0374 (4)	0.6450 (4)	1.05183 (11)	0.0394 (11)
C212	0.0522 (4)	0.6039 (4)	1.03965 (12)	0.0398 (11)
H212	0.1093	0.5929	1.0545	0.048
C213	−0.1907 (4)	0.6577 (3)	0.96762 (10)	0.0309 (9)
N214	−0.1563 (3)	0.6426 (3)	0.93546 (9)	0.0295 (7)
C215	−0.2177 (4)	0.6686 (4)	0.90885 (11)	0.0347 (10)
H215	−0.1937	0.6622	0.8868	0.042
C216	−0.3168 (4)	0.7050 (4)	0.91315 (13)	0.0387 (11)
H216	−0.3589	0.7231	0.8941	0.046
C217	−0.3531 (4)	0.7144 (4)	0.94499 (14)	0.0414 (11)
H217	−0.4210	0.7357	0.9480	0.050
C218	−0.2875 (4)	0.6918 (4)	0.97297 (12)	0.0376 (10)
H218	−0.3099	0.7001	0.9952	0.045
C219	−0.0413 (4)	0.6825 (4)	1.08797 (12)	0.0422 (11)
N220	−0.1328 (4)	0.7033 (4)	1.09973 (11)	0.0517 (12)
C221	−0.1325 (5)	0.7489 (5)	1.13068 (13)	0.0502 (14)
H221	−0.1954	0.7646	1.1401	0.060
C222	−0.0432 (4)	0.7743 (5)	1.14976 (11)	0.0433 (12)
C223	0.0473 (5)	0.7418 (5)	1.13542 (13)	0.0483 (13)
H223	0.1090	0.7521	1.1480	0.058
N224	0.0494 (4)	0.6965 (4)	1.10446 (11)	0.0488 (11)
C225	−0.0426 (4)	0.8377 (4)	1.18203 (13)	0.0432 (11)
C226	−0.0875 (4)	0.7939 (5)	1.21090 (13)	0.0455 (13)
C227	−0.1338 (5)	0.6897 (6)	1.21189 (15)	0.0571 (15)
H227	−0.1355	0.6458	1.1922	0.069
C228	−0.1763 (5)	0.6498 (7)	1.24041 (19)	0.0651 (18)
H228	−0.2073	0.5800	1.2402	0.078
C229	−0.1731 (6)	0.7157 (7)	1.27056 (15)	0.069 (2)
H229	−0.2035	0.6892	1.2902	0.083
C230	−0.1280 (6)	0.8138 (7)	1.27133 (14)	0.0627 (18)
H230	−0.1263	0.8546	1.2916	0.075
C231	−0.0819 (5)	0.8589 (5)	1.24216 (13)	0.0529 (15)
C232	−0.0358 (5)	0.9605 (6)	1.24259 (16)	0.0603 (17)
H232	−0.0340	1.0018	1.2628	0.072
C233	0.0081 (5)	1.0040 (5)	1.21419 (16)	0.0551 (15)
C234	0.0584 (6)	1.1099 (6)	1.2146 (2)	0.076 (2)
H234	0.0627	1.1507	1.2350	0.091
C235	0.0989 (7)	1.1507 (7)	1.1869 (3)	0.082 (2)
H235	0.1329	1.2188	1.1880	0.098
C236	0.0910 (7)	1.0928 (6)	1.1559 (3)	0.077 (2)
H236	0.1182	1.1241	1.1365	0.093

C237	0.0458 (6)	0.9941 (6)	1.15359 (17)	0.0645 (17)
H237	0.0411	0.9578	1.1325	0.077
C238	0.0042 (5)	0.9430 (5)	1.18289 (16)	0.0497 (14)
P1	0.34598 (12)	0.58404 (12)	0.34197 (4)	0.0441 (3)
F11	0.3908 (4)	0.5906 (4)	0.37997 (9)	0.0882 (15)
F12	0.3150 (4)	0.4592 (4)	0.34706 (13)	0.0938 (15)
F13	0.4535 (4)	0.5485 (5)	0.32928 (12)	0.0976 (17)
F14	0.3745 (4)	0.7093 (4)	0.33693 (13)	0.0952 (15)
F15	0.2377 (3)	0.6191 (4)	0.35499 (11)	0.0839 (13)
F16	0.2996 (3)	0.5763 (3)	0.30407 (9)	0.0651 (11)
P2	0.98674 (15)	0.77719 (18)	0.54018 (4)	0.0671 (5)
F21	0.9560 (6)	0.8872 (6)	0.55837 (17)	0.141 (3)
F22	0.8708 (5)	0.7615 (6)	0.52916 (17)	0.137 (3)
F23	0.9733 (4)	0.7104 (6)	0.57401 (13)	0.114 (2)
F24	1.1038 (4)	0.7978 (6)	0.55074 (13)	0.1122 (19)
F25	0.9997 (4)	0.8436 (5)	0.50585 (11)	0.0975 (17)
F26	1.0189 (6)	0.6721 (5)	0.52071 (16)	0.125 (2)
N31	0.0937 (14)	0.8798 (14)	0.0228 (4)	0.200 (6)
C32	0.1570 (14)	0.9076 (11)	0.0429 (4)	0.137 (5)
C33	0.2226 (10)	0.9270 (9)	0.0726 (3)	0.110 (4)
H33A	0.2667	0.8638	0.0766	0.165
H33B	0.1814	0.9382	0.0922	0.165
H33C	0.2638	0.9920	0.0691	0.165
N41	0.2560 (6)	0.0002 (7)	0.8290 (2)	0.092 (2)
C42	0.2087 (6)	0.0688 (6)	0.81796 (18)	0.0627 (17)
C43	0.1439 (8)	0.1547 (8)	0.8055 (3)	0.100 (3)
H43A	0.0793	0.1508	0.8164	0.150
H43B	0.1325	0.1466	0.7811	0.150
H43C	0.1758	0.2253	0.8104	0.150

Table *S2. Anisotropic displacement parameters* ($Å^2$)

	U_{11}	U_{22}	U_{33}	U_{12}	U_{13}	U_{23}
Ru	0.03192 (16)	0.02836 (14)	0.02014 (13)	−0.00168 (15)	0.00350 (9)	−0.00237 (14)
N11	0.028 (2)	0.0280 (17)	0.0258 (17)	−0.0018 (13)	0.0071 (14)	−0.0038 (13)
C12	0.040 (3)	0.046 (3)	0.027 (2)	0.0041 (19)	0.0059 (18)	−0.0002 (18)
C13	0.046 (3)	0.038 (3)	0.041 (3)	−0.004 (2)	0.013 (2)	0.004 (2)
C14	0.053 (3)	0.035 (3)	0.046 (3)	−0.012 (2)	0.007 (2)	−0.005 (2)
C15	0.048 (3)	0.037 (2)	0.032 (2)	−0.006 (2)	0.004 (2)	−0.0021 (19)
C16	0.032 (2)	0.032 (2)	0.0249 (19)	−0.0014 (17)	0.0029 (16)	−0.0034 (16)
C17	0.029 (2)	0.035 (2)	0.0236 (19)	−0.0018 (17)	0.0026 (16)	−0.0032 (16)
N18	0.029 (2)	0.0311 (19)	0.0231 (18)	0.0000 (16)	0.0003 (15)	−0.0013 (16)
C19	0.028 (3)	0.032 (2)	0.029 (2)	−0.0025 (17)	0.0047 (18)	0.0041 (17)
C110	0.029 (3)	0.036 (2)	0.032 (2)	−0.0024 (18)	0.0057 (18)	0.0000 (19)
C111	0.033 (3)	0.043 (2)	0.0176 (18)	0.0008 (18)	0.0049 (16)	−0.0043 (16)
C112	0.031 (2)	0.038 (2)	0.026 (2)	−0.0029 (17)	0.0056 (17)	−0.0064 (17)
C113	0.029 (2)	0.036 (2)	0.029 (2)	0.0008 (17)	0.0023 (16)	−0.0015 (17)
N114	0.036 (2)	0.0270 (17)	0.0279 (17)	−0.0020 (14)	−0.0013 (15)	0.0002 (14)
C115	0.048 (3)	0.038 (2)	0.033 (2)	−0.004 (2)	0.001 (2)	−0.0041 (18)
C116	0.065 (4)	0.034 (3)	0.048 (3)	−0.010 (2)	−0.002 (3)	−0.009 (2)
C117	0.065 (4)	0.034 (3)	0.058 (4)	−0.013 (2)	0.001 (3)	0.003 (2)
C118	0.047 (3)	0.038 (3)	0.038 (2)	−0.008 (2)	0.003 (2)	0.004 (2)
C119	0.028 (2)	0.046 (2)	0.025 (2)	0.0011 (18)	0.0039 (16)	−0.0028 (17)
N120	0.040 (2)	0.042 (2)	0.0252 (18)	0.0040 (16)	0.0044 (16)	−0.0011 (15)
C121	0.040 (3)	0.050 (3)	0.0220 (19)	−0.003 (2)	0.0049 (18)	0.0026 (18)
C122	0.033 (3)	0.051 (3)	0.0208 (19)	0.0045 (19)	0.0019 (18)	−0.0013 (18)
C123	0.041 (3)	0.045 (3)	0.029 (2)	−0.004 (2)	0.0054 (19)	−0.0057 (19)
N124	0.038 (2)	0.053 (2)	0.0281 (19)	−0.0067 (18)	0.0061 (17)	−0.0107 (17)
C125	0.035 (3)	0.046 (3)	0.025 (2)	0.0008 (19)	0.0077 (18)	−0.0018 (18)
C126	0.039 (3)	0.046 (2)	0.025 (2)	−0.001 (2)	0.0016 (19)	−0.0028 (18)
C127	0.045 (3)	0.054 (3)	0.030 (2)	0.009 (2)	0.006 (2)	−0.004 (2)
C128	0.064 (4)	0.051 (3)	0.032 (3)	0.008 (3)	0.004 (2)	0.004 (2)
C129	0.063 (4)	0.064 (3)	0.024 (2)	−0.002 (3)	0.002 (2)	0.003 (2)
C130	0.056 (4)	0.067 (4)	0.025 (2)	−0.002 (3)	0.008 (2)	−0.004 (2)
C131	0.038 (3)	0.058 (3)	0.027 (2)	−0.002 (2)	0.003 (2)	−0.004 (2)

A2-3 Supplementary data of single crystal structure of complexes **3b** in **Chapter 3**.

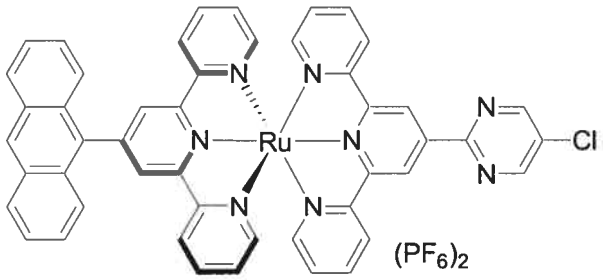

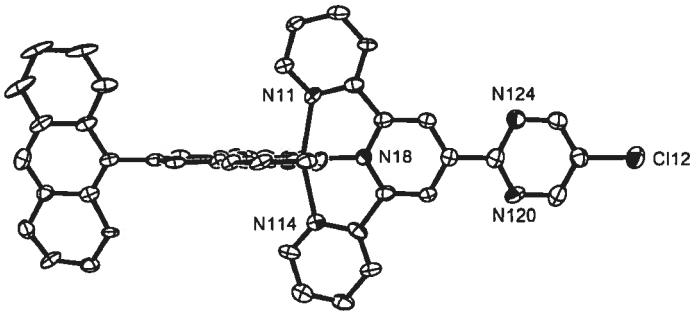

29 Jun 2004

Acta Cryst. (2004). C**60**, 000–000

Structure of Gary41

GARRY HANAN, ELAINE MEDLYCOTT AND FRANCINE BÉLANGER-GARIÉPY

Département de Chimie, Université de Montréal, C.P. 6128, Succ. Centre-ville, Montréal, Québec, Canada H3C 3J7. E-mail: [redacted]

Abstract

Here should be written a short abstract

Comment

To finish the structure, it was decided to use the *PLATON* (Spek, 2000) facility SQUEEZE to handle the disordered solvent. *PLATON* identified a remarkably large potential solvent volume of 600.8 Å^3, or 22.1% of the cell volume. The use of *PLATON*/SQUEEZE resulted in a 3.1% improvement in R1 while correcting for 168 electrons/cell. The reported structure is based on the *PLATON*/SQUEEZE corrected data. The actual solvent content is unknown, so several quantities reported in Table 1 [empirical formula, density, absorption coefficient, $F(000)$] are incorrect and should be indicated as such in future publications.

Experimental

Small details about the preparation of the compound.

Crystal data

$C_{18}H_{31}ClN_8Ru.2(F_6P)$
$M_r = 1146.27$
Triclinic
$P\bar{1}$
$a = 10.4037\,(6)$ Å
$b = 12.2602\,(7)$ Å
$c = 21.9324\,(12)$ Å
$\alpha = 80.801\,(3)°$
$\beta = 85.840\,(3)°$
$\gamma = 80.360\,(3)°$
$V = 2719.5\,(3)$ Å^3
$Z = 2$
$D_x = 1.400$ Mg m^{-3}
D_m not measured

Cu $K\alpha$ radiation
$\lambda = 1.54178$ Å
Cell parameters from 14369 reflections
$\theta = 3.70–68.28°$
$\mu = 4.059$ mm^{-1}
$T = 100\,(2)$ K
Plate
Red
0.35 × 0.12 × 0.03 mm
Crystal source: synthesized by the authors. See text

Data collection

Bruker AXS Smart 2K/Platform diffractometer
ω scans
Absorption correction:
multi-scan Sadabs (Sheldrick.1996)
$T_{min} = 0.5400$, $T_{max} = 0.9100$
21145 measured reflections
9562 independent reflections

7740 reflections with $I > 2\sigma(I)$
$R_{int} = 0.078$
$\theta_{max} = 68.53°$
$h = -11 \rightarrow 12$
$k = -14 \rightarrow 14$
$l = -24 \rightarrow 26$
189 standard reflections
every ? reflections
intensity decay: −3.62%

Refinement

Refinement on F^2
$R[F^2 > 2\sigma(F^2)] = 0.1359$
$wR(F^2) = 0.4025$
$S = 1.148$
9562 reflections
650 parameters
H-atom parameters constrained
$w=1/[\sigma^2(F_o^2) + (0.3200P)^2 + 0.0000P]$
where $P = (F_o^2 + 2F_c^2)/3$

$(\Delta/\sigma)_{max} = 0.012$
$\Delta\rho_{max} = 3.283$ e Å^{-3}
$\Delta\rho_{min} = -2.446$ e Å^{-3}
Extinction correction: *SHELXL*
Extinction coefficient: 0.0022 (6)
Scattering factors from *International Tables for Crystallography* (Vol. C)

Table 1. *Selected geometric parameters (Å, °)*

Ru1—N18	1.970 (8)	Ru1—N28	1.978 (7)

Supplementary data

The tables of data shown below are not normally printed in *Acta Cryst. Section C* but the data will be available electronically *via* the online contents pages at

http://journals.iucr.org/c/journalhomepage.html

Table *S*1. *Fractional atomic coordinates and equivalent isotropic displacement parameters (Å²)*

$$U_{eq} = (1/3)\Sigma_i\Sigma_j U^{ij} a^i a^j \mathbf{a}_i.\mathbf{a}_j.$$

	x	y	z	U_{eq}
Ru1	0.73957 (6)	0.69278 (5)	0.18709 (3)	0.0440 (4)
N11	0.5575 (8)	0.7829 (6)	0.2054 (4)	0.0469 (18)
C12	0.4704 (9)	0.8357 (7)	0.1642 (5)	0.048 (2)
H12	0.4945	0.8407	0.1214	0.058
C13	0.3447 (10)	0.8838 (7)	0.1826 (5)	0.050 (2)
H13	0.2846	0.9213	0.1525	0.060
C14	0.3082 (10)	0.8761 (9)	0.2464 (6)	0.060 (3)
H14	0.2231	0.9063	0.2604	0.072
C15	0.4018 (9)	0.8225 (7)	0.2876 (5)	0.053 (2)
H15	0.3822	0.8188	0.3308	0.063
C16	0.5217 (10)	0.7752 (7)	0.2669 (5)	0.050 (2)
C17	0.6199 (9)	0.7109 (8)	0.3091 (5)	0.049 (2)
N18	0.7287 (7)	0.6659 (6)	0.2782 (3)	0.0438 (16)
C19	0.8280 (9)	0.5966 (8)	0.3091 (5)	0.050 (2)
C110	0.8211 (9)	0.5645 (9)	0.3715 (5)	0.056 (2)
H110	0.8900	0.5145	0.3919	0.067
C111	0.7088 (11)	0.6080 (9)	0.4043 (5)	0.057 (2)
C112	0.6086 (9)	0.6765 (8)	0.3728 (5)	0.052 (2)
H112	0.5300	0.7010	0.3950	0.062
C113	0.9397 (9)	0.5573 (9)	0.2656 (5)	0.052 (2)
N114	0.9201 (7)	0.5921 (6)	0.2042 (4)	0.0448 (17)
C115	1.0134 (9)	0.5641 (8)	0.1633 (5)	0.053 (2)
H115	0.9999	0.5893	0.1207	0.063
C116	1.1325 (11)	0.4980 (9)	0.1807 (6)	0.059 (3)
H116	1.1982	0.4784	0.1503	0.071
C117	1.1523 (9)	0.4628 (10)	0.2409 (6)	0.063 (3)
H117	1.2314	0.4170	0.2539	0.075
C118	1.0538 (9)	0.4952 (7)	0.2837 (5)	0.054 (2)
H118	1.0672	0.4732	0.3266	0.065
C119	0.6927 (11)	0.5650 (8)	0.4708 (5)	0.057 (2)
N120	0.7850 (9)	0.4869 (8)	0.4971 (4)	0.063 (2)
C121	0.7706 (13)	0.4499 (10)	0.5576 (5)	0.069 (3)
H121	0.8332	0.3924	0.5776	0.083
C122	0.6620 (11)	0.4975 (9)	0.5905 (5)	0.056 (2)
C123	0.5721 (11)	0.5779 (11)	0.5615 (5)	0.065 (3)
H123	0.4964	0.6059	0.5847	0.078
N124	0.5848 (9)	0.6189 (10)	0.5027 (4)	0.071 (3)
Cl12	0.6429 (3)	0.4526 (3)	0.67016 (13)	0.0694 (8)
N21	0.6499 (7)	0.5651 (6)	0.1683 (4)	0.0446 (17)
C22	0.6010 (10)	0.4872 (7)	0.2094 (5)	0.051 (2)
H22	0.6105	0.4867	0.2522	0.062
C23	0.5375 (9)	0.4077 (8)	0.1916 (5)	0.049 (2)
H23	0.5006	0.3555	0.2217	0.058
C24	0.5289 (9)	0.4058 (8)	0.1291 (5)	0.053 (2)
H24	0.4880	0.3506	0.1158	0.064
C25	0.5797 (8)	0.4840 (6)	0.0864 (4)	0.042 (2)
H25	0.5731	0.4838	0.0434	0.051
C26	0.6403 (8)	0.5625 (7)	0.1062 (4)	0.0415 (19)
C27	0.6967 (8)	0.6527 (6)	0.0641 (4)	0.0394 (18)
N28	0.7442 (8)	0.7200 (5)	0.0957 (3)	0.0408 (16)
C29	0.7979 (9)	0.8095 (7)	0.0655 (4)	0.0448 (19)

C210	0.7971 (8)	0.8321 (7)	0.0022 (5)	0.045 (2)
H210	0.8267	0.8979	−0.0189	0.054
C211	0.7528 (8)	0.7592 (7)	−0.0316 (4)	0.044 (2)
C212	0.7014 (8)	0.6681 (6)	0.0013 (4)	0.0418 (19)
H212	0.6697	0.6172	−0.0200	0.050
C213	0.8501 (9)	0.8700 (7)	0.1078 (5)	0.0443 (19)
N214	0.8326 (7)	0.8321 (6)	0.1697 (4)	0.0454 (17)
C215	0.8837 (9)	0.8772 (8)	0.2117 (5)	0.054 (2)
H215	0.8736	0.8486	0.2543	0.065
C216	0.9524 (11)	0.9671 (9)	0.1931 (6)	0.067 (3)
H216	0.9907	0.9971	0.2234	0.080
C217	0.9656 (11)	1.0123 (9)	0.1325 (6)	0.064 (3)
H217	1.0103	1.0744	0.1204	0.077
C218	0.9105 (10)	0.9639 (8)	0.0882 (6)	0.055 (2)
H218	0.9146	0.9949	0.0457	0.066
C219	0.7570 (8)	0.7820 (6)	−0.1003 (4)	0.042 (2)
C220	0.6420 (10)	0.8284 (7)	−0.1313 (5)	0.052 (2)
C221	0.5180 (10)	0.8564 (7)	−0.1006 (6)	0.062 (3)
H221	0.5124	0.8447	−0.0567	0.074
C222	0.4088 (11)	0.8988 (8)	−0.1310 (8)	0.086 (5)
H222	0.3296	0.9174	−0.1078	0.103
C223	0.4072 (13)	0.9166 (9)	−0.1962 (9)	0.099 (6)
H223	0.3306	0.9478	−0.2179	0.118
C224	0.5227 (14)	0.8860 (10)	−0.2250 (9)	0.107 (7)
H224	0.5232	0.8919	−0.2687	0.129
C225	0.6435 (11)	0.8459 (8)	−0.1978 (6)	0.061 (3)
C226	0.7620 (13)	0.8258 (10)	−0.2300 (5)	0.068 (3)
H226	0.7651	0.8410	−0.2739	0.081
C227	0.8755 (9)	0.7842 (8)	−0.2001 (5)	0.048 (2)
C228	0.9993 (11)	0.7635 (9)	−0.2331 (5)	0.060 (3)
H228	1.0063	0.7772	−0.2770	0.072
C229	1.1032 (10)	0.7245 (7)	−0.2002 (5)	0.052 (3)
H229	1.1848	0.7204	−0.2229	0.063
C230	1.1093 (9)	0.6907 (9)	−0.1402 (5)	0.059 (3)
H230	1.1888	0.6560	−0.1218	0.071
C231	0.9940 (8)	0.7084 (7)	−0.1056 (4)	0.0432 (19)
H231	0.9944	0.6867	−0.0620	0.052
C232	0.8728 (9)	0.7587 (7)	−0.1333 (5)	0.047 (2)
P1	0.0232 (7)	0.8654 (4)	0.3860 (2)	0.134 (3)
F11	−0.0106 (9)	0.7663 (9)	0.4339 (4)	0.110 (3)
F12	−0.1197 (14)	0.8939 (14)	0.3624 (6)	0.188 (6)
F13	−0.0166 (15)	0.9472 (10)	0.4364 (5)	0.156 (5)
F14	0.1750 (11)	0.8345 (8)	0.4063 (4)	0.120 (3)
F15	0.0642 (10)	0.7851 (9)	0.3330 (4)	0.111 (3)
F16	0.0567 (15)	0.9691 (9)	0.3381 (5)	0.164 (5)
P2	0.2469 (2)	0.7344 (2)	0.04037 (12)	0.0498 (6)
F21	0.2409 (12)	0.8653 (7)	0.0370 (4)	0.119 (3)
F22	0.3975 (7)	0.7283 (9)	0.0423 (5)	0.120 (3)
F23	0.2307 (12)	0.7217 (8)	0.1126 (4)	0.119 (3)
F24	0.0929 (8)	0.7404 (10)	0.0384 (5)	0.115 (3)
F25	0.2603 (10)	0.7467 (8)	−0.0317 (4)	0.104 (3)
F26	0.2507 (12)	0.6067 (8)	0.0420 (5)	0.122 (3)

Table *S2*. *Anisotropic displacement parameters* (Å^2)

	U_{11}	U_{22}	U_{33}	U_{12}	U_{13}	U_{23}
Ru1	0.0403 (5)	0.0429 (5)	0.0511 (5)	−0.0077 (3)	−0.0051 (3)	−0.0114 (3)
N11	0.045 (4)	0.045 (4)	0.049 (4)	−0.002 (3)	−0.016 (3)	−0.001 (3)
C12	0.038 (5)	0.046 (5)	0.058 (6)	0.001 (4)	−0.009 (4)	−0.005 (4)
C13	0.049 (5)	0.042 (4)	0.057 (6)	0.006 (4)	−0.019 (4)	−0.004 (4)
C14	0.034 (5)	0.063 (6)	0.085 (8)	0.004 (4)	−0.007 (5)	−0.024 (5)
C15	0.044 (5)	0.043 (5)	0.064 (6)	0.017 (4)	−0.001 (4)	−0.012 (4)
C16	0.048 (6)	0.038 (4)	0.067 (6)	−0.002 (4)	−0.008 (4)	−0.013 (4)
C17	0.039 (5)	0.049 (5)	0.059 (6)	−0.003 (4)	−0.008 (4)	−0.012 (4)
N18	0.038 (4)	0.053 (4)	0.043 (4)	−0.008 (3)	−0.006 (3)	−0.011 (3)

A2-4 Supplementary data of single crystal structure of complexes **3d** in **Chapter 3**.

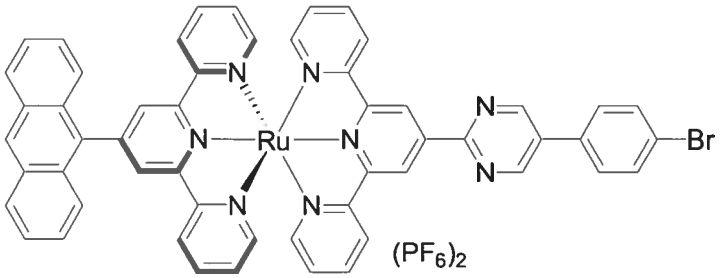

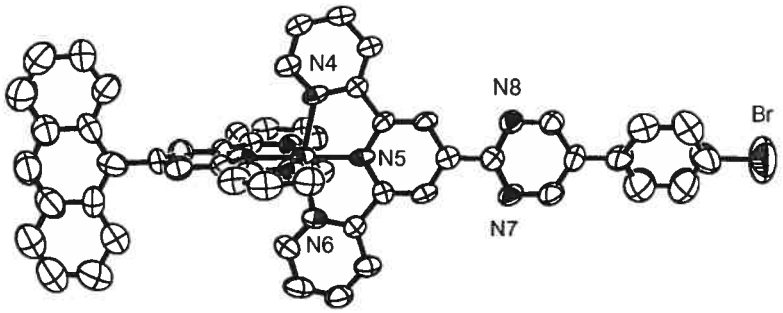

26 Feb 2004

Acta Cryst. (2003). C**59**, 000–000

Structure of Gary36

Garry Hanan, Elaine Medlycott, Joseph Wang and Francine Bélanger-Gariépy

Département de Chimie, Université de Montréal, C.P. 6128, Succ. Centre-ville, Montréal, Québec, Canada H3C 3J7. E-mail: [redacted]

Abstract

Here should be written the text of the abstract

Comment

To finish the structure, it was decided to use the *PLATON* (Spek, 2000) facility SQUEEZE to handle the disordered solvent. *PLATON* identified a large potential solvent volume of 1865.3 Å^3, or 28.6% of the cell volume. The use of *PLATON*/SQUEEZE resulted in a 2.0% improvement in R1 while correcting for 458 electrons/cell. The reported structure is based on the *PLATON*/SQUEEZE corrected data. The actual solvent content is unknown, so several quantities reported in Table 1 [empirical formula, density, absorption coefficient, $F(000)$] are incorrect and should be indicated as such in future publications.

Experimental

Small details about the preparation of the compound.

Crystal data

$C_{54}H_{35}BrN_8Ru.2(F_6P)$
$M_r = 1266.82$
Monoclinic
$P2_1/c$
$a = 25.1776\,(18)$ Å
$b = 11.4829\,(8)$ Å
$c = 23.2866\,(15)$ Å
$\beta = 104.716\,(3)°$
$V = 6511.6\,(8)$ Å^3
$Z = 4$
$D_x = 1.292$ Mg m^{-3}
D_m not measured

Cu $K\alpha$ radiation
$\lambda = 1.54178$ Å
Cell parameters from 16364 reflections
$\theta = 3.85$–$56.91°$
$\mu = 3.765$ mm^{-1}
$T = 220\,(2)$ K
Block
Red
0.50 × 0.11 × 0.04 mm
Crystal source: synthesized by the authors. See text

Data collection

Bruker AXS Smart 2K/Platform diffractometer
ω scans
Absorption correction:
multi-scan Sadabs (Sheldrick,1996)
$T_{min} = 0.6300$, $T_{max} = 0.9000$
55391 measured reflections
9043 independent reflections

4640 reflections with $I > 2\sigma(I)$
$R_{int} = 0.053$
$\theta_{max} = 58.15°$
$h = -27 \rightarrow 27$
$k = -12 \rightarrow 12$
$l = -25 \rightarrow 25$
358 standard reflections
every ? reflections
intensity decay: none

Refinement

Refinement on F^2
$R[F^2 > 2\sigma(F^2)] = 0.0550$
$wR(F^2) = 0.0992$
$S = 1.011$
9043 reflections
819 parameters
H-atom parameters constrained

$w=1/[\sigma^2(F_o^2) + (0.0259P)^2]$
where $P = (F_o^2 + 2F_c^2)/3$
$(\Delta/\sigma)_{max} = 0.001$
$\Delta\rho_{max} = 0.600$ e Å^{-3}
$\Delta\rho_{min} = -0.366$ e Å^{-3}
Extinction correction: none
Scattering factors from *International Tables for Crystallography* (Vol. C)

Table 1. *Selected geometric parameters (Å, °)*

Ru—N28	1.933 (4)	Ru—N21	2.085 (4)
Ru—N18	1.947 (5)	Br—C228	1.871 (8)
Ru—N11	2.070 (4)	N11—C12	1.325 (6)
Ru—N124	2.079 (4)	N11—C16	1.360 (6)
Ru—N214	2.080 (4)	C12—C13	1.374 (7)

Supplementary data

The tables of data shown below are not normally printed in *Acta Cryst. Section C* but the data will be available electronically *via* the online contents pages at

http://journals.iucr.org/c/journalhomepage.html

Table *S*1. *Fractional atomic coordinates and equivalent isotropic displacement parameters (Å²)*

$$U_{eq} = (1/3)\Sigma_i\Sigma_j U^{ij} a^i a^j \mathbf{a}_i.\mathbf{a}_j.$$

	Occupancy	x	y	z	U_{eq}
Ru	1	**0.352783** (18)	0.26531 (3)	**0.394653** (19)	0.05169 (17)
Br	1	0.91864 (4)	0.21172 (10)	0.80561 (5)	0.1850 (5)
N11	1	0.3628 (2)	0.1690 (3)	0.3230 (2)	0.0491 (12)
C12	1	0.4083 (3)	0.1204 (5)	0.3157 (3)	0.0566 (16)
H12	1	0.4408	0.1285	0.3460	0.068
C13	1	0.4103 (3)	0.0586 (5)	0.2657 (3)	0.0650 (18)
H13	1	0.4431	0.0234	0.2624	0.078
C14	1	0.3637 (3)	0.0496 (5)	0.2212 (3)	0.0661 (18)
H14	1	0.3641	0.0086	0.1864	0.079
C15	1	0.3157 (3)	0.1007 (5)	0.2270 (3)	0.0644 (17)
H15	1	0.2833	0.0951	0.1964	0.077
C16	1	0.3160 (3)	0.1599 (4)	0.2784 (3)	0.0497 (15)
C17	1	0.2673 (3)	0.2176 (5)	0.2897 (3)	0.0539 (15)
N18	1	0.27879 (19)	0.2718 (4)	0.3428 (2)	0.0508 (12)
C19	1	0.2395 (3)	0.3278 (5)	0.3604 (3)	0.0543 (16)
C120	1	0.1861 (3)	0.3295 (5)	0.3249 (3)	0.0657 (18)
H120	1	0.1586	0.3688	0.3379	0.079
C121	1	0.1732 (3)	0.2737 (6)	0.2703 (3)	0.0656 (17)
C122	1	0.2150 (3)	0.2166 (5)	0.2522 (3)	0.0674 (17)
H122	1	0.2079	0.1783	0.2154	0.081
C123	1	0.2588 (3)	0.3839 (5)	0.4177 (3)	0.0549 (16)
N124	1	0.3128 (2)	0.3677 (3)	0.4443 (2)	0.0522 (13)
C125	1	0.3356 (3)	0.4148 (5)	0.4964 (3)	0.0635 (18)
H125	1	0.3732	0.4028	0.5135	0.076
C126	1	0.3059 (4)	0.4809 (5)	0.5262 (3)	0.077 (2)
H126	1	0.3229	0.5145	0.5631	0.093
C127	1	0.2509 (4)	0.4968 (5)	0.5012 (4)	0.082 (2)
H127	1	0.2298	0.5408	0.5213	0.098
C128	1	0.2265 (3)	0.4492 (5)	0.4470 (3)	0.080 (2)
H128	1	0.1888	0.4600	0.4297	0.095
C129	1	0.1169 (3)	0.2686 (7)	0.2302 (4)	0.081 (2)
C130	1	0.0790 (4)	0.1863 (7)	0.2397 (4)	0.088 (2)
C131	1	0.0903 (3)	0.1086 (9)	0.2881 (4)	0.120 (3)
H131	1	0.1242	0.1132	0.3167	0.144
C132	1	0.0515 (5)	0.0242 (8)	0.2941 (5)	0.165 (4)
H132	1	0.0600	−0.0304	0.3251	0.199
C133	1	0.0000 (5)	0.0230 (10)	0.2529 (6)	0.171 (4)
H133	1	−0.0265	−0.0306	0.2586	0.205
C134	1	−0.0131 (4)	0.0936 (10)	0.2066 (5)	0.150 (4)
H134	1	−0.0474	0.0867	0.1789	0.180
C135	1	0.0257 (4)	0.1813 (8)	0.1987 (5)	0.106 (3)
C136	1	0.0122 (4)	0.2568 (10)	0.1516 (4)	0.113 (3)
H136	1	−0.0227	0.2519	0.1249	0.135
C137	1	0.0485 (4)	0.3388 (8)	0.1426 (4)	0.097 (2)
C138	1	0.0341 (4)	0.4171 (9)	0.0936 (4)	0.132 (3)
H138	1	−0.0008	0.4126	0.0668	0.158
C139	1	0.0699 (5)	0.4962 (9)	0.0858 (4)	0.148 (4)
H139	1	0.0597	0.5488	0.0539	0.178
C140	1	0.1229 (4)	0.5028 (8)	0.1244 (5)	0.133 (3)
H140	1	0.1480	0.5580	0.1171	0.160
C141	1	0.1383 (3)	0.4316 (7)	0.1713 (4)	0.106 (3)

H141	1	0.1736	0.4396	0.1969	0.127
C142	1	0.1027 (3)	0.3448 (8)	0.1832 (4)	0.083 (2)
N21	1	0.3458 (2)	0.1182 (3)	0.4448 (2)	0.0512 (12)
C22	1	0.3009 (3)	0.0546 (5)	0.4411 (3)	0.0642 (18)
H22	1	0.2683	0.0747	0.4130	0.077
C23	1	0.3013 (3)	−0.0416 (5)	0.4780 (3)	0.075 (2)
H23	1	0.2695	−0.0867	0.4743	0.090
C24	1	0.3483 (3)	−0.0689 (5)	0.5192 (3)	0.074 (2)
H24	1	0.3491	−0.1334	0.5443	0.089
C25	1	0.3946 (3)	−0.0027 (5)	0.5244 (3)	0.0638 (17)
H25	1	0.4270	−0.0206	0.5534	0.077
C26	1	0.3930 (3)	0.0921 (5)	0.4859 (3)	0.0500 (15)
C27	1	0.4396 (3)	0.1699 (5)	0.4881 (3)	0.0472 (15)
N28	1	0.42582 (17)	0.2581 (4)	0.44705 (17)	0.0449 (11)
C29	1	0.4640 (3)	0.3391 (5)	0.4442 (2)	0.0463 (15)
C210	1	0.5161 (3)	0.3357 (4)	0.4810 (3)	0.0493 (15)
H210	1	0.5416	0.3936	0.4779	0.059
C211	1	0.5316 (3)	0.2467 (5)	0.5231 (2)	0.0494 (14)
C212	1	0.4912 (3)	0.1629 (5)	0.5256 (2)	0.0530 (16)
H212	1	0.4998	0.1016	0.5532	0.064
C213	1	0.4435 (3)	0.4246 (5)	0.3981 (2)	0.0430 (14)
N214	1	0.3898 (2)	0.4090 (3)	0.3667 (2)	0.0469 (12)
C215	1	0.3669 (2)	0.4797 (5)	0.3221 (2)	0.0548 (16)
H215	1	0.3303	0.4662	0.3009	0.066
C216	1	0.3950 (3)	0.5722 (5)	0.3058 (3)	0.0590 (17)
H216	1	0.3779	0.6215	0.2742	0.071
C217	1	0.4489 (3)	0.5902 (4)	0.3371 (3)	0.0576 (17)
H217	1	0.4690	0.6526	0.3271	0.069
C218	1	0.4729 (2)	0.5166 (5)	0.3829 (2)	0.0503 (15)
H218	1	0.5096	0.5287	0.4041	0.060
C219	1	0.5863 (3)	0.2395 (5)	0.5631 (3)	0.0534 (15)
N220	1	0.5956 (2)	0.1575 (4)	0.6056 (2)	0.0605 (14)
C221	1	0.6458 (3)	0.1569 (5)	0.6412 (3)	0.0681 (19)
H221	1	0.6536	0.1015	0.6719	0.082
C222	1	0.6880 (3)	0.2322 (6)	0.6364 (3)	0.0620 (16)
C223	1	0.6729 (3)	0.3104 (5)	0.5901 (3)	0.0619 (17)
H223	1	0.6997	0.3622	0.5839	0.074
N224	1	0.6230 (2)	0.3174 (4)	0.5540 (2)	0.0601 (14)
C225	1	0.7436 (3)	0.2267 (5)	0.6754 (3)	0.079 (2)
C226	1	0.7674 (4)	0.1290 (8)	0.7013 (4)	0.142 (3)
H226	1	0.7481	0.0586	0.6923	0.170
C227	1	0.8213 (4)	0.1262 (9)	0.7423 (4)	0.157 (4)
H227	1	0.8350	0.0566	0.7617	0.188
C228	1	0.8495 (3)	0.2171 (7)	0.7517 (4)	0.120 (3)
C229	1	0.8308 (4)	0.3156 (9)	0.7256 (4)	0.138 (3)
H229	1	0.8522	0.3837	0.7330	0.165
C230	1	0.7770 (4)	0.3175 (8)	0.6854 (4)	0.135 (3)
H230	1	0.7649	0.3872	0.6650	0.162
P1	0.38 (2)	0.5603 (6)	0.2475 (13)	0.3299 (7)	0.0697 (10)
F11	0.38 (2)	0.5484 (12)	0.189 (2)	0.3873 (10)	0.108 (9)
F12	0.38 (2)	0.5006 (7)	0.3003 (17)	0.3112 (8)	0.106 (6)
F13	0.38 (2)	0.5377 (10)	0.1342 (12)	0.2936 (10)	0.080 (7)
F14	0.38 (2)	0.6193 (7)	0.192 (3)	0.3494 (10)	0.141 (9)
F15	0.38 (2)	0.5834 (10)	0.3617 (18)	0.3646 (9)	0.103 (7)
F16	0.38 (2)	0.5728 (10)	0.298 (2)	0.2712 (8)	0.094 (7)
P2	0.62 (2)	0.5692 (4)	0.2463 (8)	0.3293 (4)	0.0697 (10)
F21	0.62 (2)	0.5304 (9)	0.3558 (14)	0.3183 (5)	0.126 (6)
F22	0.62 (2)	0.6001 (6)	0.2891 (12)	0.2816 (5)	0.083 (4)
F23	0.62 (2)	0.5253 (5)	0.1785 (16)	0.2798 (5)	0.103 (5)
F24	0.62 (2)	0.5373 (7)	0.2061 (15)	0.3766 (6)	0.094 (5)
F25	0.62 (2)	0.6113 (7)	0.3141 (11)	0.3798 (5)	0.109 (4)
F26	0.62 (2)	0.6079 (5)	0.1365 (8)	0.3408 (5)	0.083 (4)
P3	0.693 (15)	0.1508 (3)	0.7687 (7)	0.4737 (4)	0.143 (2)
F31	0.693 (15)	0.2136 (5)	0.7514 (13)	0.4759 (8)	0.201 (7)
F32	0.693 (15)	0.1345 (7)	0.8460 (11)	0.4163 (5)	0.223 (7)

F33	0.693 (15)	0.1712 (6)	0.8877 (9)	0.5099 (6)	0.203 (7)
F34	0.693 (15)	0.1655 (5)	0.7034 (10)	0.5355 (5)	0.196 (5)
F35	0.693 (15)	0.1309 (3)	0.6550 (9)	0.4380 (6)	0.171 (5)
F36	0.693 (15)	0.0910 (4)	0.7864 (12)	0.4832 (6)	0.210 (5)
P4	0.307 (15)	0.1558 (6)	0.8007 (16)	0.4591 (8)	0.143 (2)
F41	0.307 (15)	0.1729 (8)	0.9102 (19)	0.4262 (9)	0.168 (10)
F42	0.307 (15)	0.0995 (6)	0.857 (2)	0.4615 (11)	0.150 (9)
F43	0.307 (15)	0.1895 (10)	0.856 (3)	0.5196 (8)	0.188 (15)
F44	0.307 (15)	0.2105 (7)	0.741 (2)	0.4532 (10)	0.098 (8)
F45	0.307 (15)	0.1268 (8)	0.739 (3)	0.3991 (10)	0.189 (11)
F46	0.307 (15)	0.1459 (11)	0.690 (2)	0.4969 (16)	0.188 (14)

Table *S2. Anisotropic displacement parameters* ($Å^2$)

	U_{11}	U_{22}	U_{33}	U_{12}	U_{13}	U_{23}
Ru	0.0650 (3)	0.0407 (3)	0.0513 (3)	−0.0001 (3)	0.0184 (2)	0.0007 (3)
Br	0.1054 (8)	0.2131 (12)	0.1917 (11)	0.0082 (8)	−0.0448 (8)	0.0090 (9)
N11	0.051 (4)	0.041 (3)	0.055 (4)	0.005 (3)	0.014 (3)	0.006 (2)
C12	0.060 (5)	0.044 (4)	0.064 (5)	−0.003 (3)	0.014 (4)	−0.008 (3)
C13	0.062 (5)	0.059 (4)	0.072 (5)	0.008 (3)	0.013 (4)	−0.010 (4)
C14	0.093 (6)	0.055 (4)	0.056 (5)	0.000 (4)	0.030 (5)	−0.007 (3)
C15	0.060 (5)	0.060 (4)	0.075 (5)	0.007 (4)	0.021 (4)	−0.004 (4)
C16	0.063 (5)	0.044 (4)	0.046 (4)	0.006 (3)	0.022 (4)	−0.003 (3)
C17	0.047 (5)	0.049 (4)	0.066 (5)	0.005 (3)	0.016 (4)	0.001 (4)
N18	0.070 (4)	0.034 (3)	0.062 (4)	−0.001 (3)	0.041 (3)	−0.004 (3)
C19	0.055 (5)	0.055 (4)	0.050 (5)	−0.010 (4)	0.008 (4)	0.003 (4)
C120	0.077 (6)	0.063 (4)	0.060 (5)	0.002 (4)	0.025 (4)	0.001 (4)
C121	0.034 (5)	0.080 (5)	0.077 (5)	0.001 (4)	0.003 (4)	0.012 (4)
C122	0.065 (5)	0.067 (4)	0.071 (5)	0.003 (4)	0.019 (5)	0.002 (4)
C123	0.070 (5)	0.040 (4)	0.062 (5)	0.000 (4)	0.030 (5)	0.004 (4)
N124	0.068 (4)	0.048 (3)	0.043 (4)	−0.003 (3)	0.019 (3)	0.001 (3)
C125	0.093 (6)	0.052 (4)	0.047 (5)	0.004 (4)	0.022 (5)	−0.005 (3)
C126	0.098 (6)	0.078 (5)	0.059 (5)	−0.008 (5)	0.024 (5)	−0.013 (4)
C127	0.112 (7)	0.074 (5)	0.071 (6)	0.004 (5)	0.046 (5)	−0.015 (4)
C128	0.098 (6)	0.064 (4)	0.085 (6)	0.010 (4)	0.039 (5)	−0.001 (4)
C129	0.082 (7)	0.060 (5)	0.114 (7)	0.001 (5)	0.048 (6)	0.006 (5)
C130	0.062 (7)	0.104 (6)	0.086 (6)	−0.001 (5)	−0.004 (5)	0.004 (5)
C131	0.081 (7)	0.139 (8)	0.137 (8)	−0.013 (6)	0.019 (6)	0.024 (7)
C132	0.122 (9)	0.160 (9)	0.211 (12)	−0.030 (8)	0.036 (9)	0.068 (8)
C133	0.090 (9)	0.184 (11)	0.226 (13)	−0.032 (8)	0.014 (9)	0.055 (10)
C134	0.087 (8)	0.164 (10)	0.190 (12)	−0.018 (8)	0.015 (8)	0.031 (8)
C135	0.077 (8)	0.103 (7)	0.141 (9)	−0.012 (6)	0.034 (8)	−0.002 (6)
C136	0.076 (7)	0.142 (8)	0.115 (8)	−0.002 (7)	0.013 (6)	0.002 (7)
C137	0.077 (8)	0.115 (7)	0.097 (7)	0.001 (6)	0.019 (6)	0.008 (6)
C138	0.121 (9)	0.136 (8)	0.118 (9)	−0.010 (7)	−0.006 (7)	0.014 (7)
C139	0.140 (10)	0.149 (9)	0.131 (9)	−0.008 (8)	−0.011 (8)	0.047 (7)
C140	0.084 (8)	0.167 (9)	0.129 (8)	−0.021 (6)	−0.009 (6)	0.042 (7)
C141	0.105 (7)	0.106 (6)	0.093 (7)	0.002 (6)	0.002 (6)	0.019 (5)
C142	0.054 (6)	0.092 (6)	0.100 (7)	−0.011 (5)	0.016 (6)	−0.008 (5)
N21	0.059 (4)	0.042 (3)	0.056 (3)	−0.004 (3)	0.022 (3)	−0.001 (2)
C22	0.058 (5)	0.061 (4)	0.076 (5)	−0.008 (4)	0.022 (4)	−0.001 (4)
C23	0.096 (6)	0.055 (5)	0.080 (5)	−0.025 (4)	0.034 (5)	0.003 (4)
C24	0.096 (6)	0.058 (4)	0.067 (5)	−0.008 (5)	0.018 (5)	0.012 (4)
C25	0.086 (5)	0.048 (4)	0.060 (5)	−0.006 (4)	0.023 (4)	0.002 (4)
C26	0.056 (5)	0.050 (4)	0.045 (4)	0.004 (4)	0.015 (4)	−0.002 (3)
C27	0.047 (5)	0.046 (4)	0.049 (4)	0.000 (4)	0.012 (4)	−0.009 (3)
N28	0.068 (3)	0.026 (3)	0.046 (3)	0.003 (3)	0.024 (3)	0.004 (3)
C29	0.063 (5)	0.038 (4)	0.034 (4)	0.004 (4)	0.007 (4)	0.001 (3)
C210	0.073 (5)	0.027 (3)	0.046 (4)	−0.002 (3)	0.011 (4)	0.003 (3)
C211	0.064 (5)	0.042 (4)	0.045 (4)	0.004 (4)	0.020 (4)	−0.011 (3)
C212	0.077 (5)	0.039 (4)	0.046 (4)	0.011 (4)	0.021 (4)	0.008 (3)
C213	0.052 (5)	0.036 (4)	0.042 (4)	0.006 (3)	0.014 (4)	−0.006 (3)
N214	0.073 (4)	0.032 (3)	0.039 (3)	0.009 (3)	0.019 (3)	0.005 (2)
C215	0.074 (5)	0.047 (4)	0.045 (4)	0.002 (4)	0.018 (4)	−0.002 (3)
C216	0.076 (5)	0.053 (4)	0.050 (4)	0.009 (4)	0.020 (4)	0.013 (3)

A2-5 Supplementary data of single crystal structure of complexes **2c** in **Chapter 4**.

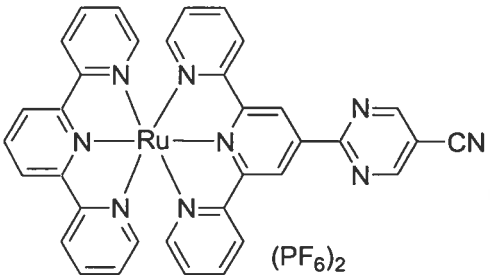

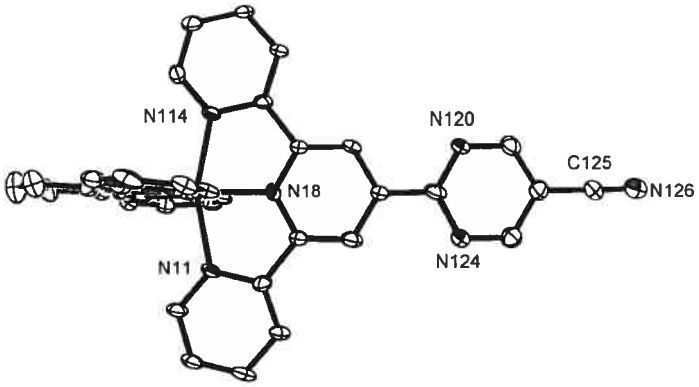

20 Jul 2004

Acta Cryst. (2004). C**60**, 000–000

Structure of Gary43 avec squueze

GARRY HANAN, ELAINE MEDLYCOTT, JOSEPH WANG AND FRANCINE BÉLANGER-GARIÉPY

Département de Chimie, Université de Montréal, C.P. 6128, Succ. Centre-ville, Montréal, Québec, Canada H3C 3J7. E-mail: [redacted]

Abstract

Here should be written a short abstract

Comment

To finish the structure, it was decided to use the *PLATON* (Spek, 2000) facility SQUEEZE to handle the disordered solvent and PF6 anion (2 by asymmetric unit). *PLATON* identified a remarkably large potential solvent/anion volume of 847.2 Å^3, or 39.6% of the cell volume. The use of *PLATON*/SQUEEZE resulted in a 20% improvement in R1 while correcting for 435 electrons/cell. The reported structure is based on the *PLATON*/SQUEEZE corrected data. The actual solvent content is unknown, so several quantities reported in Table 1 [empirical formula, density, absorption coefficient, $F(000)$] are incorrect and should be indicated as such in future publications.

Experimental

Small details about the preparation of the compound.

Crystal data

$C_{35}H_{23}N_9Ru$
$M_r = 670.69$
Triclinic
$P\bar{1}$
$a = 8.6267\,(4)$ Å
$b = 8.8957\,(3)$ Å
$c = 28.2782\,(11)$ Å
$\alpha = 81.425\,(2)°$
$\beta = 86.118\,(2)°$
$\gamma = 86.135\,(2)°$
$V = 2137.29\,(15)$ Å^3
$Z = 2$
$D_x = 1.042$ Mg m^{-3}
D_m not measured

Cu $K\alpha$ radiation
$\lambda = 1.54178$ Å
Cell parameters from 10132 reflections
$\theta = 3.17$–$68.00°$
$\mu = 3.202$ mm^{-1}
$T = 100\,(2)$ K
PLATE
Red
0.20 × 0.10 × 0.03 mm
Crystal source: synthesized by the authors. See text

Data collection

Bruker AXS Smart 4K/Platform diffractometer
ω scans
Absorption correction:
multi-scan Sadabs (Sheldrick,1996)
$T_{min} = 0.4400$. $T_{max} = 0.9100$
27039 measured reflections
7540 independent reflections

5577 reflections with $I > 2\sigma(I)$
$R_{int} = 0.059$
$\theta_{max} = 68.58°$
$h = -9 \rightarrow 10$
$k = -10 \rightarrow 10$
$l = -34 \rightarrow 33$
182 standard reflections
every ? reflections
intensity decay: none

Refinement

Refinement on F^2
$R[F^2 > 2\sigma(F^2)] = 0.0996$
$wR(F^2) = 0.2812$
$S = 1.076$
7540 reflections
406 parameters
H-atom parameters constrained

w=$1/[\sigma^2(F_o^2) + (0.1771P)^2 + 4.1539P]$ where $P = (F_o^2 + 2F_c^2)/3$
$(\Delta/\sigma)_{max} = 0.000$
$\Delta\rho_{max} = 2.222$ e Å^{-3}
$\Delta\rho_{min} = -2.504$ e Å^{-3}
Extinction correction: none
Scattering factors from *International Tables for Crystallography* (Vol. C)

Supplementary data

The tables of data shown below are not normally printed in *Acta Cryst. Section C* but the data will be available electronically *via* the online contents pages at

http://journals.iucr.org/c/journalhomepage.html

Table *S*1. *Fractional atomic coordinates and equivalent isotropic displacement parameters (Å²)*

$$U_{eq} = (1/3)\Sigma_i\Sigma_j U^{ij} a^i a^j \mathbf{a}_i.\mathbf{a}_j.$$

	x	y	z	U_{eq}
Ru	0.04718 (7)	0.01817 (6)	0.26569 (2)	0.0338 (3)
N11	−0.0387 (8)	0.2414 (7)	0.2503 (2)	0.0348 (15)
C12	−0.1065 (11)	0.3340 (8)	0.2802 (3)	0.041 (2)
H12	−0.1159	0.2962	0.3134	0.050
C13	−0.1633 (11)	0.4812 (9)	0.2651 (3)	0.044 (2)
H13	−0.2090	0.5423	0.2878	0.052
C14	−0.1536 (11)	0.5387 (10)	0.2172 (3)	0.048 (2)
H14	−0.1954	0.6382	0.2059	0.057
C15	−0.0794 (11)	0.4446 (8)	0.1855 (3)	0.043 (2)
H15	−0.0640	0.4825	0.1524	0.052
C16	−0.0299 (11)	0.2993 (8)	0.2025 (3)	0.0387 (19)
C17	0.0481 (10)	0.1924 (8)	0.1708 (3)	0.0367 (18)
N18	0.0877 (10)	0.0551 (7)	0.1948 (2)	0.0415 (18)
C19	0.1561 (10)	−0.0586 (8)	0.1723 (3)	0.0374 (19)
C110	0.1887 (11)	−0.0338 (8)	0.1240 (3)	0.042 (2)
H110	0.2380	−0.1128	0.1081	0.051
C111	0.1493 (11)	0.1088 (9)	0.0977 (3)	0.041 (2)
C112	0.0818 (11)	0.2235 (9)	0.1221 (3)	0.042 (2)
H112	0.0590	0.3224	0.1054	0.051
C113	0.1910 (10)	−0.2004 (8)	0.2060 (3)	0.0363 (18)
N114	0.1402 (8)	−0.1951 (7)	0.2528 (2)	0.0328 (14)
C115	0.1616 (10)	−0.3215 (9)	0.2844 (3)	0.0387 (19)
H115	0.1295	−0.3182	0.3170	0.046
C116	0.2281 (11)	−0.4559 (9)	0.2718 (3)	0.043 (2)
H116	0.2382	−0.5440	0.2951	0.051
C117	0.2799 (11)	−0.4613 (8)	0.2249 (3)	0.043 (2)
H117	0.3308	−0.5513	0.2156	0.052
C118	0.2562 (10)	−0.3345 (8)	0.1923 (3)	0.0374 (19)
H118	0.2851	−0.3383	0.1594	0.045
C119	0.1925 (12)	0.1356 (9)	0.0471 (3)	0.046 (2)
N120	0.2653 (11)	0.0220 (8)	0.0250 (2)	0.054 (2)
C121	0.3030 (12)	0.0472 (10)	−0.0204 (3)	0.052 (2)
H121	0.3468	−0.0345	−0.0360	0.062
C122	0.2810 (13)	0.1895 (10)	−0.0467 (3)	0.051 (2)
C123	0.2034 (11)	0.3039 (10)	−0.0228 (3)	0.046 (2)
H123	0.1809	0.4018	−0.0403	0.055
N124	0.1612 (9)	0.2780 (8)	0.0233 (2)	0.0449 (18)
C125	0.3356 (13)	0.2231 (11)	−0.0971 (3)	0.056 (3)
N126	0.3765 (14)	0.2431 (10)	−0.1353 (3)	0.080 (3)
N21	0.2487 (8)	0.0911 (6)	0.2882 (2)	0.0349 (15)
C22	0.3707 (9)	0.1505 (8)	0.2616 (3)	0.0347 (18)
H22	0.3718	0.1541	0.2279	0.042
C23	0.4945 (10)	0.2064 (8)	0.2804 (3)	0.040 (2)
H23	0.5772	0.2499	0.2602	0.048
C24	0.4946 (13)	0.1973 (9)	0.3296 (3)	0.051 (2)
H24	0.5786	0.2352	0.3434	0.062
C25	0.3752 (12)	0.1344 (10)	0.3587 (3)	0.049 (2)
H25	0.3761	0.1250	0.3926	0.058
C26	0.2503 (10)	0.0837 (7)	0.3362 (3)	0.0368 (19)
C27	0.1195 (12)	0.0104 (9)	0.3644 (3)	0.047 (2)
N28	0.0118 (10)	−0.0181 (7)	0.3369 (2)	0.0411 (18)

C29	−0.1241 (12)	−0.0831 (9)	0.3546 (3)	0.049 (2)
C210	−0.1555 (13)	−0.1204 (13)	0.4039 (4)	0.063 (3)
H210	−0.2465	−0.1694	0.4170	0.076
C211	−0.0427 (14)	−0.0803 (16)	0.4328 (4)	0.075 (4)
H211	−0.0617	−0.0967	0.4666	0.090
C212	0.0902 (12)	−0.0197 (12)	0.4144 (3)	0.054 (2)
H212	0.1648	0.0029	0.4351	0.065
C213	−0.2274 (11)	−0.1078 (9)	0.3166 (3)	0.045 (2)
N214	−0.1695 (8)	−0.0630 (7)	0.2713 (2)	0.0369 (16)
C215	−0.2640 (10)	−0.0822 (9)	0.2349 (3)	0.040 (2)
H215	−0.2305	−0.0487	0.2026	0.048
C216	−0.4041 (11)	−0.1483 (10)	0.2443 (4)	0.049 (2)
H216	−0.4656	−0.1593	0.2186	0.058
C217	−0.4554 (12)	−0.1976 (10)	0.2896 (4)	0.060 (3)
H217	−0.5522	−0.2441	0.2954	0.072
C218	−0.3690 (12)	−0.1816 (9)	0.3280 (4)	0.051 (2)
H218	−0.4027	−0.2178	0.3601	0.061

Table *S2. Anisotropic displacement parameters* (Å^2)

	U_{11}	U_{22}	U_{33}	U_{12}	U_{13}	U_{23}
Ru	0.0481 (5)	0.0175 (3)	0.0360 (4)	0.0003 (2)	0.0053 (3)	−0.0094 (2)
N11	0.038 (4)	0.024 (3)	0.044 (4)	0.001 (3)	0.008 (3)	−0.015 (3)
C12	0.050 (6)	0.022 (4)	0.054 (5)	0.004 (3)	0.003 (4)	−0.012 (3)
C13	0.046 (6)	0.025 (4)	0.061 (5)	0.001 (4)	0.011 (4)	−0.018 (4)
C14	0.043 (6)	0.035 (4)	0.068 (6)	0.016 (4)	−0.007 (4)	−0.026 (4)
C15	0.058 (6)	0.021 (4)	0.051 (5)	0.004 (4)	0.001 (4)	−0.010 (3)
C16	0.054 (6)	0.022 (3)	0.041 (4)	−0.004 (3)	−0.005 (4)	−0.004 (3)
C17	0.050 (6)	0.025 (4)	0.036 (4)	0.006 (3)	−0.005 (3)	−0.008 (3)
N18	0.076 (6)	0.027 (3)	0.024 (3)	−0.009 (3)	0.002 (3)	−0.011 (2)
C19	0.052 (6)	0.025 (4)	0.034 (4)	0.005 (3)	0.000 (3)	−0.006 (3)
C110	0.064 (6)	0.025 (4)	0.039 (4)	0.004 (4)	0.000 (4)	−0.015 (3)
C111	0.060 (6)	0.027 (4)	0.034 (4)	0.007 (4)	−0.002 (4)	−0.008 (3)
C112	0.050 (6)	0.029 (4)	0.051 (5)	0.006 (4)	−0.005 (4)	−0.015 (3)
C113	0.047 (5)	0.017 (3)	0.044 (4)	−0.006 (3)	0.009 (4)	−0.006 (3)
N114	0.035 (4)	0.024 (3)	0.040 (3)	0.003 (3)	0.005 (3)	−0.011 (3)
C115	0.046 (5)	0.040 (4)	0.031 (4)	−0.005 (4)	0.005 (3)	−0.008 (3)
C116	0.059 (6)	0.023 (4)	0.048 (5)	−0.004 (4)	−0.005 (4)	−0.008 (3)
C117	0.060 (6)	0.018 (3)	0.048 (5)	0.003 (4)	0.011 (4)	−0.001 (3)
C118	0.053 (6)	0.021 (3)	0.038 (4)	0.008 (3)	−0.003 (4)	−0.011 (3)
C119	0.061 (6)	0.029 (4)	0.052 (5)	−0.001 (4)	0.003 (4)	−0.019 (4)
N120	0.092 (7)	0.031 (3)	0.038 (4)	0.007 (4)	0.008 (4)	−0.011 (3)
C121	0.075 (7)	0.038 (5)	0.045 (5)	−0.013 (5)	0.009 (5)	−0.014 (4)
C122	0.071 (7)	0.040 (5)	0.040 (5)	−0.009 (4)	0.003 (4)	−0.004 (4)
C123	0.049 (6)	0.039 (4)	0.048 (5)	−0.007 (4)	0.003 (4)	−0.004 (4)
N124	0.063 (5)	0.035 (3)	0.037 (4)	0.003 (3)	0.002 (3)	−0.010 (3)
C125	0.083 (8)	0.045 (5)	0.041 (5)	0.006 (5)	0.007 (5)	−0.013 (4)
N126	0.130 (10)	0.048 (5)	0.057 (6)	0.013 (5)	0.015 (6)	−0.008 (4)
N21	0.036 (4)	0.019 (3)	0.051 (4)	0.010 (3)	0.000 (3)	−0.015 (3)
C22	0.037 (5)	0.020 (3)	0.046 (4)	0.003 (3)	0.008 (3)	−0.009 (3)
C23	0.042 (5)	0.018 (3)	0.058 (5)	−0.004 (3)	0.010 (4)	−0.004 (3)
C24	0.075 (7)	0.028 (4)	0.053 (5)	0.001 (4)	0.001 (5)	−0.012 (4)
C25	0.064 (7)	0.040 (4)	0.042 (5)	0.005 (4)	0.004 (4)	−0.012 (4)
C26	0.046 (5)	0.014 (3)	0.051 (5)	0.000 (3)	0.007 (4)	−0.012 (3)
C27	0.071 (7)	0.034 (4)	0.036 (4)	0.002 (4)	0.005 (4)	−0.012 (3)
N28	0.076 (6)	0.027 (3)	0.021 (3)	−0.001 (3)	0.003 (3)	−0.008 (2)
C29	0.066 (7)	0.030 (4)	0.049 (5)	−0.007 (4)	0.018 (4)	−0.003 (3)
C210	0.058 (7)	0.084 (8)	0.051 (6)	−0.009 (6)	0.001 (5)	−0.019 (5)
C211	0.071 (9)	0.111 (10)	0.048 (6)	−0.027 (7)	0.002 (5)	−0.015 (6)
C212	0.045 (6)	0.068 (6)	0.050 (5)	−0.005 (5)	0.011 (4)	−0.015 (4)
C213	0.054 (6)	0.029 (4)	0.053 (5)	0.008 (4)	0.008 (4)	−0.013 (4)
N214	0.037 (4)	0.021 (3)	0.054 (4)	0.010 (3)	−0.005 (3)	−0.015 (3)
C215	0.031 (5)	0.031 (4)	0.064 (5)	0.008 (3)	−0.010 (4)	−0.025 (4)
C216	0.043 (6)	0.045 (5)	0.064 (6)	0.006 (4)	−0.006 (4)	−0.029 (4)
C217	0.051 (7)	0.037 (5)	0.099 (8)	−0.010 (4)	0.008 (6)	−0.038 (5)

A2-6 Supplementary data of single crystal structure of complexes **1a** in **Chapter 5**.

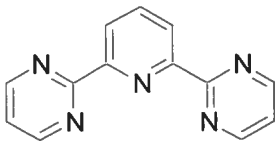

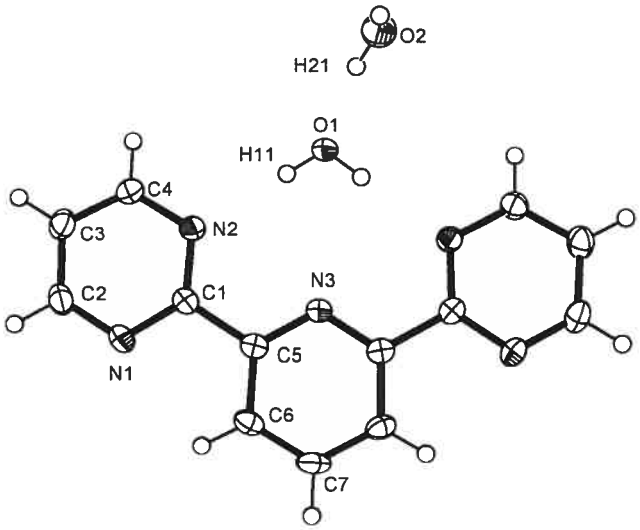

4 Mar 2005

Acta Cryst. (2004). C**60**, 000–000

Structure of Gary74

GARRY HANAN, ELAINE MEDLYCOTT, JIANHUA WANG AND FRANCINE BÉLANGER-GARIÉPY

Département de Chimie, Université de Montréal, C.P. 6128, Succ. Centre-ville, Montréal, Québec, Canada H3C 3J7. E-mail: [redacted]

Abstract

Here should be written a short abstract

Comment

Here should be written the text of the article

Experimental

Small details about the preparation of the compound.

Crystal data

$C_{13}H_9N_5.3(H_2O)$
$M_r = 289.30$
Orthorhombic
Pb_{cn}
$a = 15.4015\,(3)$ Å
$b = 13.4558\,(3)$ Å
$c = 6.72570\,(10)$ Å
$V = 1393.83\,(5)$ Å^3
$Z = 4$
$D_x = 1.379$ Mg m^{-3}
D_m not measured

Cu $K\alpha$ radiation
$\lambda = 1.54178$ Å
Cell parameters from 4152 reflections
$\theta = 2.87$–$72.60°$
$\mu = 0.848$ mm^{-1}
$T = 100\,(2)$ K
Block
Colourless
0.36 × 0.27 × 0.17 mm
Crystal source: synthesized by the authors. See text

Data collection

Bruker Smart 2000 diffractometer
ω scans
Absorption correction:
multi-scan Sadabs (Sheldrick,1996)
$T_{min} = 0.9000$, $T_{max} = 0.9000$
11258 measured reflections
1378 independent reflections
1295 reflections with
$I > 2\sigma(I)$
$R_{int} = 0.025$

$\theta_{max} = 72.74°$
$h = -18 \rightarrow 19$
$k = -13 \rightarrow 15$
$l = -8 \rightarrow 8$
119 standard reflections
every ? reflections
intensity decay: 0.03%

Refinement

Refinement on F^2
$R[F^2 > 2\sigma(F^2)] = 0.0528$
$wR(F^2) = 0.1383$
$S = 1.185$
1378 reflections
109 parameters
H atoms treated by a mixture of independent and constrained refinement

$w=1/[\sigma^2(F_o^2) + (0.0536P)^2 + 1.2468P]$
where $P = (F_o^2 + 2F_c^2)/3$
$(\Delta/\sigma)_{max} = 0.001$
$\Delta\rho_{max} = 0.305$ e Å^{-3}
$\Delta\rho_{min} = -0.250$ e Å^{-3}
Extinction correction: none
Scattering factors from *International Tables for Crystallography* (Vol. C)

Table 1. *Selected geometric parameters (Å, °)*

N1—C2	1.334 (3)	C1—C5	1.494 (3)
N1—C1	1.342 (2)	C2—C3	1.382 (3)
N2—C1	1.338 (3)	C3—C4	1.379 (3)
N2—C4	1.339 (2)	C5—C6	1.396 (3)
N3—C5	1.338 (2)	C6—C7	1.377 (2)
N3—C5^{i}	1.338 (2)	C7—C6^{i}	1.377 (2)
C2—N1—C1	116.48 (17)	C4—C3—C2	116.53 (19)
C1—N2—C4	116.29 (16)	N2—C4—C3	122.57 (19)
C5—N3—C5^{i}	117.6 (2)	N3—C5—C6	122.92 (17)
N2—C1—N1	125.66 (17)	N3—C5—C1	117.36 (17)
N2—C1—C5	118.41 (16)	C6—C5—C1	119.72 (16)
N1—C1—C5	115.92 (17)	C7—C6—C5	118.73 (18)
N1—C2—C3	122.45 (18)	C6^{i}—C7—C6	119.1 (2)

Symmetry codes: (i) $1 - x, y, \frac{1}{2} - z$.

Table 2. *Hydrogen-bonding geometry (Å, °)*

D—H···*A*	*D*—H	H···*A*	*D*···*A*	*D*—H···*A*
O2—H22···O2^{i}	0.84	1.914 (9)	2.750 (3)	173 (7)
O2—H21···O1	0.84	1.935 (6)	2.763 (2)	168 (3)
O1—H11···N2	0.84	1.993 (2)	2.8329 (19)	178 (3)

Supplementary data

The tables of data shown below are not normally printed in *Acta Cryst. Section C* but the data will be available electronically *via* the online contents pages at

http://journals.iucr.org/c/journalhomepage.html

Table *S*1. *Fractional atomic coordinates and equivalent isotropic displacement parameters (Å²)*

$$U_{eq} = (1/3)\Sigma_i\Sigma_j U^{ij} a^i a^j \mathbf{a}_i.\mathbf{a}_j.$$

	x	y	z	U_{eq}
N1	0.72392 (10)	0.99693 (13)	0.1260 (2)	0.0239 (4)
N2	0.64983 (10)	0.84411 (12)	0.1841 (2)	0.0228 (4)
N3	1/2	0.94974 (16)	1/4	0.0188 (5)
C1	0.65349 (12)	0.94331 (14)	0.1738 (3)	0.0203 (4)
C2	0.79586 (13)	0.94593 (16)	0.0837 (3)	0.0292 (5)
H2	0.8471	0.9815	0.0505	0.035
C3	0.79857 (13)	0.84331 (16)	0.0862 (3)	0.0310 (5)
H3	0.8500	0.8077	0.0542	0.037
C4	0.72279 (12)	0.79521 (15)	0.1377 (3)	0.0268 (5)
H4	0.7223	0.7246	0.1403	0.032
C5	0.57280 (11)	1.00123 (14)	0.2156 (3)	0.0195 (4)
C6	0.57552 (13)	1.10492 (14)	0.2147 (3)	0.0249 (5)
H6	0.6285	1.1390	0.1902	0.030
C7	1/2	1.1568 (2)	1/4	0.0282 (6)
H7	1/2	1.2274	1/4	0.034
O1	1/2	0.72652 (13)	1/4	0.0272 (5)
H11	0.5436 (11)	0.7629 (17)	0.232 (5)	0.054 (9)
O2	0.47301 (11)	0.59256 (13)	0.5552 (3)	0.0381 (4)
H21	0.4887 (16)	0.6331 (15)	0.467 (3)	0.038 (7)
H22	0.486 (5)	0.589 (4)	0.676 (3)	0.18 (3)

Table *S*2. *Anisotropic displacement parameters* (Å²)

	U_{11}	U_{22}	U_{33}	U_{12}	U_{13}	U_{23}
N1	0.0229 (8)	0.0260 (8)	0.0229 (8)	−0.0051 (7)	0.0007 (6)	0.0027 (6)
N2	0.0218 (8)	0.0216 (8)	0.0251 (8)	0.0001 (6)	−0.0013 (6)	0.0028 (6)
N3	0.0218 (10)	0.0184 (10)	0.0163 (10)	0.000	−0.0014 (8)	0.000
C1	0.0221 (9)	0.0240 (10)	0.0149 (8)	−0.0026 (7)	−0.0027 (7)	0.0015 (7)
C2	0.0204 (9)	0.0357 (12)	0.0315 (11)	−0.0041 (8)	−0.0007 (8)	0.0068 (8)
C3	0.0225 (10)	0.0356 (12)	0.0348 (11)	0.0040 (8)	−0.0005 (8)	0.0068 (9)
C4	0.0250 (10)	0.0246 (10)	0.0310 (10)	0.0032 (7)	−0.0006 (8)	0.0045 (8)
C5	0.0256 (9)	0.0200 (9)	0.0130 (8)	−0.0014 (7)	−0.0025 (7)	0.0002 (6)
C6	0.0323 (11)	0.0213 (10)	0.0212 (10)	−0.0053 (7)	0.0028 (8)	0.0009 (7)
C7	0.0450 (17)	0.0141 (13)	0.0256 (14)	0.000	0.0068 (13)	0.000
O1	0.0257 (10)	0.0172 (10)	0.0389 (11)	0.000	0.0066 (9)	0.000
O2	0.0396 (9)	0.0429 (10)	0.0318 (9)	0.0045 (7)	0.0009 (7)	0.0130 (7)

Table *S*3. *Geometric parameters (Å, °)*

N1—C2	1.334 (3)	C3—H3	0.95
N1—C1	1.342 (2)	C4—H4	0.95
N2—C1	1.338 (3)	C5—C6	1.396 (3)
N2—C4	1.339 (2)	C6—C7	1.377 (2)
N3—C5	1.338 (2)	C6—H6	0.95
N3—C5^{i}	1.338 (2)	C7—C6^{i}	1.377 (2)
C1—C5	1.494 (3)	C7—H7	0.95
C2—C3	1.382 (3)	O1—H11	0.8400 (2)
C2—H2	0.95	O2—H21	0.84000 (12)
C3—C4	1.379 (3)	O2—H22	0.8400 (3)

A2-7 Supplementary data of single crystal structure of complexes **2a** in **Chapter 5**.

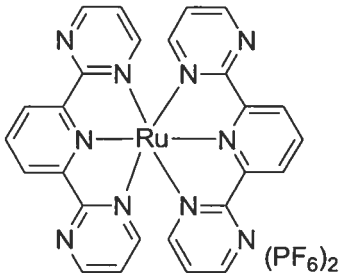

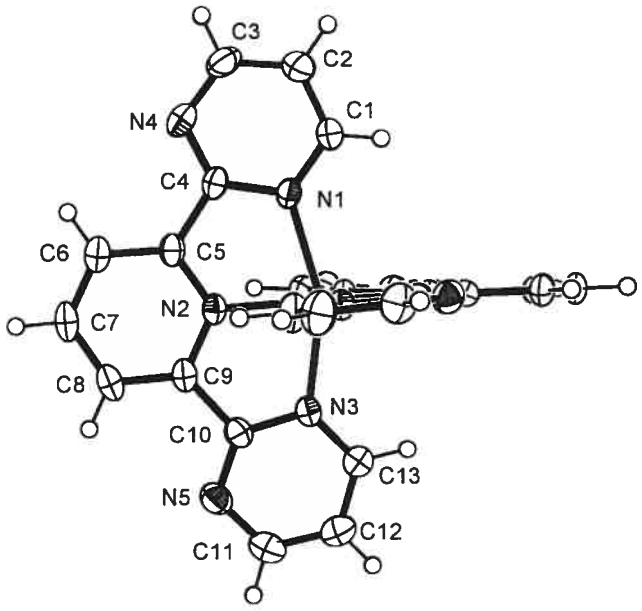

Table 1. Crystal data and structure refinement for GH4.

Identification code	gh4	
Empirical formula	C31 H25.50 F12 N12.50 O0 P2 Ru	
Formula weight	964.15	
Temperature	125(2) K	
Wavelength	0.71070 Å	
Crystal system	Triclinic	
Space group	P-1	
Unit cell dimensions	a = 12.9633(18) Å	α= 87.483(3)°.
	b = 14.844(2) Å	β= 88.590(2)°.
	c = 19.220(3) Å	γ = 78.648(2)°.
Volume	3622.1(9) $Å^3$	
Z	4	
Density (calculated)	1.768 Mg/m^3	
Absorption coefficient	0.629 mm^{-1}	
F(000)	1924	
Crystal size	0.50 x 0.25 x 0.10 mm^3	
Theta range for data collection	1.60 to 28.30°.	
Index ranges	-17<=h<=17, -19<=k<=19, -25<=l<=25	
Reflections collected	41687	
Independent reflections	17852 [R(int) = 0.0396]	
Completeness to theta = 28.30°	99.0 %	
Absorption correction	Multiscan	
Max. and min. transmission	0.9398 and 0.7439	
Refinement method	Full-matrix least-squares on F^2	
Data / restraints / parameters	17852 / 3 / 1050	
Goodness-of-fit on F^2	1.031	
Final R indices [I>2sigma(I)]	R1 = 0.0464, wR2 = 0.1158	
R indices (all data)	R1 = 0.0800, wR2 = 0.1340	
Largest diff. peak and hole	1.327 and -0.633 $e.Å^{-3}$	

Table 2. Atomic coordinates (x 10^4) and equivalent isotropic displacement parameters ($Å^2$x 10^3) for GH4. U(eq) is defined as one third of the trace of the orthogonalized U^{ij} tensor.

	x	y	z	U(eq)
Ru(1)	3293(1)	7865(1)	265(1)	23(1)
P(1)	2639(1)	8167(1)	3280(1)	37(1)
F(1)	2077(2)	9002(2)	3739(1)	54(1)
F(2)	1589(2)	7758(2)	3309(1)	54(1)
F(3)	3204(2)	7325(2)	2832(1)	54(1)
F(4)	3703(2)	8555(2)	3263(1)	53(1)
F(5)	2262(2)	8741(2)	2584(1)	54(1)
F(6)	3021(2)	7585(2)	3981(1)	46(1)
N(1)	3803(2)	8789(2)	890(1)	27(1)
N(2)	3126(2)	8978(2)	-361(1)	26(1)
N(3)	2755(2)	7388(2)	-633(1)	28(1)
N(4)	4047(2)	10348(2)	872(2)	35(1)
N(5)	2200(2)	7919(2)	-1776(2)	38(1)
N(6)	1830(2)	8082(2)	768(1)	27(1)
N(7)	3423(2)	6746(2)	884(1)	25(1)
N(8)	4807(2)	7197(2)	30(1)	25(1)
N(9)	885(2)	7398(2)	1660(2)	33(1)
N(10)	5980(2)	5757(2)	248(2)	31(1)
C(1)	4152(3)	8670(2)	1543(2)	36(1)
C(2)	4438(3)	9380(3)	1881(2)	43(1)
C(3)	4373(3)	10209(3)	1526(2)	42(1)
C(4)	3769(2)	9646(2)	579(2)	29(1)
C(5)	3373(2)	9756(2)	-135(2)	28(1)
C(6)	3239(3)	10551(2)	-555(2)	33(1)
C(7)	2852(3)	10525(2)	-1216(2)	38(1)
C(8)	2601(3)	9725(3)	-1440(2)	35(1)
C(9)	2741(2)	8949(2)	-1001(2)	29(1)
C(10)	2543(2)	8039(2)	-1156(2)	28(1)
C(11)	2088(3)	7063(3)	-1903(2)	51(1)
C(12)	2328(3)	6352(3)	-1426(2)	47(1)
C(13)	2651(3)	6533(3)	-782(2)	37(1)

C(14)	1011(3)	8770(2)	689(2)	37(1)
C(15)	100(3)	8797(3)	1093(2)	43(1)
C(16)	76(3)	8108(3)	1580(2)	39(1)
C(17)	1719(3)	7415(2)	1254(2)	28(1)
C(18)	2618(3)	6643(2)	1313(2)	28(1)
C(19)	2681(3)	5861(2)	1742(2)	32(1)
C(20)	3581(3)	5185(2)	1715(2)	34(1)
C(21)	4400(3)	5297(2)	1265(2)	30(1)
C(22)	4305(2)	6088(2)	852(2)	26(1)
C(23)	5089(2)	6346(2)	350(2)	26(1)
C(24)	6679(3)	6053(2)	-187(2)	34(1)
C(25)	6498(3)	6912(2)	-512(2)	33(1)
C(26)	5532(3)	7469(2)	-398(2)	31(1)
Ru(1A)	3454(1)	2739(1)	5230(1)	23(1)
P(1A)	6900(1)	6867(1)	1933(1)	38(1)
F(1A)	6360(2)	7770(2)	2331(1)	53(1)
F(2A)	5804(2)	6527(2)	1965(1)	54(1)
F(3A)	7430(2)	5970(2)	1536(1)	57(1)
F(4A)	7977(2)	7235(2)	1891(1)	52(1)
F(5A)	6572(2)	7389(2)	1202(1)	53(1)
F(6A)	7226(2)	6350(2)	2663(1)	51(1)
N(1A)	2072(2)	2935(2)	5808(1)	26(1)
N(2A)	3677(2)	1608(2)	5846(1)	25(1)
N(3A)	4961(2)	2094(2)	4933(1)	25(1)
N(4A)	1229(2)	2223(2)	6740(2)	33(1)
N(5A)	6231(2)	718(2)	5152(2)	31(1)
N(6A)	2767(2)	2273(2)	4384(1)	25(1)
N(7A)	3119(2)	3874(2)	4634(1)	25(1)
N(8A)	4062(2)	3660(2)	5809(1)	24(1)
N(9A)	1972(2)	2820(2)	3299(2)	35(1)
N(10A)	4158(2)	5253(2)	5804(2)	35(1)
C(1A)	1258(3)	3643(3)	5797(2)	38(1)
C(2A)	427(3)	3680(3)	6264(2)	45(1)
C(3A)	445(3)	2961(3)	6735(2)	40(1)
C(4A)	2007(2)	2241(2)	6294(2)	27(1)
C(5A)	2913(3)	1476(2)	6302(2)	27(1)

C(6A)	3028(3)	691(2)	6721(2)	34(1)
C(7A)	3949(3)	39(2)	6669(2)	36(1)
C(8A)	4736(3)	183(2)	6204(2)	32(1)
C(9A)	4574(3)	980(2)	5787(2)	27(1)
C(10A)	5310(3)	1266(2)	5266(2)	26(1)
C(11A)	6883(3)	1029(2)	4690(2)	33(1)
C(12A)	6619(3)	1868(2)	4341(2)	34(1)
C(13A)	5637(3)	2389(2)	4472(2)	30(1)
C(14A)	2653(3)	1417(2)	4246(2)	33(1)
C(15A)	2216(3)	1235(3)	3636(2)	43(1)
C(16A)	1872(3)	1962(3)	3177(2)	43(1)
C(17A)	2424(3)	2940(2)	3886(2)	28(1)
C(18A)	2587(2)	3864(2)	4038(2)	27(1)
C(19A)	2261(3)	4663(2)	3641(2)	32(1)
C(20A)	2480(3)	5479(2)	3867(2)	33(1)
C(21A)	3011(3)	5489(2)	4484(2)	33(1)
C(22A)	3319(2)	4673(2)	4862(2)	27(1)
C(23A)	3882(3)	4540(2)	5527(2)	28(1)
C(24A)	4680(3)	5086(2)	6399(2)	38(1)
C(25A)	4934(3)	4224(2)	6711(2)	36(1)
C(26A)	4604(3)	3515(2)	6399(2)	29(1)
P(1B)	740(1)	1386(1)	1007(1)	49(1)
F(1B)	-22(2)	2265(2)	660(2)	74(1)
F(2B)	1680(2)	1924(2)	976(2)	91(1)
F(3B)	1483(2)	509(2)	1356(2)	75(1)
F(4B)	-208(2)	847(2)	1028(1)	62(1)
F(5B)	1076(2)	994(2)	264(2)	80(1)
F(6B)	394(2)	1764(2)	1753(1)	69(1)
P(1C)	4865(1)	2589(1)	2495(1)	28(1)
F(1C)	4164(2)	3458(1)	2857(1)	42(1)
F(2C)	5863(2)	2738(2)	2911(1)	45(1)
F(3C)	5567(2)	1718(1)	2140(1)	44(1)
F(4C)	3868(2)	2444(2)	2084(1)	45(1)
F(5C)	5170(2)	3239(1)	1870(1)	43(1)
F(6C)	4562(2)	1940(1)	3121(1)	43(1)
N(1B)	1029(4)	684(4)	5486(3)	111(2)

C(1B)	300(4)	1211(4)	5301(2)	57(1)
C(2B)	-555(4)	1908(4)	5080(3)	89(2)
N(1C)	-1024(4)	1632(5)	3415(3)	110(2)
C(1C)	-643(4)	956(5)	3142(3)	74(2)
C(2C)	-166(4)	110(4)	2798(3)	69(1)
N(1D)	-155(5)	4030(4)	4412(3)	122(2)
C(1D)	-703(5)	3980(6)	3998(4)	99(2)
C(2D)	-1365(7)	4050(7)	3519(5)	175(5)
N(1F)	-1134(3)	4363(3)	-284(2)	57(1)
C(1F)	-307(3)	4006(3)	-378(2)	44(1)
C(2F)	768(2)	3558(3)	-518(2)	67(1)
N(1E)	275(2)	5120(2)	2404(2)	110(2)
C(1E)	511(2)	4540(2)	2032(1)	68(1)
C(2E)	546(2)	3878(2)	1506(2)	88(3)
N(1K)	275(2)	5120(2)	2404(2)	110(2)
C(1K)	511(2)	4540(2)	2032(1)	68(1)
C(2K)	1135(2)	3792(2)	1635(2)	88(3)

A2-8 Supplementary data of single crystal structure of complexes **2b** in **Chapter 5**.

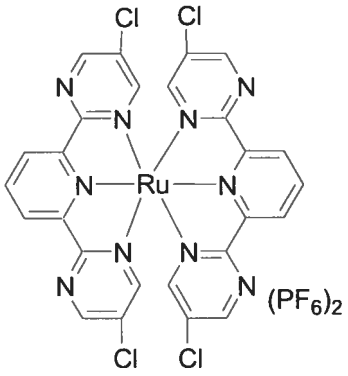

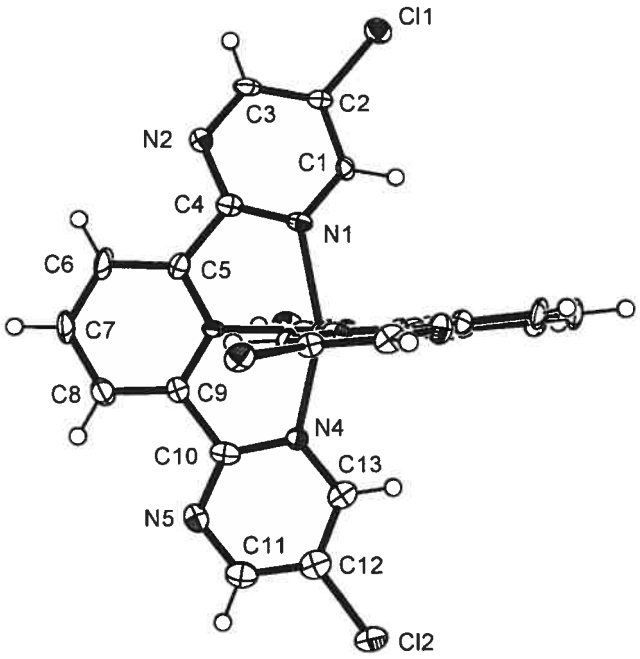

Table 1. Crystal data and structure refinement for ggh6.

Identification code	ggh6	
Empirical formula	C30 H24 Cl4 F12 N12 O2 P2 Ru	
Formula weight	1117.42	
Temperature	125(2) K	
Wavelength	0.71070 Å	
Crystal system	Monoclinic	
Space group	P2/c	
Unit cell dimensions	a = 11.877(3) Å	α= 90°.
	b = 10.666(2) Å	β= 119.990(11)°.
	c = 17.361(3) Å	γ = 90°.
Volume	1904.8(7) $Å^3$	
Z	2	
Density (calculated)	1.948 Mg/m^3	
Absorption coefficient	0.887 mm^{-1}	
F(000)	1108	
Crystal size	0.30 x 0.10 x 0.05 mm^3	
Theta range for data collection	1.91 to 28.25°.	
Index ranges	-15<=h<=15, -14<=k<=14, -23<=l<=23	
Reflections collected	20615	
Independent reflections	4678 [R(int) = 0.0643]	
Completeness to theta = 28.25°	99.2 %	
Absorption correction	Multiscan	
Max. and min. transmission	0.9570 and 0.7767	
Refinement method	Full-matrix least-squares on F^2	
Data / restraints / parameters	4678 / 54 / 308	
Goodness-of-fit on F^2	1.115	
Final R indices [I>2sigma(I)]	R1 = 0.1066, wR2 = 0.2791	
R indices (all data)	R1 = 0.1267, wR2 = 0.2930	
Largest diff. peak and hole	2.593 and -2.551 $e.Å^{-3}$	

Table 2. Atomic coordinates (x 10^4) and equivalent isotropic displacement parameters ($Å^2$x 10^3) for ggh6. U(eq) is defined as one third of the trace of the orthogonalized U^{ij} tensor.

	x	y	z	U(eq)
Ru(1)	5000	2682(1)	2500	11(1)
Cl(1)	1183(2)	6091(2)	-92(2)	23(1)
Cl(2)	9187(2)	-977(2)	4077(2)	28(1)
N(1)	3514(7)	3996(7)	1976(5)	17(2)
N(2)	2028(8)	5042(8)	2313(6)	22(2)
N(3)	4491(7)	2743(7)	3430(5)	14(1)
N(4)	6255(7)	1352(8)	3402(5)	17(2)
N(5)	6727(8)	362(8)	4769(5)	22(2)
C(1)	2961(8)	4568(8)	1180(6)	16(2)
C(2)	1913(9)	5358(8)	933(6)	18(2)
C(3)	1466(9)	5584(9)	1514(6)	21(2)
C(4)	2997(8)	4247(9)	2489(6)	17(2)
C(5)	3589(9)	3573(9)	3348(6)	19(2)
C(6)	3293(10)	3702(11)	4029(7)	26(2)
C(7)	3902(10)	2926(11)	4759(7)	27(2)
C(8)	4811(10)	2021(10)	4819(7)	25(2)
C(9)	5079(9)	1969(9)	4128(6)	18(2)
C(10)	6080(9)	1171(9)	4112(6)	20(2)
C(11)	7682(10)	-284(10)	4750(7)	27(2)
C(12)	7940(10)	-134(9)	4061(7)	25(2)
C(13)	7220(9)	708(9)	3389(7)	20(2)
P(1A)	0	1653(4)	2500	28(1)
F(1A)	-220(30)	1260(30)	1584(13)	124(11)
F(2A)	1486(10)	1628(17)	2806(14)	47(5)
F(3A)	-1471(19)	1570(40)	2160(30)	180(20)
F(4A)	250(30)	1970(20)	3430(11)	88(7)
F(5A)	-180(20)	3043(14)	2224(13)	80(7)
F(6A)	190(20)	249(13)	2787(13)	73(6)
P(1F)	5000	7618(3)	2500	15(1)
F(1F)	5292(5)	6532(6)	1971(4)	26(1)
F(2F)	5280(6)	8698(6)	1972(4)	29(1)

F(5F)	3489(5)	7558(6)	1738(4)	26(1)
N(1A)	1575(12)	6984(12)	4317(8)	49(3)
C(1A)	1761(12)	7425(11)	3809(8)	35(3)
C(2A)	2002(12)	8055(14)	3171(9)	40(3)
O(1B)	802(13)	7367(13)	5416(10)	75(4)

A2-9 Supplementary data of single crystal structure of complexes **3b** in **Chapter 5**.

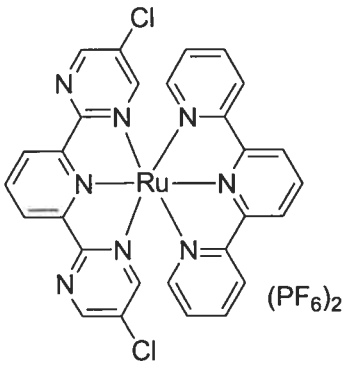

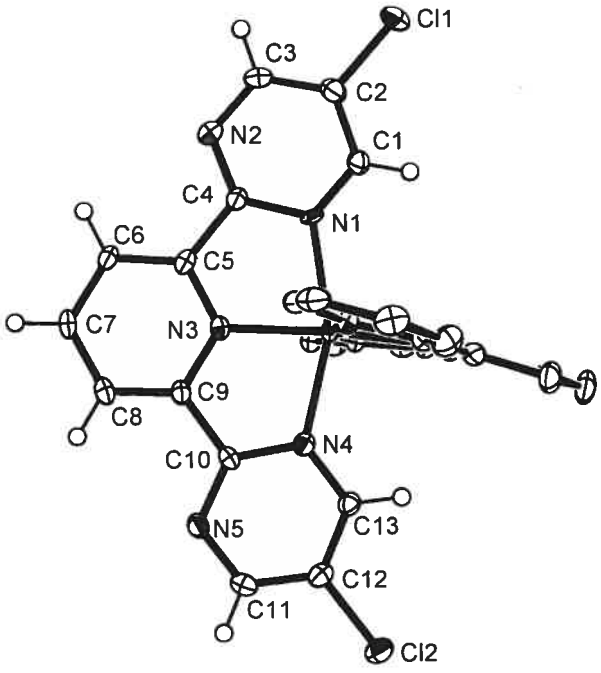

21 Apr 2005

Acta Cryst. (2004). C**60**, 000–000

Structure of Gary75

GARRY HANAN, ELAINE MEDLYCOTT, JIANHUA WANG AND FRANCINE BÉLANGER-GARIÉPY

Département de Chimie, Université de Montréal, C.P. 6128, Succ. Centre-ville, Montréal, Québec, Canada H3C 3J7. E-mail: [redacted]

Abstract

Here should be written a short abstract

Comment

Here should be written the text of the article

Experimental

Small details about the preparation of the compound.

Crystal data

$C_{28}H_{18}Cl_2N_8Ru.2(PF_6).2(C_2H_3N)$
$M_r = 1010.52$
Orthorhombic
Fd_{d2}
$a = 16.3846\,(2)$ Å
$b = 62.8985\,(8)$ Å
$c = 14.5581\,(2)$ Å
$V = 15003.1\,(3)$ Å^3
$Z = 16$
$D_x = 1.790$ Mg m^{-3}
D_m not measured

Cu $K\alpha$ radiation
$\lambda = 1.54178$ Å
Cell parameters from 7885 reflections
$\theta = 2.81$–$72.87°$
$\mu = 6.435$ mm^{-1}
$T = 100\,(2)$ K
Block
Red
0.48 × 0.25 × 0.07 mm
Crystal source: synthesized by the authors.
See text

Data collection

Bruker Smart 2000 diffractometer

ω scans

Absorption correction:

multi-scan Sadabs (Sheldrick,1996)

$T_{min} = 0.3400$, $T_{max} = 0.7300$

45518 measured reflections

7327 independent reflections

7121 reflections with

$I > 2\sigma(I)$

$R_{int.} = 0.053$

$\theta_{max} = 72.97°$

$h = -19 \rightarrow 18$

$k = -77 \rightarrow 77$

$l = -17 \rightarrow 17$

357 standard reflections

every ? reflections

intensity decay: 0.03%

Refinement

Refinement on F^2

$R[F^2 > 2\sigma(F^2)] = 0.0277$

$wR(F^2) = 0.0685$

$S = 1.024$

7327 reflections

588 parameters

H-atom parameters constrained

w=$1/[\sigma^2(F_o^2) + (0.0495P)^2 + 0.0000P]$

where $P = (F_o^2 + 2F_c^2)/3$

$(\Delta/\sigma)_{max} = 0.002$

$\Delta\rho_{max} = 0.680$ e Å^{-3}

$\Delta\rho_{min} = -0.398$ e Å^{-3}

Extinction correction: none

Scattering factors from *International Tables for Crystallography* (Vol. C)

Absolute structure: Flack H D (1983), XXXX

Friedel Pairs

Flack parameter = 0.050 (5)

Supplementary data

The tables of data shown below are not normally printed in *Acta Cryst. Section C* but the data will be available electronically *via* the online contents pages at

http://journals.iucr.org/c/journalhomepage.html

Table *S*1. *Fractional atomic coordinates and equivalent isotropic displacement parameters (Å²)*

$$U_{eq} = (1/3)\Sigma_i\Sigma_j U^{ij} a^i a^j \mathbf{a}_i.\mathbf{a}_j$$

	Occupancy	x	y	z	U_{eq}
Ru1	1	**−0.209893** (11)	**0.172144** (3)	**0.684553** (14)	0.01342 (6)
N1	1	−0.33569 (12)	0.16741 (3)	0.67513 (16)	0.0127 (4)
N2	1	−0.43126 (15)	0.13823 (4)	0.66493 (17)	0.0195 (5)
N3	1	−0.21447 (14)	0.14072 (3)	0.6797 (2)	0.0156 (4)
N4	1	−0.08716 (13)	0.16475 (4)	0.69328 (17)	0.0164 (4)
N5	1	0.00172 (14)	0.13429 (3)	0.69510 (18)	0.0186 (5)
N6	1	−0.19858 (14)	0.17986 (4)	0.54596 (18)	0.0162 (5)
N7	1	−0.19543 (13)	0.20369 (3)	0.6911 (2)	0.0174 (5)
N8	1	−0.21928 (14)	0.17721 (4)	0.82446 (17)	0.0164 (5)
Cl1	1	−0.55600 (4)	**0.191623** (11)	0.68180 (7)	0.03056 (16)
Cl2	1	0.13958 (4)	**0.185780** (12)	0.70296 (5)	0.02673 (17)
C1	1	−0.39689 (17)	0.18087 (4)	0.6751 (2)	0.0187 (5)
H1	1	−0.3862	0.1957	0.6761	0.022
C2	1	−0.47681 (18)	0.17372 (5)	0.6737 (2)	0.0216 (6)
C3	1	−0.49211 (17)	0.15216 (5)	0.6672 (2)	0.0206 (6)
H3	1	−0.5469	0.1472	0.6643	0.025
C4	1	−0.35612 (16)	0.14580 (4)	0.67060 (19)	0.0158 (5)
C5	1	−0.28719 (16)	0.13087 (4)	0.6745 (2)	0.0163 (6)
C6	1	−0.29219 (17)	0.10875 (4)	0.6751 (2)	0.0180 (6)
H6	1	−0.3436	0.1018	0.6731	0.022
C7	1	−0.21994 (17)	0.09703 (4)	0.6786 (2)	0.0201 (6)
H7	1	−0.2217	0.0819	0.6790	0.024
C8	1	−0.14595 (16)	0.10750 (4)	0.6816 (2)	0.0185 (5)
H8	1	−0.0965	0.0996	0.6820	0.022
C9	1	−0.14402 (15)	0.12949 (4)	0.6840 (2)	0.0160 (5)
C10	1	−0.07210 (16)	0.14325 (4)	0.6912 (2)	0.0153 (5)
C11	1	0.06632 (18)	0.14731 (4)	0.6980 (2)	0.0191 (6)
H11	1	0.1198	0.1415	0.6990	0.023
C12	1	0.05622 (18)	0.16921 (4)	0.6994 (2)	0.0194 (6)
C13	1	−0.02142 (17)	0.17753 (4)	0.69873 (19)	0.0173 (5)
H13	1	−0.0288	0.1925	0.7022	0.021
C21	1	−0.19922 (17)	0.16646 (5)	0.4742 (2)	0.0198 (6)
H21	1	−0.2013	0.1516	0.4855	0.024
C22	1	−0.1970 (2)	0.17362 (5)	0.3844 (2)	0.0245 (7)
H22	1	−0.1971	0.1638	0.3349	0.029
C23	1	−0.19469 (19)	0.19512 (5)	0.3674 (2)	0.0260 (7)
H23	1	−0.1964	0.2003	0.3062	0.031
C24	1	−0.18985 (18)	0.20910 (5)	0.4411 (2)	0.0240 (6)
H24	1	−0.1858	0.2240	0.4308	0.029
C25	1	−0.19098 (17)	0.20110 (5)	0.5296 (2)	0.0175 (6)
C26	1	−0.18346 (17)	0.21438 (4)	0.6127 (2)	0.0180 (6)
C27	1	−0.15949 (19)	0.23559 (5)	0.6156 (2)	0.0235 (6)
H27	1	−0.1513	0.2434	0.5606	0.028
C28	1	−0.1478 (2)	0.24508 (5)	0.7009 (2)	0.0279 (7)
H28	1	−0.1313	0.2595	0.7042	0.033
C29	1	−0.1600 (2)	0.23368 (5)	0.7808 (2)	0.0252 (6)
H29	1	−0.1514	0.2401	0.8390	0.030
C30	1	−0.18519 (18)	0.21251 (5)	0.7748 (2)	0.0191 (6)
C31	1	−0.20148 (17)	0.19767 (5)	0.8507 (2)	0.0193 (6)
C32	1	−0.19980 (19)	0.20343 (5)	0.9418 (2)	0.0258 (7)
H32	1	−0.1849	0.2175	0.9591	0.031

C33	1	−0.22029 (19)	0.18834 (6)	1.0089 (2)	0.0263 (7)
H33	1	−0.2195	0.1921	1.0721	0.032
C34	1	−0.24154 (19)	0.16813 (5)	0.9825 (2)	0.0246 (7)
H34	1	−0.2568	0.1578	1.0268	0.029
C35	1	−0.24013 (18)	0.16317 (5)	0.8894 (2)	0.0200 (6)
H35	1	−0.2546	0.1492	0.8711	0.024
P1	1	−0.71632 (4)	**0.111539** (11)	0.68014 (7)	0.01984 (14)
F11	0.70	−0.6886 (5)	0.0901 (2)	0.6265 (9)	0.0267 (12)
F12	0.70	−0.7743 (4)	0.09707 (8)	0.7457 (5)	0.0278 (10)
F13	0.70	−0.6428 (9)	0.1091 (2)	0.7486 (10)	0.029 (2)
F14	0.70	−0.6524 (9)	0.1232 (2)	0.6175 (9)	0.044 (3)
F15	0.70	−0.7901 (5)	0.11428 (12)	0.6120 (5)	0.0313 (15)
F16	0.70	−0.7454 (4)	0.13225 (14)	0.7353 (6)	0.0330 (14)
F111	0.30	−0.7084 (15)	0.0906 (5)	0.628 (2)	0.062 (8)
F112	0.30	−0.7886 (11)	0.1043 (3)	0.7445 (15)	0.050 (4)
F113	0.30	−0.651 (2)	0.1040 (5)	0.758 (2)	0.031 (5)
F114	0.30	−0.660 (2)	0.1267 (5)	0.608 (2)	0.037 (5)
F115	0.30	−0.7820 (13)	0.1191 (3)	0.5975 (14)	0.052 (6)
F116	0.30	−0.7214 (12)	0.1345 (4)	0.728 (2)	0.060 (6)
P2	1	0.05209 (5)	**0.220275** (12)	0.94247 (7)	0.03008 (18)
F21	1	0.12202 (17)	0.23669 (4)	0.91313 (17)	0.0621 (8)
F22	1	0.11425 (12)	0.20102 (3)	0.9276 (2)	0.0492 (6)
F23	1	0.02255 (16)	0.21836 (4)	0.83809 (16)	0.0484 (6)
F24	1	−0.0107 (2)	0.23941 (4)	0.95773 (18)	0.0690 (9)
F25	1	0.07975 (18)	0.22230 (3)	1.04753 (15)	0.0503 (6)
F26	1	−0.01721 (13)	0.20364 (3)	0.97234 (17)	0.0412 (5)
C41	1	−0.5918 (3)	0.25158 (7)	0.6753 (4)	0.0678 (15)
H41A	1	−0.5658	0.2510	0.7358	0.102
H41B	1	−0.6125	0.2660	0.6642	0.102
H41C	1	−0.5518	0.2479	0.6279	0.102
C42	1	−0.6591 (2)	0.23657 (5)	0.6722 (3)	0.0382 (8)
N43	1	−0.7112 (2)	0.22461 (5)	0.6710 (3)	0.0421 (8)
C51	1	0.0307 (2)	0.20455 (7)	0.4802 (3)	0.0444 (9)
H51A	1	0.0679	0.2006	0.5301	0.067
H51B	1	−0.0048	0.1925	0.4655	0.067
H51C	1	−0.0028	0.2167	0.4995	0.067
C52	1	0.0776 (2)	0.21034 (5)	0.3997 (2)	0.0297 (7)
N53	1	0.1152 (2)	0.21498 (5)	0.3362 (2)	0.0408 (7)

Table *S2. Anisotropic displacement parameters* (Å^2)

	U_{11}	U_{22}	U_{33}	U_{12}	U_{13}	U_{23}
Ru1	0.01377 (9)	0.00815 (8)	0.01833 (9)	−0.00001 (7)	0.00116 (8)	0.00036 (8)
N1	0.0078 (10)	0.0173 (11)	0.0130 (11)	−0.0045 (7)	−0.0004 (9)	0.0051 (10)
N2	0.0183 (12)	0.0201 (12)	0.0200 (13)	−0.0040 (9)	0.0000 (9)	−0.0001 (9)
N3	0.0185 (11)	0.0119 (10)	0.0162 (11)	0.0008 (8)	−0.0001 (9)	0.0018 (12)
N4	0.0173 (11)	0.0153 (10)	0.0165 (11)	−0.0015 (8)	0.0018 (10)	−0.0008 (10)
N5	0.0188 (12)	0.0150 (10)	0.0220 (13)	0.0030 (8)	0.0032 (10)	0.0018 (10)
N6	0.0141 (11)	0.0113 (12)	0.0234 (13)	−0.0006 (8)	0.0009 (9)	0.0011 (10)
N7	0.0172 (11)	0.0103 (9)	0.0247 (12)	0.0007 (7)	0.0027 (11)	0.0006 (11)
N8	0.0151 (12)	0.0148 (11)	0.0192 (13)	−0.0002 (9)	−0.0005 (9)	−0.0003 (10)
Cl1	0.0193 (3)	0.0266 (3)	0.0457 (4)	0.0083 (3)	0.0040 (3)	0.0035 (4)
Cl2	0.0187 (3)	0.0255 (3)	0.0360 (4)	−0.0047 (3)	0.0019 (3)	−0.0041 (3)
C1	0.0200 (13)	0.0158 (12)	0.0203 (14)	0.0004 (10)	0.0012 (12)	0.0024 (11)
C2	0.0195 (13)	0.0219 (14)	0.0234 (17)	0.0043 (11)	0.0028 (13)	0.0015 (12)
C3	0.0142 (13)	0.0275 (14)	0.0201 (15)	−0.0013 (11)	−0.0004 (11)	−0.0004 (11)
C4	0.0181 (13)	0.0143 (12)	0.0151 (14)	−0.0021 (10)	0.0033 (10)	−0.0015 (10)
C5	0.0196 (13)	0.0141 (12)	0.0152 (15)	−0.0043 (10)	0.0012 (11)	−0.0002 (11)
C6	0.0199 (13)	0.0131 (12)	0.0211 (16)	−0.0048 (10)	0.0011 (11)	0.0004 (11)
C7	0.0281 (15)	0.0095 (11)	0.0226 (14)	0.0010 (10)	0.0002 (13)	0.0020 (12)
C8	0.0243 (14)	0.0137 (12)	0.0176 (13)	0.0043 (9)	0.0015 (13)	0.0023 (12)
C9	0.0189 (13)	0.0121 (11)	0.0170 (12)	0.0006 (9)	0.0016 (12)	0.0008 (12)
C10	0.0174 (13)	0.0140 (11)	0.0145 (12)	0.0040 (9)	0.0002 (11)	0.0012 (11)
C11	0.0158 (13)	0.0237 (14)	0.0180 (15)	0.0037 (10)	0.0010 (11)	0.0015 (12)
C12	0.0190 (13)	0.0205 (14)	0.0188 (17)	−0.0041 (10)	0.0016 (11)	−0.0028 (11)